CONSIGLIO NAZIONALE DELLE RICERCHE
ISTITUTO DI RADIOASTRONOMIA

PROCEEDINGS OF THE

14th Working Meeting on European VLBI for Geodesy and Astrometry

Castel San Pietro Terme
8 - 9 September 2000

Edited by : P. Tomasi
F. Mantovani
M. Perez Torres

Proceedings of the

14th Working Meeting on European VLBI for Geodesy and Astrometry

Castel San Pietro Terme
8 – 9 September 2000

Edited by: P. Tomasi
F. Mantovani
M. Pérez-Torres

Foreword

The 14th Working Meeting on European VLBI for Geodesy and Astrometry, organised by the Istituto di Radioastronomia of the National Research Council (CNR), has been held in Castel San Pietro Terme, a town not far from Bologna and the Medicina VLBI antenna. The meeting has been a great success, with 35 participants and 27 oral presentations, divided in four sessions.

The young researchers connected to the Training and Mobility programme of the European Community inside the European VLBI network, were a large fraction of the total. Several contributions presented geodetic results from the European VLBI network. The combinations and comparisons of data obtained with different spatial techniques, like GPS, were also presented.

It is now clear that the VLBI solutions are improving and that different centres are producing convergent results also for the vertical component. Moreover, the GPS can be used to densify the observing network and to produce useful information on the wet zenith path delay. A lot of work has been done in order to improve the local tie using classical and GPS techniques, in particular for those sites (like Ny Ålesund and Medicina) where nothing appears to be really stable. New link using GPS has been determined for the VLBI antenna in Onsala. A large effort has been devoted in the technical development at the stations. All the European Stations are now equipped with MARK IV terminal. A new MARK IV correlator is working at JIVE institute (Dwingeloo, The Netherlands) mainly for astronomical data. A second correlator has been recently installed at the Max-Planck-Institute für Radioastronomie (Bonn, Germany) for the correlation of both Geodetic and Astronomical observations. Two very interesting papers have been presented into the astrometric session: one on spatial astrometric VLBI with the Japanese satellite VSOP and the other opening the way to the Global phase-delay Astrometry.

A fraction of the working time has been spent in general discussions and in informal meetings. A visit to the Medicina Station was organised. The weather conditions were perfect and helped to enjoy the visit. The closing dinner at the nearby Trattoria La Fiorentina has been as interesting as the rest of the meeting. Good Italian pasta and meat, with a lot of wine have been served.

I hope everyone enjoyed the meeting and the good time spent in Castel San Pietro Terme.

Paolo Tomasi

Acknowledgments

We thank the Istituto di Radioastronomia for the generous funding to support the meeting and the printing of the proceedings. We thank also the 'Pro-Loco', Castel San Pietro Terme for his help in organising the meeting.

We thank R. Primavera for his help in the preparation of the Proceedings.

The meeting has been organised under the auspices of the TMR-Contract FMRX-CT96-0071, "Measurement of Vertical Crustal Motion in Europe by VLBI".

The Local Organising Committee:
Paolo Tomasi
Franco Mantovani
Miguel Pérez-Torres

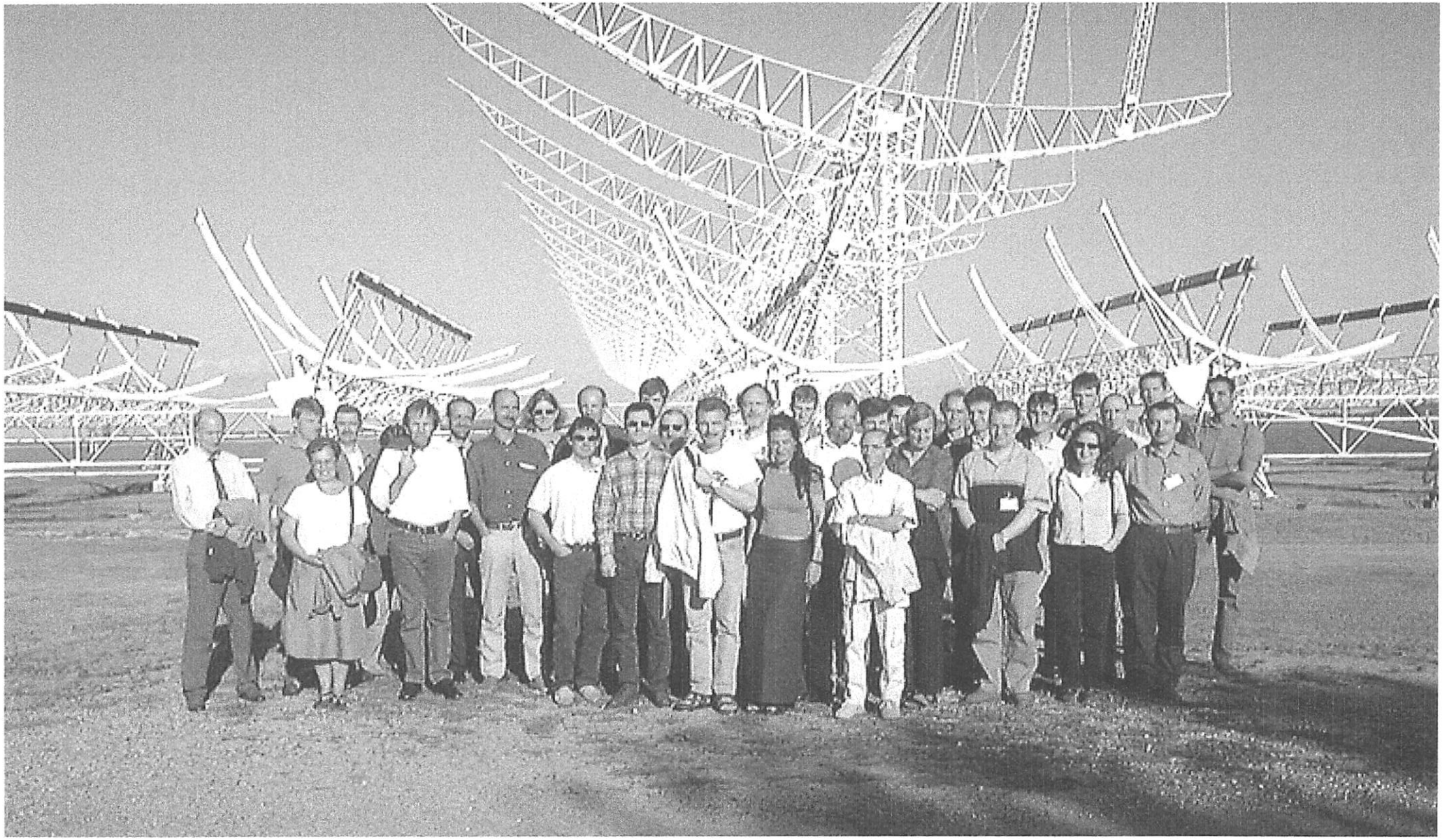

Contents

The European Geodetic VLBI Project

An Overview

The European Geodetic VLBI Project - An Overview -

James Campbell, Geodetic Institute, University of Bonn

Abstract: As the European Geodetic VLBI Project is about to reach the end of its second EU-funded operations period, the past decade of intensive observing and analysis activities is coming to fruition. At the present conference, the participating groups will put forward their most recent results concerning the horizontal and vertical site motions in the European network that has now grown to a total of 11 stations. In this presentation some of the relevant statistics pertaining to the work program of the project will be laid out and future directions of the European network will be indicated.

1. Introduction

The second funding phase of the European Geodetic VLBI Project is drawing closer to its end after 4 years of contract time plus one year of extension for completion of the work programme until the end of September 2001.

The main aim of the geodetic VLBI campaigns in Europe is the determination of horizontal and vertical crustal motions in the european region (Campbell 1988, Campbell & Nothnagel 2000). Looking back at the development of the project, an initial phase of observations in the frame of the NASA Crustal Dynamics Project (CDP) preceded the actual start of the pure European VLBI campaigns in the late eighties. These occasional experiments were carried out by the the participating observatories at their own expense, until funding for regular operations could be obtained from the European Commission under the 2nd Framework Programme "Science". In this first phase under the title "European VLBI for Crustal Dynamics" the work was concentrated on the measurement of horizontal crustal motions, because these were expected to show up first in the observed time series. The continuation and expansion of the project was accepted in June 1996 by the European Commission under the 4th Framework Programme "Training and Mobility of Researchers (TMR)", enabling a second phase of funding of regular geodetic VLBI observations in Europe.

In the second phase of the EU funding scheme, the TMR-network comprises eight participants from six different countries. In addition, several institutions and groups that are not explicitly part of the TMR program are taking part in the observing programs nonetheless, such as Yebes, (Instituto Geografico Nacional, Spain), Effelsberg (Max-Planck-Institut für Radioastronomie, Germany) and Simeis (Crimean Astrophysical Observatory, Crimea, Ukraine). At present, the European Network consists of 10 stations, six of which have an observing record longer than 7 years. In Octber 1994 the new 20m antenna established by the Norwegian Mapping Agency at Ny Ålesund on the arctic archipelago of Spitsbergen has begun to take part routinely in the European VLBI experiments. The 15m antenna of the Instituto Geografico Nacional at Yebes, about 80km east of Madrid, has been equipped for geodetic VLBI and made its first experiments in November 1996. With a MkIIIA-VLBI terminal on loan from NASA the station of Simeiz in Crimea (Ukraine) has been enabled to take part in several of the European geodetic sessions from August 1994 and has increased its participation substantially since June 1997. Finally, the astronomical radio observatoy of Effelsberg (Germany) has been making its 100m antenna available for the geodetic campaigns at a level of one 24h-session per year since December 1991.

COMMISSION OF THE EUROPEAN UNION

Framework Programme for EU-activities in the field of research, technical development and demonstration:

Stimulation	**Science**	**Human Capital and Mobility**	**Training and Mobility**	**Sustainable Growth**
1983 - 88	**1988 - 92**	**1990 - 94**	**1994 - 98**	**1998 - 2002**
Proposal:	***1991***		***June 1995***	***Jan. 2001[2])***
European VLBI:		**Phase I**	**Phase II**	
Start/End:		*Jan. 1993*	*Jan. 1996 Oct. 1996*	*Sept. 2001[1])*

[1]) *including extension of 1 yr*
[2]) *planned new proposal*

Tab. 1: Overview of the EU-funding scheme for the European VLBI project

Between January 1990 and September 2000 a total of 58 observing sessions in slightly varying configurations have been carried out, all of which were processed at the MkIIIA-correlator at the Max-Planck-Institute for Radioastronomy, Bonn. On average, six purely European sessions have been observed and processed each year (Tab.1).

In addition to the work directly associated with the running of the observing campaigns, such as experiment scheduling, sending, receiving and archiving of tapes, data transfer etc, several supplementary tasks to ensure the optimal use of the result have been and are still being taken care of by the different participants in the project:

- monitoring of antenna stability by local surveys
- development of models and methods for controlling temperature effects on antenna mounts
- studies of tropospheric path delay corrections, in particular the influence of water vapour
- include GPS data taken at the VLBI sites, both in terms of tropospheric delay studies as well as site positions and velocities.
- comparisons and combinations with GPS results
- analysis of different sources of vertical motions at the sites
- connections to tide gauges, comparisons of relative vertical motions
- concepts and ideas for geophysical interpretations

In the following sections, we will summarise the status of the activities in several of these fields and give the corresponding references for more detailed information.

$90JAN26X	EUROPE-1/90	WET-ONS-MED-MAD-NOT
$90SEP05AN	EUROPE-2/90	WET-ONS-MED-MAD-NOT-MAT
$90DEC20XE	EUROPE-3/90	WET-ONS-MED-MAD-NOT-MAT
$91JAN06X	EUROPE-1/91	WET-ONS- MAD- MAT
$91SEP08X	EUROPE-2/91	WET-ONS-MED-MAD-NOT-MAT
$91DEC01X	EUROPE-3/91	WET- MED-MAD- MAT-EFL
$92JAN14X	EUROPE-1/92	WET-ONS-MED-MAD-NOT-MAT
$92APR08XE	EUROPE-3/92	ONS-MED-MAD-NOT-MAT
$92MAY12XA	EUROPE-4/92	MED-MAD- MAT- MV2
$92JUL07X	EUROPE-5/92	ONS-MED-MAD- MAT- MV2
$92NOV03XA	EUROPE-7/92	WET-ONS-MED-MAD- MAT
$92DEC01XA	EUROPE-8/92	WET-ONS-MED-MAD- MAT-EFL
$93FEB16XA	EUROPE-1/93	WET-ONS-MED-MAD-NOT-MAT
$93APR27XA	EUROPE-2/93	WET- MED-MAD-NOT-MAT
$93AUG18XA	EUROPE-3/93	WET-ONS-MED-MAD- MAT
$93DEC11XE	EUROPE-4/93	WET-ONS-MED-MAD- MAT-EFL
$94FEB09XN	EUROPE-1/94	WET- MED- not-MAT
$94APR27XE	EUROPE-2/94	WET-ONS-MED-MAD-not-MAT-EFL
$94JUN29XE	EUROPE-3/94	WET-ONS-MED-MAD-not-MAT
$94AUG31XE	EUROPE-4/94	WET-ONS-MED-MAD-not-MAT- CRI
$94OCT26XE	EUROPE-5/94	WET-ONS-MED- not-MAT-EFL-CRI-NYA
$94DEC28XA	EUROPE-6/94	WET-ONS-MED-MAD-not-MAT- NYA
$95FEB01XE	EUROPE-1/95	WET-ONS-MED-MAD-not-MAT- CRI-NYA
$95APR12XA	EUROPE-2/95	WET-ONS-MED-MAD-not-MAT-EFL-CRI-NYA
$95JUN08XA	EUROPE-3/95	WET-ONS-MED-MAD-not-MAT- CRI-NYA-YEB
$95AUG31XA	EUROPE-4/95	WET-ONS- MAD- NYA
$95NOV09XA	EUROPE-5/95	WET-ONS-MED-MAD-NOT-MAT-
$95DEC06XA	EUROPE-6/95	WET-ONS-MED-MAD-NOT-MAT-EFL- NYA
$96FEB07XM	EUROPE-1/96	WET-ONS-MED-MAD-NOT-MAT
$96APR25XA	EUROPE-2/96	WET-ONS- MAD- CRI-NYA
$96JUN12XA	EUROPE-3/96	WET-ONS- MAD-NOT-MAT
$96SEP09XA	EUROPE-4/96	WET-ONS- MAD-NOT-MAT
$96NOV03XA	EUROPE-5/96	WET-ONS-MED-MAD-NOT-MAT-EFL- NYA-YEB
$96DEC05XA	EUROPE-6/96	WET-ONS-MED-MAD-NOT-MAT-EFL- NYA-YEB
$97JAN29XA	EUROPE-1/97	WET-ONS-MED- MAT
$97MAR17XA	EUROPE-2/97	WET-ONS-MED- MAT- YEB
$97JUN16XA	EUROPE-3/97	WET-ONS-MED- NOT-MAT- CRI-NYA-YEB
$97AUG25XA	EUROPE-4/97	WET-ONS-MED- NOT-MAT CRI-NYA
$97OCT30XE	EUROPE-5/97	WET-ONS-MED-MAD-NOT-MAT- CRI-NYA
$97DEC08XA	EUROPE-6/97	WET-ONS-MED-MAD-NOT-MAT-EFL-CRI-NYA- TIG
$98FEB02XA	EUROPE-41	WET-ONS-MED-MAD-NOT-MAT- CRI-NYA
$98APR20XA	EUROPE-42	ONS-MED- NOT-MAT- CRI-NYA
$98JUN22XA	EUROPE-43	WET-ONS- NOT-MAT- CRI-NYA- TIG
$98AUG17XA	EUROPE-44	WET-ONS-MED- MAT- CRI-NYA- TIG
$98OCT12XB	EUROPE-45	WET-ONS-MED-MAD-NOT-MAT- CRI-NYA
$98DEC14XD	EUROPE-46	WET- MED-MAD-NOT-MAT-EFL-CRI-NYA- TIG
$99FEB01XA	EUROPE-47	WET-ONS-MED- NOT- NYA- TIG
$99APR26XA	EUROPE-48	WET-ONS-MED-MAD-NOT-MAT- NYA-YEB
$99JUN28XA	EUROPE-49	WET-ONS-MED-MAD-NOT-MAT- NYA-YEB-TIG
$99AUG16XA	EUROPE-50	WET-ONS-MED-MAD-NOT-MAT- CRI-NYA- TIG
$99OCT11XA	EUROPE-51	WET-ONS- MAD-NOT-MAT- CRI-NYA- TIG
$99DEC13XA	EUROPE-52	WET-ONS-MED-MAD-NOT-MAT-EFL-CRI-NYA- TIG
$00JAN27XA	EUROPE-53	WET-ONS-MED- NOT-MAT- CRI-NYA-YEB-TIG
$00FEB07XA	EUROPE-54	WET-ONS-MED- NOT-MAT- CRI-NYA-YEB-TIG
$00MAR16XA	EUROPE-55	WET-ONS-MED- CRI-NYA-YEB
$00MAY15XA	EUROPE-56	WET-ONS-MED-MAD-NOT-MAT-
$00AUG07XA	EUROPE-57	WET-ONS- NOT-MAT- NYA
$00SEP04XA	EUROPE-58	WET-ONS- NOT-MAT- CRI-NYA
$00OCT02XA	EUROPE-59	WET-ONS-MED- NOT-MAT- CRI- YEB
$00DEC06XA	EUROPE-60	WET-ONS-MED-MAD- EFL-CRI

Tab. 1: Listing of the european geodetic VLBI experiments carried out or planned till December 2000

2. Data Analysis and Results

In the frame of the European VLBI Project, the data are being analysed by several of the participating groups and the results are compared and discussed at regular intervals (see e.g. Börger 1999). Most of the groups are using the CALC/SOLVE analysis software developed at the NASA GSFC (Ma et al. 1992), but the strategies and the amount of data used in the solution are left to the discretion of each team. A compilation and comparison of the most recent solutions available at this moment (Sept. 2000) is given in a related paper in these proceedings (Campbell, this volume).

Here, we just mention the most important differences in the solution strategies:

a. global solutions using the entire global VLBI data set or a large part of it (> 90%). These solutions allow the simultaneous determination of source coordinates (CRF), Earth orientation parameters (EOP) and site coordinates as well as velocities (Ma et al. 1992).
b. global solutions using only a smaller part of the global data set (<10%). These solutions require the a priori input of the CRF and the EOP (except nutation offsets) (Gueguen et al. 2000).
c. regional solutions using only the data of the EUROPE experiments. These solutions also require the a priori input of the CRF and the EOP (Haas et al. 2000)

The solutions of cathegory a) are normally referred to the NUVEL-1A frame of global NNR, while the European solutions of cathegories b) and c) are referred to the Eurasian plate or to one station on this plate (e.g. Wettzell). By subtracting the NUVEL motion of the Eurasian plate from solution a), we of course also obtain the velocities with respect to the Eurasian plate. By contrast, the vertical motions are the result of an average zero vertical motion in the global solutions a), while in the cases b) and c) they are referred to an arbitrarily chosen zero motion of any one fixed station (e.g. Wettzell).

3. Atmospheric path delays

In the total VLBI error budget, the mismodeling of the atmospheric path delays, especially regarding the wet part of the correction, is still considered to be the biggest contribution. Estimated parameters in the VLBI solutions tend to weaken the target parameters, in particular the vertical compnent. Therefore, the idea that GPS data taken at the VLBI sites during the VLBI observing sessions could improve the estimated vertical component of position has been pursued in several of the groups (Rioja and Tomasi 1999, Behrend et al. 2000, Haas et al. 1999, Boehm et al. 2000, Gradinarsky et al. 2000). The first results are encouraging and suggest the implementation of routine procedures to apply this technique in future analyses.

In parallel, however, the water vapour radiometry technique remains a serious option that is being followed on, in spite of the additional technical and logistical efforts needed to run the somewhat delicate systems (Gradinarsky et al. 2000).

4. Local Ties for telescope reference points

The importance of local geodetic measurements for the correct interpretation of the space geodetic determinations of global and regional crustal motions has been stressed at many occasions (Bosworth 1999, Carter et al. 1980). Nevertheless, these supplementary activities

have often received less attention than they should have. In any event, one should be aware that the local measurements serve several distinct purposes:

- local ties of the telescope reference points to the ground markers and between different space techniques (Niell and Nelson 1999)
- deformation monitoring of the telescope structure during and between measurements
- deployment of a local footprint network to monitor local crustal motions or ground motions (Plag 1999)

In the European VLBI network geodetic surveys for local ties of the telescope reference points have been carried out at all of the sites, although the methods applied and the quality achieved vary to some extent. However, in recent years, the investigations for local effects at the telescopes have gained momentum and are yielding improved results. In particular, the influence of thermal expansion on the telescope reference points (Nothnagel et al. 1995) is being monitored at Onsala and Wettzell comparing models to direct measurements, e.g. with invar wires (Elgered 1996, Elgered and Carlsson 1995, Elgered et al. 1996, Johansson et al. 1996, Kilger 1997, Zernecke 1999)

At the sites of Effelsberg (100m Radiotelescope) (Nothnagel 1999), Madrid (Robledo DSS65 Antenna) (Behrend and Rius 1999) and Bologna (Medicina), extensive local geodetic measurements have been carried out to check the location (and possible motion) of the VLBI reference points on the antennas.

Examples of local ground surveys for tying the different space techniques together are given e.g. by (Kipar et al. 1986, Schlüter et al. 1999) for the site of Wettzell and by (Rius and Calero 1983, Behrend and Rius 1999) for Madrid (DSS Robledo).

4. Training activities

An important part of the EU-Funding sceme under the TMR program is formed by the **training activities** that are designed to propagate expert knowledge to the young researchers employed by the project. Among these, we mention those with more specific subjects:

> Course and observational tests on Water Vapour Radiometry, GPS-Iononspere and Troposphere at the Institut d'Estudis Espacials de Catalunya (IEEC), Barcelona, Spain, October 15-23, 1998.
>
> Course on Water Vapour Radiometry and related subjects at Chalmers Technical University, Gothenburg, Sweden, 28 April - 16 May 1999.
>
> Course on Differential GPS and its applications in Positioning and Navigation, IEEC, Barcelona, Spain, 28-29 Oct. 1999
>
> Course on Crustal Loading Effects in Theory and Practice at Chalmers Technical University, Gothenburg, Sweden, 22-24 May 2000
>
> Course on aspects of VLBI for Astronomy and Geodesy at the Istituto di Radioastronomia (CNR), Bologna, Italy, 11-13 Sept. 2000

A course on geophysical aspects of geodetically observed site motions is being planned by the Norwegian National Mapping Agency for May 2001.

5. Outlook

From this overview it becomes clear that the most important task that remains to be done in the frame of the TMR project is the implementation of a final combined solution for the complete set of stations in the European geodetic VLBI network. This final solution has to include the "best" presently available GPS-solution for the VLBI sites and should be made in conjunction with an extensive variance-covariance analysis in order to establish a realistic weighting balance beteeen the VLBI and GPS inputs.

In parallel, still more work has to be invested in the geophysical interpretation, keeping in mind of course that in the frame of this project, only some very broad outlines can be given. The VLBI results will be useful in particular to provide answers about the type and degree of present-day motions of points (i.e. monuments) fixed to the Earth´s crust. In this regard, the most important advantage of the VLBI results is the low level of biases on very long distances bewteen points. In this context, the results will be of particular value as boundary conditions for the sum of possible local and regional motions over long distances. This is valid for both the horizontal as well as the vertical motions.

6. References

Behrend, D., A. Rius: Geodetic Conrol of the Madrid DSS65 VLBI Antenna. *Proc. of the 13th Working Meeting on European VLBI for Geodesy and Astrometry*, Viechtach/Wettzell, Feb. 12-13, 1999, Eds. W. Schlüter, H. Hase, Publ. by BKG, Wettzell, p. 42-50, 1999

Behrend, D., L. Cucurull, J. Vila, R. Haas: An Intercomparison Study to Estimate Zenith Wet Delays Using VLBI, GPS and NWP Models. *Earth, Planets, Space, Journal of the Japanese Societies for Earth and Planetary Sciences*, in print, 2000

Behrend, D., R. Haas, L. Cucurull, J. Vila: ZWS´s from VLBI, GPS, and NWP Models. *this Volume,* 2000

Boehm, R., R. Haas, H. Schuh, and R. Weber: Comparison of tropospheric gradients determined from VLBI and GPS. *this volume*, 2000

Bosworth, J.M.: Collocation of Systems at Space Geodetic Observatories: Best Practices to Ensure Correct Scientific Interpretation of Combined Solutions. *Proc. Of the International Workshop on Geodetic Measurements by the collocation of Space Techniques on Earth (GEMSTONE)*, held Jan. 25-28, 1999 at the Communications Research Laboratory, Koganei, Tokyo, Japan, p. 10-14, 1999

Börger, K.: Comparison of European network solutions. *Proc. of the 13th Working Meeting on European VLBI for Geodesy and Astrometry*, Viechtach/Wettzell, Feb. 12-13, 1999, Eds. W. Schlüter, H. Hase, Publ. by BKG, Wettzell, p. 121-137, 1999

Campbell, J.: European VLBI for Geodynamics. *Proc. of the 3rd Int. Conf. on the WEGENER/MEDLAS Project*, Bologna, May 25-27, 1987, P. Baldi, S. Zerbini Eds., The University of Bologna, p. 361-374, 1988

Campbell, J.: Comparison of European VLBI solutions from different Analysis Centers. *this volume,* 2000

Campbell, J., A. Nothnagel: European VLBI for Crustal Dynamics. *Journal of Geodynamics*, Vol. 30, p. 321-326, 2000

Carter, W.E., A.E.E. Rogers, C.C. Counselman III, and I.I. Shapiro: Comparison of Geodetic and Radio

Interferometric Measurements of the Haystack-Westford Base Line Vector. *Journ. Geophys. Res.*, Vol. 85, p. 2685-2687, 1980

Elgered, G.: Geodetic Very-Long-Baseline Interferometry at the Onsala Space Observatory 1995-1996. *Proc. of the 11th Working Meeting on European VLBI for Geodesy and Astrometry*, Göteborg, Sweden, Sept 1996, Ed. G. Elgered, Research Report No. 177, Chalmers University of Technology, p. 55-61, 1996

Elgered, G., R.T. Carlsson: Temperature Stability of the Onsala 20-m Antenna and Its impact on Geodetic VLBI. *Proc. of the 10th Working Meeting on European VLBI for Geodesy and Astrometry*, Matera, Italy, May 24-25, 1995, Eds. R. Lanotte, G. Bianco, Centro di Geodesia Spaziale, Matera, Italy p. 69-78, 1995

Gradinarsky, L.: Comparison of atmospheric parameters estimated from VLBI, GPS and microwave radiometer data. *Proc. of the 13th Working Meeting on European VLBI for Geodesy and Astrometry*, Viechtach/Wettzell, Feb. 12-13 1999, Eds. W. Schlüter, H. Hase, Publ. by BKG, Wettzell, p. 161-165, 1999

Gradinarsky, L., R. Haas, G. Elgered, J.M. Johansson: Wet path delay and delay gradients inferred from microwave radiometer, GPS and VLBI observations. *Earth, Planets, Space, Journal of the Japanese Societies for Earth and Planetary Sciences*, in print, 2000

Haas, R., L.P. Gradinarsky, J.M. Johansson, G. Elgered: The Atmospheric Propagation Delay: A Common Error Source for Colocatad Space Techniques of VLBI and GPS. *Proc. Of the International Workshop on Geodetic Measurements by the collocation of Space Techniques on Earth (GEMSTONE)*, held Jan. 25-28, 1999 at the Communications Research Laboratory, Koganei, Tokyo, Japan, p. 230-234, 1999

Johansson, L.-A., F. Stodne, S. Wolf: The PISA Project: Variations in the height of the Foundation of the 20 Meter Radio Telescope. *Research Report No. 178, Chalmers University of Technology*, Göteborg 1996

Kilger, R.: Status Report of RT-Wettzell. *Proc. of the 12th Working Meeting on European VLBI for Geodesy and Astrometry*, Hönefoss, Norway, Sept 12-13, 1997, Ed. B. Petterson, Publ. by Statens Kartverk, Hönefoss, Norway, p. 35-37, 1997

Kipar, O., W. Schlüter, H. Seeger, U. Stichling: Ergebnisse der Neuvermessung des lokalen Festpunktfeldes der Fundamentalstation Wettzell. *Veröff. Bayer. Komm. Int. Erdmess.*, Astron.-Geod. Arbeiten, Heft Nr. 48, p. 104-111, München 1986

Ma, C., J.W. Ryan, D.S. Caprette; Crustal Dynamics Project - Data Analysis--1991, VLBI Geodetic Results 1979-90; *NASA Technical Memorandum* 104552, Greenbelt, p. 1-24, 1992

Niell, A.., V. Nelson: The VLBI to GPS Tie at Westford. *Proc. Of the International Workshop on Geodetic Measurements by the collocation of Space Techniques on Earth (GEMSTONE)*, held Jan. 25-28, 1999 at the Communications Research Laboratory, Koganei, Tokyo, Japan, p. 61-67, 1999

Nothnagel, A., M. Pilhatsch, R. Haas: Investigations of Thermal Height Changes of Geodetic VLBI Radio Telescopes. *Proc. of the 10th Working Meeting on European VLBI for Geodesy and Astrometry*, Matera, Italy, May 24-25, 1995, Eds. R. Lanotte, G. Bianco, Centro di Geodesia Spaziale, Matera, Italy p. 121-133, 1995

Nothnagel, A.: Local Survey at the Effelsberg Radio Telescope 1997 - Preliminary Results. *Proc. of the 13th Working Meeting on European VLBI for Geodesy and Astrometry*, Viechtach/Wettzell, Feb. 12-13, 1999, Eds. W. Schlüter, H. Hase, Publ. by BKG, Wettzell, p. 25-31, 1999

Plag, H.-P.: Measurement of vertical crustal motion in Europe by VLBI: Station Report for Ny-Alesund; Norwegian Mapping Authority. *Proc. of the 13th Working Meeting on European VLBI for Geodesy and Astrometry*, Viechtach/Wettzell, Feb. 12-13 1999, Eds. W. Schlüter, H. Hase, Publ. by BKG, Wettzell, p. 65-77, 1999

Rioja, M., P. Tomasi: Integrating GPS zenith path delay measurements into the analysis of geodetic VLBI observations from the European network. *Proc. of the 13th Working Meeting on European VLBI for Geodesy and Astrometry*, Viechtach/Wettzell, Feb. 12-13 1999, Eds. W. Schlüter, H. Hase, Publ. by BKG, Wettzell, p. 152-160, 1999

Rius, A., E. Calero: Comparison of VLBI and Conventional Surveying of the Madrid Deep Space Network Antennas. *Techniques d'Interferometrie a Tres Grande Base*, Toulouse, 31 Aug.-2 Sept. 1982, CNES-Publication, p. 33-39, 1983

Schlüter, W., H. Hase, K. Böttcher, R. Stöger, H. Lang, R. Zernecke: Actual Results of the Local Survey at the FS-Wettzell. *Proc. Of the International Workshop on Geodetic Measurements by the collocation of Space Techniques on Earth (GEMSTONE)*, held Jan. 25-28, 1999 at the Communications Research Laboratory, Koganei, Tokyo, Japan, p. 73-79, 1999

Zernecke, R.: Seasonal Variations in Height demonstrated at the Radiotelescope Reference Point. *Proc. of the 13th Working Meeting on European VLBI for Geodesy and Astrometry*, Viechtach/Wettzell, Feb. 12-13 1999, Eds. W. Schlüter, H. Hase, Publ. by BKG, Wettzell, p. 15-18, 1999

Acknowledgements:

The project has been supported by the EU from Feb. 1993 to August 1996 (grant SCI*CT920829) and from Oct. 1996 onwards (grant FMRX CT96 0071).

Section 1

Geodetic VLBI Analysis and Comparison between Different Techniques

Comparison of European VLBI solutions from different Analysis Centers

James Campbell, Axel Nothnagel
Geodetic Institute, University of Bonn

Abstract: In the frame of the European Geodetic VLBI Project several groups are involved in the analysis of the VLBI observing campaigns, producing solutions for site coordinates as well as the change of these coordinates with time. The solutions may be classified in three cathegories: global solutions containing virtually all VLBI data observed world wide, semi-global solutions containing only a smaller fraction of the global data, and the pure european solutions containing only the so-called EUROPE observing sessions. Fortunately, in addition to the solutions with the widely used CALC/SOLVE system, a solution produced with a completely independent software OCCAM is also available for comparison. The results from the past decade of european VLBI observations show a steadily improving level of agreement, which demonstrates the robustness and integrity of the accumulated VLBI data set.

1. Introduction

The fact that research teams at different institutions around the world are working hard to derive optimal solutions from the same data has long been recognised as a positive incentive for improving the final results. It is useful in prompting discussions among the groups, fostering the birth of new ideas and enabling the discovery of hidden errors. Of course, in the end one 'official' solution should be the result of the all the efforts invested. In this concrete case perhaps the best one is the combined solution.

The comparisons will be made at the level of the site velocities, because these are of greatest interest in the present project. The effect of the translations between solutions can be taken into account by requesting all groups to refer their solutions to one station fixed (e.g. Wettzell), which means in essence that this station is moving in agreement with the Eurasian plate. For the vertical velocities the reference can be chosen arbitrarily (in the range of, say, ±5 mm/y). To first order, a simple algebraic differencing is sufficient to change the zero velocity level.

Still, rotations between solutions do exist and will become obvious at the stations that are farthest away from the chosen fixed station. The rotations normally are also time dependent and hence will affect the velocities, both horizontal and vertical. From the stability of the global EOP solution (the relation between the ITRS and the ICRS) we know that over short as well as long perids of time, the deviations can be at most 0.3 mas, which corresponds to a displacement at the end of a 3000km-baseline vector of about 5 mm (Ny Ålesund is at about 3280 km from Wettzell). These system related motions are embedded in the observed motions and have to be taken into account when setting up the final error budget (Herring 1986).

2. Description of the Solutions

2.1 GIUB (Geodetic Institute, University of Bonn) A. Nothnagel, V. Thorandt

This solution is a global solution that contains about 90% of the total VLBI data base (2282 sessions) covering a period from Jan. 1984 to Dec. 1999, and corresponds to the offical input to the IERS. The software used is CALC 8.2/f-SOLVE. The solution is referred to the ITRF97 terrestrial frame by constraining the sum of the adjustments of 12 selected global sites to zero. The evolution of the

velocity field is constrained by a similar condition for 5 sites. Parameters for episodic site motion are included for Madrid, Effelsberg and Medicina (in Europe). This solution is as usual to be found in one of the next IERS Technical Reports.

2.2 OSO (Onsala Space Observatory) R. Haas, A. Nothnagel

The OSO solution used here belongs to the type of two-stage solutions that allow the explicit representation of the baseline and site coordinate time series (Haas et al. 2000). The solution only contains the data from the EUROPE sessions in the period from Jan. 1990 to May 2000. The software used is the CALC 8.2/f-SOLVE including a frequency and latitude dependent solid Earth tide model, an fcn-period of 430 days, the ocean loading got99.2 model plus interpolated tides, the ERP from Goddard solution for IERS, nutation offsets estimated and the reference station Wettzell fixed to NUVEL-1A NNR. For the stations Effelsberg, Madrid (DSS65) and Medicina the 'jumps' associated with the wheel and track repairs were estimated. In addition, for the stations of Matera, Medicina, Noto and Yebes annual signals in the time evolution of the coordinates were estimated. The wrms of the time series is around ±1.5 to ±2.5 mm for the horizontal components and ±9 to ±16 mm in the vertical.

2.3 CNR (Consiglio Nazionale delle Ricerche) P. Tomasi, E. Gueguen

The CNR 2000 VLBI solution has been presented at the 10th General Assembly of the WEGENER Project (Gueguen et al. 2000). It contains all sessions (also global sessions) that include at least three european stations. In addition, it has been made sure that all data bases with Ny Ålesund take part in the analysis. This makes a total of 198 observing sessions covering the time period from 1986 to December 1999. The CALC 9.1/f-SOLVE software has been used, taking the positions and velocities of the European sites as solve-for parameters except the velocities for Yebes and TIGO-Wettzell, which were not estimated. For the antennas of Effelsberg, Madrid and Medicina, additional parameters for episodic motion at the dates of the wheel-and-track repairs were introduced in the adjustment. The position of Wettzell was fixed in the adjustment to move with the NUVEL-1A-NNR plate model (Eurasia-fixed solution).

2.4 SPbU (Saint Petersburg University) O. Titov

This solution, which contains only 47 European VLBI experiments in the period from 1990 to 2000, is the only one made with a completely different VLBI software, the OCCAM version in use at the Saint Petersburg University (Titov and Zarraoa 1997, Titov 1999).

3. Comparison

On the whole, both the horizontal as well as the vertical site velocities are in a surprisingly good agreement between the analysis centers. This shows, how well the main trends of motion at all the european sites are reproduced by analyses that are using widely different data samples and strategies, even completely different software systems.

There are, however, some differences between solutions of up to 1.5 mm/y in extreme cases, which is not negligible. We can see that nearly all of the velocities of the OSO solution seem to be significantly smaller than those in the three other solutions. This is clearly a matter that needs to be investigated. Possibly, this is an effect of the introduction of additional parameters introduced to take out apparent annual signals in the VLBI time series. This option is presently being tested.

Horizontal velocities with respect to Wettzell fixed (mm/y)					
Station	North East	VLBI (GIUB)	VLBI (OSO)	VLBI (CNR)	VLBI (SPbU)	ITRF97
Ny Ålesund		+ 0.3 ±0.1 - 2.7 ±0.1	- 0.2 ±0.7 - 1.0 ±0.4	- 0.5 ±0.1 - 2.2 ±0.1	- 0.3 ±2.4 - 1.6 ±2.0	+ 0.6 - 2.8
Onsala		- 0.3 ±0.2 - 1.2 ±0.2	- 0.6 ±0.2 - 0.7 ±0.1	- 0.7 ±0.1 - 0.9 ±0.1	- 0.9 ±0.7 - 0.5 ±0.8	- 0.3 - 1.3
Effelsberg		- 0.3 ±0.4 - 0.3 ±0.4	- 0.7 ±0.3 + 0.3 ±0.3	- 1.1 ±0.2 + 1.2 ±0.2	-.- -.-	-.- -.-
Wettzell		+ 0.0 + 0.0	+ 0.0 + 0.0	+ 0.0 + 0.0	+ 0.0 + 0.0	+ 0.0 + 0.0
Madrid (DSN)		- 0.9 ±0.2 + 0.2 ±0.1	- 0.1 ±0.2 + 0.1 ±0.2	- 0.2 ±0.1 + 0.6 ±0.1	- 0.9 ±1.4 + 0.6 ±0.8	- 0.9 + 0.7
Yebes		- 2.2 ±0.7 - 0.1 ±0.7	- 0.6 ±0.6 + 0.2 ±0.6	-.- -.-	-.- -.-	-.- -.-
Medicina		+ 1.7 ±0.1 + 2.0 ±0.1	+ 1.1 ±0.2 + 1.5 ±0.2	+ 1.4 ±0.1 + 2.3 ±0.1	+ 2.1 ±0.7 + 1.1 ±0.7	+ 1.8 + 2.5
Matera		+ 4.0 ±0.1 + 1.8 ±0.1	+ 2.8 ±0.1 + 1.0 ±0.1	+ 4.1 ±0.1 + 1.5 ±0.1	+ 4.3 ±0.8 + 0.6 ±1.0	+ 4.7 + 1.7
Noto		+ 4.1 ±0.1 - 0.1 ±0.1	+ 3.0 ±0.1 - 0.4 ±0.1	+ 4.4 ±0.1 - 0.4 ±0.1	+ 4.6 ±1.1 - 1.0 ±0.9	+ 4.8 + 0.1
Crimea		+ 1.1 ±0.3 + 1.9 ±0.3	+ 0.9 ±0.7 + 1.0 ±0.8	+ 1.6 ±0.3 + 0.5 ±0.3	-.- -.-	-.- -.-

Tab. 1: Horizontal site motions determined by VLBI. Solutions referred to Wettzell in the Eurasian Plate have been provided by GIUB, OSO, CNR and SPbU. The ITRF97 velocities are given as a reference representing a mean of all space techniques involved.

Vertical velocities with respect to Wettzell fixed (mm/y)					
	VLBI (GIUB)	VLBI (OSO)	VLBI (CNR)	VLBI (SPbU)	ITRF97
Ny Ålesund	+ 5.3 ±0.3	+ 5.6 ±1.8	+ 6.4 ±0.3	+ 5.0 ±6.3	+ 2.75
Onsala	+ 3.7 ±0.2	+ 2.0 ±0.7	+ 2.9 ±0.3	+ 4.2 ±3.1	+ 3.76
Effelsberg	- 4.3 ±1.6	+ 1.3 ±2.9	- 0.8 ±0.8	-.-	-.-
Wettzell	+ 0.0	+ 0.0	+ 0.0	+ 0.0	+ 0.00
Madrid (DSN)	+ 2.8 ±0.6	+ 1.2 ±0.8	+ 2.8 ±0.3	+ 2.4 ±3.0	+ 3.71 + 2.97 [1])
Yebes	- 7.5 ±3.1	+ 0.6 ±4.2	-.-	-.-	-.-
Medicina	- 2.7 ±0.4	- 4.1 ±1.0	- 1.2 ±0.3	- 3.0 ±2.6	- 1.01
Matera	+ 0.2 ±0.3	+ 0.4 ±0.6	+ 1.0 ±0.3	+ 0.4 ±3.3	+ 1.80
Noto	- 1.2 ±0.4	- 0.5 ±0.8	- 1.2 ±0.3	- 1.6 ±4.0	- 1.91
Crimea	+ 3.5 ±1.1	- 1.0 ±4.5	+ 4.3 ±1.1	-.-	-.-

Tab. 2: Vertical site motions in comparison between different analysis groups. [1]) GPS-station of Villafranca near Madrid

The errors given together with the different solutions in tables 1 and 2 are the formal errors that are determined primarily by the numbers of total degrees of freedom, which in turn are mainly governed by the number of observations used in the solution. There is of course a big difference between the global solutions and those using only the pure European sessions. Apart from this effect, however, the relations of the errors within a solution are quite informative and show for example, that there is a core set of stations, i.e. Onsala, Medicina, Matera, and Noto, which, together with Wettzell have produced excellent results. Madrid and Ny Ålesund are following closely, while the stations of Effelsberg, Yebes and Crimea, chiefly due to the much smaller number of successful observing sessions are still only of marginal quality. Effelsberg has only one session per year, and Yebes as well as Crimea (Petrov et al. 1999) initially suffered from severe technical problems.

4. References

Gueguen, E., R. Haas, P. Tomasi, A. Nothnagel, J. Campbell: Vertical crustal motion in Europe by means of VLBI. Comparison with geological and geophysical data. *Proc.* of *the 10th GENERAL Assembly of the WEGENER Project,* held at San Fernando, Spain, Sept. 18-20, 2000

Haas, R., E. Gueguen, H.-G. Scherneck, A. Nothnagel, J. Campbell: Crustal Motion Results derived from observations in the European Geodetic VLBI network. *Earth, Planets, Space*, Japan, Vol.xx, (in print) 2000

Herring, T.A.: Precision of Vertical Position Estimates from Very Long Baseline Interferometry. *JGR*, Vol. 91, p. 9177-9182, 1986

Petrov, L., O. Volvach, N. Nesterov: Measurements of horizontal motion of the station Simeiz using very long baseline interferometry. Submitted to *Astronomy Letters* in Dec. 1999

Titov, O.: Tectonic Motion of European VLBI Sites. *Proc. of the 13th Working Meeting on European VLBI for Geodesy and Astrometry*, Viechtach/Wettzell, Feb. 12-13 1999, Eds. W. Schlüter, H. Hase, Publ. by BKG, Wettzell, p. 186-191, 1999

Titov, O., N. Zarraoa: OCCAM 3.4 User's Guide. *Communications of the IAA,* Saint Petersburg, No. 69, 1997

Comparison of the Results Obtained by Different VLBI Networks

Volker Tesmer [1], *Harald Schuh* [2]

[1] Deutsches Geodätisches Forschungsinstitut, Germany, *tesmer@dgfi.badw.de*
[2] Institute of Geodesy and Geophysics, Vienna University of Technology, Austria, *hschuh@luna.tuwien.ac.at*

Abstract

The general subject of this investigation is the analysis of Earth orientation parameters (EOPs) determined by VLBI. A modified version of the OCCAM 4.0 software was used for the VLBI data analysis. The EOP series show different offsets relative to the IERS C 04 series, depending on the specific VLBI network configuration. The offsets are quite similar to those derived by MacMillan et al. (1999) who used the CALC/SOLVE software. EOP series from two different networks observing simultaneously were also determined. The differences between EOPs obtained by the parallel experiments are bigger by at least factor two than their formal errors. Another topic under investigation was whether EOPs in high time resolution show systematic differences depending on the network and whether there are jumps or discontinuities between results of sessions on subsequent days.

1. Introduction

The CORE (Continuous Observations of the Rotation of the Earth) program consists of several VLBI networks, each of them observing on different days of the week. Till now (summer 2000), usually three 24h sessions per week take place only, but it is planned to increase the number of observing sessions aiming at continuous observations by the year 2003. One goal of this study is the investigation of the dependence of EOP series on different VLBI network configurations to get hints on the capability of determining the EOPs from the complete CORE program. Since 1997 two different VLBI networks, CORE-A and NEOS-A, have been observing simultaneously, i.e. on the same day, about twice a month. This allows to compare the results obtained by the two parallel networks. All calculations presented here were done using the OCCAM 4.0 VLBI software, which was extended by a standard least-squares-fit based on the Gauss-Markov-model.

2. EOP series from different VLBI networks

In VLBI, the EOPs are determined with the celestial and terrestrial reference frames kept fixed. In a single VLBI session, usually only a few (four to six) radio telescopes are involved, representing the terrestrial reference frame. Thus, special care has to be taken when chosing the station coordinates. An additional problem is the short North-South extension of most of the observing networks. To get an insight in the dependence of EOPs on network configurations, we analysed observational data from all suitable NEOS-A, CORE-A, CORE-B and IRIS-S sessions between 1997 and the end of 1999.

The solutions were carried out with the International Reference Frame 1997 (ITRF97) station coordinates and velocities, and the International Celestial Reference Frame (ICRF) extension 1 kept fixed. As recommended by the International Earth Rotation Service (IERS Gazette No 13, 1997),

we entered the daily IERS C 04 series with the Lagrangian interpolation scheme and applied the Ray et al. (1994) model for the semidiurnial/diurnial variations of Earth rotation due to the ocean tides.

The EOPs from the various VLBI networks show different and mostly significant offsets relative to the C 04 series (table 1). There seem to be insufficiencies in the models which contribute to the realisation of the terrestrial reference frame in the VLBI software, e.g. the treatment of the permanent tide. Especially the big offsets of dUT1 (dUT1 is the difference between Universal Time 1 (UT1) based on Earth rotation velocity and a very stable atomic time), which are common to solutions from all networks, point to systematic inconsistencies.

Table 1. Offsets between EOP series obtained by different VLBI networks and IERS C 04, (from 1997 till end of 1999)

VLBI network	number of sessions	X_p offset [mas]		Y_p offset [mas]		dUT1 offset [ms]	
NEOS-A	149	-0.089	+/- 0.014	0.073	+/- 0.013	0.0211	+/- 0.0006
CORE-A	62	-0.016	+/- 0.024	0.194	+/- 0.020	0.0182	+/- 0.0011
CORE-B	44	-0.083	+/- 0.029	0.005	+/- 0.034	0.0160	+/- 0.0020
IRIS-S	34	-0.019	+/- 0.034	0.097	+/- 0.039	0.0163	+/- 0.0038

3. EOPs determined from simultaneous NEOS-A and CORE-A sessions

EOPs determined from two completely independent networks monitored simultaneously can help to assess the accuracy of EOP series observed by VLBI. As can be seen in figure 1, the differences between the two EOP series consist of offsets and scatter. The offsets NEOS-A minus CORE-A, determined from 58 simultaneous sessions are -0.033 mas in X_p, -0.129 mas in Y_p and 0.004 ms in dUT1. Some of the individual values are more than two times bigger than their formal errors. All results are very similar to those determined by MacMillan et al. (1999) who used the CALC/SOLVE software package.

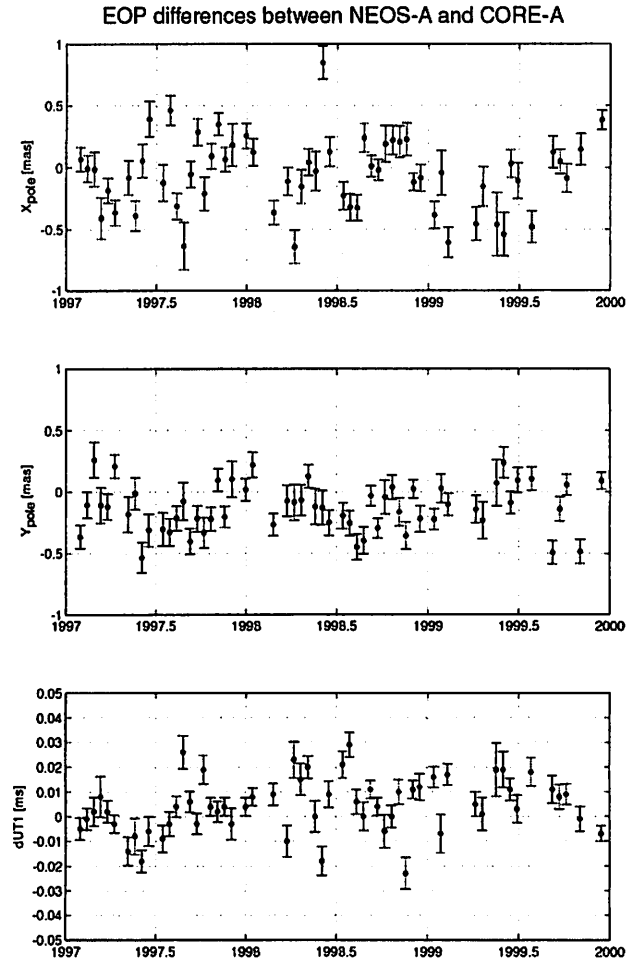

Figure 1. EOP differences between NEOS-A and CORE-A using modified OCCAM 4.0

4. EOPs in high time resolution from sessions on the same and subsequent days

EOPs determined in very high, subdaily time resolution can help to identify reasons for the differences between the results of different networks. EOPs with a temporal resolution of two hours were obtained from the following session constellations:

1. different networks (NEOS-A and CORE-A), observing on the same day,
2. different networks (IRIS-S, NEOS-A and CORE-B), observing on subsequent days,
3. the same network (CONT94, CONT95), observing on subsequent days.

4.1 NEOS-A and CORE-A sessions on the same days

We determined EOPs in high time resolution from the same parallel sessions used in section 3. The results of both networks on February 24th, 1998 (figure 2) show a similar temporal behaviour. An explanation for this good agreement of all three components of Earth orientation could be that the North-South extension of both networks is very long: NEOS-A contains Fortaleza (Brazil) and Ny Ålesund (Spitsbergen), CORE-A is with Fairbanks (Alaska), Hartebeesthoek (South Africa) and Hobart (Australia). However, there are clear offsets between the results of both networks. It is remarkable that in most of the parallel sessions, the results for dUT1, which depend on the East-West component of the networks show the best agreement. On the other hand, the EOPs in high time resolution do not coincide at all for some other simultaneous VLBI sessions as can be seen in figure 3. The reasons for the disagreement could be insufficient modelling of local effects at some of the participating stations. Further investigations on that are needed.

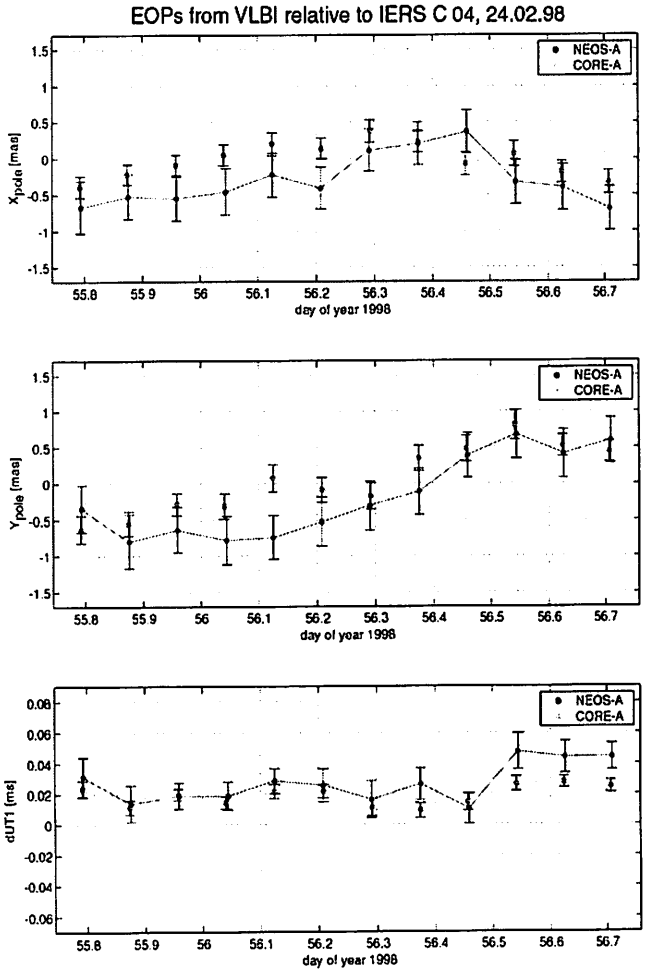

Figure 2. EOPs in high time resolution from NEOS-A and CORE-A, obtained by modified OCCAM 4.0 (24.02.98)

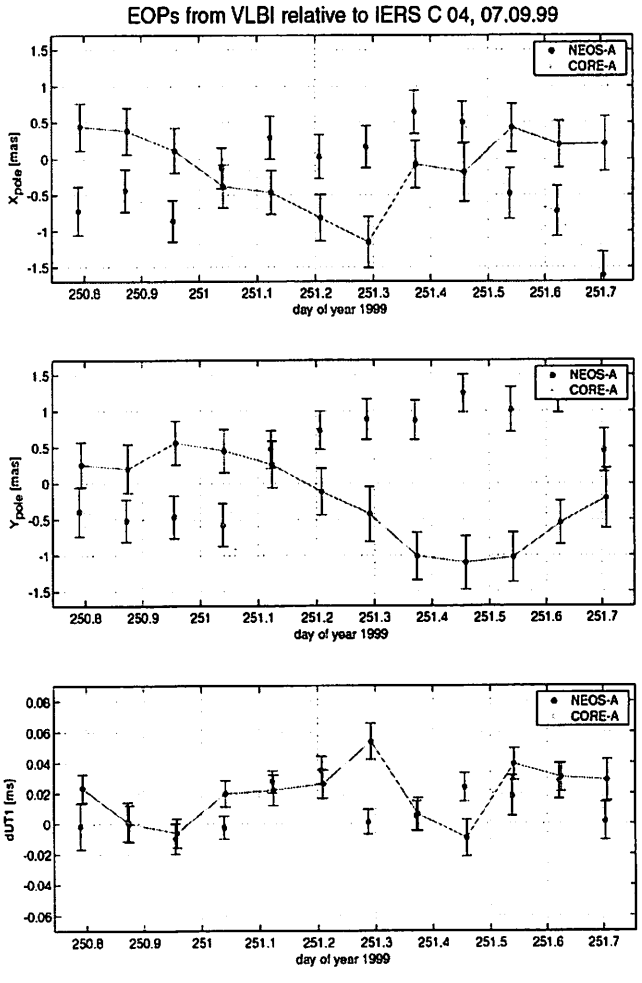

Figure 3. EOPs in high time resolution from NEOS-A and CORE-A, obtained by modified OCCAM 4.0 (07.09.99)

4.2 IRIS-S, NEOS-A and CORE-B sessions on subsequent days

This section also presents EOPs in high time resolution, but now from subsequent VLBI sessions. In figure 4 typical results are shown for EOPs in a temporal resolution of two hours determined from IRIS-S, NEOS-A and CORE-B sessions on subsequent days. The curves are in general 'smooth' and fairly well continuing over several days. Sometimes, small discontinuities and/or offsets dependent on the network can be seen.
Even if the formal errors (plotted as error bars in figure 4) are multiplied by factor two to get more realistic errors, the deviations of the two hourly results from an average value are significant. This shows that there are high frequency variations in the EOPs. One explanation could be that the a-priori model for oceanic tidal influences on the EOPs (Ray et al., 1994) needs improvement. It is also rather likely that further short-period variations of the EOPs exist which are not due to the tides. In this context we refer to IERS Technical Note 28 'High Frequency Oscillations of Earth Rotation' (2000).

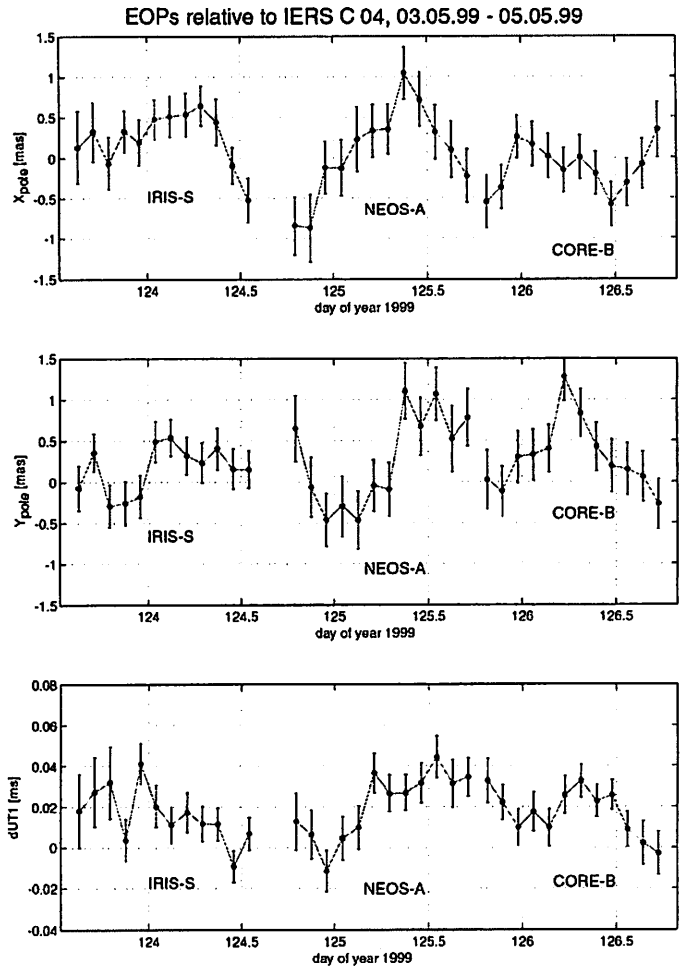

Figure 4. EOPs in high time resolution from IRIS-S, NEOS-A and CORE-B, obtained by modified OCCAM 4.0 (03.05. – 05.05.99)

4.3 CONT94 and CONT95 sessions

In the CONT sessions 1994 and 1995 almost always the same stations observed over a time span of several days. In general the EOPs from CONT94 in two hourly resolution are 'continuous' curves with no offsets from one 24 hour subset to the other as can be seen in figure 5. However, the deviations of the individual two hourly results from average values are significant again.
The existence of offsets between EOPs obtained by different network configurations becomes visible in the results from CONT95 (figure 6). An obvious discontinuity in X_p and Y_p occured on the third day (marked with stars) what is due to the fact that the Westford radio telescope (Massachusetts, U.S.A.) did not observe on that day.

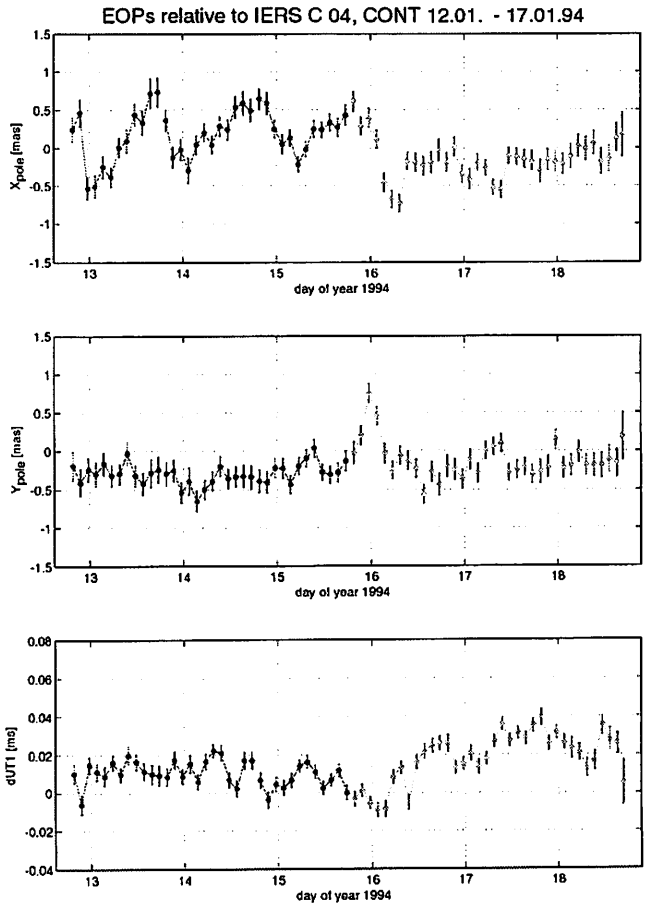

Figure 5. EOPs in high time resolution from CONT94, obtained by modified OCCAM 4.0 (12.01. – 17.01.94)

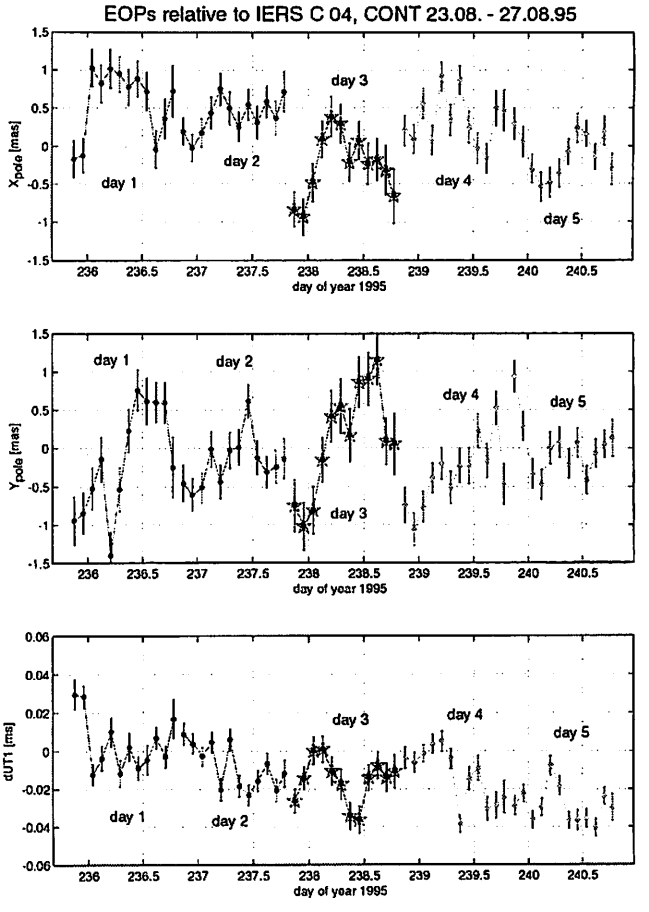

Figure 6. EOPs in high time resolution from CONT95, obtained by modified OCCAM 4.0 (23.08. – 27.08.95)

5. Conclusions

To avoid systematic offsets between EOPs obtained from different VLBI networks, we will determine a terrestrial reference frame with the modified OCCAM 4.0 software, keeping fixed the ICRF and the IERS C 04 EOPs in a first step. This will help to explore the reasons for the network dependent offsets between the EOP series. Those may be due to inconsistent models within OCCAM or due to differences between OCCAM and those software packages which were used to generate the a-priori station coordinates.

The scatter in the differences between EOPs determined by various networks observing simultaneously are a measure for the uncertainty of EOPs from VLBI. Universal Time 1, respectively dUT1 is usually the most accurate and stable component of the Earth's rotation vector observed by a VLBI network. This is due to the fact that in most of the networks the East-West extension is longer and is determined by more stations than the North-South component. The VLBI system of TIGO (Transportable Integrated Geodetic Observing System) which will be located in Chile in 2001 will improve the geometry of some of the networks.

Acknowledgements

The authors acknowledge Dr. N. Vandenberg from Nasa Goddard Space Flight Center (GSFC) for providing the observational data and Dr. A. Nothnagel from Geodetic Institute of the University of Bonn (GIUB) for helpful suggestions in context with this study.

References

Kolaczek, B., Schuh, H., Gambis, D. (eds.): High Frequency Oscillations of Earth Rotation. IERS Technical Note 28, Observatoire de Paris, 2000

McCarthy, D.D. (ed.): IERS Conventions (1996), IERS Technical Note 21, Observatoire de Paris, 1996

MacMillan, D.S., Himwich, W.E., Thomas, C.C., Vandenberg, N.R., Bosworth, J.M., Chao, B., Clark, T.A. and Ma, C.: CORE, High-Accuracy Earth Orientation Measurements. In: Schlüter, W., Hase, H. (eds): 13th Working Meeting on European VLBI for Geodesy and Astrometry, pp 166-171, Viechtach, 1999

Ray, R., Steinberg, D.J., Chao, B.F. and Carthwright, D.E.: Diurnial and Semidiurnial Variations in the Earth's Rotation Rate Induced by Oceanic Tides, Science, 264, pp 830-832, 1994

Schuh, H.: The Rotation of the Earth Observed by VLBI, Acta Geod. Geoph. Hungarica, Vol. 34(4), pp 1-12, 1999

First steps towards rigorous combinations of VLBI Earth orientation parameter series

Axel Nothnagel and Christoph Steinforth
Geodetic Institute of the University of Bonn, Nussallee 17, D-53115 Bonn, Germany
Tel.: ++49 (228) 733574, Fax: ++49 (228) 732988, E-mail: nothnagel@uni-bonn.de

Abstract

On March 1, 1999, the International VLBI Service for Geodesy and Astrometry (IVS) was officially inaugurated. One of the primary objectives of this service is to provide high quality results from Very Long Baseline Interferometry (VLBI) observations for a variety of applications. Optimal analysis models and data flow procedures are a prerequisite for successful contributions to the worldwide investigations in Earth rotation. The current operation of the IVS provides initial comparisons of the results of individual IVS Analysis Centers as a feedback to their submissions. Procedures are being established for combinations in order to provide to the users reliable and consistent Earth orientation parameters (EOP) series.

Introduction

On March 1, 1999, the International VLBI Service for Geodesy and Astrometry (IVS) was officially inaugurated and since then has made considerable progress towards its realization (IVS 1999). By now the IVS has become a fully qualified service of the International Association of Geodesy (IAG) and of the International Astronomical Union (IAU).

One of the primary objectives of this service is to provide high quality VLBI (Very Long Baseline Interferometry) results for a variety of users and applications. Earth orientation parameters (EOP) as a prime product of the IVS are of special importance since VLBI is the only technique which can provide all EOP components without additional information from other techniques.

Currently, the IVS comprises 75 components of which 19 serve as IVS Analysis Centers. According to their proposals the tasks have been distributed between the analysis centers taking into account their special capacities and interests. The IVS Terms of Reference (ToR) distinguish between IVS Analysis Centers and IVS Associate Analysis Centers. IVS Analysis Centers routinely process VLBI data and submit their products in a complete and timely manner while IVS Associate Analysis Centers concentrate on special research efforts and submit specialized products (IVS 2000).

1 Data flow within the IVS

Routinely, the observation data of the VLBI sessions are correlated using one of the primary Mark IIIa/IV VLBI hardware correlators at Bonn (Germany), Haystack near Westford, MA (USA) and Washington D.C. (USA). The raw data is prepared for analysis by the responsible IVS Operation Center and submitted to the nearest IVS Data Center which exist at NASA Goddard Space Flight Center (Greenbelt MD, USA), Observatoire de Paris (Paris, France) and Bundesamt für Kartographie (Leipzig, Germany) (Fig. 1). The contents of the data centers are mirrored on a six-hourly basis so that all data is close to current at all the data centers at any time.

IVS Analysis Centers then collect the observational data from the data centers and carry out their data analyses. At present four IVS Analysis Centers regularly submit earth orientation parameters to the IVS Data Centers: Bundesamt für Kartographie und Geodäsie (BKG), Leipzig in Germany, NASA Goddard Space Flight Center (GSFC), Greenbelt MD USA, Institute for Applied Astronomy (IAA), and St. Petersburg University SPbU both at St. Petersburg in Russia. The analysis centers store their results in the IVS Data Centers in a predefined data structure. The data is also available to any user who may retrieve it from here.

The IVS Analysis Coordinator is responsible for coordinating the analysis activities of the IVS and for stimulating VLBI product development and delivery. In this context he is responsible for forming the official products of IVS using combinations of the analysis results submitted by the IVS Analysis Centers. For this purpose the results of the individual Analysis Centers are routinely copied to the IVS Analysis Coordinator's office for comparisons and combination.

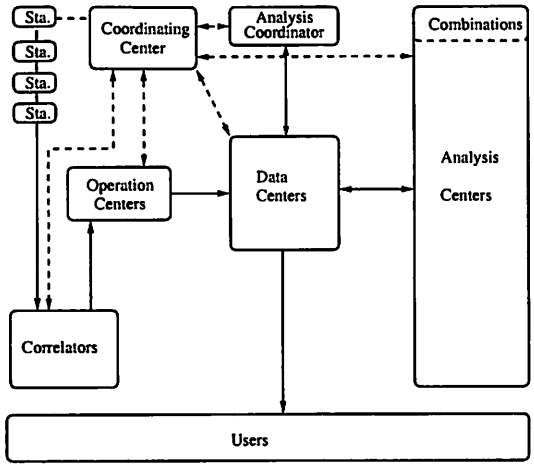

Figure 1: IVS data flow.

2 Results of Comparisons

For the comparisons the question arises of how to establish relative weights for the individual analysis centers since weighted averages have to be computed as a reference. It is quite clear that these cannot only depend on the formal errors assigned by the analysis centers alone. For this purpose the scatter of the nutation results appears to be a suitable indicator. The celestial reference frame as such is very stable at the sub-milliarcsecond level and deficiencies of individual sources average out in the large number of sources used in geodetic VLBI series. Therefore, most of the scatter to be found in the individual nutation offset series can be attributed to the way the analysis is carried out.

In a first step of the comparison procedure the scatter of the nutation angles $d\psi$ and $d\epsilon$ is analysed. Initial mean values are computed for each epoch where the input is weighted only according to the formal errors. These values are used to determine biases and rates which are mainly due to reference frame differences. From the unbiased series a weighted root mean squared error (wrms) is computed for each analysis center combining both nutation components in a root sum squared error (rss) sense:

$$wrms_{nut,i} = \sqrt{wrms^2_{d\epsilon,i} + wrms^2_{d\psi \sin \epsilon_0,i}} \tag{1}$$

with i being the index of analysis centers. The combined wrms of the nutation offsets is then used as a new weighting factor for each of the analysis centers. For fine tuning the process is then repeated applying the weighting factors to the input data.

At present, the comparisons of the Earth orientation parameters concentrate on the results of the 24 hour sessions. Due to delays caused by tape transportation, correlation and IVS start-up friction EOPs are currently submitted with a delay of roughly 3 to 4 weeks for the weekly EOP observing series. Table 1 gives an impression of the current level of agreement of the four analysis centers. The biases of the nutation components are computed relative to the weighted means while for polar motion and UT1-UTC they are computed relative to the IERS C04 series. At present some numerical obstacles in the weighting process inhibit the use of weights for polar motion and UT1-UTC. Therefore, only the unweighted RMS is presented here for polar motion and UT1-UTC.

Table 1: Current average statistics of comparisons from 4 analysis centers (Status: 2000.06.01

component	| bias |	wrms
$d\psi \cdot \sin \epsilon$	17 μas	58 μas
$d\epsilon$	32 μas	51 μas
component	| bias |	rms
UT1-UTC	15 μs	6 μs
x_p	74 μas	92 μas
y_p	82 μas	88 μas

The results of the comparisons are regularly being made available both graphically and numerically on the IVS Web page http:/ivscc.gsfc.nasa.gov or its mirrors (click on Analysis Coordinator's page). An example is printed in fig. 2. Analysis centers are invited to use these comparisons to monitor their performance and users have first hand information on the quality of the IVS products.

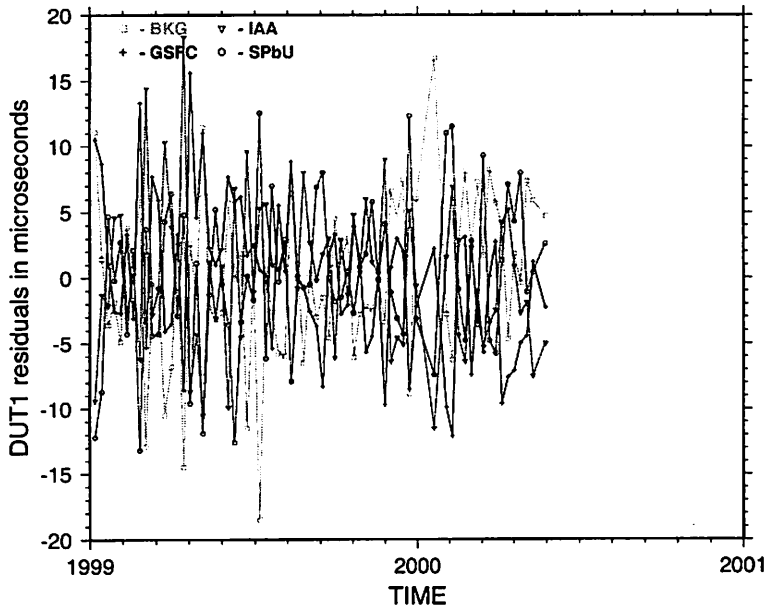

Figure 2: UT1-UTC residuals of all analysis centers.

3 Combination Procedures

Since users of the combined series will also rely on the long term stability of EOP series this requirement has to be taken into account in the combination process. While the nutation offset series are fairly uncritical due to their young history and their direct connection to VLBI observations, polar motion and UT1-UTC series have a long history. Consistency with the reference series C04 of the International Earth Rotation Service (IERS) (e.g. IERS 1999) is considered to be of importance and should, therefore, be maintained.

The first step before combination is, thus, the determination of offsets between the individual series and the IERS C04 series. Biases are computed from data sets of each individual analysis center which cover at least periods from 1984 to dates immediately prior to the first epoch of combination. As long as no changes in the strategy of the solution are introduced the biases are frozen. For each data point the respective bias of the analysis center is subtracted before a weighted average is computed yielding the combined EOP value.

4 Outlook

The International VLBI Service for Geodesy is currently establishing the basis for the realization of a true geodetic service. The production and dissemination of combined EOP series are important contributions to this service.

The first combined IVS EOP series will be published in the near future. A regular update is planned always concurrent with the production of individual series by the IVS Analysis Centers. In parallel, more refined analyses of the combination residuals of the individual analysis centers have to be carried out investigating reasons for the differences in the results.

One of the unsolved problems are systematic differences between EOP results from different VLBI networks which observe at the same day (MacMillan and Ma 2000). There are a number of promising

investigations and the reasons for the differences may soon be discovered leading to an even better stability of the combined EOP series.

References

IERS (1999) 1998 IERS Annual Report, Observatoire de Paris, Paris

IVS (1999) International VLBI Service for Geodesy and Astrometry, Annual Report 1999, N.R. Vandenberg (ed.); NASA/TP-1999-209243, Greenbelt MD

IVS (2000) International VLBI Service for Geodesy and Astrometry, Terms of References, available electronically from http://ivscc.gsfc.nasa.gov

MacMillan D.S, C. Ma (2000) Improvement of VLBI EOP accuracy and precision, Proceedings of the First IVS General Meeting, Kötzting, Germany, Feb. 21–23, 2000

Using a Knowledge-Based System for the VLBI Data Analysis

Wolfgang Schwegmann

Istituto di Radioastronomia (CNR), Via P. Gobetti, 101, 40129 Bologna, Italy,
Tel.:+39/051-639-9414, Fax: +39/051-639-9431, e-mail: schwegma@ira.bo.cnr.it

Abstract

An important contribution to the acceleration of the VLBI procedure is a faster and semiautomatic data analysis, in particular in view of the increasing amount of VLBI data to be processed in the next years. The VLBI data analysis is a very complex process and still needs a lot of manual interactions. A Knowledge-Based System (KBS) is being developed to support the analyst during the data analysis and to automate it. In the KBS the knowledge about the VLBI data analysis is stored and processed according to specific rules and instructions. Whenever the KBS is going to be activated all necessary data and information have to be transferred from the existing software. This information is evaluated by the KBS and possible errors are corrected. The results are sent back to the analysis software and the regular analysis is continued. Examples will be given how the KBS is going to check the decisions done by the analyst and how the data analysis is accelerated.

1 Introduction

The geodetic VLBI data analysis is a very complex process and needs a lot of manual interactions. Most tasks require a comprehensive knowledge of the whole procedure of data analysis. Thus, it is very time consuming and a partial automation would be very useful to accelerate the VLBI procedure in particular with regard to the increasing number of geodetic observing sessions to be expected in the future. According to the description of a *Knowledge-Based System* (KBS) (Sundermeyer, 1991) a KBS can be used to model the knowledge needed for the VLBI data analysis and to apply this knowledge for solving the complex problems within the data analysis automatically. A KBS is less susceptible to errors, allows to conserve the analyst's knowledge and to check his decisions. More detailed information about KBS can be found in Schnupp et al. (1989).

In the VLBI data analysis a KBS can be used to dispatch certain tasks:

- support the analyst during the data analysis,
- automate the data analysis,
- teach less experienced analysts,
- check and verify data and
- resolve problems.

Investigations of the *MarkIII Data Analysis System*, a widely used VLBI software system (Ryan et al., 1980), have shown that almost all steps of the data analysis can be supported by at least one of the above applications of a KBS (Schwegmann and Schuh, 1999).

Thus, a Knowledge-Based System for support and guidance of the analyst is developed to automate to a high degree the geodetic VLBI data analysis. It is an important component of a general concept for VLBI in near real-time (Schuh and Schwegmann, 2000). In this KBS the knowledge about the data analysis is stored and processed according to specific rules and instructions. The concept and the implementation of this *Intelligent Assistant for Data Analysis in VLBI* (IADA) will be described in section 2. The KBS can be adapted to different geodetic VLBI software packages by developing an interface for the existing data analysis software. The interface is used to transfer data and information between both the existing software and the KBS. At present an interface is being built for the MarkIII Data Analysis System in particular for the program SOLVE, that is used for analyzing geodetic VLBI observations. Whenever the KBS is activated the interface collects all necessary data from SOLVE. This information is evaluated by the KBS and possible errors are

corrected. The results are transferred back to SOLVE and the regular analysis is continued. The development of this interface will be described in section 3 and examples for the dataflow between the two systems using the interface will be given in section 4.

A first successful realization of an on-line VLBI-System is the Japanese Keystone project. In this project four radiotelescopes in the Tokyo area produce geodetic results in near real-time. It is part of the Japanese Earthquake Prediction Programme (Koyama et al., 1998).

2 Development of the Knowledge-Based System

The most important and even critical task when developing a KBS is to build the Knowledge Base (KB), the main component of a KBS, because its efficiency depends on the qualitiy of the KB, which should be modular, flexible and extensible. The knowledge needed for the problem must be collected, structured and organized first (*Knowledge Acquisition*). Then it has to be formally represented and stored in the Knowledge Base (*Knowledge Representation*).

As mentioned in section 1 the KBS should be able to fulfill several purposes during the data analysis. Considering all these possible applications of the KBS four so called *Modes* were defined (cf. table 1). These *Modes* have to be taken into account when building the Knowledge Base. For example it should be possible to call the *Diagnosis Mode* from the *Interactive Mode* to investigate problems which occured during the analysis in the *Interactive Mode.*

Because the general procedure of VLBI data analysis is very similar in all VLBI analysis programs, the system can be designed to be transferable to other VLBI software packages like OCCAM (developed at the Universities of Bonn, Madrid and Sanct Petersburg) or MASTERFIT/MODEST (developed at Jet Propulsion Laboratory, Pasadena, CA).

Table 1: Modes of the Knowledge-Based System.

INTERACTIVE	- to check all decisions done by the analyst
	- to support the analyst during the data analysis
AUTOMATIC	- to perform the steps of the data analysis automatically
DIAGNOSIS	- to investigate problems and find possible solutions
	- to check the results of the data analysis
TUTORIAL	- to teach less experienced analysts

2.1 Knowledge Acquisiton

To collect the knowledge about the VLBI data analysis its general procedure has to be described, i.e. a *Concept* of the VLBI data analysis procedure has to be set up. This was done in accordance with the *User's guide to interactive* SOLVE (Petrov, 2000). The *Concept* is divided into three main parts: *Analysis Steps*, *Analysis Substeps* and *Substep Description.* The first part defines the global frame of the VLBI data analysis procedure. The *Analysis Steps* are performed one by one in the standard data analysis and are subdivided into substeps to describe the tasks of the data analysis in detail. Table 2 lists the *Analysis Steps* and its *Substeps.* The KBS can be applied for the whole process of the data analysis or for single steps or substeps. Each substep is characterized by the so-called *Substep Description* to define the parameterizations and calibrations that should be used. By comparing these specifications to the current settings within the analysis software, the system is able to check all actions done by the analyst in the *Interactive Mode.* In the *Automatic Mode* the specifications are applied to set up the correct parameterization automatically. In order to be able to evaluate the results of a substep *Evaluation Criteria* can be specified within the *Substep Description.* Additionally, methods can be designated to overcome problems during this substep of the data analysis, for example if the results don't meet the evaluation criteria. Examples for such a description are given in table 3.

Table 2: Steps and Substeps of the VLBI data analysis procedure.

ANALYSIS STEPS	Data Loading	Initial Solution	Intermediary Solution	Final Solution	Database Update
ANALYSIS SUBSTEPS	-	Initial Settings	Initial Settings	Initial Settings	-
		A priori Clock	Outlier Elimination	Outlier Elimination	
		Ambiguity Solution	Check Solution	Examine Solution	
		Inspect Residuals		Final Outlier Elim.	
				Source Positions	
				Check Cable Cal	
				Inspect Residuals	

Table 3: Description of the substeps of the VLBI data analysis procedure.

STEP/ SUBSTEP	Parameterization	Evaluation Criteria	Problem Handling
		⋮	
Initial Solution/ A priori clock	- clock polynomials of order 0,1,2	- clock offset should be less than 100000 nsec - clock rate should be less than 100000D-14	- set a priori clock model
		⋮	
Intermediary Solution/ Check Solution	- estimate station positions (except the reference station) - estimate baseline-dependent clocks - estimate atmosphere path delay - estimate clock parameters	- solution is good if the total wrms is in the range [15,100] psec and more than 80% of observations are in solution - solution is poor if the total wrms is in the range [100-250] and between 50% and 80% of observations are in solution - solution is unsatisfactory if wrms is more than 250 psec and/or less than 50% of observations are in solution	- check calibration - check para-meterization - check for clock breaks
		⋮	

2.2 Knowledge Representation

The *Concept* of the VLBI data analysis procedure has to be transformed and stored in the Knowledge Base of the KBS. Several knowledge representation techniques are applied to formalize the knowledge. The most important formalisms are:

- *FRAMES* to represent knowledge about objects, for example a VLBI station. They consist of several *slots* to describe the attributes of an object. In frames both dynamic knowledge (e.g. the current parameterization related to a VLBI station, ...) and static knowledge (e.g. a priori coordinates, clock behavior of a VLBI station, ...) is stored. In contrast to the static knowledge the dynamic knowledge depends on the current experiment and changes during the course of the data analysis. While the static knowledge is a part of the Knowledge Base the dynamic knowledge has to be collected from the analysis software and loaded into the Knowledge Base at each step of the data analysis.

- *RULES* to model knowledge which depends on conditions. They are applied to check whether the current parameterization is correct (e.g. with respect to rank deficiencies, ...), to examine the results of the analysis and so on. Therefore they use the information within the frames of the Knowledge Base. Rules are organized in so-called *rule-sets*. Each rule-set combines rules which are used for a specific task, e.g. for the check of the correct parameterization. Depending on the step of the data analysis specific rule-sets are going to be applied. This is specified in the *Instruction Part* of the Knowledge Base.

The *Status Description* is an important part of the *Concept* of the VLBI data analysis procedure, because it contains the knowledge about the correct parameterization and the parameters that have to be checked at each substep of the data analysis. This knowledge is considered to be dynamic, i.e. it is not hard-coded within the Knowledge Base but stored in external files. It can be modified easily without profound knowledge about the knowledge representation techniques used in the Knowledge Base. Thus, the KBS can be adapted to a specific analysis program without modifying the Knowledge Base, because the procedure of the VLBI data analysis itself is very similar in all programs. It just has to be specified which *Analysis Steps* and/or *Substeps* and which parameterizations and calibrations are supported by the specific software.

3 The interface between SOLVE and IADA

To apply the KBS during the data analysis using a specific software an interface has to be developed to manage the dataflow between these two systems. The interface is part of the analysis software and has to perform the following tasks:

1. Extract the data needed by the KBS to control and/or automate the data analysis.
2. Send the data to the KBS and receive results from the KBS.
3. Read the results from the KBS and perform the steps proposed by the system.

At present an interface is going to be developed for the MarkIII/IV data analysis software package SOLVE. Figure 1 shows the dataflow between SOLVE and the KBS, when the latter is used to control or automate the data analysis in SOLVE, i.e. in *Interactive* or *Automatic Mode*. When applying the KBS in *Diagnosis* or *Tutorial Mode* the control switches over to the KBS in order to be able to investigate problems or to get help in the data analysis procedure. The KBS is called IADA: *Intelligent Assistant for Data Analysis in VLBI.*

When the user invokes SOLVE to analyze geodetic VLBI observations the program OPTIN starts and displays the main SOLVE menu. In order to use IADA for the data analysis, the user calls the program IADAO to specify that point of the data analysis where to start and in which mode the KBS shall be used. Then program INTF can be launched.

INTF extracts the data and informations needed by IADA from the *scratch files* which contain all the informations about the current status of the data analysis of an experiment. The data are extracted with respect to the *Step* and *Substep* of the analysis and written into a data file. This file is read by IADA and depending on *Mode*, *Step* and *Substep* of the data analysis the data within this file are investigated. The results are written into a result file which is read by program INTF. The results are processed by INTF, the data in the *scratch files* are updated and the data analysis continues depending on the *Mode* of IADA. In *Interactive Mode*, control switches back to program IADAO and the user is able to perform another step of the data analysis with IADA or to go back to OPTIN. In *Automatic Mode* the next *Substep* of the data analysis with respect to the *Concept* in table 2 will be chosen and program INTF starts again.

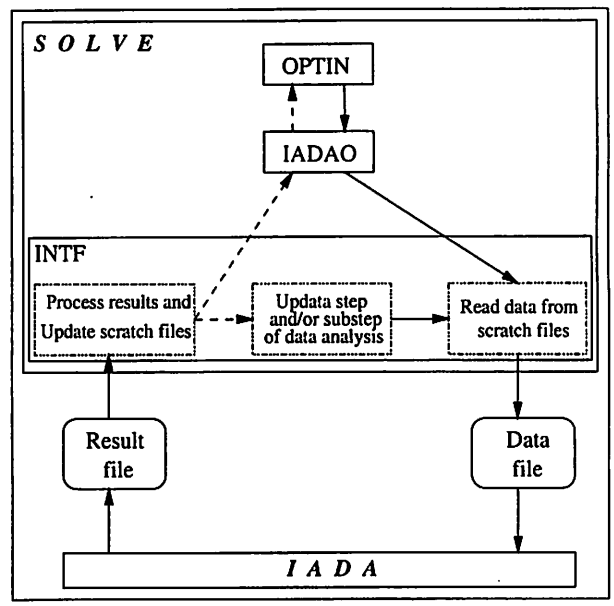

Figure 1: INTF *- the interface between* SOLVE *and* IADA.

4 Examples

An example for the application of IADA in *Interactive Mode* is given in figure 2. The *Analysis Step* is `Initial Solution` and the *Substep* is `A priori clock`. This *Step* is carried out when the experiment is analyzed the first time. Its purposes are equivalent to the associated *Substeps* in table 2: set a priori clock models if necessary (substep `A priori clock`), resolve group delay ambiguities (`Ambiguity solution`) and check for clock breaks and remove very large outliers (`Inspect Residuals`).

At first the interface collects the data needed by the KBS to check if the parameterization is correct for this *Substep* and if the results match the *Evaluation Criteria* (cf. table 3). In this example the parameterization is correct but an a priori clock model has to be applied for one of the stations. The user decides whether to apply the changes proposed by IADA automatically; then he can continue with the next step of the data analysis or go back to OPTIN. In *Automatic Mode* the changes are going to be applied automatically and INTF proceeds with the next *Substep* of the data analysis. User interaction is only necessary if problems occur that cannot be resolved automatically.

```
SOLVE
Interface SOLVE-IADA (INTF):
---------------------------

Mode: Interactive  Step: InitialSolution  Status: AprioriClock

=====================================================================

1. Collecting information for IADA...

 - Checking for applied a priori clock models...
   -> No a priori clock models are applied!
 - Running least squares solution in order to determine
   values of clock offsets and rates...
   -> Least squares solution has been made.
 - Information for IADA is going to be extracted...

2. Waiting for results of IADA...

3. Reading results of IADA...

   - Parameterization is OK!

   The following changes are proposed by IADA:

   - Applying a priori clock model for station: TIGOWTZL

   Do you want me to do it? (Y/N) > Y

Hit 0 to return to optin or C to continue with next step > C
```

Figure 2: Using IADA *in interactive mode.*

The KBS can be called in *Diagnosis Mode* to investigate problems or look at the results of the data analysis. In this case control switches over from SOLVE to IADA and depending on the current *Step/Substep* of the data analysis several default options are presented. Figure 3 shows these options for step `Intermediary Solution` and substep `Check Solution`. The user is able to check the results of the data analysis (option 1) by comparing it to the evaluation criteria for this substep (cf. table 3). According to the methods for problem handling in the *Status Description* of this substep further options are listed to investigate the reason why the check of the solution failed. Figure 4 shows the results of an overall check of the results of this substep. Because the results are considered being 'poor' the system checks whether there are wrong calibrations or parameterization and whether the clock breaks were selected correctly. The result of the diagnosis is a possible clock break at one station. This has to be examined by looking at the residuals' plots of the particular station.

```
IADA
DIAGNOSIS MENU:
---------------

Step  : INTERMEDIARYSOLUTION                    Substep: CHECKSOLUTION
=====================================================================

1. Check solution              4. Check for clock breaks

2. Check calibrations          5. Do all

3. Check parameterization      6. User input.

                               7. Exit

---> 
```

Figure 3: IADA *in diagnosis mode.*

```
IADA
DIAGNOSIS PROCESS MENU
----------------------

Step  : INTERMEDIARYSOLUTION                    Substep: CHECKSOLUTION
=====================================================================

Results of Option 5 - Do all:

  - Checking solution:
    Total wrms:              120.2 psec
    Observations in Solution: 96.17%
    => Intermediary solution is considered POOR.

  - Check calibrations
    --> Calibrations settings are ok.
  - Check parameterization
    --> Parameterization is ok.
  - Check for clock breaks by examining the residuals:
    --> There may be a clock break for station CRIMEA!
        Check it by looking at the residuals plot of this station!
-----
1. Explain
2. Return to DIAGNOSIS MENU
---> 
```

Figure 4: Results of option 5 in figure 3.

5 Conclusions

The application of knowledge-based techniques for the automation of the VLBI data analysis yields many benefits because they allow an explicit modelling of the multifaceted knowledge needed for these tasks. Thus, the knowledge of several analysts can be conserved and applied by the KBS to automate considerable parts of the data analysis. The very general *Concept* of the KBS allows to adapt the system to different VLBI software packages without modifying the Knowledge Base of the KBS. The interface between the VLBI data analysis software package SOLVE and IADA allows to exchange data and information between these two systems to control and/or to automate by the KBS the regular analysis done in SOLVE.

Acknowledgements

The concept for the KBS has been developed at DGFI, Munich, within a research project called 'Applications of Methods of AI for the VLBI Data Analysis'. This project was supported by the Deutsche Forschungsgemeinschaft (DFG), project Schu 1103/2-1. The author is currently supported by the European Union within the TMR programme under contract FMRX-CT960071.

References

[1] Koyama, Y., Kurihara, N., Kondo, T., Sekido, M., Takahashi, Y., Kiuchi, H. and Heki, K., Automated Geodetic Very Long Baseline Interferometry Observation and Data Analysis System, *Earth Planets Space*, **50**, 109–722, 1998.

[2] Petrov, L., User's Guide to Interactive SOLVE, *http : //gemini.gsfc.nasa.gov/solve_root/solve_help/solve_guide_01.html*, May 2000.

[3] Ryan, J. W., Ma, C. and Vandenberg, N. R., The Mark III VLBI Data Analysis System, NASA Goddard Space Flight Center, publication X-945-80-25, 1980.

[4] Schnupp, P., Huu, C. T. N. and Bernhard, L. W., *Expert Systems Lab Course*, Springer-Verlag, Berlin/Heidelberg, 1989.

[5] Schuh, H. and Schwegmann, W., A Vision Towards Automated Real-Time VLBI, *Accepted by Physics and Chemistry of the Earth*, 2000.

[6] Schwegmann, W. and Schuh, H., On the Automation of the Mark III VLBI Data Analysis System, in Proceedings of the 13^{th} Working Meeting on European VLBI for Geodesy and Astrometry, held at Viechtach, February 12-13, 1999, edited by W. Schlüter and H. Hase, Bundesamt für Kartographie und Geodäsie, Wettzell, 1999.

[7] Sundermeyer, K., Knowledge-Based Systems: terminology and references, BI-Wissenschaftsverlag, Mannheim/Wien/Zürich, 1991.

Integrating GPS zenith path-delay measurements into VLBI analysis of geodetic observations with the European network

By María J. Rioja[1,2], Paolo Tomasi[1,3], Pierguido Sarti[4] and Miguel A. Pérez-Torres[1]

[1]Istituto di Radioastronomia, Bologna, Italy

[2]Observatorio Astronómico Nacional, Alcalá, Spain

[3]Istituto di Tecnologia Informatica Spaziale CNR, Italy

[4]Universita di Bologna, Distart, Bologna, Italy

The aim of this work is to contribute to the effort of increasing the accuracy of VLBI geodetic parameters. We are investigating a route to disentangle the coupling between the values of the vertical coordinates and the tropospheric contributions at each site, estimated from the VLBI analysis. We present results from a novel route of analysis which implements external GPS tropospheric estimates, computed every hour, in the VLBI analysis using the CALC/SOLVE package. Our working database consists of the six European VLBI geodetic observations from 1998. We have performed repeatability tests using both standard VLBI analysis and introducing GPS tropospheric estimates. The results are very encouraging and justify a deeper investigation of the potential of a route of analysis combining the products from both geodetic techniques. Also, astronomical observations at millimeter wavelengths, with coherence times as short as a few tens of seconds, would benefit from a better modeling of the wet component of the troposphere, allowing longer integration times.

1. Introduction

The radio signals observed with telescopes at the Earth are affected by the propagation medium, mainly the ionosphere and the troposphere. Since simultaneous observations at 8.4 and 2.3 GHz are carried out in geodetic VLBI, the ionosphere contribution is exactly corrected. Unfortunately, variations in the distribution of the water vapor content in the troposphere (hereafter wet component) are one of the main error sources in the geodetic measurements with VLBI. A common way to correct for the extra path delay due to the wet component of the troposphere is to assume a horizontally stratified atmosphere to estimate the equivalent zenith wet delay from the data themselves using mapping functions to estimate values at appropriate elevation angles. However, given the close functional dependence of the tropospheric and geometric contributions in the mathematical formulation of the group delay, errors in the tropospheric modeling will corrupt the least squares adjustment of the vertical component of the site position. We intend to contribute to the effort of investigating the potential of new routes of analysis to increase the accuracy of the VLBI geodetic parameters. In particular we have tried to combine the products from two different geodetic techniques, namely GPS and VLBI.

The observational strategy used in VLBI to sample the atmosphere consists of a rapid switching of the antenna between radio sources in different directions to cover the whole sky, including low elevation angles. Instead, a GPS antenna collects the radio signals arriving **simultaneously** from the observations of a number of satellites from different directions. In principle, the latter observational configuration would be more favorable to estimate unknown spatial and temporal irregularities of the wet component in the

troposphere. For sites with both GPS and VLBI antennas, one could use the GPS tropospheric estimates in the analysis of the VLBI observations. Other authors have made attempts in that direction with no conclusive results (Carlsson et al. 1995).

2. Data Analysis and Results

Our working data set are the series of six EUROPE campaigns of VLBI observations in 1998, 24-hour long each and separated by ca. 2 months. The number of participating antennas per epoch ranges from 7 to 9, and at all epochs more than half of the sites had simultaneous GPS tropospheric estimates from the analysis of IGS data from Berna University (Markus Rothacher, priv. comm.) The VLBI experiments were processed with the least squares estimation program SOLVE. We have performed parallel analyses using two different approaches to account for the wet delay: 1) in the so called *standard route*, the wet zenith path delays at all sites were estimated from the data themselves, using continuous piecewise linear functions in segments of 60 minutes; 2) in the novel route, *hybrid route* from now on, we took GPS tropospheric estimates from simultaneous observations, wherever available, and fed them into the VLBI analysis without any further adjustment.

The strong coupling between errors in the tropospheric modeling and inaccurate estimates of the vertical components follows from the close functional dependence of the tropospheric and the geometric (in particular, the vertical component of the position of the VLBI sites) contributions in the mathematical formulation of the interferometric delay. Any elevation dependent error (such as errors in modeling the tropospheric path delay) in the group delay model that correlates with the sine of the elevation, will corrupt the least squares adjustment of the vertical component of the site position. In addition, an error introduced into the estimate of the vertical component of the position of either site (Δr) introduces a corresponding error in the estimate of the length of the baselines between the sites (ΔD):

$$\Delta D \approx \frac{D}{2r_e}\Delta r \tag{1}$$

where D is the baseline length and r_e is the radius of the Earth.

Hence longer baselines are more sensitive to errors in the vertical components of any or both of the stations that form it. A first and simple diagnosis tool to make a comparison between the results from both routes of analysis is to compare the slopes of the linear fits to plots with the baseline length errors as a function of the baseline length.

Figure 1 shows the difference between wet zenith delay estimates with GPS and VLBI versus time at Onsala, for 5 observing epochs. For all stations the agreement between the estimates from both techniques looks good, with correlation coefficients close to 1. However, there is an offset of several millimeters, which changes from site to site and between epochs. The same effect has also been found by other authors in different data sets (Carlsson et al. 1995). No doubt, the existing offset is partially due to the height difference between the GPS and VLBI antennas. A rough estimate of the contribution to the observed delay from an extra layer of troposphere 10 meters long, is ca. 10 picoseconds or 3 millimeters. This is very close to the differences shown in Figure 1 for Onsala, and for other sites.

We computed the baseline length repeatabilities from the analysis of the 6 experiments in 1998, and used them to quantify the errors in the baseline length estimates. Figure

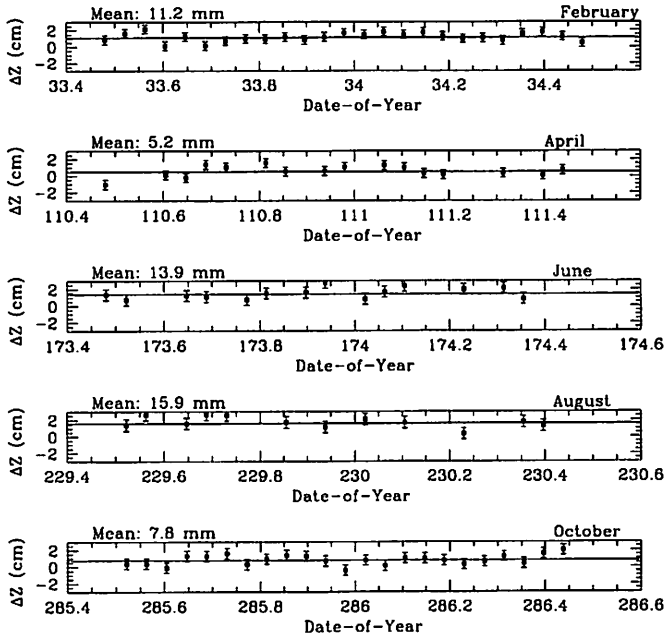

FIGURE 1. Differences between the estimated tropospheric wet zenith delays for the Onsala site from GPS and VLBI, as a function of time, at 5 epochs of observations in 1998.

2 displays the baseline length errors (baseline repeatabilities) as a function of baseline length for all participating sites, using the two different methods to correct the wet zenith path delay. The best fit of a straight line to the estimates from the *standard route* is $1.80 + 0.64 \times 10^{-9}D$; for the second type of VLBI solution, with GPS tropospheric estimates, the best fit of a straight line is $1.80 + 0.37 \times 10^{-9}D$. The rms residual from both fits is 1.4mm. The comparison of the slopes of the best fits to the results from both analysis shows an improvement in the overall performance of the VLBI solution using the *hybrid route* (see formula 1).

3. Results and Conclusions

We can summarize the current status of the project as follows:

- We have established a working interface that integrates external tropospheric data in the analysis of VLBI observations with SOLVE.
- We confirm the evidence found by other authors too, that the inferred wet delay contributions estimated from GPS and VLBI exhibit similar short term variations but with an apparent long term bias.
- Our results from repeatability tests indicate a promising perspective for the combination of both geodetic techniques. Figure 1 shows an overall improvement of the network in the VLBI solution using the *hybrid route* of analysis, which implements external GPS tropospheric estimates into the VLBI analysis, as an alternative option to the auto-calibration from the VLBI data themselves.

This is a report from a work which is still in progress. The results shown in that contribution are very encouraging to investigate further in detail the potential of this new route of analysis. We are currently investigating the effects of decreasing the solution

interval of GPS tropospheric estimates, testing new strategies in the analysis, and trying to understand the meaning of the bias between tropospheric estimates.

Astronomical observations with VLBI would also benefit from an improved modeling of the troposphere using GPS estimates in the analysis. Phase reference and astrometric observations are becoming nearly standard at centimeter wavelengths, and a detailed modeling of the atmospheric contribution would help to increase the angular separation across which the phase connection is possible. Certainly, if GPS could provide tropospheric estimates every few minutes, or at even shorter time intervals, this would be of great relevance for millimeter astronomy, since it would significantly increase the coherence time for VLBI observations. The short coherence time, of the order of some tens of seconds at most, limited by unknown fluctuations in the wet component of the troposphere, sets a main constraint in the sources reachable at millimeter wavelengths with VLBI.

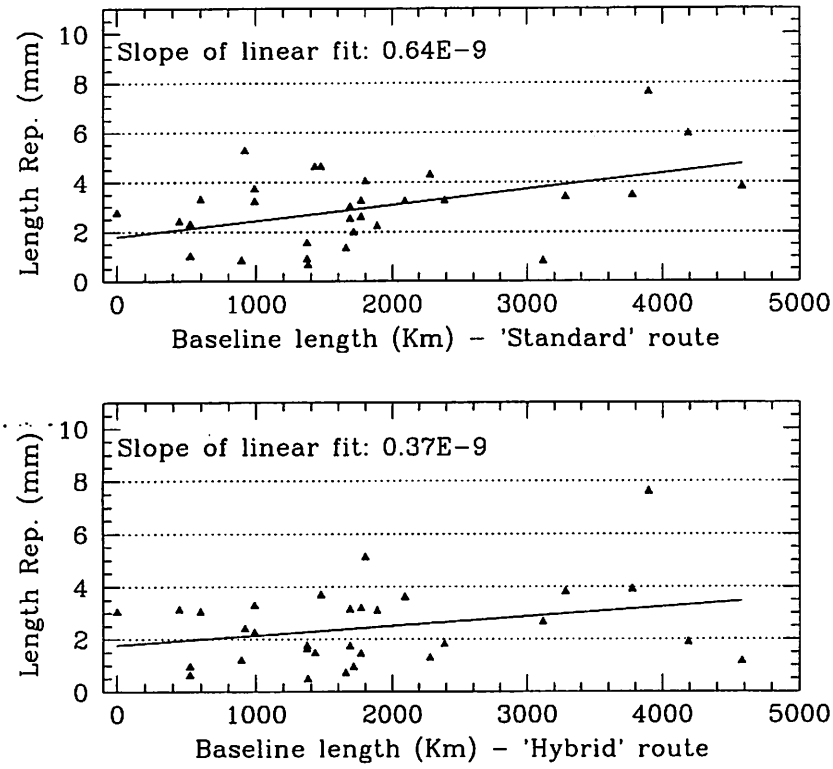

FIGURE 2. Baseline length repeatability as a function of baseline length, computed with the estimates from the *standard route* (*Upper plot*), and the hybrid route (*Lower plot*) which combines VLBI and GPS products. The slopes of the best fit of straight lines are indicated in each plot. The slope is proportional to the magnitude of elevation dependent errors in the analysis.

REFERENCES

CARLSSON, T.R., ELGERED, G., & JOHANSSON, J.M. 1995 *Proc. 10th Working Meeting on European VLBI for Geodesy and Astrometry*, p. 148.

ZWDs from VLBI, GPS, and NWP Models

Dirk Behrend[a], Rüdiger Haas[b], Lídia Cucurull[a], and Jordi Vilà[c]

[a]Institut d'Estudis Espacials de Catalunya, CSIC Research Unit, Gran Capità 2-4, 08034 Barcelona, Spain
[b]Onsala Space Observatory, Chalmers University of Technology, SE-439 92 Onsala, Sweden
[c]Department of Meteorology and Air Quality, Wageningen University, 6701 AP Wageningen, The Netherlands

Abstract

Humidity plays a crucial role in atmospheric processes over a wide range of scales in space and time. The amount of humidity integrated along the signal path of VLBI or GPS measurements is nearly proportional to the signal delay caused by the presence of the water vapour. In geodesy this tropospheric delay constitutes a nuisance parameter that needs to be removed for a precise position determination. In meteorology, on the other hand, information on the humidity distribution and its variation is used for improving numerical weather prediction (NWP) models with the improvement strongly depending on the knowledge of the statistical characteristics of the respective parameters. Thus, an inter-comparison study of zenith wet delay (ZWD) values is presented. For the station Robledo de Chavela (Madrid) we compare ZWDs derived from geodetic space techniques (GPS and VLBI) with ZWDs retrieved from NWP models (the non-hydrostatic MM5 and the hydrostatic HIRLAM model). The results of the different techniques agree to the sub-centimetre level with correlation values of 0.87 (GPS vs. MM5), 0.81 (GPS vs. HIRLAM), and 0.84 (MM5 vs. HIRLAM). The correlation VLBI vs. MM5 of 0.78 is based on a short VLBI time series and should be considered preliminary. Further studies with longer time series are necessary to confirm this value. The bias and RMS difference values are all contained in the margin provided by the internal errors.

1 Introduction

A primary task of algorithms of geodetic space techniques (such as the Global Positioning System [GPS] and Very Long Baseline Interferometry [VLBI]) is to calibrate the delay or "equivalent excess path length" introduced by the refractivity of the Earth's atmosphere (Businger *et al.*, 1996). Unlike the retardation of the signal in the dispersive ionosphere, the delay caused by the electrically neutral atmosphere (troposphere) cannot be removed by using measurements on two frequencies. Hence, the tropospheric delay is either estimated from the GPS or VLBI data as part of the overall least squares inversion (Businger *et al.*, 1996) or the tropospheric parameters are injected from independent sources (e.g., Rioja and Tomasi, 1999; Elgered *et al.*, 1991).

GPS appears to have an advantage over VLBI in modelling atmospheric parameters, as it employs omni-directional antennas facilitating a complete sky scan in a short period of time. VLBI, on the other hand, uses directional antennas that scan a specific radio source for a limited time, usually between 90 and 180 s, before they are steered to the next source. In this way also the entire sky is covered, but sequentially and in a much longer time span. However, VLBI has the benefit of not being contaminated by satellite orbit errors that propagate into the estimated parameters.

Unlike geodesy, where the tropospheric delays are considered nuisance parameters or even noise, in meteorology they constitute one of the key variables. Instead of using tropospheric parameters as input parameters, it is also possible to retrieve them from numerical weather prediction (NWP) models. Such models (e.g. MM5 and HIRLAM) are run operationally at national or international weather services and make use of physical models (governing equations), initial atmospheric conditions, and observations (e.g. radiosonde profiles, ground meteorological data) for predicting variables such as temperature, pressure, and humidity (Behrend *et al.*, 2000). The interest is usually focused on forecast rather than nowcast or hindcast.

The inter-comparison of zenith wet delays (ZWDs) resp. precipitable water (PW) derived from different techniques and models provides basic information on the inherent error budget. In previous studies sets of pairs of the aforementioned methods have been analysed with some recent examples being: GPS vs. VLBI (Haas *et al.*, 1999; Behrend *et al.*, 1999), GPS vs. HIRLAM (Yang *et al.*, 1999; Cucurull *et al.*, 2000), and GPS

vs. MM5 (Cucurull and Vandenberghe, 1999). Here we present an inter-comparison of all three techniques (VLBI, GPS, and NWP models) including a comparison between VLBI and MM5 (a non-hydrostatic NWP model). The analysis is limited to investigating the temporal behaviour of the ZWD for the site Robledo de Chavela (Madrid) where VLBI and GPS are collocated.

2 Data Description and Analysis

2.1 GPS Data

In December 1996 (Dec. 3-15) GPS data in a network of 5 stations were acquired in the Madrid Sierra, Spain, employing Trimble 4000SSE GPS receivers. Fig. 1 shows the geographical location of the sites involved in this experiment. The intersite separations are between 5 km and 50 km. The observations consisted of data streams—from 6 to 8 satellites—of undifferenced dual-frequency carrier-phase and pseudo-range measurements taken at a sampling rate of 30 s (Elósegui *et al.*, 1998).

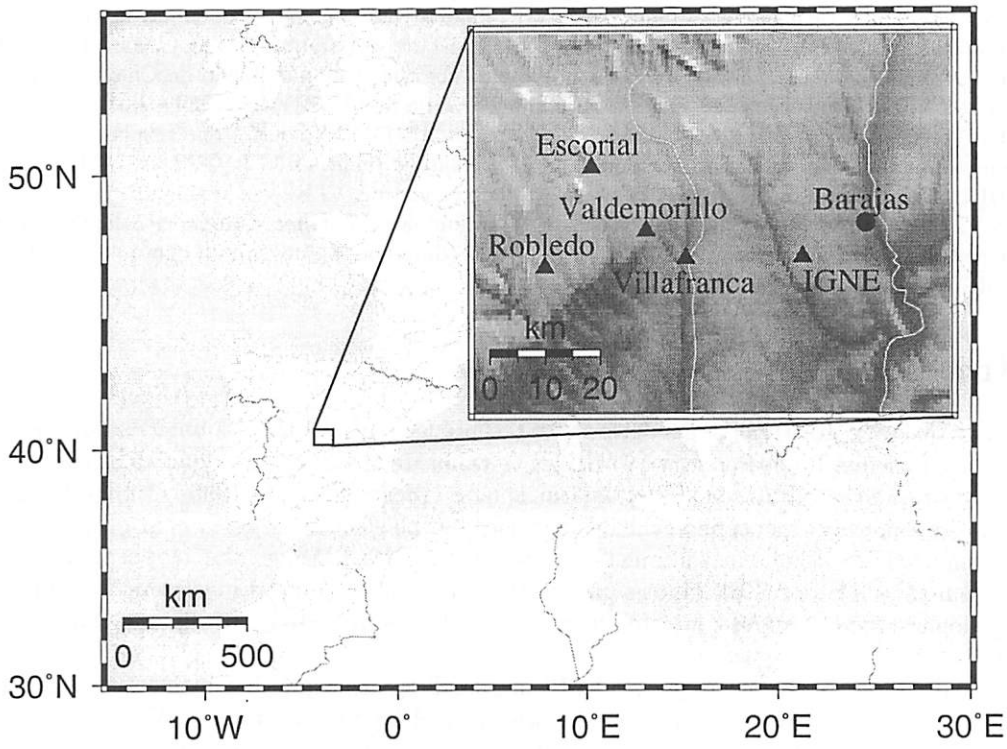

Figure 1: Sites of the December 1996 GPS campaign in the Madrid Siera. The GPS sites are shown as triangles. Barajas is the airport of Madrid. IGNE is the Spanish National Geographic Institute located close to the center of Madrid.

We used the GIPSY/OASIS-II (v.4) software package (Webb and Zumberge, 1993) with a *point positioning strategy* to estimate zenith wet delays (ZWD) at the GPS sites with a precision of 5 mm (Elósegui *et al.*, 1998). The necessary estimates of the satellite clock corrections and orbits as well as consistent earth-rotation parameters were provided by the IGS (International GPS Service for Geodynamics) and JPL (Jet Propulsion Laboratory). The tropospheric delay was modelled as a *random walk* ($\sigma^2 = d^2 \cdot t$) with a drift rate of $d = 2.5$ mm/$\sqrt{\text{h}}$. The drift rate for the gradient parameters was 0.3 mm/$\sqrt{\text{h}}$. We used a cut-off elevation angle of 7° and an estimation interval of 30 min. For comparison purposes later on, an additional data set was created by averaging the 30 min time series to 3 hour values. In this study we merely utilize the data for the station Robledo de Chavela, as it is collocated to a VLBI station.

The zenith wet delay ΔL_w^z is obtained from the total delay ΔL^z through subtracting the hydrostatic part ΔL_h^z:

$$\Delta L^z = \Delta L_h^z + \Delta L_w^z \,. \tag{1}$$

The hydrostatic delay ΔL_h^z can be estimated well from surface pressure measurements: an error of 0.4 hPa in pressure causes a delay error of less than 1 mm (Elgered *et al.*, 1991). For the station Robledo pressure data were available from the station meteorological package with a precision of 0.3 hPa.

2.2 VLBI Data

On December 6, 1996, the European geodetic VLBI experiment EUROPE 6/96 was performed at the Madrid Deep Space Communications Complex (MDSCC) using the DSS65 34 m antenna. The nominal observation time of a EUROPE experiment is 24 hours. Unfortunately, Madrid was scheduled only for the second half of this specific experiment due to other commitments leaving an actual observation period of 12 hours. This period was further reduced to 9.5 hours due to bad data at the beginning of the experiment that had to be edited out. Thus, EUROPE 6/96 can be considered an uncommon experiment with an unusually short time series. But as there are no other geodetic VLBI sessions at Madrid in the first two weeks of December 1996, it constitutes the only information source available. However, the data are still useful to derive indicative if not significant results.

The VLBI data were analysed using the SOLVE software (Ma *et al.*, 1990). The positions of the radio sources and the station coordinates have been taken from a recent global VLBI solution. Clock parameters were estimated hourly with respect to a reference clock of the European VLBI network. ZWDs as well as horizontal delay gradients were determined using the *piecewise linear constrained approach.* The estimation interval was chosen to 30 min for wet delays and 3 hours for gradients. For the upper bound constraints 15 mm/$\sqrt{\text{h}}$ for the wet delays and 0.82 mm/$\sqrt{\text{h}}$ for the gradients were taken. The precision (standard deviation) of the ZWD values is in the range of 15 to 20 ps which translates to 4...8 mm in terms of length units.

2.3 MM5 Data

For the same region and time as the GPS campaign a numerical simulation using the non-hydrostatic Mesoscale Model (MM5) was performed. We set up three (2-way nested) domains with a resolution ranging from 45 km down to 5 km. Gridded precipitable water (PW) values were simulated in the finest domain. The grid values were calculated by integrating the specific humidity in the vertical, in this case over 23 vertical layers. In order to estimate point values for the VLBI and GPS sites (in the horizontal) the grid values were bilinearly interpolated from the four closest grid points. The individual PW values were averaged over 30 min intervals to obtain values that are coherently comparable with the GPS and VLBI results. The precision of the PW is about 2 mm (Cucurull and Vandenberghe, 1999). As was done with the GPS data, the 30 min time series was averaged to 3 hour values in order to create an additional data set for comparison purposes.

The PW were then converted to ZWD values. The functional relationship between ΔL_w^z and PW can be formulated as follows (Tregoning *et al.*, 1998):

$$PW = \Pi(T_m, \varrho_v)\, \Delta L_w^z \tag{2}$$

with

$$\Pi = \frac{10^6}{\varrho_v R_v \left[(k_3/T_m) + k_2'\right]} \,. \tag{3}$$

ϱ_v is the density of liquid water ($\varrho_v = 0.998205$ kg dm^{-3}), R_v is the specific gas constant for water vapour ($R_v = 461.5$ J kg^{-1} K^{-1}), T_m is the mean temperature of the atmosphere, k_3 and k_2' are physical constants ($k_3 = 3.776 \cdot 10^5$ K^2 hPa^{-1}; $k_2' = 17$ K hPa^{-1}). For the location and time under investigation the dimensionless conversion factor was chosen to $\Pi \approx 0.15$ (Emardson and Derks, 1999).

2.4 HIRLAM Data

The HIRLAM (HIgh Resolution Limited Area Modelling) short-range NWP model is a complete analysis and forecast system. It is a regional system jointly developed by the weather services in the Nordic countries, Holland, Ireland and Spain (Yang *et al.*, 1999). As the operational model of the Spanish Weather Service (INM) it is routinely run with two horizontal resolutions, 0.5° × 0.5° and 0.2° × 0.2°, and 31 vertical levels. The forecast model is hydrostatic with Eulerian grid-point numbers and provides time series of 3 hours. The accuracy of HIRLAM's predictions of pressure fields is better than 1.5 hPa, and of the order of 15 mm for ZWD (Cucurull *et al.*, 2000).

For obtaining ZWDs two different approaches were followed: (1) calculation of PW by integrating the specific humidity in the vertical followed by the conversion of the PW to ZWD like in the MM5 case; (2) generation of refractivity profiles from HIRLAM's temperature, pressure, and humidity profiles followed by integration of the refractivity along the zenith direction yielding directly ZWD. The difference between the two procedures is negligible (less than 0.5 mm in PW) which may be considered a verification of the chosen conversion factor Π. To estimate point values for the VLBI and GPS sites again bilinear interpolation from the four closest grid points was used. A thorough description of the HIRLAM analysis is given in Cucurull *et al.* (2000).

3 Comparison and Results

The formal errors of the four techniques have already been mentioned in section 2. For convenience, Table 1 provides a compilation of these errors. The measurement techniques provide ZWDs two to three times higher in precision than the retrievals from the NWP models. As any observation with a smaller error adds information to the model, PW or ZWD values from GPS or VLBI may be used for improving the NWP models in a data assimilation context (see also Cucurull *et al.*, 2000).

Table 1: Precision of ZWD and PW derived from geodetic space techniques (GPS, VLBI) and NWP models (MM5, HIRLAM).

Method	ZWD	PW
GPS	~ 5 mm	~ 1 mm
VLBI	~ 4...8 mm	~ 1...2 mm
MM5	~ 15 mm	~ 2 mm
HIRLAM	~ 15 mm	~ 2 mm

Fig. 2 shows the time series of the ZWD values of the station Robledo de Chavela for the period 3-15 Dec. 1996 and a blow-up of the series around the VLBI experiment. The variation of the ZWD between 30 mm and 160 mm can mainly be attributed to the passage of two frontal systems (December 4–5 and 12–14). These winter frontal systems are identifiable by initial increases in the atmospheric moisture followed by decreases after the passage of the front. The rapid increase on day 5 could be associated with fluctuations in the water vapour fields due to the passage of the first front. The agreement between the independent ZWD profiles is reasonably well and shall be quantified by computation of correlation as well as bias and RMS difference values between sets of pairs of the involved techniques (correlation analysis). From the blow-up (right panel in Figure 2 one may conclude that the GPS time series contains high frequency variations of the humidity field which are not resolvable with a model of limited spatial or temporal resolution (e.g., Yang *et al.*, 1999). One has to bear in mind that the backbone of operational NWP models are radiosonde measurements that have a limited spatial and temporal coverage. The larger variation of the VLBI data may be attributed to inhomogeneous or incomplete sky coverage with radio sources during the observation.

The results of the correlation analysis are summarized in Table 2 and are depicted in the scatter plots of Fig. 3 to 6. The GPS vs. MM5 comparison was done with two time resolutions (30 min and 3 h) and two lengths for the time series (2 weeks and 9.5 h). Lowering the time resolution from 30 min to 3 h has no significant effect, as correlation, bias, and RMS difference stay almost the same. In contrast to this,

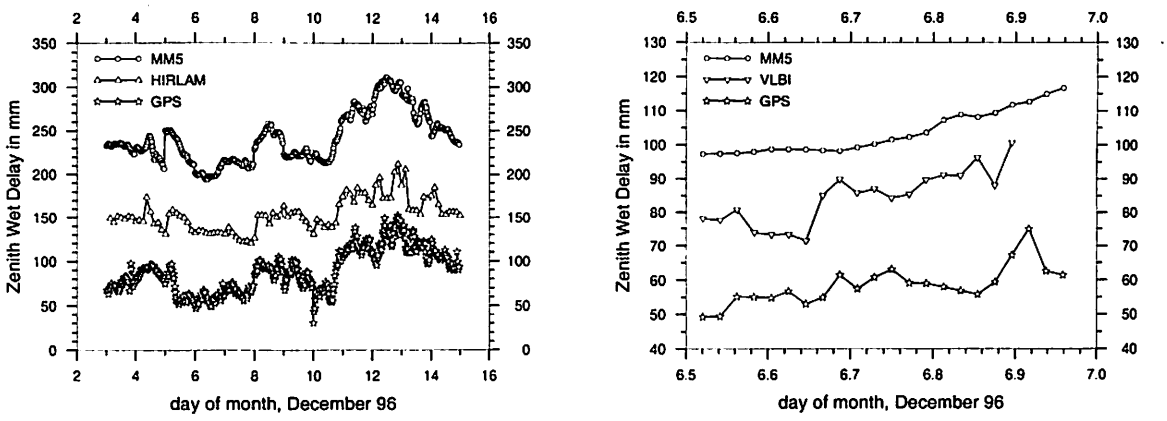

Figure 2: Time series of ZWD values at Robledo de Chavela. *Left panel:* MM5, HIRLAM and GPS for the two weeks of the GPS campaign (MM5 and HIRLAM offset by 150 mm resp. 75 mm for mapping purposes). *Right panel:* MM5, VLBI and GPS for the length of the VLBI experiment (MM5 and VLBI offset by 50 mm resp. 25 mm for mapping purposes).

the confinement of the time span to the length of the VLBI experiment (9.5 h) causes a decrease of the RMS difference value (as was to be expected due to the lesser number of input values), a reduction of the correlation coefficient, and a change of the bias value from 2.23 mm to −5.31 mm. The latter may be attributed to the fact that the bias between GPS and MM5 is not constant, but depends on the degree of moisture: MM5 overestimates the water vapour content for high moisture values and underestimates it for low moisture values (see Fig. 3 and 4).

Table 2: Comparison of GPS, VLBI, MM5, and HIRLAM derived ZWD values. Unit of bias and RMS difference: mm.

Meth. 1	Meth. 2	#points	Resolution	Correlation	Bias	RMS diff.
GPS	MM5	564	30 min	0.874	2.23	14.09
GPS	MM5	95	3 h	0.864	2.38	14.48
GPS	MM5	19	30 min	0.550	−5.31	4.23
GPS	HIRLAM	95	3 h	0.812	−9.97	14.40
VLBI	MM5	19	30 min	0.781	−7.52	5.20
VLBI	GPS	19	30 min	0.654	−2.21	6.10
MM5	HIRLAM	95	3 h	0.835	−12.35	16.51

The time series of the VLBI data is too short in order to give significant results regarding systematic errors of VLBI with respect to the other methods. But since the VLBI vs. GPS comparisons obtained with the short data set (cf. Table 2) agree reasonably well with results reported in Haas *et al.* (1999), Gradinarsky *et al.* (1999), Behrend *et al.* (1999), and Gradinarsky *et al.* (2000), the comparison results may at least be considered indicative. The VLBI experiment was run in a period of low moisture during which MM5 tends to underestimate the ZWDs (see above). When comparing the VLBI-derived with the MM5-derived ZWD values (Table 2 and Fig. 4) the RMS difference is slightly higher than in the GPS vs. MM5 case. This holds true also for the bias values, where the increase is equal to the bias VLBI vs. GPS. The correlation value of 0.78 is significantly higher than the GPS vs. MM5 one (short time series) suggesting a better agreement between VLBI and MM5 than between GPS and MM5 for this special case. With sufficiently long time series (e.g. two weeks) correlation values on the order of the GPS vs. MM5 results may be expected. This is to be verified by further studies using more data material, but the initial results are promising.

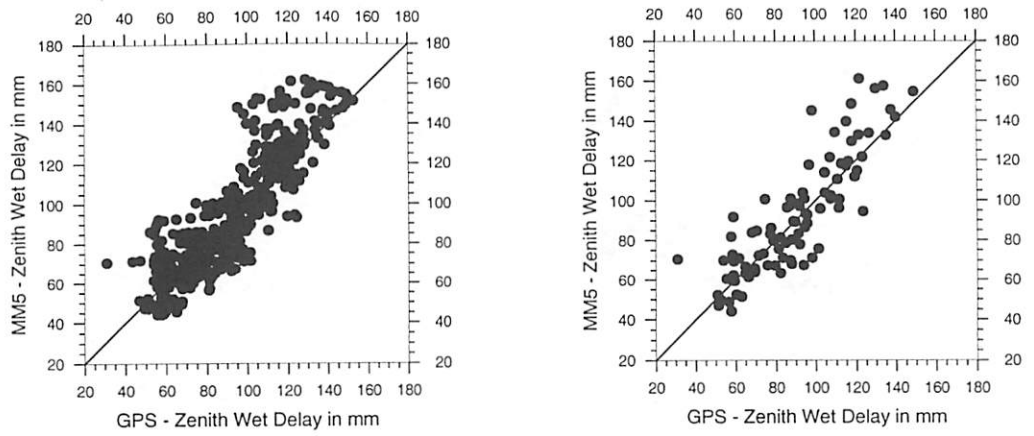

Figure 3: Scatter plots of ZWD values. *Left panel:* GPS vs. MM5. Time span: Dec. 3-15, 1996. Sampling rate: 30 min. *Right panel:* GPS vs. MM5. Time span: Dec. 3-15, 1996. Sampling rate: 3 h.

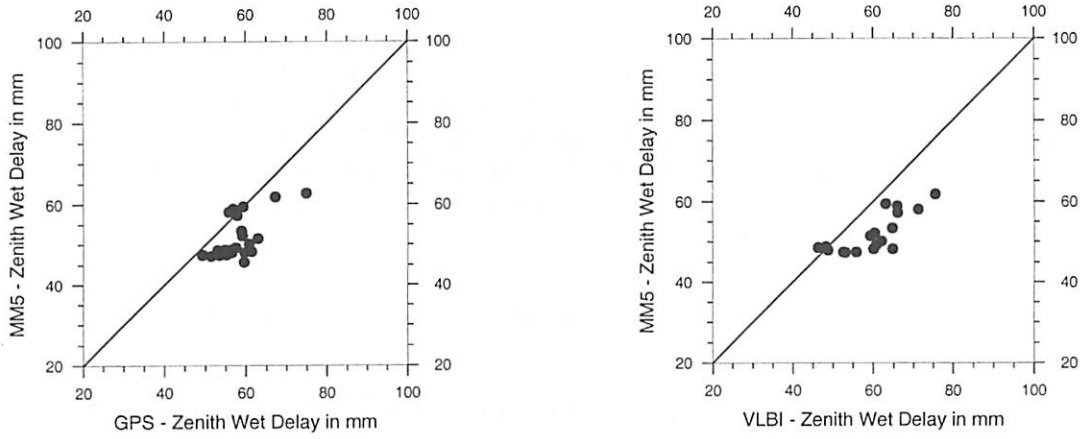

Figure 4: Scatter plots of ZWD values. *Left panel:* GPS vs. MM5. Time span: Dec. 6, 1996 (9.5 h). Sampling rate: 30 min. *Right panel:* VLBI vs. MM5. Time span: Dec. 6, 1996 (9.5 h). Sampling rate: 30 min.

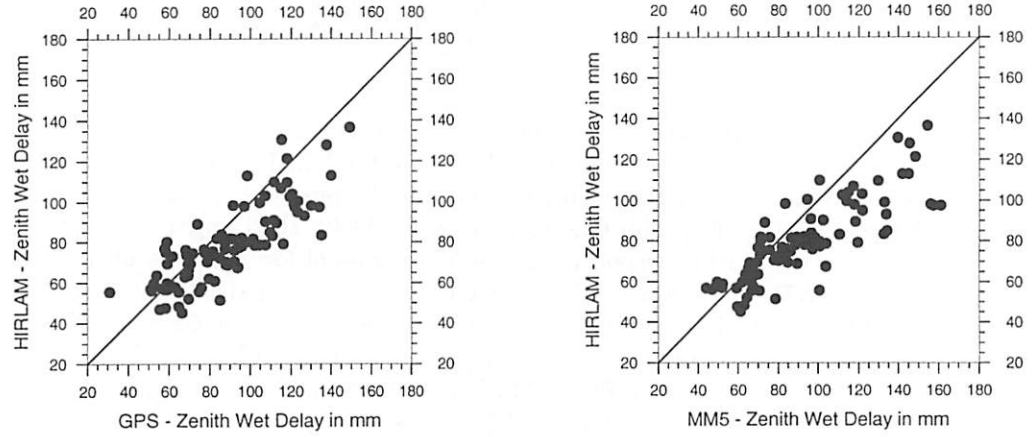

Figure 5: Scatter plots of ZWD values. *Left panel:* GPS vs. HIRLAM. Time span: Dec. 3-15, 1996. Sampling rate: 3 h. *Right panel:* MM5 vs. HIRLAM. Time span: Dec. 3-15, 1996. Sampling rate: 3 h.

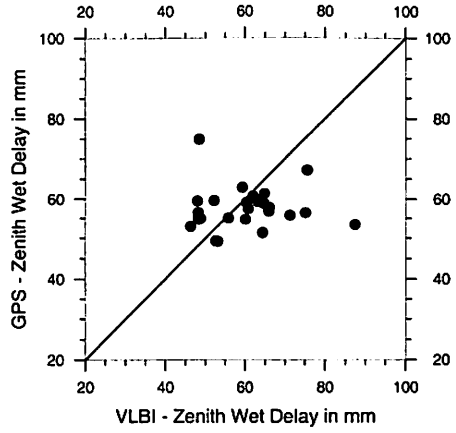

Figure 6: Scatter plot of ZWD values. VLBI vs. GPS. Time span: Dec. 6, 1996 (9.5 h). Sampling rate: 30 min.

As the HIRLAM-derived ZWDs are available at a sampling rate of 3 hours, the ZWDs are compared only with the GPS-derived and the MM5-derived ZWDs over the two weeks of the GPS campaign (cf. Table 2 and Fig. 5). The correlation values are in the 0.80...0.85 range. The biases are somewhat larger than the previous ones with values of about 10...12 mm (HIRLAM lower than GPS and MM5) indicating that HIRLAM underestimates the moisture content of the troposphere as compared to GPS and MM5. This corroborates the findings of Yang *et al.* (1999) who state that HIRLAM tends to underestimate when moisture becomes large. The RMS difference is around 15 mm corresponding to the error margin given by the formal errors of each technique (cf. Table 1).

4 Conclusions

We inter-compared ZWD values derived from GPS, VLBI, MM5, and HIRLAM data for the station Robledo de Chavela (Madrid), Spain. The results agree to the sub-centimetre level. The correlation values obtained from a time series of two weeks amount to 0.87 (GPS vs. MM5), 0.81 (GPS vs. HIRLAM), and 0.84 (MM5 vs. HIRLAM); the bias and RMS difference values fall within the error frames provided by the internal accuracies of the respective methods. The VLBI data employed in the comparison cover a time span of 9.5 hours, so that the comparison results should be considered indicative only. With a correlation value of 0.78 (VLBI vs. MM5) they, nevertheless, look promising.

The geodetic space techniques (VLBI and GPS) provide estimates of the ZWD at the 5 mm level, whereas the NWP models (MM5 and HIRLAM) give ZWD values with an accuracy of about 15 mm, i.e. the geodetic space techniques furnish ZWD estimates superior to the NWP-derived values by a factor of about 3. Thus, both VLBI and GPS can be employed to validate NWP models and may be utilized as additional information source for the models in a data assimilation context. Due to the favourable spatial distribution of GPS stations, the low operational costs (as compared to VLBI) and the near-real-time availability, GPS constitutes the obvious choice for improving NWP models. VLBI, on the other hand, lends itself to independent checks at selected sites. Furthermore, both GPS and VLBI can provide data for climate studies, as this meteorological application does not make demands related to timing.

Acknowledgments

Dirk Behrend and Rüdiger Haas are supported by the European Union within the TMR programme under contract FMRX-CT960071.

5 References

BEHREND, D., L. CUCURULL, J. VILÀ, and R. HAAS: An Inter-comparison Study to Estimate Zenith Wet Delays Using VLBI, GPS, and NWP Models. *Earth, Planets and Space*, in press, 2000.

BEHREND, D., A. RIUS, R. HAAS, L.P. GRADINARSKY, J.M. JOHANSSON, and S.J. KEIHM: Comparison of Independently Derived Atmospheric Parameters. *IUGG XXII General Assembly*, Birmingham, England, 1999.

BUSINGER, S., S.R. CHISWELL, M. BEVIS, J. DUAN, R.A. ANTHES, C. ROCKEN, R.H. WARE, M. EXNER, T. VANHOVE, and F.S. SOLHEIM: The Promise of GPS in Atmospheric Monitoring. *Bull. Amer. Meteor. Soc.*, **70(1)**, 5-18, 1996.

CUCURULL, L., B. NAVASCUES, G. RUFFINI, P. ELÓSEGUI, A. RIUS, and J. VILÀ: On the Use of GPS to Validate NWP Systems: the HIRLAM Model. *J. Atmos. and Ocean. Tech.*, **17(6)**, 773-787, 2000.

CUCURULL, L. and F. VANDENBERGHE: Comparison of PW Estimated from MM5 and GPS Data. *MM5 Workshop '99*, Boulder, Colorado, USA, 1999.

ELÓSEGUI, P., A. RIUS, J.L. DAVIS, G. RUFFINI, S.J. KEIHM, B. BÜRKI, and L.P. KRUSE: An Experiment for Estimation of the Spatial and Temporal Variations of Water Vapor Using GPS Data. *Phys. Chem. Earth*, **23(1)**, 125–130, 1998.

EMARDSON, T.R. and H.J.P. DERKS: On the Relation Between the Wet Delay and the Integrated Precipitable Water Vapor in the European Atmosphere. *Meteorol. Appl.*, **6**, 1–12, 1999.

ELGERED, G., J.L. DAVIS, T.A. HERRING, and I.I. SHAPIRO: Water Vapor Radiometry for Estimation of the Wet Delay. *J. Geophys. Res.*, **96**, 6541-6555, 1991.

GRADINARSKY, L.P., R. HAAS, J.M. JOHANSSON, and G. ELGERED: Comparison of Atmospheric Parameters Estimated from VLBI, GPS and Microwave Radiometer Data. *Proc. 13th Work. Meet. Europ. VLBI f. Geod. Astrom.*, 161–165, Viechtach, 1999.

GRADINARSKY, L.P., R. HAAS, G. ELGERED, and J.M. JOHANSSON: Simultaneous Observation of Atmospheric Parameters with Independent Collocated Space Geodetic and Remote Sensing Techniques at Onsala Space Observatory. *Earth Planets and Space*, in press, 2000.

HAAS, R., L.P. GRADINARSKY, J.M. JOHANSSON, and G. ELGERED: The Atmospheric Propagation Delay: A Common Error Source for Colocated Space Techniques of VLBI and GPS. *Proc. Int. Work. "Geod. Meas. Coll. Space Tech. Earth" (GEMSTONE)*, 230–234, Koganei, Tokyo, 1999.

MA, C., J.M. SAUBER, L.J. BELL, T.A. CLARK, D. GORDON, and W.E. HIMWICH: Measurement of Horizontal Motions in Alaska Using Very Long Baseline Interferometry. *J. Geophys. Res.*, **95(B13)**, 21991–22011, 1990.

RIOJA, M. and P. TOMASI: Integrating GPS Zenith Path-Delay Measurements into the Analysis of Geodetic VLBI Observations from the European Network. *Proc. 13th Work. Meet. Europ. VLBI f. Geod. Astrom.*, 152-160, Viechtach, 1999.

TREGONING, P., R. BOERS, D. O'BRIEN, and M. HENDY: Accuracy of Absolute Precipitable Water Vapor Estimates from GPS Observations. *J. Geophys. Res.*, **103(D22)**, 28701–28710, 1998.

WEBB, F.H. and J.F. ZUMBERGE: An Introduction to GIPSY/OASIS-II. *JPL Publication*, **D-11088**, 1993.

YANG, X., B.H. SASS, G. ELGERED, J.M. JOHANSSON, and T.R. EMARDSON: A Comparison of Precipitable Water Vapor Estimates by an NWP Simulation and GPS Observations. *J. Applied Meteorology*, **38**, 941–956, 1999.

ZUMBERGE, J.F., M.B. HEFLIN, D.C. JEFFERSON, M.M. WATKINS, and F.H. WEBB: Precise Point Positioning for the Efficient and Robust Analysis of GPS Data from Large Networks. *Geophys. Res. Lett.*, **102**, 5005–5017, 1997.

Comparison and Combination of Recent European VLBI- and GPS-Solutions

Matthias Becker [1]), James Campbell [2]), Axel Nothnagel [2]), Ch. Steinforth[2])

[1]) Bundesamt für Kartographie und Geodäsie, Frankfurt/Main
[2]) Geodätisches Institut, Universität Bonn

Abstract: In recent years, GPS permanent stations in Europe have accumulated data records and produced time series of high quality that allow the significant determination of site motions. On the other hand, the European VLBI-network has now been operational for a decade and is able to provide long term site motions in a stable inertial reference frame. Here, we present the first results of a comparison between a recent GPSsolution based on 4 years of EUREF combination results and a VLBI global solution used for the annual IERS submission of 1999. The VLBI global solution contains the European VLBI network observations as a subset and provides a homogeneous solution in terms of ICRF, Earth orientation parameters and terrestrial frame realisation. Hence, in a combined global VLBI and European GPS solution, the GPS station velocities can be adjusted to the collocated VLBI/GPS sites in order to achieve a densified velocity field tied to the European part of the global VLBI network.

1. Introduction

One of the primary goals of the second phase of the European VLBI project is the comparison of the site motions obtained by VLBI with the results from other space techniques, in particular GPS. Presently, almost all of the VLBI stations in Europe are equipped with permanent GPS receivers, although some have begun regular observations fairly late. A reliable velocity determination for all of the sites, which requires at least 2.5 years of continuous data (Blewitt and Lavallée 2000), is now becoming feasible.

The following presentation contains a preliminary comparison of VLBI and GPS velocities at the european level made in the frame of the present project. Similar work is being pursued by other groups, for example by the Centro di Geodesia Spaziale (CGS) at Matera, Italy (Putigliano et al. 2000, Devoti et al. 2000).

The fact that the permanent GPS observations are carried out on an ever increasing number of sites and thus provide a much denser coverage of the european area than VLBI, constitutes an enormous benefit that will be derived from the use of these GPS data for the interpretation of the present kinematic scenario of tectonic (as well as man-induced) crustal motions. To ensure a coordinated observing and processing procedure, most of the permanent stations have joined the EUREF Permanent GPS Network (EPN), an element of the realization of the ITRS and the European Reference System ETRS89 (Becker et al. 2000). An overview of the data record of the permanent stations relevant to this study is shown below:

NYAL /NYA1 [1])			====	=====	=====	=====	==	====	=====	==
VILL [2])					=====	=====	=====	=====	=====	==
MADR [3])		===	=====	=====	=====	=====	=====	=====	====	
MATE		====	=====	=====	=====	=====	=====	=====	=====	==
NOTO						=====	=====	=====	=====	==
MEDI						===	=====	=====	=====	==
ONSA		=	=====	=====	=====	=====	=====	=====	=====	==
WTZR					====	=====	=====	=====	=====	==
WETT [4])	=====	=====	=====	=====	=====	==				
WSRT [5])							===	=====	=====	==
KOSG [6])		=	=====	=====	=====	=====	=====	=====	=====	==
	1991	1992	1993	1994	1995	1996	1997	1998	1999	2000

[1]) The first site NYAL was replaced in 1997 by a more stable site NYA1
[2]) The station of Villafrance is located close to the city of Madrid
[3]) At Madrid (DSN-VLBI station Robledo) the GPS data show many irregular jumps in the period from Jan. 1996 to March 1999
[4]) The old GPS receiver at the site WETT was replaced by a new one in 1995. Both receivers had a period of parallel observations during 1995/1996
[5]) At the Dutch Radio Observatory of Westerbork (site of the array) a permanent GPS receiver was installed in 1997
[6]) The site of the former satellite station Kootwijk (University of Delft, Holland), about 80km south of Westerbork

Unfortunately, not all of the available GPS data are actually used in the EUREF solutions. This is partly due to the fact that certain quality criteria have to be fulfilled for the data to be accepted for processing (Bruyninx 1997). Moreover, some of the sites have had changes that led to the exclusion of the older data. In this way, for Ny Ålesund only the data taken at NYA1 from March 1999 onwards are included in the EUREF processing.

2. Data Analysis of the GPS Permanent Stations

For the large number of permanently observing GPS stations, the concept of distributed processing has been adopted, whereby a certain number of analysis centers (presently 12) are taking care of the data from sub-networks with some degree of overlap (Blewitt et al. 1995), in a way that each GPS station is processed by at least three of the 12 AC's. At the website of the Central Bureau of the EPN, the Royal Observatory of Brussels, the weekly solutions of the AC's as well as the weekly combination solution are permanently accessible (Bruyninx 1997, http://homepage.oma.be/euref/). The computation of weekly combinations has been fully implemented from July 1996 onwards. Details of the combination method used in conjunction with the module ADDNEQ of the Bernese GPS software are given by Brockmann and Gurtner (1996).

The time series generated from the weekly solutions represent the evolution of each site in terms of its coordinates in East, North and Up referred to the ITRF96 (depending on the epoch: from GPS-week 1021 onwards, the reference is ITRF97). The connection to this reference frame is made by forcing the total free coordinate solution (of each weekly combination) to have no translation and no rotation for a selected number of fiducial sites in the ITRF, i.e. for the stations of Brussels, Graz, Kootwijk, Matera, Onsala, Wettzell and Zimmerwald. This means that the observed velocities at the fiducial sites are made - on average - to agree with the velocities given by the ITRF. What we actually see in the published time series is how well the 'observations', i.e. the weekly combinations, agree with the extrapolated ITRF velocities. For the non-fiducial stations, we can evaluate the change of position with time in this frame. For the fiducials, the agreement of course only refers to the inner deformations of the weekly combinations and not to the transformations and rotations (and scale) because these are constantly adapted to zero mean with respect to the ITRF-values.

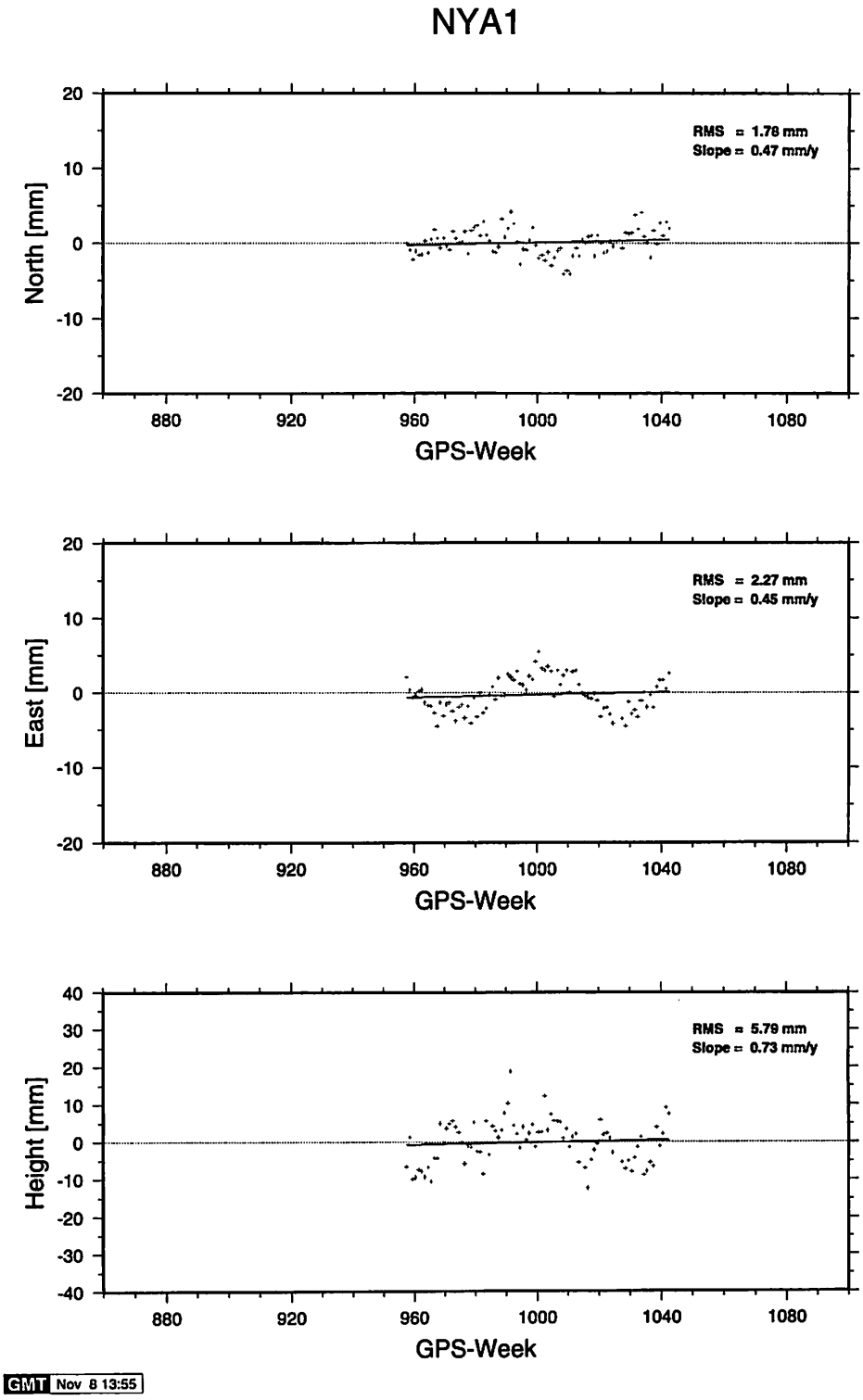

Fig. 1: Time series for the GPS-permanent site NYA1 in the european CODE solution. The linear fits are with respect to the ITRF 97 velocities as a priori´s.

For the combination we have used one of the multi-year combinations of weekly results that are being prepared for the input to the ITRF2000. This solution has the following characteristics:

- data span from June 30, 1966 to Jan 1, 2000 (GPS-week 860-1042)
- number of stations in the solution: 95
- selected set of reference sites for connection to ITRF97
- type of solution: free network (loose constraints on reference stations)

An example of the time series of the european CODE solution (BKG) is shown in fig. 1.

3. VLBI solution

The VLBI solution considered for the combination is one that already provides the required SINEX format, i.e. the GIUB global solution that has been sent to the IERS for the 1999 Annual combination of Earth rotation parameters (Campbell, this volume).

4. Comparison and combination

The comparison and combination of the results of different space techniques involves two aspects that may be treated separately:

a. the site coordinates at a given reference epoch
b. the velocities.

The site coordinates have to rely on the accuracy and integrity of the eccentricities between the reference points or markers that represent each of the techniques at every site. The quality of the local surveys may not be up to the highest standard everywhere and changes in the monumentation and setting up of the measuring systems and antennas do occur at many sites. This is why a comparison of the adjustments for the eccentricities (if no constraints are applied) will be informative of the consistency of the available data on these eccentricities.

The velocities can be used for comparison and combination even if there are still problems with the eccentricities (as long as these are constant for the entire time period considered). Before the final combination it is advisable to examine the time series in order to make sure there are no jumps that indicate uncorrected changes at the stations. One such station that has shown several jumps in the time series is MADR (see section 1). In this case, it is necessary to introduce additional offset parameters for unknown episodic motion. Because of the problems at MADR, in the comparison we have also included the station of VILL (Villafranca) which is located close to Madrid.

The solutions that will be used for the combination can be compared in terms of velocities with respect to the NUVEL-1 velocities of Eurasia (i.e. in a Eurasia-fixed frame). In this presentation, only the vertical motions are shown (tab. 1).

In the comparisons we have also included two more GPS-solutions:

a. the global CODE solution as input to the ITRF2000 (Springer, pers. comm.) which has been computed at the Astronomical Institute Bern (AIUB), Switzerland

b. the global IGS solution posted at the IGS website at JPL (Heflin et al., see http://sideshow.jpl.nasa.gov/mbh/series.html)

These solutions provide an additional background for the assessment of the degree of significance of the site motions observed by GPS, because they partially have longer series of data and a better datum definition due to the global distribution of sites.

5. First Evaluation of the Comparisons

Although the actual combination is still in progress, the comparison has already shown some interesting aspects concerning the velocities determined by VLBI and GPS. For one thing, there are still some rather large differences between the global IGS time series (JPL) and the European based GPS solutions CODE and BKG. This is primarily due to the difference in length of data sets and the modelling of offsets and outliers. Another aspect is of course the quality of the orbits and EOP used in the different solutions.

Vertical velocities with respect to Wettzell fixed (mm/y)					
	VLBI (GIUB)	GPS (BKG)	GPS (CODE)	GPS (IGS)	ITRF97
Ny Ålesund	+ 5.3 ±0.3	+ 2.9 ±2.0	+ 3.2 ±1.9	+ 6.4 ±1.6	+ 2.75
Onsala	+ 3.7 ±0.2	+ 2.9 ±0.9	+ 3.0 ±0.8	+ 1.6 ±0.1	+ 3.76
Effelsberg	- 4.3 ±1.6	-.-	-.-	-.-	-.-
Wettzell	+ 0.0	+ 0.0 ±0.7	+ 0.0	+ 0.0	+ 0.00
Madrid (DSN)	+ 2.8 ±0.6	-.-	-.-	+ 2.0 ±0.3	+ 3.71
Villafranca	-.-	+ 2.4 ±0.9	+ 2.3 ±0.6	- 1.2 ±0.2	+ 2.97
Yebes	- 7.5 ±3.1	-.-	-.-	-.-	-.-
Medicina	- 2.7 ±0.4	- 1.0 ±0.7	- 4.5 ±0.6	- 2.1 ±0.4	- 1.01
Matera	+ 0.2 ±0.3	+ 1.1 ±0.8	+ 1.4 ±0.7	- 0.9 ±0.3	+ 1.80
Noto	- 1.2 ±0.4	+ 0.4 ±0.9	- 3.6 ±0.8	- 2.1 ±0.3	- 1.91
Crimea	+ 3.5 ±1.1	-.-	-.-	-.-	-.-

Tab. 1: Comparison of vertical site motions in the European VLBI Network. The BKG and CODE values still have to be regarded as preliminary.

At the moment, the final results for both the european and the global CODE solutions for 2000 are not yet available. Therefore, the values given in table 1 have to be considered preliminary.

On the whole, considering the small size of the quantities in question, the GPS results agree fairly well with the VLBI results, even the vertical velocities. This holds in spite of the fact that there is still a considerable amount of annual and quasi-periodic variations in the continuous GPS position records.

If we take a closer look at the vertical motions, we see a persistent divergence of motion of about 3 mm/y between Onsala and Wettzell (Onsala going up while Wettzell is going down). How much of this relative motion is actually assigned to either of the sites remains open. All we can suggest is that in an averaged global sense Onsala should be moving upward by about 1 mm/y in the postglacial rebound scenario (Scherneck et al. 2000). In that case, there remains a significant downward trend for Wettzell of about 2 mm/y (whatever may be the cause). This means that we have to take this

downward motion into account when trying to interpret the motions of the other european sites in a more absolute sense.

The steep rise of Ny Ålesund of about + 5 mm/y in relation to Wettzell fixed could still be an effect of the short observational time series on the new site of NYA1, although the VLBI solution uses data from Oct. 1994 onwards. In VLBI, the strong upward trend has been observed earlier by several groups with independent software (see e.g. Titov 1999 and Campbell, this volume). The european (BKG) and global CODE (AIUB) solutions are closer to the ITRF97 value, but these solutions are not yet final.

The subsidence at Medicina of about -2mm/y in relation to Wettzell fixed is an effect that is present in both the VLBI and the GPS solutions. This subsidence is even more pronounced if we turn to a more absolute reference by taking into account the downward motion of the reference station Wettzell.

At this point it is clear that the connection of the GPS results to the tide gauges has to be investigated in detail, in order to establish a 'stable' central european reference. Only then, we can embark on any serious type of interpretation of the vertical motions. Moreover, it is obvious from the error levels of the velocity determinations that one or two more years of data (especially GPS-data) will improve the situation significantly and permit to draw significant conclusions.

6. References

Becker, M., G. Weber, C. Bruyninx and G. Stangl: The EUREF Permanent GPS Network. *Proc. of the 10th General Assembly of the WEGENER Project*, held at San Fernando, Spain, Sept. 18-20, 2000

Blewitt, G., Y. Bock, and J. Kouba: Constructing the IGS polyhedron by distributed processing. *Proc. of the IGS Workshop*, ed. by J. Zumberge, IGS Central Bureau, Pasadena, Calif., USA, p. 21-36, 1995

Blewitt, G., D. Lavallée: Effect of Annually Repeating Signals on Geodetic Velocity Estimates. *Proc. of the 10th General Assembly of the WEGENER Project*, held at San Fernando, Spain, Sept. 18-20, 2000

Brockmann, E., W. Gurtner: Combination of GPS Solutions for Densification of the European Network: Concepts and Results Derived from 5 European Associated Analysis Centers of the IGS. *Veröff. Bayer. Komm. Int. Erdmess.*, Astron.-Geod. Arbeiten, Heft Nr. 57, Subcommission for Europe (EUREF), Publ. No. 5, p. 152-157, München 1996

Bruyninx, C.: The EUREF Permanent GPS Network - Activities May '96 - May '97 and Future Plans - . *Veröff. Bayer. Komm. Int. Erdmess.*, Astron.-Geod. Arbeiten, Heft Nr. 58, Subcommission for Europe (EUREF), Publ. No. 6, p. 39-49, München 1997

Campbell, J.: Comparison of European VLBI Solutions from Different Analysis Centers. *This volume*

Devoti, R., C. Ferraro, R. Lanotte, V. Luceri, A. Nardi, R. Pacione, P. Putigliano, C. Sciarretta, R. Sabadini, I. Jiménez-Munt, E. Gueguen, F. Vespe: Deformations and stress field in the Mediterranean area from geodetic and geophysical approaches. *Proc. of the 10th General Assembly of the WEGENER Project*, held at San Fernando, Spain, Sept. 18-20, 2000

Putigliano, P., C. Ferraro, R. Devoti, R. Lanotte, V. Luceri, A. Nardi, R. Pacione, C. Sciarretta, C. Doglioni, E. Gueguen, F. Vespe: Vertical Motions in the Western Mediterranean area from geodetic and geological data. *Proc. of the 10th General Assembly of the WEGENER Project*, held at San Fernando, Spain, Sept. 18-20, 2000

Scherneck, H.-G., J.M. Johansson, R. Haas: BIFROST Project: Studies of Variations of Absolute Sea Level in Conjunction With the Postglacial Rebound of Fennoscandia. *IAG Sympos. "Towards an Integrated Global Geodetic Observing System (IGGOS)*, Munich, Oct. 5-9, 1998, Vol. 120, p. 241-244, Springer, 2000

Titov, O.: Tectonic Motion of European VLBI Sites. *Proc. of the 13th Working Meeting on European VLBI for Geodesy and Astrometry*, Viechtach/Wettzell, Feb. 12-13 1999, Eds. W. Schlüter, H. Hase, Publ. by BKG, Wettzell, p. 186-191, 1999

Comparison of tropospheric gradients determined by VLBI and GPS

Johannes Böhm (1), Rüdiger Haas (2), Harald Schuh (1), Robert Weber (1)

(1) Institute of Geodesy and Geophysics, Vienna University of Technology, Austria
(2) Onsala Space Observatory, Chalmers University of Technology, Sweden

Abstract
The estimation of geodetic parameters from GPS and VLBI requires the modeling of tropospheric refraction in order to account for the path delays of the radio signals being emitted by extragalactic radio sources and satellites, respectively. Precise models consider the deviation from the azimuthal symmetry by introducing horizontal tropospheric gradients. While the estimation of gradients had been included in the VLBI and GPS software packages SOLVE and GIPSY several years ago it was implemented in the BERNESE GPS software package (version 4.2) and in the VLBI software OCCAM (modified version 4.0) quite recently. We present a comparison of tropospheric gradient estimates derived with the four software packages mentioned above. The parameters have been estimated for the fundamental station Wettzell (Germany) for four VLBI experiments in the first half of 1999 (Euro48, Euro50, Iris136, Iris139) and for simultaneous GPS observations. The analysis of the rms-differences shows that the two VLBI solutions (SOLVE, OCCAM) agree rather well independently of the constraints and time intervals used for the determination of the tropospheric parameters. On the other hand when comparing results from the different techniques (GPS and VLBI) the agreement is poor except a common offset. An interesting feature in all comparisons is that the rms-differences of east gradients are smaller than those of the corresponding north gradients.

1. Introduction

It has been shown that azimuthal asymmetries in the tropospheric path delay lead to errors of the estimated horizontal and vertical station coordinates (MacMillan, 1995). Tropospheric gradients have been introduced in many geodetic software packages:

$$\Delta L(\varepsilon,\kappa) = m(\varepsilon)\cot(\varepsilon)\left[\Sigma_n \cos\kappa + \Sigma_e \sin\kappa\right] \qquad (1)$$

$\Delta L(\varepsilon,\kappa)$ is the total path delay, ε the elevation angle and κ the azimuth. The mapping function $m(\varepsilon)$ describes the elevation dependence of the path delay, and Σ_n and Σ_e are the north and east components of the horizontal gradient vector Σ. The $\cot(\varepsilon)$ factor accounts for the increase in the horizontal change of refractivity along the signal path when the elevation decreases.
Daily average gradient effects consisting of a dry and a wet part can be as large as 50 mm of delay at 7° elevation. The dry (hydrostatic) atmospheric gradients produced by pressure or temperature gradients have a relatively large spatial scale of ~100 km and a temporal scale of days. Wet atmospheric gradients are functions of water vapour content and temperature. They have a smaller spatial scale (<10 km) and can vary more rapidly on time scales of hours and less (MacMillan, 1995). (Mind that a gradient of 1 mm produces a delay contribution of ~65 mm for an observation at 7° elevation and a delay of ~33 mm at 10°.)
The linear model of Equation 1 is similar to that used by Davis et al. (1993) and is approximately equivalent to tilting the atmosphere about a horizontal axis through the site (Rothacher et al., 1998).

While the estimation of gradients had been included in the VLBI and GPS software packages SOLVE by MacMillan (1995) and GIPSY (Webb and Zumberge, 1996) several years ago it was implemented in the BERNESE GPS software package (version 4.2) (Rothacher et al., 1998) and in the VLBI software package OCCAM (modified version 4.0) (Titov and Zarraoa, 1997) quite recently. This lead us to a comparison of tropospheric gradients calculated by these four independent software packages.
Additionally, different algorithms were applied for the parameter estimation: While the Kalman Filter technique was used to derive the tropospheric parameters with GIPSY, we applied a Gauß-Markoff least-squares model (Koch, 1997) with OCCAM, SOLVE and BERNESE to estimate the gradients as piecewise linear functions. Similarily to GIPSY we also modeled the tropospheric parameters in SOLVE as random walk stochastic processes.
Apart from BERNESE (where we used $1/\sin(\varepsilon)$ as mapping function) the Niell mapping functions (Niell, 1996) were applied to account for the elevation dependence of the path delays. In the GPS software packages we introduced a cutoff angle of 10° elevation and standard meteorological data, while for the VLBI data we used a cutoff angle of 5° and measured values for pressure, temperature and relative humidity. In order to derive tropospheric parameters for Wettzell a subset of the EUREF network was processed with the BERNESE software package, whereas with GIPSY the Precise-Point-Positioning method (Zumberge et al., 1997) was applied.

2. Data comparison

Our comparison of tropospheric gradients at Wettzell is based on the analysis of four VLBI experiments and simultaneous GPS observations in 1999: Euro48 (26.04.1999), Euro50 (16.08.1999), Iris136 (15.03.1999) and Iris139 (14.06.1999). Table 1 shows the constraints applied for the estimation of the tropospheric parameters with SOLVE, OCCAM, GIPSY and BERNESE.

Table 1: Constraints for the zenith wet delays (zwd) and the horizontal gradients. Mind the difference in the units ([mm/sqrt(h)] for the random walk parameters, [mm/h] for the sigmas of the pseudo-observations).

	SOLVE/GIPSY [mm/sqrt(h)]		OCCAM [mm/h]		BERNESE [mm/h]	
Constraint	zwd	gradient	zwd	gradient	zwd	gradient
1	1	0.1	1	0.02	1	0.02
2	1.5	0.15	1.5	0.03	1.5	0.03
3	2	0.2	2	0.04		
4	3	0.3	3	0.06	3	0.06
5	4	0.4	4	0.08		
6	5	0.5	5	0.1		
7	6	0.6	6	0.12		

As far as the constraints for OCCAM are concerned the weights ($= 1/\sigma^2$) for the pseudo-observations were further adapted to the number of observations that are contributing to a certain tropospheric parameter. This procedure is equivalent to repeatedly adding pseudo-observations for the rates of the piecewise linear functions to the Gauß-Markoff model. Moreover four different time intervals (1.5 hours (a), 3 hours (b), 6 hours (c), 12 hours (d)) were chosen to check their impact on the tropospheric gradients.
With the BERNESE software package only the following combinations of time intervals and constraints were processed for each of the four sessions: b4 (3h time interval, 3mm/h for zenith wet delay, 0.06mm/h for north and east gradient), c1, c2, d1.

As typical examples how gradients derived by VLBI and GPS behave we show the north and east gradients for session Euro50 with the time interval (b) and the constraints (4) (Fig. 1a) and the time interval (a) and the constraints (7) (Fig. 1b).

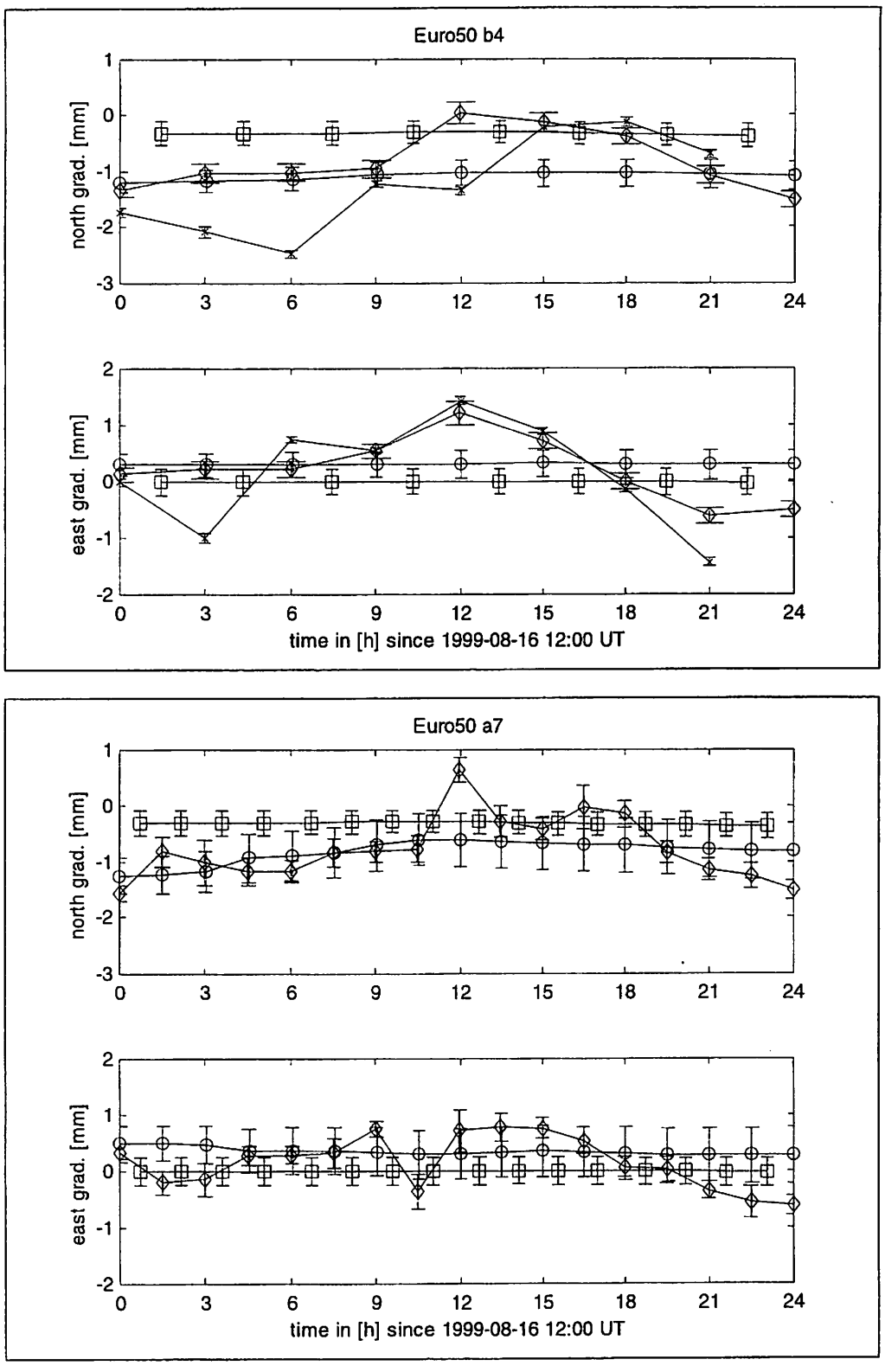

Fig. 1a,b: North and east gradients for session Euro50 with a 3hours/90min time interval (a/b) and the $4^{th}/7^{th}$ set of constraints (Table 1) for the tropospheric parameters. Different markers are used for the software packages: squares (SOLVE), diamonds (GIPSY), crosses (BERNESE), circles (OCCAM); There is no BERNESE data for the solution Euro50 a7.

The corresponding root-mean-square (rms) differences in [mm] for this experiment are given in Table 2a and 2b. Table 3 presents the rms-differences in [mm] for all experiments (Euro48, Euro50, Iris136 and Iris136) and all combinations of time intervals and constraints with available BERNESE results.

Table 2a,b: Rms-differences in [mm] of north and east gradients for the VLBI experiment Euro50 and simultaneous GPS observations. Time intervals of 3hours/90min and the $4^{th}/7^{th}$ set of constraints in Table 1 have been used. There is no BERNESE data for the solution Euro50 a7.

north / east	OCCAM	GIPSY	BERNESE
SOLVE	0.75 / 0.31	0.63 / 0.56	1.13 / 0.91
OCCAM		0.52 / 0.51	0.71 / 0.96
GIPSY			0.78 / 0.53

north / east	OCCAM	GIPSY
SOLVE	0.55 / 0.36	0.68 / 0.45
OCCAM		0.44 / 0.45

Table 3: Overall rms-differences in [mm] of north and east gradients for all VLBI experiments and simultaneous GPS observations.

north / east	OCCAM	GIPSY	BERNESE
SOLVE	0.37 / 0.22	0.86 / 0.53	0.87 / 0.54
OCCAM		0.88 / 0.58	0.79 / 0.58
GIPSY			0.91 / 0.55

Firstly it is evident that GPS gradients are more variable than VLBI gradients (Fig. 1a,b) which is certainly due to the different numbers of observations used for the estimation of the parameters. But further tests showed that weakening the constraints for VLBI gradients did not result in a variation that is similar to that of GPS gradients.

When comparing the atmospheric gradients calculated by the four software packages we see that gradients derived from SOLVE and OCCAM agree rather well whereas gradients from the different techniques (GPS and VLBI) do not show more than a common offset. The rms-differences between tropospheric gradients determined by GIPSY and BERNESE are quite large. This might be caused by the different strategies used for the analysis of the GPS experiments (processing of a network solution with the BERNESE software based on a Gauß-Markoff least-squares model, application of the Precise-Point-Positioning method with GIPSY using the Kalman Filter technique). In any case, more experiments have to be analysed in order to derive reliable conclusions concerning the deviation of the GPS gradients obtained by different analysis strategies.

Another interesting feature is indicated by Figure 2 where tropospheric gradients are plotted against gradients determined by a different software package. In the ideal case of 100% correlation the data would lie on the bisector of the angle. It is evident that the correlation for the east gradients is better than for the north gradients. This effect is confirmed in Table 3 where the overall rms-differences of the east gradients are significantly better than those of the north gradients. Possibly the lack of GPS satellites in the north (Fig. 3) is contributing to this effect but this has to be investigated in the future.

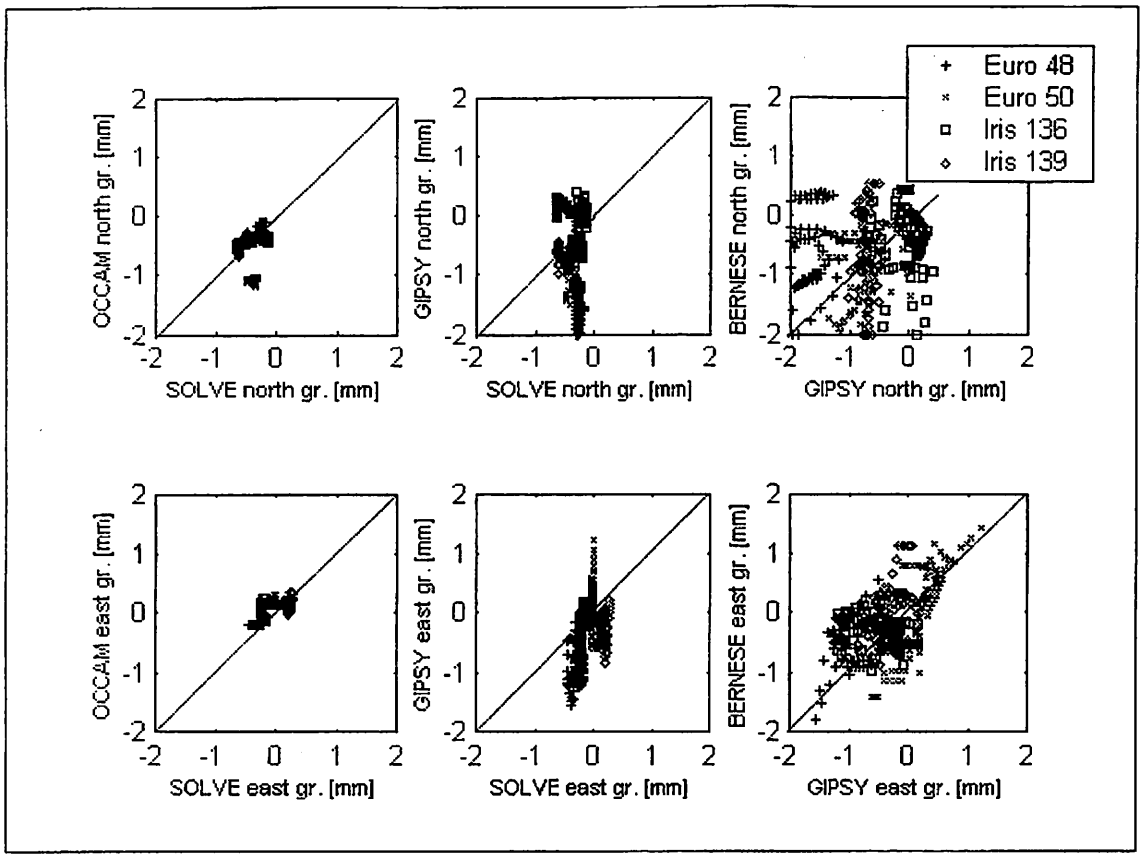

Fig. 2: North and east gradients are plotted against the corresponding gradients derived from different software packages. In the ideal case of 100% correlation the data would lie on the bisector of the angle. With these comparisons only those combinations of constraints and time intervals are included where BERNESE data were available. East gradients agree in a better way than north gradients do and north gradients tend to be negative for each technique.

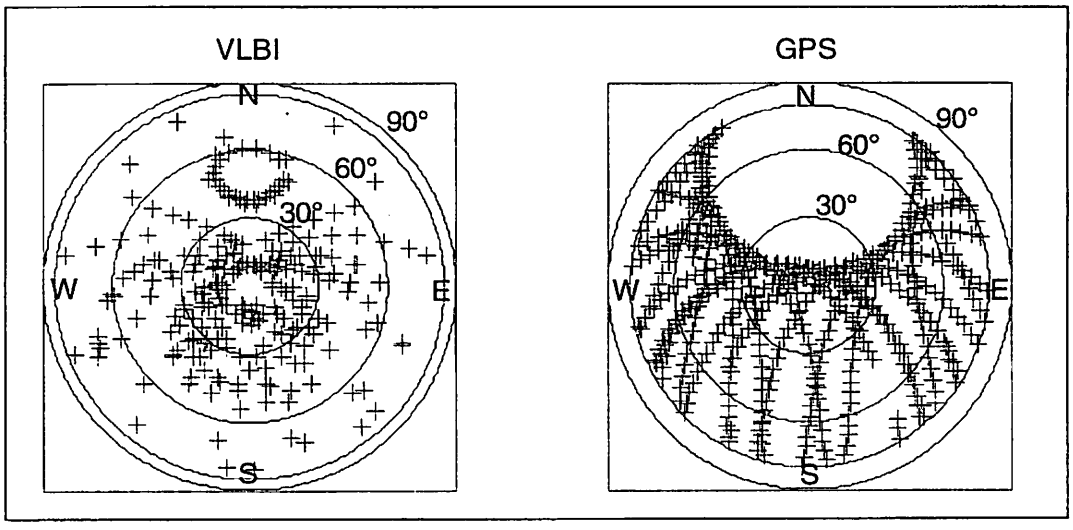

Fig. 3: Distribution of radio sources and GPS satellites during the VLBI experiment Euro50 (1999-08-16) for the fundamental station Wettzell. Mind the different elevation cutoff angles (5° with VLBI, 10° with GPS for reducing multipath effects). The lack of GPS satellites in the north is likely to contribute to larger rms-differences of north gradients when GPS data is involved in the comparison (Fig. 2).

Additionally, the north gradients from each technique tend to be negative (Fig. 2) because Wettzell is situated at a northern latitude of 49° and therefore the north gradients are sensitive to the increase of the tropospheric height towards the south (Chen and Herring, 1997).

3. Conclusions

A pure comparison of horizontal gradients estimated for four VLBI experiments and simultaneous GPS observations in 1999 was presented. We find that the gradients derived from the two VLBI software packages SOLVE and OCCAM agree reasonably well. The gradients from the two GPS analysis software packages show a better agreement for the east than for the north component. Comparing the results from the different techniques, VLBI and GPS, the agreement is rather poor except a common offset. In order to confirm these results more experiments have to be analysed. Also the quality of the gradients remains to be judged by the repeatability of station coordinates or baseline lengths or by comparisons to WVR (water vapour radiometer) data. Further investigations have to be done, e.g. concerning the influence of the geometry (sky distribution) of the radio sources on the gradients.

References

Chen G. and Herring T., Effects of Atmospheric Azimuthal Asymmetry on the Analysis of Space Geodetic Data, J. Geophys. Res., 102 (B9), pp. 20489-20502, 1997.

Davis J.L., Elgered G., Niell A.E. and Kuehn C.E., Ground-based measurements of gradients in the "wet" radio refractivity of air, Radio Science, 28 (6), pp. 1003-1018, 1993.

Koch K.R., Parameterschätzung und Hypothesentests in Linearen Modellen, 3. Auflage, Ferdinand Dümmler Verlag, Bonn, 1997.

MacMillan D.S., Atmospheric Gradients from Very Long Baseline Interferometry Observations, Geophys. Res. Letters, 22 (9), pp. 1041-1044, 1995.

Niell A.E., Global Mapping Functions for the Atmospheric Delay at Radio Wavelengths, J. Geophys. Res., 101 (B2), pp. 3227-3246, 1996.

Rothacher M., Springer T.A., Schaer S. and Beutler G., Processing Strategies for Regional GPS networks, IAG Symposia, 118, pp. 93-101, 1998.

Titov O. and Zarraoa N., OCCAM 3.4 User's Guide, Communications of the Institute of Applied Astronomy, Russian Academy of Sciences, 1997.

Webb F.H. and Zumberge J.F., An Introduction to GIPSY/OASIS-II, JPL Publication D-11088, Jet Propulsion Laboratory, Pasadena, California, 1993.

Zumberge J.F., Precise Point Positioning for the Efficient and Robust Analysis of GPS Data from Large Networks, J. Geophys. Res., 102, pp. 5005-5017, 1997.

Section 2

Stations Reports and Local Ties

Foot-Print Study at the Space-Geodetic Observatory, Ny-Ålesund, Svalbard

Hans-Peter Plag[1], Lars Bockmann, Halfdan P. Kierulf, Oddgeir Kristiansen
Norwegian Mapping Authority, Kartverksveien, N-3511 Hønefoss, Norway

Abstract

The Space-Geodetic Observatory at Ny-Ålesund, Svalbard, which is operated by the Norwegian Mapping Authority, has developed over recent years into a fundamental geodetic station. Currently, there are permanent receivers for five space- and satellite-geodetic techniques as well as a tide gauge and a cryogenic gravimeter. At such fundamental sites, detailed knowledge of the stability of the station, both locally and with respect to the region, is essential for geodetic and geophysical applications of the observations. Therefore, the Norwegian Mapping Authority has initiated and contributed to an extensive foot-print study for the observatory. Own studies include repeated GPS campaigns on a 50 km by 30 km control network and repeated classical surveys of the inner control network extending 400 m by 40 m. In the frame of the Large Scale Facility Ny-Ålesund, a number of projects have contributed to the foot-print study through establishing local ties between VLBI and GPS, surveying the local network and the VLBI antenna, and carrying out absolute gravity measurements. Results from the GPS campaigns reveal local movement of at least one monument of the permanent sites.

1 Introduction

The Norwegian Mapping Authority (NMA) participates in the VLBI experiments within the EU-Project *Measurement of vertical crustal motion in Europe by VLBI* with the Geodetic Observatory in Ny-Ålesund, Svalbard. Moreover, NMA contributes with various research activities to the project (see Plag, 1999, for more details on NMAs contribution to the EU project). The observatory in Ny Ålesund is a fundamental geodetic station located at 78.9 °N and 11.9 °E on the West coast of Spitsbergen, the main island of Svalbard.

The observatory is located on the southern coast of King's Bay (Kongsfjorden) (see Figures 1). An overview over the infrastructure at the station is given in Table 1 and the location of the different techniques is indicated on Figure 2. The main part of the observatory is on a NW-SE striking ridge, which is elevated approximately 45 m above sea level. The ridge top is covered with several meters of cracked perma-frost material. Geologically, Ny-Ålesund is situated on Cretacious/Permian material, with a small tertiary unit close to the observatory (Figure 1). The map also indicates some faults relatively close to the observatory. Geologists assume these faults to be locked, however, they may still be moving, as is indicated by some seismic activity close to Ny-Ålesund (see e.g. Figure 6.20 in Høgden, 1999).

Fundamental geodetic stations allow to establish the relation between different space- and satellite-geodetic techniques. These stations form the back-bone of the geodetic networks and the International Terrestrial Reference Frame (ITRF). Knowledge of the stability of the monuments as well as ties between the different techniques are of crucial importance (Long & Bosworth, 2000). Of equal importance is the stability of the station in relation to the surrounding region.

In order to monitor the stability of the different monuments in Ny Ålesund and to determine site stability, NMA has in 1994 established a local control network around the station (Grimstveit & Rekkedal, 1998). This network consists of 8 pillars, which are connected to the bedrock and isolated against temperature effects (see Tomasi et al., 2000). The pillars are suited for both classical and GPS measurements. In 1995, 1998, and 2000, a total of 12 additional GPS markers were established first in the inner part of King's Bay and then covering a total area of 50 km by 30 km (see Figure 1).

In this report, we will summarise the measurements and analyses carried out so far by NMA. The Geodetic Observatory is part of the Large Scale Facility Ny-Ålesund (LSF), and in the frame of this programme, a number of projects were carried out, which contribute to the foot-print study. Therefore, below we first introduce the LSF and give an overview over the projects carried out so far. We then discuss the design of the control network in more detail and give an overview over the classical and GPS campaigns. In the final section, we present preliminary results from analysis of the GPS observations.

[1]phone: +47-32118100, fax: +47-32118101, Email: plag@statkart.no

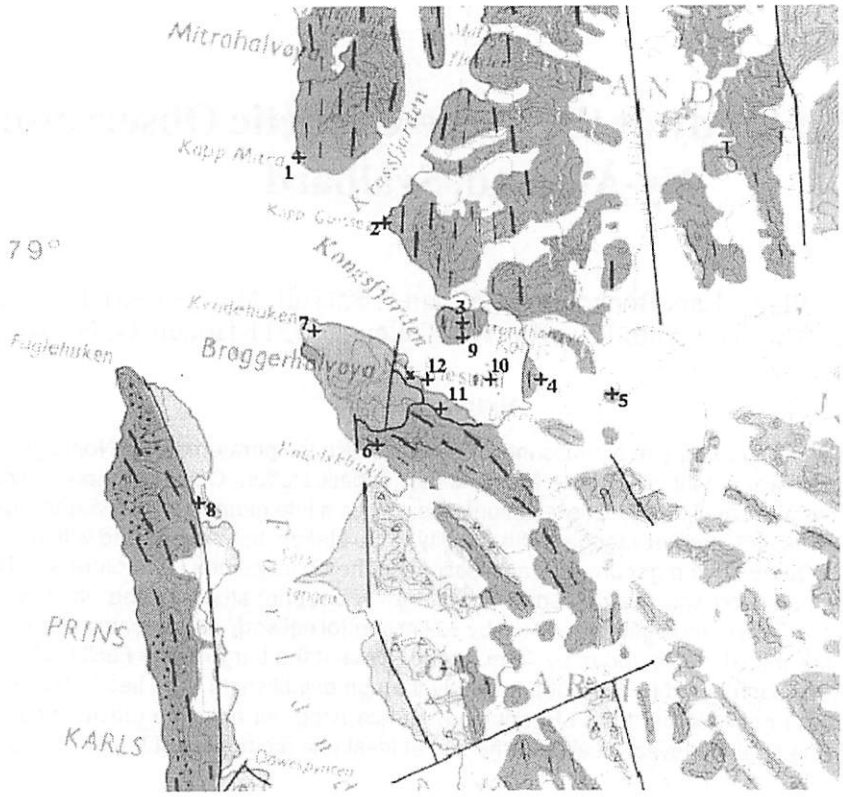

Figure 1: Geology of the King's Bay area.
Dark grey: Proterozoic; light grey: tertiary, intermediate grey (on Brøggerhalvøya): cretatious-permian. Note the fault system on Brøggerhalvøya and the small tertiary unit close to the geodetic observatory. The numbers 1-8 denote the GPS markers established in 1998; those with number 9-11 were established in 1995, while number 12 is closed to the tide gauge and was established in 2000 (see also Table 4). The map is taken from National atlas for Norway, Main topic 2, Rocks and sediments, sheet 2.2.2: Geology of Svalbard and Jan Mayen, Norwegian Mapping Authority, 1996 (translated from Norwegian title).

2 The Large Scale Facility in Ny-Ålesund

The Large Scale Facility *Large Scale Environmental Research and Monitoring Facilities in the European Arctic*[2] has been supported by the European Commission since 1996. Scientific institutes of the LSF are the

- Atmospheric Climate and Biological Research Facilities (NP);
- Atmospheric Air Research Facility (NP / NILU);
- Ozone/Stratospheric and Climate Research Facilities (AWI);
- Space-Geodetic Observatory (NMA);
- Nerc Research Station (NERC);

The projects hosted since 1998 at NMA's Observatory are listed in Table 2. From the project titles it is obvious that the majority of the projects are related to site surveys and the determination of local ties between the different techniques. More3over, the LSF projects oriented towards a geophysical interpretation of the available observations are helping to understand the environmental conditions at and around the fundamental station and to elucidate their effect on the geodetic measurements.

3 The control network in Ny-Ålesund

A description of the inner part of the network, which has been measured fully or in part in 1994, 1997, 1999 and 2000 with classical geodetic measurements can be found in Grimstveit & Rekkedal (1998); Tomasi et al. (2000). Here, we concentrate on the GPS measurements.

At points outside the inner control network with its elaborated pillars, the GPS markers are brass screw bolts drilled and

[2]see http://www.npolar.no/nyaa-lsf/

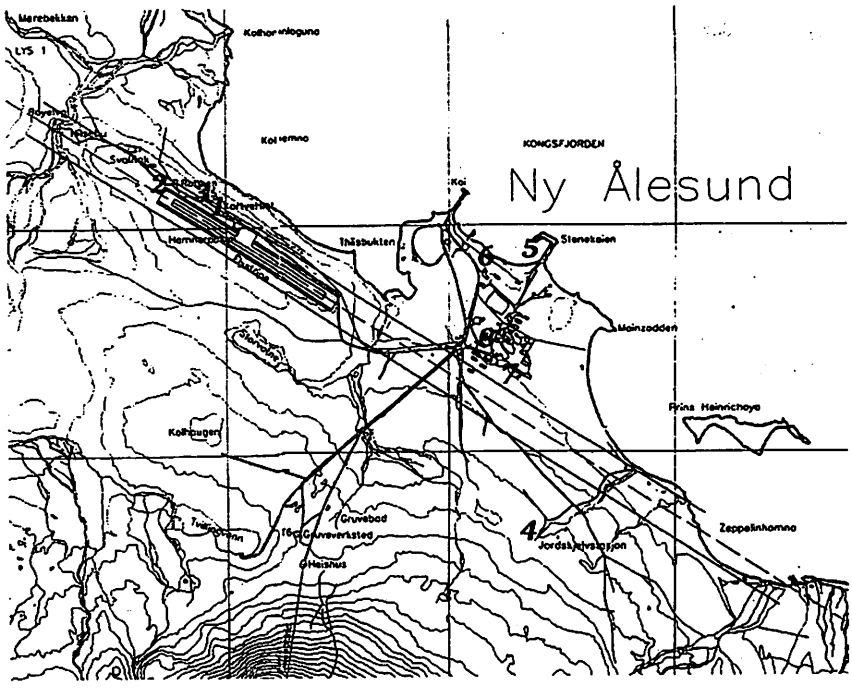

Figure 2: Location of the Geodetic Observatory's infrastructure in Ny-Ålesund.
1: VLBI antenna; 2: SATREF, CHAMP and GLONASS receivers; 3: IGS receiver NYAL and NYA1 as well as cryogenic gravimeter and absolute gravity point; 4: Relative LCR Earth tide gravimeter, also seismic observatory; 5: tide gauge; 6: Tide gauge bench mark; 7: DORIS; 8: Water vapour radio meter and ballon sounding.

Table 1: Geodetic and ancillary infrastructure at the Geodetic Observatory, Ny-Ålesund.

Technique	Since	Application
	Space- and satellite geodesy	
GPS	1999	SATREF, real-time
GPS	1991	IGS, hourly data files
GPS/GLONASS	1999	IGS, hourly files
GPS	2000	CHAMP, LEOs, 15 minutes files
VLBI	1994	IVS (VLBI Europe, CORE, NEOS), EVN
PRARE	1995	PRARE Experiment
DORIS[1]	1992	DORIS network
	Gravity	
relative	1996	Earth tides studies
absolute	1998, 2000	foot-print, geodynamics, sea-level studies, calibration
gryogenic	1999	Earth studies within Global Geodynamics Project (GGP)
	others	
tide gauge	1991	Global Sea Level Observing System (GLOSS)
Control network		
inner part 400 by 40 m	1994, 1997, 2000	monument stability and foot-print study
outer part 50 by 30 km	1998	annual campaigns, foot print study

[1] supported by NMA

zemented into solid rock. Elevation of the top of the bolt above ground is of the order of 10 cm. In the reconnaisance much care has been taken to find suitably flat outcrops of solid rocks, which provide acceptable horizons for GPS observations. Moreover, locations are choosen to cover all major geological units in the area.

GPS campaigns were carried out in 1998, 1999, and 2000 (Table 3). In 1998, seven points established in 1998 were measured. In both, 1999 and 2000, all points suitable for GPS measurements were occupied in two consecutive campaigns. However, the eastern-most point of the control network (point 5 on Figure 1) could not be occupied in 1998 due to weather conditions over the ice preventing access with a helicopter. Therefore, it was decide to abandon this point and not use it in subsequent campaigns.

Table 2: List of LSF Projects since 1998.

P.I.	Country	Year	Title
Susanna Zerbini	Italy	1998	Design, establishing and measuring a local GPS network in the Arctic environment
Antonio Rius	Spain	1998	GPS Tomography of the Ionosphere and the Troposphere in the Arctic environment
Bernd Richter	Germany	1998	Absolute gravity measurements for the detection of ice load changes
John Ponsonby	U.K.	1999	Study of the atomic time and frequency standards at the Statens kartverk's VLBI radio observatory, especially the hydrogen maser standards
Paolo Tomasi	Italy	1999	Geodetic link of the VLBI antenna at Ny-Alesund to the control network
Detlef Wolf	Germany	1999	Present-day changes in the ice-caps in West Spitsbergen: geophysical implications
Alexander Braun	Germany	1999	Calibration of ERS altimetric data in the western Spitsbergen shelf through tide gauge data
Trevor Baker	U.K.	1999	A test of ocean tide models in the Arctic
Paolo Tomasi	Italy	2000	Reference point for geodetic VLBI antenna at Ny-Alesund using GPS receivers. Determination of the position and possible low time scale variability due to thermal expansion
Antonius Rius	Spain	2000	Tidal effects in the determination of tropospheric water vapour using geodetic space techniques
Axel Nothnagel	Germany	2000	Conventional survey tie between VLBI and GPS reference point at Ny Alesund
Rüdiger Haas	Sweden	2000	A new GPS-VLBI tie at Ny-Alesund
Jacques Hinderer	France	2000	Absolute gravity measurements in Svalbard: long term evolution and accurate calibration of the superconducting gravimeter

Table 3: GPS campaigns on the control network.
The number of points given are the points of the control network plus the permanent points available during the campaign.

Year	Period	Number of points
1998	September 2-6	7 + 2 points
1999	August 15-18	7 + 2 points
	August 19-24	6 + 3 points
2000	August 12-17	5 + 3 points
	August 18-21	6 + 3 points
	August 26-30	1 + 3 points
	September 2-12	1 + 3 points

Table 4: Coordinates of the GPS markers in the control network.
Coordinates are for the FNW solution and given in ITRF97. N is the geoid height at the point. Numbers n are those used on Figure 1. They are determined for the first full day of the 1998 campaign, i.e. 2 September 1998.

ID	n	**Latitude** °N	**Longitude** °E	**Height** m	N m
BRAT	3	78.982768831	12.068829975	403.8167	36.6399
ENGL	6	78.857537511	11.732618315	235.4424	36.8548
KAPG	2	79.066166494	11.652208521	41.8508	36.7947
KAPM	1	79.114289272	11.171813793	37.4250	36.9660
KNOC	8	78.802450239	10.807748806	79.9473	37.8627
KVAD	7	78.958063400	11.399361921	56.8751	36.9650
NYA1	x	78.929553865	11.865306635	84.1949	36.7346
NYAL	x	78.929583936	11.865083329	78.4706	36.7347
SARS	4	78.937312744	12.510997616	368.9046	36.4328

Table 5: Horizontal site movements for the markers in the control network.
For each component, the first column is the linear velocity and the second column the standard deviation of the residuals. The last three lines give the velocities for NUVEL-1A-NNR (DeMets et al., 1994) and the long-term velocities for VLBI (Ma, 1998, personal communication) and the NYAL IGS series, which starts in 1991 (Heflin, 2000).

ID	campaigns	North		East	
		mm/yr	mm	mm/yr	mm
BRAT	3	15	3	10	3
ENGL	3	15	3	8	4
KAPG	3	15	4	10	3
KAPM	3	15	3	10	2
KNOC	3	13	3	11	4
KVAD	3	15	3	10	3
NYA1	3	14	9	9	5
NYAL	3	15	3	14	2
SARS	3	15	3	11	2
NUVEL		13.60		12.95	
VLBI		13.50 ± .17		11.75 ± .17	
NYAL		14.03 ± 0.07		10.64 ± 0.08	

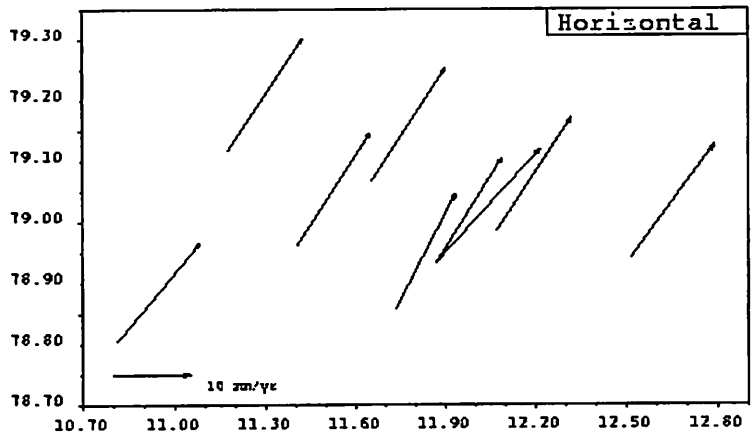

Figure 3: Horizontal movements of the control network.
The X- and Y-axis give longitude in °E and latitude in degree W, respectively.

In each campaign, the points were occupied for at least 4 complete days and in most cases for five full days. Care was taken to occupy, whereever possible, a given point each year with the same receiver and antenna pair. All campaigns were carried out by the same observer (LB).

So far, preliminary analyses were carried out with GIPSY, using a free network analysis (FNW) as well as a precise point positioning (PPP, see Zumberge et al., 1997). JPL precise orbits, EOP and clocks were used. Cut-off elevation for both solutions was set to 7 °. In addition, a ppp solution with cut-off elevation of 15 °was computed. For transformation to ITRF, JPL's global transformation parameters were used. In the analysis, no ambiguity resolution was made. Point coordinates are given in Table 4. Table 4 also includes the IGS points NYAL and NYA1, which have been monitoring continuously over the total period from 1998 - 2000.

For the FNW solution, the daily coordinates for each station show a day-to-day scatter over a total range of approximately 20 mm in the height component and about 10 mm in the north and east components. For the horizontal components, the results from the three years fit a linear velocity very well. The linear horizontal velocities derived from the three campaigns are given in Table 5. The linear horizontal velocities derived from the FNW solutions agree with those derived from the PPP solutions (both the one with 7 °and 15 °cut-off elevation) on the 1 mm/yr level for all stations.

The spatial pattern of the horizontal velocities is rather homogeneous on the 1 mm/yr level (Figure 3). The only exception is NYAL, where a significantly higher velocity is found towards east. Over the two years covered by the three compaigns, NYAL has a total anomalous horizontal movement with respect to the other points of approximately 8 mm. This indicates a local movement of the monument at NYAL. Considering that the antenna is on a steel gitter tower of 5 m height, then

a tilting of approximately 5 arcseconds would be sufficient to explain this movement. It should also be pointed out here that the east rate for NYAL deviates from the long-term rate determined by VLBI and the long-term rate determined from the GPS observations at NYAL.

In height, for all sites, a non-linear temporal behaviour is found in the FNW solution with the 1999 heights in general plotting above the linear regression line through the three campaigns. Vertical rates determined from the FNW and the PPP solutions agree on the 1-2 mm/yr level. However, selecting a 15 °cut-off elevation, vertical rates change very much. The differences to the solution with 7 °cut-off elevation may be as large as 8 mm/yr and for some sites, trends of 3 mm/yr and -3 mm/yr are found for the FNW and PPP solutions, respectively. Particularly large differences are found for those sites with bad horizon towards north (ENGB, BRAT, KAPG). The dependency of the heights and the vertical rates on the cut-off elevation has to be invertigated further in more detail.

4 Summary

The results obtained from the GPS measurements so far underline the usefulness of the repeated GPS campaigns to monitor monument stability as well as to study the foot-print of the station. Particularly the combination of campaigns with the permanent sites proves helpful (as could be expected from the MOST approach described in Bevis et al., 1997). Nevertheless, problems related to the determination of the height component remain to be solved before any potential vertical movement in the geological faults system close to the station.

Acknowledgements

The following NMA staff members have participated in or supported the establishment of the control network and/or the GPS campaigns carried out: Svein Rekkedal, Helge Digre, Leif Morten Tangen, Leif Grimstveit and David C. Holland. The authors would like to thank these persons for their contributions and support.

References

Bevis, M., Bock, Y., Fang, P., Reilinger, R., Herring, T., Stowell, J., & Smalley, R. j., 1997. Blending old and new approaches to regional GPS geodesy, *EOS, Trans. Am. Geophys. Union*, **78**, 61, 64, 66.

DeMets, C., Gordon, R. G., Argus, D. F., & Stein, S., 1994. Effect of recent revisions to the geomagnetic reversal time scale on estimates of current plate motions, *Geophys. Res. Lett.*, **21**, 2191–2194.

Grimstveit, L. & Rekkedal, S., 1998. Geodetic control of permanent sites in Tromsø and Ny-Ålesund, in *Book of Extended Abstracts for the Ninth General Assembly of the Working group of European Geoscientists for the Establishment of Networks for Earth-science Research. Second Edition*, edited by H.-P. Plag, pp. 25–28, Norwegian Mapping Authority.

Heflin, M. B., 2000. GPS time series, http://sideshow.jpl.nasa.gov/mbh/series.html.

Høgden, S., 1999. *Seismotectonics and crustal structure of the Svalbard Region*, Ph.D. thesis, Department of Geology, University of Oslo.

Long, J. L. & Bosworth, J. M., 2000. The importance of local surveys for tying techniques together, in *International VLBI Service for Geodesy and Astrometry 2000 General Meeting Proceedings*, edited by N. R. Vandenberg & K. D. Baver, pp. 113–117, NASA, Greenbelt, MD, USA.

Plag, H.-P., 1999. Measurements of vertical crustal motion in Europe by VLBI. Station report for Ny-Ålesund, Norwegian Mapping Authority, in *Proceed. 13-th Working Meeting of European VLBI for Geodesy and Astrometry, Viechtach/Wettzell, February 12-13, 1999*, edited by W. Schlüter & H. Hase, pp. 65–77, Bundesamt für Kartographie und Geodäsie, Frankfurt.

Tomasi, P., Sarti, P., & Rioja, M., 2000. The determination of the reference point of the VLBI antenna in Ny Ålesund, *Memoirs of National Institute of Polar Research, Japan*, **54**, In press.

Zumberge, J. F., Heflin, M. B., Jefferson, D. C., & Watkins, M. M., 1997. Precise point positioning for the efficient and robust analysis of GPS data from large networks, *J. Geophys. Res.*, **102**, 5005–50017.

Activities of the BKG VLBI group in the frame of the IVS

Volkmar Thorandt[1], Gerald Engelhardt[1], Dieter Ullrich[1], Reiner Wojdziak[1]

Abstract

Information on the status and the development of the IVS (International VLBI Service) Data Center at BKG (Bundesamt für Kartographie und Geodäsie) Leipzig will be given.
Furthermore the consecutive analysis works of the BKG analysis center in close cooperation with the VLBI group at the university of Bonn (Germany) will be explained.

1. Introduction

The BKG Data Center in Leipzig is one of three primary IVS Data Centers. In close cooperation with CDDIS (Crustal Dynamics Data Information System) in Greenbelt U.S.A. and Paris Observatory, France it has been established in 1999. The three data centers mirror the data several times per day.
The BKG also mirrors the IVS home page (http://www.leipzig.ifag.de/IVS) with CDDIS.

The VLBI analysis group at BKG started its work in 1994. Together with the VLBI group of the University of Bonn the BKG is one of the IVS Analysis Centers (BKG Analysis Center). At present session series Earth orientation parameter (EOP) solutions and annual solutions for EOP, Terrestrial Reference Frame (TRF) and Celestial Reference Frame (CRF) as a contribution to the IERS (International Earth Rotation Service) are submitted. It is planned to produce a TRF solution on the first day of each quarter of the year according to the IVS instructions and first test solutions of the Intensive Series EOP. The VLBI group at BKG uses the MarkIII / IV data analysis Software CALC / SOLVE originated mainly by VLBI groups at the Goddard Space Flight Center (GSFC) on the basis of a HP9000/D280/1 workstation.

[1] Bundesamt für Kartographie und Geodäsie, Außenstelle Leipzig,
Karl-Rothe-Straße 10-14, 04105 Leipzig
Fax: +49-341-5634415; Tel.: +49-341-5634285; email: vt@leipzig.ifag.de and engelhardt@leipzig.ifag.de

2. The IVS Data Center at BKG Leipzig

2.1. The Primary IVS Data Centers

The BKG Data Center in Leipzig is one of three primary IVS Data Centers. In 1999 it has been established in close cooperation with CDDIS in Greenbelt, U.S.A., and Paris Observatory, France. The three data centers mirror the data several times per day. So it is always guaranteed to have the whole data stock available at each of the centers.
The IVS Analysis Centers (respectively operation centers, correlators or network stations) put their data (experiment databases, logfiles, analysis products etc.) into the so-called incoming area by ftp (at BKG ftp.leipzig.ifag.de). At this area a script "ivs2incoming" checks the syntax of the received data and either decides to move it to the regular data center area or to put it into a bad file area. In the second case the incoming script sends a message to the data center manager.
A distinctive feature at the BKG Data Center is the "dserver". It serves the IVS Analysis Center of the Bonn University. The dserver looks into a special area in Bonn and if there is a new analysis product or database waiting for delivery to the data center it moves the files to Leipzig. After checking the files they will be moved to the data center directories.
Both scripts compress the experiment databases. It is planned to put all VLBI data of the former years into this structure. The CDDIS Data Center will manage this process.
A general view of the data center including the interfaces is shown in Figure 1.

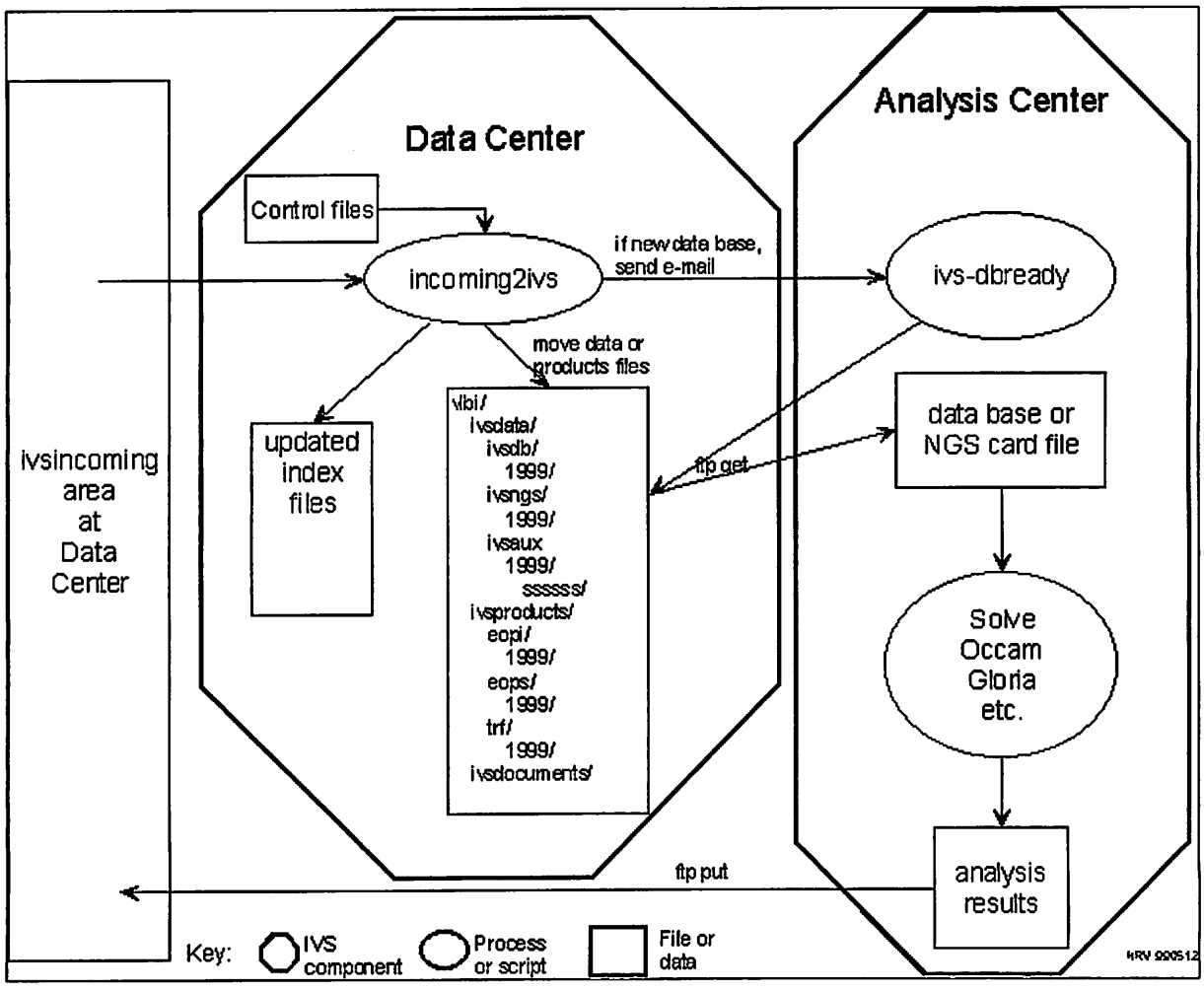

Figure 1: IVS Data Center and interfaces (drawn from http://roxy.leipzig.ifag.de/IVS/service/dc2prod.gif)

2.2. The structure of the IVS Data Center

The following table gives an overview about the structure of the IVS Data Center.

IVS Data Center - Structure		
ivscontrol	ac-codes.txt, dcstructure.txt, filemames.txt, indexformat.txt, ivsdata.txt, category.txt, masterfiles, mirror.txt, ns-codes.txt, submit.txt	
ivsdata	aux .skd, .txt, .corr, .log, .cb, .wx	1994 . . 2000
	db X- and S-band database files in compressed format: yymmmddcc_Vnnn.gz	1979 . . 2000
	sinex yymmmddcc_Xnnn.gz (currently empty)	. . . .
	ngs X- and S-band NGS database files in compressed format: yymmmddcc_Nnnn.gz	1994 . . 2000
ivsdocuments	description files: bkgi0001.eops.txt, gsfc1122.eops.txt, gsfc1122.trf.txt, iaao9907.eops.txt, usno9903.eopi.txt, usno9903.eops.txt, usno9903.trf.txt, spbu0001.eops.txt, spbu0001.eopi.txt	
ivsproducts	crf Celestial Reference Frame aaaacccc.crf aaaacccc.stats.crf	currently empty
	eopi intensive EOP aaaacccc.eopi aaaacccc.stats.eopi	usno9903.eopi, spbu0001.eopi
	eops session EOP aaaacccc.eops aaaacccc.stats.eops	bkgi0001.eops, bkgi0001.stats.eops, gsfc1122.eops, gsfc1122.stats.eops, iaao9907.eops, iaao9907.stats.eops, usno9903.eops, spbu0001.eops
	trf Terrestrial Reference Frame aaaacccc.trf aaaacccc.stats.trf	gsfc1122.trf, gsfc1122.stats.trf
ivs-iers	IERS submission files	bkgira99..., bkgtra99..., ffiera99..., gsfcra99..., iaa1ra99..., iaa2ra99..., iaa3ra99..., oparra99...

2.3. The technical equipment of the IVS Data Center at BKG

The IVS Data Center at BKG is running on a HP 9000/D280/1 machine with about 190 Gbytes disc space and 2 Gbytes memory. The operating system is HP UNIX 10.20. A DIGITAL TL 894 tape library is used as backup system. The internet rate has been upgraded to 2 Mbit/sec in August 2000.

3. The IVS Analysis Center at BKG Leipzig

The VLBI group at BKG was established in 1994. In close cooperation with the VLBI group at the University of Bonn global solutions as a contribution to the IERS annual solutions were produced. The BKG catalogue system contains about 6000 X-band databases and so-called superfiles for analysis purposes. It covers the time span from 1976 to 2000. Since March 1, 1999, the inauguration date for the IVS, the VLBI group at BKG has been operating as an IVS Analysis Center together with the VLBI group at the University of Bonn. At present so-called session series Earth orientation parameters and IVS-IERS annual solutions for EOP, TRF and CRF are produced with the Mark III / IV VLBI analysis software CALC / SOLVE (GSFC / NASA, 2000).

3.1. The Mark III / IV data analysis system

The Mark III / IV VLBI data analysis system is a program system which supports scheduling, operating, processing, archiving and analysis of VLBI experiments. It is mainly maintained by several VLBI groups at NASA / GSFC. The VLBI analysis software CALC / SOLVE is a part of that program system and allows to estimate parameters such as EOP, station coordinates, station velocities and many others. It also offers the possibility to manipulate with databases of the VLBI experiments.
At BKG the CALC / SOLVE software is installed on a HP9000/D280/1 workstation with operating system HP-UX10.20.

3.2. The processing of single VLBI experiments

The first processing step of single experiments (IRIS-S, EUROPE, COHIG) is the transfer of the version 1 X-band and S-band databases and the related log files from the Bonn correlator at MPIfR (Max Planck Institut für Radioastronomie) to the BKG Leipzig. In the second step the program APRIORI provides the necessary ephemeris, UT1 and polar motion information. After that CALC calculates theoretical values, partial derivatives, contributions and corrections according to the geophysical models. As of now CALC 8.2 Y2K is in use, but it is planned to upgrade to CALC 9.11. The fourth analysis step is to run F-SOLVE to fit the databases with the partial derivatives, theoretical values, contributions and corrections calculated by CALC and to add an ionosphere correction by using the S-band database. It also includes the group delay ambiguity resolution for X- and S-band databases. The result is the version 4 of X-band database. Currently F-SOLVE version 2000.03.31 is in use. In step 5 the program XLOG prepares the log files for the calibration of the databases with meteorological and cable data. This program was made by the VLBI people at DGFI (Deutsches Geodätisches Forschungsinstitut) in Munich, Germany and replaced the old PWXCP. It is faster and more convenient. The output of this step are the calibration files for DBCAL, the next processing step. It enters the weather and cable data into the database by interpolating the measured data for the observation epoch. Output is the version 5 of X-band database. F-SOLVE provides the final parameterization according to the purpose of the experiment and the least squares solution. It includes the inspection of the residuals and procedures for outliers elimination. The output files are the listing of results and after update the X-band database version 6. The last step is to upload the databases and related files into the incoming area of the BKG IVS Data Center and into the local data area. After mirroring the files are available at all primary data centers.

3.3. The evaluation procedure to derive the IVS products

At present the BKG Analysis Center computes consecutive session series EOP products and IVS-IERS annual solutions for EOP, TRF and CRF.

3.3.1. The Session Series EOP product

After the preprocessing of each new VLBI experiment a new solution on the basis of delays with the latest version of the databases is produced to derive session series EOP for the IVS. The features of the solution, called bkgi0001.eops, are described in the technical description and are available in the IVS data centers in the directory ivsdocuments (e.g. ftp://ftp.leipzig.ifag.de/vlbi/ivsdocuments/bkgi0001.eops.txt). The solution is put into the so-called IVS incoming area. After checking the syntax the solution will be moved to the regular data

center area (e.g. ftp://ftp.leipzig.ifag.de/vlbi/ivsproducts/eops/bkgi0001.eops). The solution includes the estimated EOP (xpol, ypol, ut1-utc) and the nutation offsets (dPsi, dEps) including the corresponding uncertainties and correlation. Together with the solution a solution statistics summary file (bkgi0001.stats.eops) is given. Figure 2 to Figure 4 show first comparisons with results of the IVS analysis center GSFC. Differences to the IERS C04 series (IERS, 1999) give an impression of the EOP variations between both solutions. Apart from some outliers both solutions fit quite well. But two other facts are remarkable. Firstly, after test solutions with different a-priori TRF, NAVY 1998-10 (USND, 1997) and ITRF97 (Boucher C. et al., 1998), an offset of about 20 microseconds in UT1-UTC between the green and red curves shown in Figure 2 can be seen. Secondly, the differences in the nutation component dPsi are approximately three times bigger than the ones in the nutation component dEps (Figure 3 and 4). That corresponds quite well with the difference in the estimated formal program errors of dPsi and dEps.

Figure 2: Comparison between BKG and GSFC in UT1-UTC

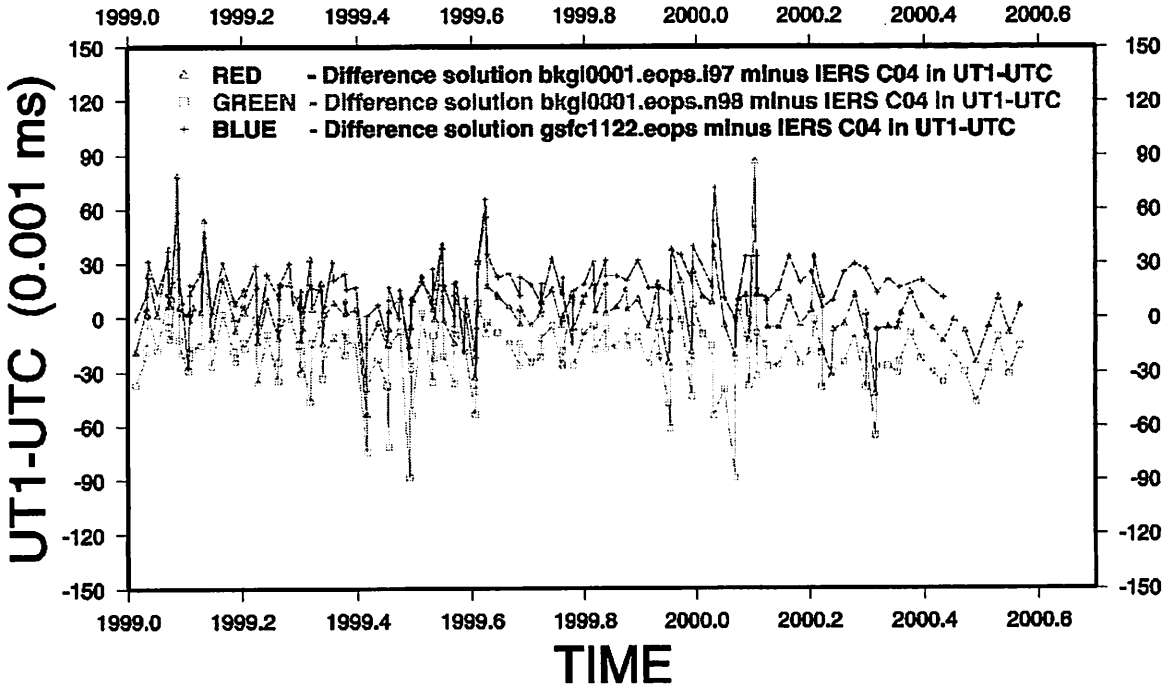

Figure 3: Comparison between BKG and GSFC in nutation offset dPsi

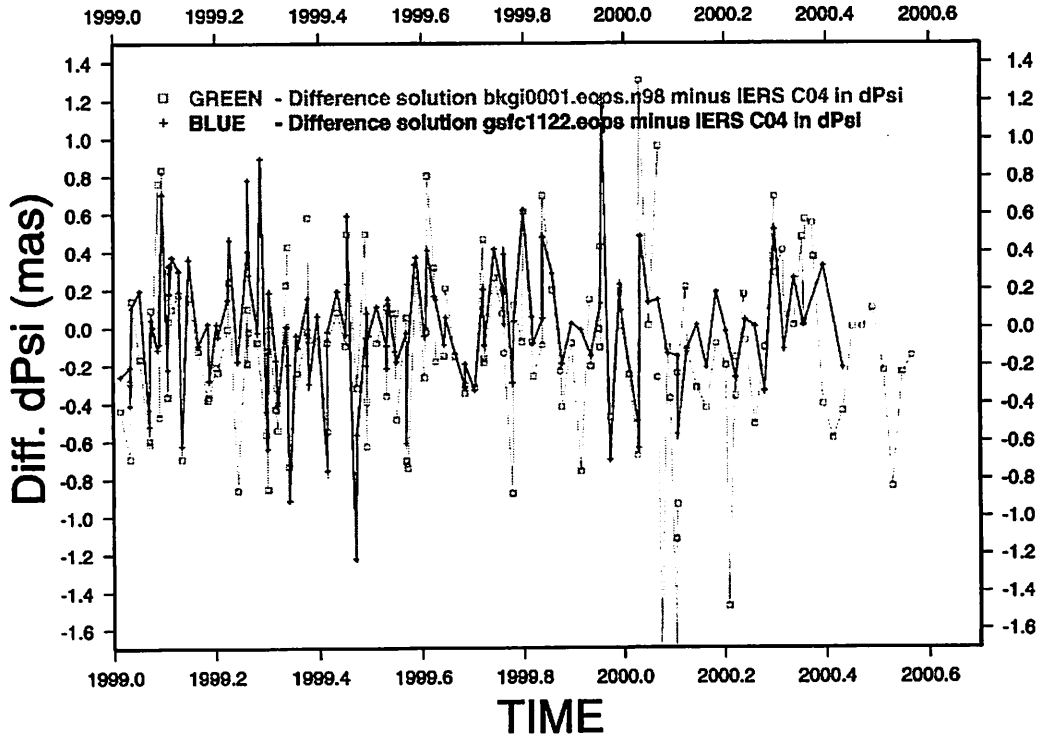

Figure 4: Comparison between BKG and GSFC in nutation offset dEps

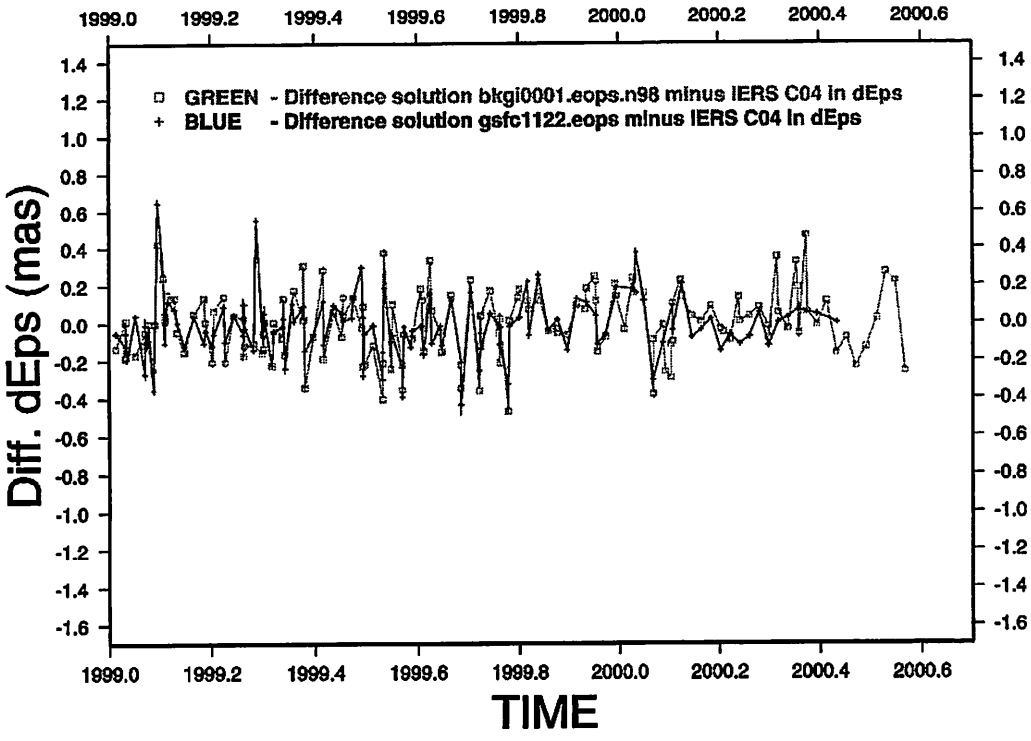

3.3.2. The IVS-IERS annual solution

In addition to the session solution a combined global solution is computed to estimate the EOP, station coordinates and velocities as well as the radio source positions. This annual solution is a contribution to the IERS. The solution type for the TRF is called bkgtra99 and corresponds to a quasi free network solution. The technical description of this solution is available in e.g. ftp://ftp.leipzig.ifag.de/vlbi/ivs-iers/bkgtra99.des. The file format is SINEX (Solution Independent Exchange Format) and can be found in the IVS data structure under e. g. ftp://ftp.leipzig.ifag.de/vlbi/ivs-iers/bkgtra99.snx.gz. The solution type for the EOP and CRF is called bkgira99 and the corresponding technical description can be found in e.g. ftp://ftp.leipzig.ifag.de/vlbi/ivs-iers/bkgira99.des. The format for the two files is IERS standard EOP format and IERS standard source position format, respectively. These two files are also available in the IVS data structure under e. g. ftp://ftp.leipzig.ifag.de/vlbi/ivs-iers/bkgira99.eop and ftp://ftp.leipzig.ifag.de/vlbi/ivs-iers/bkgira99.rsc.

4. Outlook

On the basis of comparisons between our session series EOP solution and solutions of other analysis centers outliers in the residuals have to be investigated. In the future it is planned to produce the Terrestrial Reference Frame IVS solution four times per year each on the first day of each quarter of the year. Finally the analysis group at BKG is preparing first test solutions of the intensive series EOP for future IVS submissions. In the near future the current version of the CALC / SOLVE software will be installed (GSFC / NASA, 2000).

References

Boucher C. et al., (1999): The 1997 International Terrestrial Reference Frame (ITRF97), IERS Technical Note 27, Observatoire de Paris.

Goddard Space Flight Center / NASA (2000): Release of Mark IV VLBI Analysis Software CALC / SOLVE from July, 26th, 2000-09-04 (web-reference: http://gemini.gsfc.nasa.gov/solve).

IERS (1999): Data publically available under the web-reference: http://hpiers.obspm.fr/webiers/results/eop/README.html.

USNO (1997): U. S. Naval Observatory IERS-Annual Report for 1997.

Determination of the 1996 Displacement of the Medicina Radio Telescope by Local Surveys

Axel Nothnagel and Bernd Binnenbruck
Geodetic Institute of the University of Bonn, Nussallee 17, D-53115 Bonn, Germany
Tel.: ++49 (228) 733574, Fax: ++49 (228) 732988, E-mail: nothnagel@uni-bonn.de

Abstract

The replacement of the track of the Medicina VLBI telescope caused a significant displacement of the antenna in summer 1996. In late 1998 a local survey was carried out for the determination of the VLBI reference point in the frame of a local control network. The measurements are described and the results are compared to a survey carried out in 1988. Thermal expansion is an important factor and has to be taken into account. While the horizontal displacements are marginal an uplift of the telescope of 18.5 ± 2 mm was detected.

1 Introduction

The long term stability of radio telescope reference points is one of the great advantages which geodetic VLBI has upon other space geodetic techniques. Unlike GPS antennas the phase center of a VLBI antenna always has a well determined geometric position relative to the reference point or invariant point. The long term stability of the VLBI reference point, however, does not last indefinitely and various reasons may cause a local displacement of the invariant point at irregular intervals.

At the Medicina 32 m radio telescope of the Istituto di Radioastronomia (CNR) near Bologna, Italy, the replacememt of the drive track in summer 1996 caused a significant displacement of the VLBI reference point after almost eight years of operation. In order to correct the long term geodetic VLBI time series for the displacement, precise local surveys should be carried out shortly before and after the repair work. At Medicina the pre-repair measurements had already been made in 1988 (CENCI et al. 1988) while the post-repair surveying was done in October 1998. Here, we report on the latter measurements, their analyses, results and implications.

2 Local Survey Network

At the time of the telescope construction in 1988 five survey pillars with brass marks had been erected mainly on the east side of the telescope (Fig. 1). In order to stabilize the pillars in the soil of the Po-plane where no stable bed rock is within reach two of them, A and C, were founded as deep as 22 meters (TOMASI, pers. communication). In addition to the pillars a concrete pad for mobile satellite laser ranging (SLR) systems with a central reference marker (O) as well as two brass marks on the telecope pedestal (D and E) were established. In 1988 the coordinates of the VLBI reference point were determined with respect to these markers in a local topocentric (north, east, up) system (CENCI et al. 1988). In 1995 the measurements were repeated but the VLBI reference point was spared at that time (DEL ROSSO et al. 1995).

In October 1998 the Medicina control network was revisited with leveling instrument and tachymeter for a re-determination of the VLBI reference point after the track repair. The method of choice was a three dimensional triangulation of the end points of the elevation axis in different azimuth positions of the telecope. For this procedure two auxiliary survey points, HPN and HPS, were established since the existing survey monuments alone did not provide full coverage around the telecope. For the determination of the coordinates of these two points relative to the beacons a number of basic measurements had to be performed.

2.1 Precise Levelling

In a first step levelling was carried out between the three pillars, A, B, C, and the markers on the pedestal, D and E. Unfortunately, it was assumed that the pillars had been stable over the years and the height difference to the SLR pad (O) was not observed. After analysis of the levelling data it turned out that the resulting height values of the pillars were quite contradictory, not for measurement reasons, which are quite accurate, but for the results. In order to resolve the discrepancies we decided to fix the heights of pillar B and of marker D at the values of 1988. The reasons for this decision were a) that the relative heights of only these two points stayed identical to the 1988 values and b) that we want to

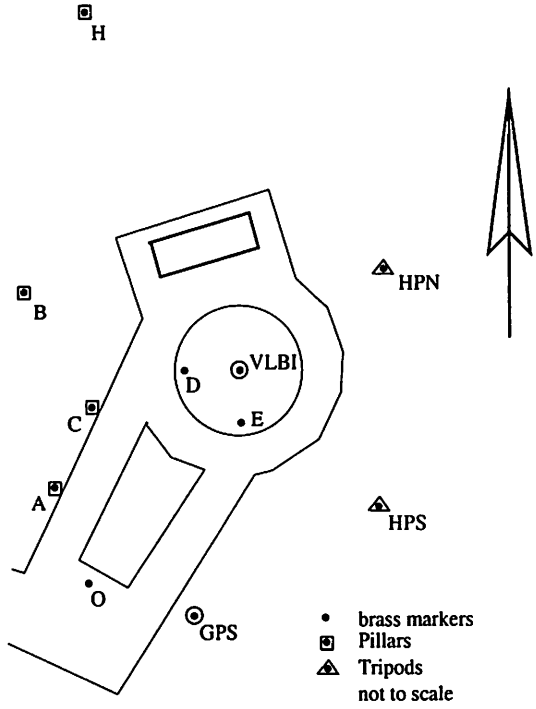

Figure 1: Layout of Medicina control network.

determine a height change of the telescope which places special importance on the identity of marker D. The height change can be computed from the heights relative to marker D which is located on the pedestal and should, therefore, have encountered the same long term movements as the telescope itself. Table 1 contains the height components of the pillars and markers.

Table 1: Results of precise levelling

Point	1988 Height [m]	1998 Height [m]	Difference [mm]
A	2.1320	2.1377	+5.7
B	2.0586	2.0586	-
C	2.1452	2.1466	+1.4
D	1.9421	1.9421	-
E	1.9449	1.9414	-3.5

Normally, one would expect that survey beacons only show a tendency of subsidence and an increase in height may be impossible. However, there may be two reasons why an uplift could be possible. The first one is that the marker on top of the pillar may have been modified for some other measurements (TOMASI, pers. communication) which may be a reasonable assumption for pillar A with such a large positive height difference. The second reason could be the elastic response of the soil close to a heavy mass like the telescope pedestal which sinks and at the same time presses soil to the outside causing an uplift next to the telescope (GUEGUEN, pers. communication). This may well be the case for pillar C.

The subsidence of brass marker E which is located on the south edge of the telescope's pedestal may be an indication that the pedestal has not subsided directly vertically but that some tilting has occured. However, without a third reference point on the pedestal the position angle of the major tilt axis cannot be determined.

2.2 Triangulation and Trilateration

For the determination of the VLBI reference point the existing network had to be checked and the two auxiliary points, HPN and HPS, had to be linked in. For this purpose, conventional triangulation and trilateration of points A, B, C, D, H, HPS and HPN was carried out. Each point was occupied with a

Wild TC1600 tachymeter and distances and directions were measured to almost all other points. Only the line between point B and auxiliary point HPS was not observed since the control building blocks the view. In addition, the monumentation of the permanent GPS antenna was measured to be determined by intersection.

The analysis of the observations was carried out with the least squares adjustment program PANDA (GEOTEC 1998). In a first step a free network adjustment was computed. The results of this analysis indicated that the measurements were performed with high accuracy and that coordinates with formal errors at the 1 mm level had been achieved. However, a comparison with the 1988 coordinates and distances also showed that the reference network was not as stable as anticipated and displacements of the pillars must have occured at the several millimeter level. Most prominent was the difference for pillar A where a modification of the marker had already been suspected for the extra-ordinary positive height change.

With such a small number of common points at the two epochs and in the absence of a point which could be assumed as being unchanged over the years, a compromise for the datum of the 1998 network had to be sought. Similar to the considerations made for the height determination one of the most important aspects is that the aim of these measurements is the determination of the relative displacement of the VLBI reference point. Therefore, marker D on the pedestal of the telescope is considered to be the point onto which the 1998 coordinates could best be projected. The 1988 coordinates of marker D were, therefore, carried over to 1998. In addition, the coordinate translations for point D necessary to shift the 1998 results of the initial adjustment to the 1988 coordinates were then used for fixing the datum by applying a rectangular translation to the initial coordinate results of all other points to transform them onto the 1988 values as best as possible.

Table 2 contains the topocentric coordinates of all fixed beacons used in 1998. The 1988 coordinates are taken from CENCI et al. (1988) after a fixed offset of 1000 m in the north and east components was added to have only positive numbers. The coordinates of the initial 1998 solution were translated onto the 1988 datum by fixed offsets in the north and east components as described above.

Table 2: Topocentric coordinates of pillars

	1988		1998		Difference	
Point	East [m]	North [m]	East [m]	North [m]	East [mm]	North [mm]
A	992.0877	1024.9403	992.0703	1024.9355	-17.4	-4.8
B	987.6672	1067.4279	987.6681	1067.4405	0.9	12.6
C	1001.8831	1042.5173	1001.8881	1042.5196	5.0	2.3
D	1025.3524	1050.6353	1025.3524	1050.6353	-	-
H			999.7434	1124.2031		
GPS			1025.6874	991.0410		

Assuming the datum as described above the final least squares adjustment with no further constraints yielded the coordinates of the pillars and the temporary points for the subsequent determination of the VLBI reference point as listed in table 3.

Table 3: Topocentric coordinates and formal errors of beacons used for telescope measurements; * estimated

Point	East [m]	F.E. [m]	North [m]	F.E. [m]	Height [m]	F.E. [m]
A	992.0703	±0.0003	1024.9355	±0.0004	2.1416	±0.001
B	987.6681	±0.0003	1067.4405	±0.0004	2.0593	±0.001
HPN	1069.7866	±0.0003	1074.7981	±0.0004	0.4573	±0.002*
HPS	1065.6466	±0.0003	1018.4515	±0.0004	0.5622	±0.002*

3 Telescope measurements

For an alt-azimuth antenna the VLBI reference point is the intersection of azimuth and elevation axis. If they do not intersect, as is the case at Medicina, it is the point of the azimuth axis where the distance to the elevation axis is smallest. When rotating in azimuth each end point of the elevation axis ideally describes a circle about the VLBI reference point. The average height of the two end points represents

the height of the VLBI reference point. In order to determine the reference point at Medicina, the end points of the elevation axis were materialized by a small screw mounted on a metal bar which in turn was temporarily mounted onto the bearing structures at both ends of the axis. Determining the 3D positions of these markers at different positions will subsequently permit the computation of the VLBI reference point as the center of the circles.

On the ground, beacons A and B together with the temporary points HPN and HPS were then occupied pairwise with a Wild T2 theodolite and a Wild TC1600 tachymeter for trigonometric intersection and trigonometric levelling. In order to check whether the target marks were mounted centric and indeed represented the elevation axis, several measurements were made at a fixed azimuth but varying elevation angles for computations of 3D coordinates by horizontal and vertical angles. Both targets did not show any movements larger than 1.5 mm both in the horizontal nor in the vertical component. Since 1.5 mm is just above the noise floor of the measurement accuracy the excentricities can safely be ignored.

For the determination of the end points of the declination axis at different azimuth positions of the telescope, the antenna was driven in azimuth into positions where the pairs of instruments could aim at the markers. Often the markers were obstructed by metal beams and the telescope had to be moved in incremental steps until the markers became visible. 17 azimuth positions were observed for the marker of the right end of the elevation axis and 16 measurements were successful for the left target. In all positions horizontal directions and zenith distances were observed with both theodolites as well as reference directions relative to point H. All measurements were carried out in double-sighting in order to eliminate collimation errors and errors of the transverse axis.

In the analysis the trigonometric intersects provided horizontal coordinates in the frame of the local coordinate system. The accuracy of the points were computed with the error propagation law resulting in errors in the coordinate components of the axis end points of 1 - 4 mm RMS.

4 Determination of VLBI Reference Point

Under the assumption that the telescope rotates around a central azimuth axis the end points of the elevation axis should describe circles around this axis. The radii of these circles need not necessarily be identical since they depend on the location where the target marks are mounted. Taking the coordinates of the end points at different azimuth positions as inputs two least squares adjustments can be performed solving for the coordinates of the centers and the radii of the circles. Table 4 lists the coordinates and radii of the targets at the left (TL) and at the right end of the elevation axis (TR). The weighted averages of the two materializations are taken as the final coordinates of the VLBI reference point in the local system for the 1998 epoch. In addition, for each of the horizontal positions the trigonometric levelling yielded height values. Averages of these were formed to determine the average heights of the target marks. The heights of target TL and target TR may differ slightly due to inaccuracies in the construction of the telescope. The magnitude and the scatter of the residuals do not show any significant systematics and confirm the small formal errors of the parameters.

Table 4: Parameters of the circles fitted to the series of positions with their formal errors and the final coordinates in the local system

Target	East [m]	F.E. [m]	North [m]	F.E. [m]	Radius [m]	F.E. [m]	Height [m]	F.E. [m]
TL	1035.2545	±0.0004	1050.6651	±0.0005	7.1537	±0.0003	17.7390	±0.0010
TR	1035.2536	±0.0004	1050.6657	±0.0004	7.1497	±0.0003	17.7378	±0.0007
W. Avg.	1035.2541	±0.0003	1050.6654	±0.0003			17.7382	±0.0007

5 Displacement

One of the environmental factors which has to be considered in addition to the purely geometrical circumstances is thermal expansion. The metal structure up to the elevation axis is 15.8 m high. During the measurements the ambient temperature increased from 9° C in the morning to 20° C in the afternoon. Assuming a time lag of 2 hours which are needed for the ambient temperature to migrate into the metal and actually causing the expansion (NOTHNAGEL et al. 1995) the average temperature for the time of the measurements was 13.5° C. In 1988 the measurements were carried out on July 11 and 12. Here, the temperature increased from 27° C at 10:00 in the morning to 33° C at 15:30 in the afternoon resulting in an average temperature of 30° C.

With an expansion coefficient for steel of 1.2×10^{-5} a one degree C increase causes a height increase of 0.2 mm. The temperature difference of 16.5° C, thus, results in a 3.3 mm height correction which has to be added to the 1998 height in order to determine the height difference at the same temperature. In table 5 3.3 mm are, therefore, added to the 1998 height value in table 4.

From the three dimensional coordinates of the VLBI reference point before and after the repair work, the displacement can be computed by simple differencing. Table 5 contains the final coordinates of both measurements together with their errors as well as the displacement in the local coordinate system. In view of the assumptions which had to be made with respect to the long term behaviour of the beacons (see 2.2) the formal errors of the horizontal components of the 1998 measurements as listed in table 4 are not representative and were, therefore, inflated by quadratically adding 2 mm to each formal error. The vertical component was left unchanged. For the 1988 coordinates the accuracies had to be estimated since they are not available from the reference (CENCI et al. 1988).

Table 5: Displacement of VLBI reference point = Difference in local coordinates of 1988 and 1998 (* estimated) at a reference temperature of 30°C

Target	East [m]	F.E. [m]	North [m]	F.E. [m]	Height [m]	F.E. [m]
1988	1035.2500	±0.0020*	1050.6680	±0.0020*	17.7230	±0.0020*
1998	1035.2540	±0.0020	1050.6654	±0.0020	17.7415	±0.0007
Displ.	0.0040	±0.0028	-0.0026	±0.0028	0.0185	±0.0021

6 Discussion

There are several aspects which deserve some considerations with respect to the local surveys which have been and which will be carried out at the Medicina radio telescope and its control network in the direct vicinity. Although two of the beacons are founded as deep as 22 m the soil of the Po-plains does not in any respect form an adequate foundation for a stable control network. Even with a larger number of pillars there will always be the dilemma of not being able to discriminate a stable reference. The only solution to this is a regular monitoring of a few of these beacons within a so-called footprint measurement (e.g. COMBRINCK 2000) connected to a more stable part of the Apenin.

Since the measurements carried out in 1988 and the ones reported here lack the respective links, some compromise is necessary in order to still achieve some meaningful results. The assumption that the brass marker at the pedestal of the telescope (D) has not changed its position relative to the foundation of the telescope is quite plausible. In addition, since this marker is the closest marker to the VLBI reference point observed in the 1998 measurements it is quite practical to link all results to this marker. The orientation of the control network may have an uncertainty which is caused by possible errors of a few millimeters of points A and C. However, since the network hinges on point D the lever arm to points A and B of about 40 m scales down by a factor of about 4 when the respective rotation is computed for the VLBI reference point. The largest effect is then in the north component of the VLBI reference point while the east component is hardly affected. For this reason, the horizontal displacement in the north component between 1988 and 1998 has to be treated with caution and may not be significant.

The vertical change, on the other hand, is much more reliable. Again referred to marker D the direct height relationship between 1988 and 1998, this time in only one dimension, is established within the accuracy as indicated by the formal errors.

One other factor which also deserves some discussion is the subsidence of brass marker (E) of 3.5 mm on the south-east side of the pedestal. As mentioned already only a third height reference on the pedestal would give an indication of the main axis of subsidence. Assuming that maximum subsidence occurs at the southern edge while the northern edge has remained stable the pedestal would be tilted by 38". At the height of the VLBI reference point of 15.8 m this would correspond to a shift of 2.9 mm to the south which agrees quite favourably with the displacement of 2.6 mm from table 5.

Contrary to these arguments there is another fact which was reported by TOMASI (pers. communication). Prior to the track repair the azimuth axis was apparently tilted by 35" at an azimuth of about 120° which was corrected with the new track. The correction would result in a displacement of the reference point by 2.3 mm to the west and 1.3 mm to the north.

Finally, the displacement computed here can be compared to those estimated from VLBI observations. HAAS ET AL. (2000) quote displacements of 2.2 ± 1.8 mm to the west, 2.1 ± 1.9 mm to the north and 18.1 ± 10.0 mm in the up component. The agreement in the up component is quite striking although

the VLBI determination is weakest for this component. The horizontal components appear to be in opposite directions. However, from a statistical point of view the horizontal VLBI displacements are only marginally significant.

All in all the information on the horizontal displacement available is quite contradicting for several reasons. The pillars and reference points around the telescope as a basis for the 1998 measurements have not been stable over the last 10 years. Secondly, the 1988 measurements do not provide error estimates of the coordinates determined in those days inhibiting a proper judgement of significance. At least the theory of the 35" tilting agrees quite well with the VLBI results and may be an indication that this is the most probable magnitude and direction of the horizontal displacement.

References

Cenci A., G. Vicomanni, G. Bianco (1988) *Determination of the invartiant point and of the axes offset for the VLBI antenna at Medicina*, Telespazio, Roma

Combrinck L. (2000)*Local surveys of VLBI telescopes*, IVS 2000 General Meeting Proceedings, N.R. Vandenberg and K.D. Baver (eds.), NASA/CP-2000-209893, Greenbelt MD, 118-127

Del Rosso D., F. Ambrico (1995) *Survey of the Medicina site - September 1995*, Nuova Telespazio, Roma

Geotec (1998) *Panda für Windows, Version 2.12*, Systemhandbuch, GeoTec GmbH, Laatzen

Haas R., A. Nothnagel, D. Behrend (2000) *VLBI determinations of local telescope displacements*, IVS 2000 General Meeting Proceedings, N.R. Vandenberg and K.D. Baver (eds.), NASA/CP-2000-209893, Greenbelt MD, 133-137

Nothnagel A., M. Pilhatsch, R. Haas (1995) *Investigations of thermal height changes of geodetic VLBI telescopes*, Proc. of the 10th Working Meeting on European VLBI for Geodesy and Astrometry, R. Lanotte and G. Bianco (eds.), Matera, 121-133

GPS and classical survey of the VLBI antenna in Medicina: invariant point determination

Sarti P.*, Vittuari L.*, Tomasi P.**

(*) DISTART – Topografia e Geodesia, Università di Bologna
(**) Istituto di Tecnologia Informatica Spaziale, Consiglio Nazionale delle Ricerche – Matera

Abstract

During a three days measurement campaign we have used both classical topographic methods and GPS technique, following an innovative survey approach, in order to determine the reference point of the VLBI antenna situated at the radioastronomical observatory of Medicina.
We have determined the azimuth axes, the plane containing the elevation axis and the intersection between these to 3-D surfaces (VLBI antenna reference point) with both methodologies within two different reference frames. The azimuth axis expressed as a 3-D straight line within the local reference frame is:

$$\begin{cases} x_{loc} = -5.143 \cdot 10^{-5} z_{loc} + 21.582 \\ y_{loc} = 6.719 \cdot 10^{-6} z_{loc} + 45.534 \end{cases}$$

determined using a couple of total stations and retroreflecting mirrors.
Using GPS technique the azimuth axis, represented as a 3-D straight line in a reference system translated of $r \equiv (4461000.000, 919000.000, 4449000.000)$ with respect to ITRF97, is:

$$\begin{cases} x = 0.998z - 188.202 \\ y = 0.202z + 484.134 \end{cases}$$

Reference point's coordinates, obtained intersecting the planes π with the corresponding 3-D lines, have been obtained in both local and ITRF97 reference frame:

$$P_{loc} \equiv (21.581 \pm 0.001, 45.534 \pm 0.001, 17.699 \pm 0.001)$$
$$P_{ITRF97} \equiv (4461369.94 \pm 0.01, 919596.83 \pm 0.01, 4449559.16 \pm 0.01)$$

but results obtained using GPS must be considered very preliminary.

Introduction

Measuring and monitoring the stability of the reference point of the VLBI antennae within a local reference network is nowadays a very important task for all the geodetic observatories equipped with VLBI technique. VLBI is able to provide high precision estimates of relevant geodetic parameters and allows the determination of baselines and stations' positions with a few mm accuracy over global scale. The position of the VLBI antenna is expressed using the coordinates of the reference or "invariant" point because its position does not change when the antenna dish is moved both in azimuth and/or in zenith. For antennae with azimuth-elevation mounting (it is usual for single dish radio telescope) this point is located along the azimuth axis of the antenna. It coincides with the intersection of the elevation and azimuth axis if the two axes intersect. If the two axes do not intersect it is the projection of the elevation axis onto the azimuth axis.

Monitoring its stability within a local reference frame is of great importance for understanding the reliability of the VLBI estimates and subtract a possible local motion from the global tectonic motion that has to be measured.
Usually, the approach that has been followed by different research groups for measuring and determining the coordinates of the reference point was based on the use of classical topographic methods. Triangulation and trilateration using theodolites, total stations and other high precision devices have been promising and rewarding methods (Tomasi et al., Nothnagel et al. Bianco et al.). Nevertheless, basing the determination on this approach can be very time consuming (a minimum of three days must be taken into consideration) and it requires a complete inactivity of the VLBI antenna. We have therefore pursued the same task using GPS measurements, expecting lower precisions but performing a bulk number of observations in much shorter time (a few hours).

Field operations and measurements

In order to assure a complete and straightforward 3-D determination of the reference point surveyed from the local network we have modified the pillars' tops inserting a forced 3-D centring device. An extension of the local network toward east by means of daily installed tripods has been necessary in order to assure measurements on both sides of the antenna. Figure 1 shows a comprehensive view of the ground local control network.

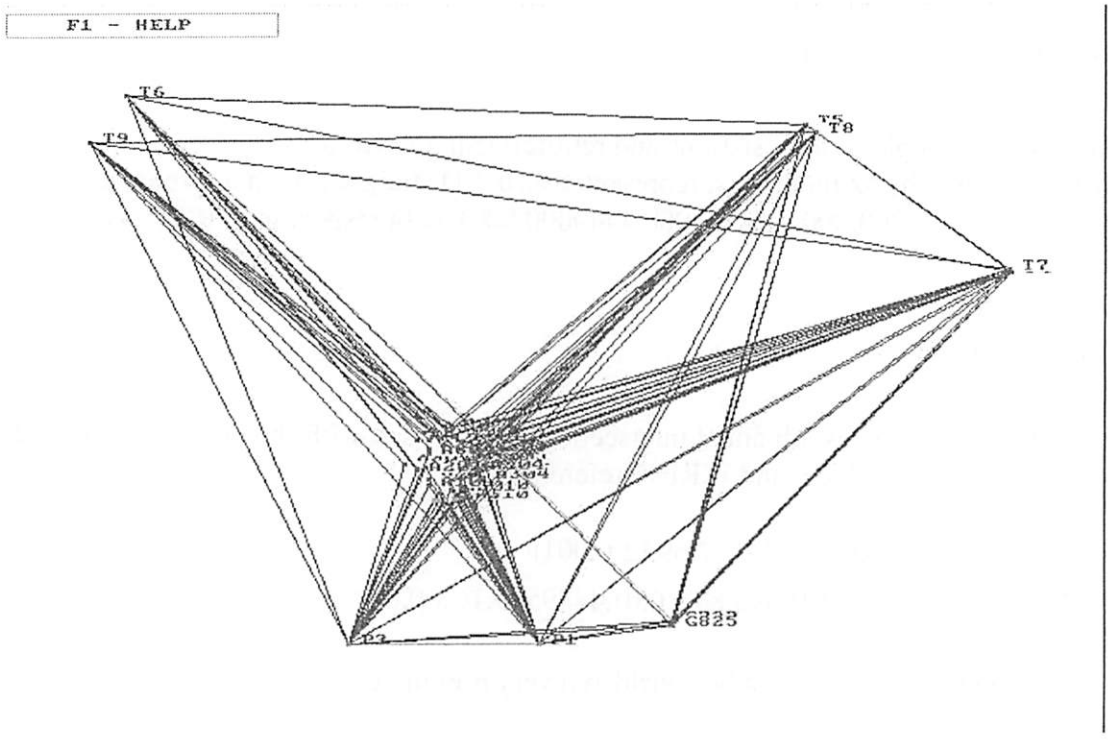

Figure 1: the local control network

Classical topographic measurements have been carried out using two high precision Leica total stations: one TCA2003 (with automatic target recognition device) and one TC2003. Every control point (fig.2) has been observed using triangulation and redundant forward intersection. Only retroreflecting mirrors have been used in order to obtain the highest accuracy on distance determination. Tribrachs and other high precision devices have been also employed. Eight mirrors

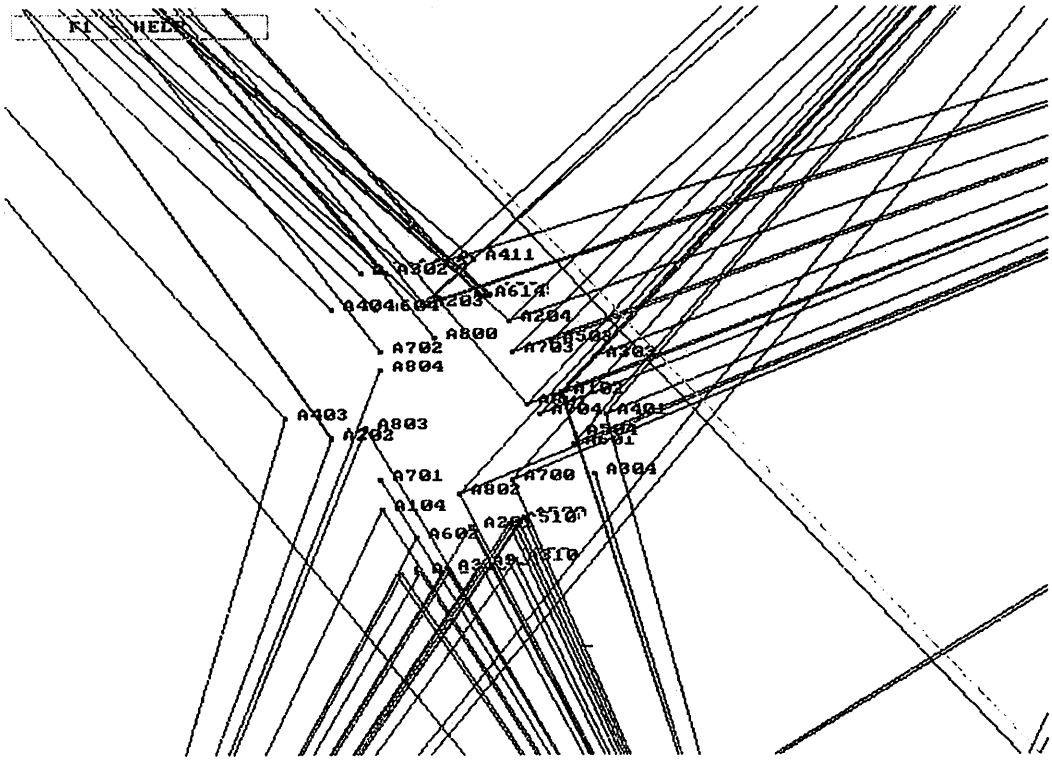

Figure 2: the control points on the VLBI antenna

have been placed on the antenna structure, distributed on both the azimuth-zenith rotating part (integral with the antenna dish) and the azimuth-only rotating part. The antenna has been rotated with stepwise intervals into six different azimuth positions at a fixed elevation. For each position every visible target has been collimated and measured. While rotating in azimuth the different points are contained in an equal number of planes and describe a circle whose centre is the intersection of the azimuth axis with these planes. Identically, for a fixed azimuth position, a rotation in elevation of the VLBI dish determines a rotation of the mirrors and each mirror therefore individuates a corresponding plane containing its rotation and whose centre is the intersection between the plane and the elevation axis.
Once these centres have been determined, following a 3-D analytical geometry least squares approach the plane containing the elevation axis is determined and its intersection with the azimuth axis is calculated thus obtaining the coordinates of the reference point.
A similar approach has been followed using five double frequency GPS receivers, acquiring data every second. Two GPS antennae have been placed on almost opposite sides of the antenna dish (approximately parallel to the elevation axis, figg.3b,3c), using a specially designed device (fig. 3a) that rotates around an axis that contains the phase centre and maintains the GPS antenna horizontal while the VLBI dish moves in elevation.

Data processing

Classical data have been processed using STAR*NET 3-D least squares adjustment software from Starplus Software Inc.. We have obtained 95% confidence error ellipses with semi-axes within a range from 1 to 3 mm. Results have been obtained in a local reference frame having a planimetric origin in pillar P3 and the altimetric origin in point G7; bearing has been fixed from pillar P3 to pillar P1.
GPS data have been analysed using Geotracer V.2.29a and data pre-analysis has been performed using Terrasat GPS-edit. For each roving GPS antenna the position has been calculated from three different reference stations. Validation of results has been carried out comparing the stability of the value of the reciprocal distance between the two roving GPS antennae, as computed from simultaneous independent solutions (i.e.: distance calculated for antenna 1 from reference station A

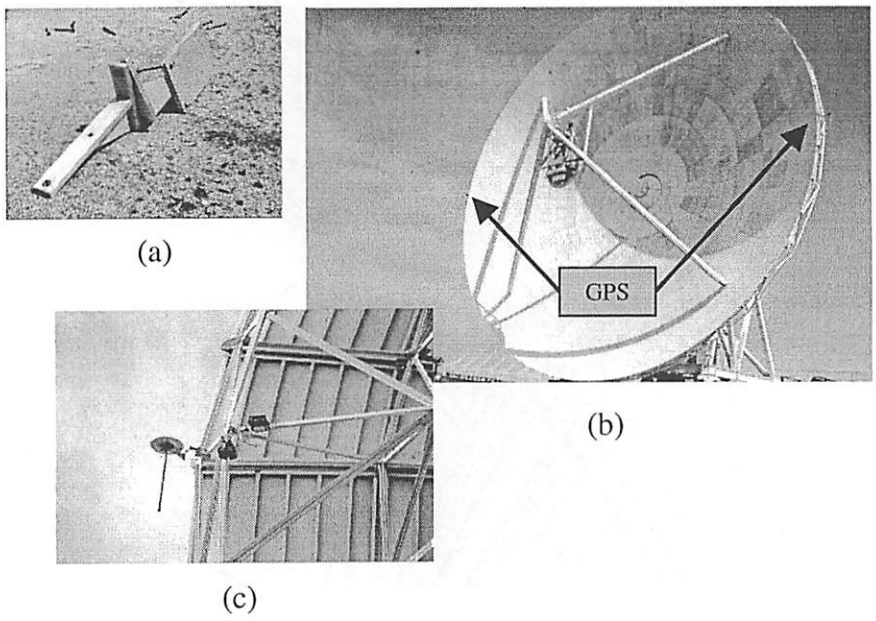

Figure 3: GPS antennae on the VLBI dish

and the simultaneous antenna 2 position obtained from reference station B). A further comparison that can be affected by cycle slips occurred at one roving antenna, is based on the calculation of the position of a single antenna by two different reference stations (Fig.4).

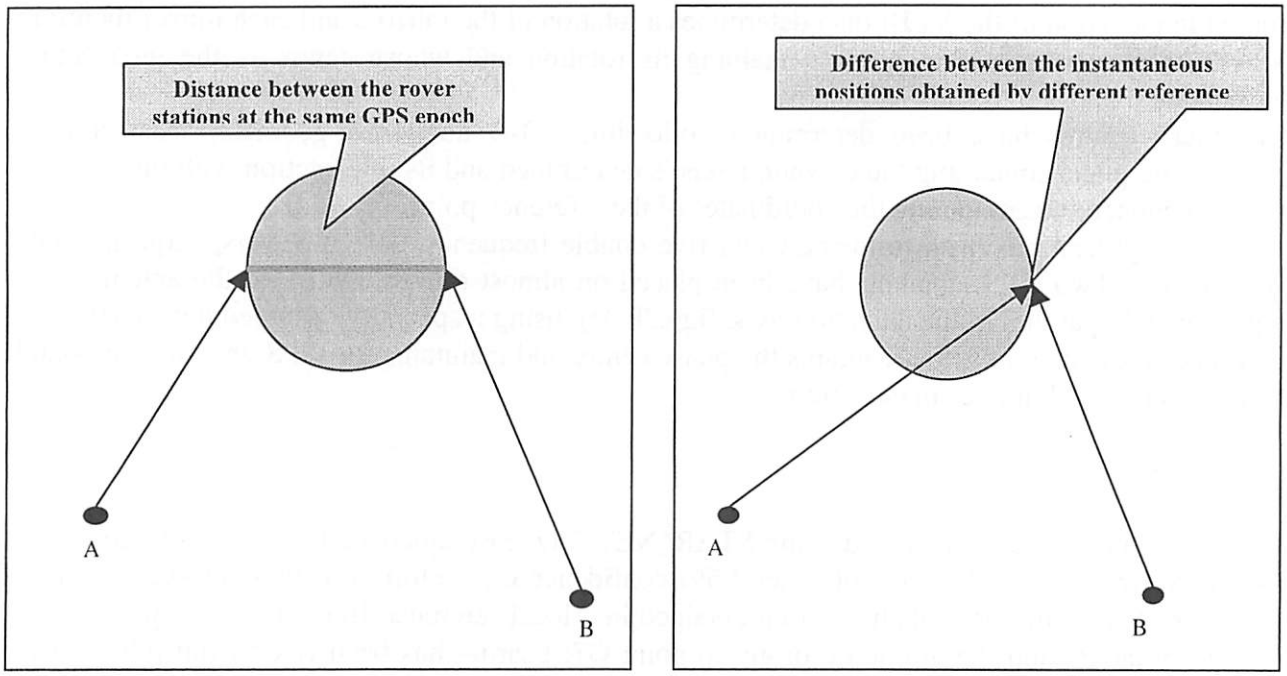

Figure 4: GPS observation schemes

With both sets of results we have started a post-processing analysis based on a 3-D least squares analytical geometry approach. We have extracted the positions of the rotating point describing the same circle and using those position we have calculated the best fit plane containing that circle. Once the 3-D plane has been obtained its coefficients have been used in order to estimate the

parameters (radius and centre's coordinates) of the best fitting circle resulting from the intersection of the best fitting sphere containing the points and the plane itself. The circle's centre coordinates represent the best fit position of different points belonging to the rotation axes of the VLBI antenna. In order to give a mathematical result the azimuth axis has been expressed as 3-D straight line. They have been calculated with a 2-D best fit approach using the projection of all the circle's centres on two of the three co-ordinated planes.

Results

Results obtained from the classical data processing and post-processing expressed in the local reference frame are:

$$\begin{cases} x_{loc} = -5.143 \cdot 10^{-5} z_{loc} + 21.582 \\ y_{loc} = 6.719 \cdot 10^{-6} z_{loc} + 45.534 \end{cases}$$

$$P_{loc} \equiv (21.581 \pm 0.001, 45.534 \pm 0.001, 17.699 \pm 0.001)$$

Using GPS technique the azimuth axis, represented as a 3-D straight line in a reference system translated of $r \equiv (4461000.000, 919000.000, 4449000.000)$ with respect to ITRF97, is:

$$\begin{cases} x = 0.998z - 188.202 \\ y = 0.202z + 484.134 \end{cases}$$

Reference point's coordinates, obtained intersecting the planes π with the corresponding 3-D lines, have been obtained in both local and ITRF97 reference frame:

$$P_{ITRF97} \equiv (4461369.94 \pm 0.01, 919596.83 \pm 0.01, 4449559.16 \pm 0.01)$$

but results obtained using GPS must be considered very preliminary.
In fact, despite very promising internal consistency of the large amount of GPS data acquired, the results must best more accurately post-processed and the statistical approach used for results validation must be optimised. The GPS kinematic approach for VLBI antenna's reference point determination is far from be standardized and a bulk amount of work has to be done in order to permit a proper processing of such a large amount of data. The results shown above are indeed obtained processing only a subset of the acquired and available data.

Conclusion

The classical methodology demands a heavy amount of time in order to perform measurements but the use of high precision automatic target recognition device has made field operation relatively faster avoiding the slow procedure of target collimation. It requires only a first scheduling of observation of the points composing the strata and the subsequent measurements are carried out automatically. The data processing is well known and standardized and results have fulfilled the high precision standards that are usually required. Nevertheless the procedure itself is slow and requires long VLBI antenna inactivity.
On the other hand, GPS approach has required a much faster survey and permits the acquisition of a much larger set of data. Results are not as precise as those obtained with the classical approach and this influences also the post processing step. The consistency of the method is based on a proper statistical approach that can take advantage of the large amount of measurements performed and the

first results obtained are very promising. Furthermore the methods allows a direct determination of the reference point within the ITRF.
Both methods require a careful post processing of the results which is not standardized and is based on a proper 3-D analytical geometry least squares approach.

Bibliography

Bianco, G., A. Caporali, A. Cenci and G. G. Vicomann, 1990; "Geodetic Connection of the SLR Pad to the VLBI Antenna at Medicina" Proc. 4th Int'l Confr. WEGENER/MEDLAS Project, T. U. Delft, pp. 67-78.

Nothnagel A. and Binnenbruck B., 2000; "1996 Displacement of the Medicina radio telescope determined by local surveys" Proceedings of the 14th Working Meeting on European VLBI for Geodesy and Astrometry, Castel San Pietro Terme (Bologna), Italy, 8-9 September 2000

Tomasi P., Sarti P., Rioja M.J., 2000, "The determination of the invariant point of the VLBI antenna in Ny Ålesund" Accepted and to be published on 54th Special Issue of Memoires of National Institute of Polar Research, Japan.

Establishing a new GPS-VLBI tie at Ny Ålesund

Rüdiger Haas, Sten Bergstrand, Jan M. Johansson

Onsala Space Observatory, Chalmers Centre for Astrophysics and Space Science, SE-439 92 Onsala (Sweden)

Contact author: Rüdiger Haas, e-mail: haas@oso.chalmers.se

Abstract

During July 16-31, 2000 we performed a project to establish a new GPS-VLBI tie at the Ny Ålesund Space Geodetic Observatory on Svalbard archipelago (Norway). This new tie was established by attaching a GPS choke-ring antenna near the vertex position of the 20 m VLBI telescope and installing the necessary receiver and cable connections. In this paper we describe the field work done during our stay at Ny Ålseund and we present first results from the analysis of the GPS data acquired between July and September 2000.

1. Introduction

The Ny Ålesund Space Geodetic Observatory plays an important role for the International Terrestrial Reference Frame (ITRF) due to its northern location and the availability of collocated space geodetic techniques, especially Very Long Baseline Interferometry (VLBI) and the Global Positioning System (GPS). The precise knowledge of the local geodetic tie between the GPS and the VLBI reference points and the monitoring of its stability over time is of particular importance for the maintenance of the ITRF. Furthermore it is a crucial prerequisite for a combined use and interpretation of VLBI and GPS data for geophysical and geodynamical studies. Therefore, our project was to establish a new tie by installing a permanent GPS-antenna on top of the VLBI telescope itself. The funding of our project was granted under the Access to Research Infrastructures Activity of the Human Potential Programme of the European Community. The necessary hardware to establish the new tie was supplied by the Norwegian Mapping Authority (NMA).

2. Desired characteristics of a new GPS-VLBI tie

Before applying for access to the Large Scale Facility Ny Ålesund, we discussed the desired characteristics of a new GPS-VLBI tie. We defined that the new tie should be independent with respect to other possible realisations in order to produce complementary results. It should be frequently repeatable and in the ideal case a permanent monitoring of the tie should be possible. Furthermore, the measurement of the tie should be more or less automatic and independent of weather conditions. From these considerations and our experience with a similar project at the Onsala Space Observatory conducted during 1999, we concluded to install a permanent GPS-antenna on top of the VLBI telescope itself in order to establish the new tie. To guarantee high accurate measurements we decided to design a fixed attachment instead of a movable one using for example a gimbal system. Positioning the VLBI telescope in its stow-position during the times it is not used for geodetic VLBI will ensure that the GPS-antenna always gets back into the same position.

3. Installing the GPS equipment

In contrast to the 20 m telescope at Onsala, the 20 m telescope at Ny Ålesund is not a secondary focus antenna but a prime focus one. Therefore, a position near the vertex of the parabola turned out to be the ideal location to install a GPS-antenna. A 30 cm high aluminium antenna mounting device was produced prior to our travel to Svalbard at a workshop at Chalmers University of Technology (Fig. 1). This mounting device can be attached to the thedolite mount near the vertex position of the parabola and hold a usual Wild tribrach for the mounting of a choke-ring GPS-antenna (Fig. 2). The GPS-antenna was horizonted using the level of the Wild tribrach while the 20 m telescope was pointed to its stow-position at 88.5 degree elevation. Figure 3 shows the GPS-antenna mounted on the VLBI telescope. Though the telescope is not pointed exactly to zenith (90 degree elevation) in its stow-position, it is positioned in a stable parking position that avoids to great extend slight wiggling due to wind forces. We oriented the GPS-antenna towards north using the special marking on it and a compass. First we tried to re-use an already existing cable on the telescope that was not used anymore in order to connect the Ashtech choke-ring GPS-antenna with the Ashtech Z-surveyor GPS-receiver situated in the control building of the Geodetic Observatory. Unfortunately this cable turned out to be damaged and therefore we had to install a new piece of cable. Both, the GPS-antenna and the GPS-receiver were supplied by NMA. Since July 19, 2000, GPS-data are

Figure 1. The aluminium antenna mounting device equipped for test purposes with tribrach and GPS-antenna.

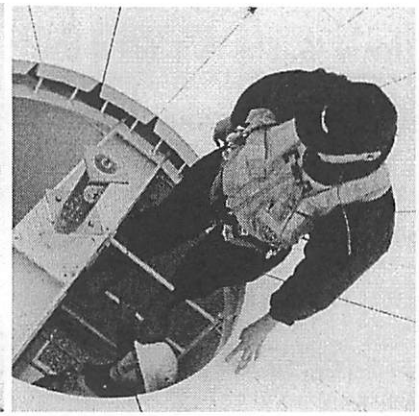

Figure 2. Attaching the antenna mounting device for the GPS-antenna NVTX to the thedolite mount.

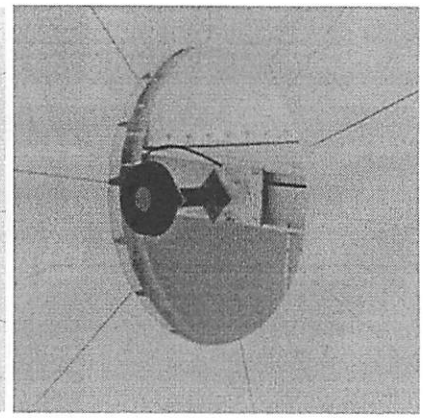

Figure 3. GPS-antenna NVTX mounted on the VLBI telescope.

recorded with this antenna/receiver combination named Ny Ålesund VerTeX (NVTX). Data are recorded with 30 second sampling interval and an elevation cut-off of 15 degrees.

4. Local eccentricity measurements

Since the new GPS-antenna NVTX ontop of the VLBI telescope is situated close to the vertex position of the parabola, it is located with some eccentricity with respect to the geodetic reference point of the 20 m telescope. Latter is the intersection of the azimuth and elevation axes of the telescope. In order to determine the eccentricity we performed a classical geodetic survey. The coordinates of the reference point of the VLBI telescope and the coordinates of the survey pillars surrounding the telescope are given in a local coordinate system by Tomasi *et al.* (2000). We therefore decided to refer the position of the reference point of the GPS-antenna NVTX also to the surrounding survey pillars. This will allow to refer to the results of the measurements performed by Nothnagel *et al.* (2000) in their repeated classical survey project, too, and thus includes inherently a redundant check.

We approached the determination of the horizontal position of the reference point of the GPS-antenna NVTX in the coordinate system of the surrounding survey pillars by measuring forward cuts with two thedolites to a survey target that was set up on the third balcony of the VLBI telescope. This survey target was realised as a bolt of brass attached to a usual tribrach and positioned vertically below the GPS-antenna NVTX when the telescope was in its stow-position (Fig. 4 and 5). The survey target was positioned horizontally using the optical plummet of the tribrach holding the GPS-antenna NVTX. Theodolite measurements with the two theodolites of type Wild T2 available at the Geodetic Observatory were performed from the survey pillars (Fig. 6). Unfortunately, the survey target was only visible from the two pillars #96 and #98. Since the weather conditions were unfavourable with rain and heavy wind the survey target was displaced horizontally which was detected by repeated survey checks. Therefore, the survey target had to be re-positioned and the measurements had to be repeated several times. Nevertheless we finally achieved measurement accuracies for the two angles measured of ± 1 milligon which allows to determine the horizontal position of the GPS-antenna NVTX in the local coordinate system with accuracies of ± 1 millimetre in both horizontal components.

In order to determine the vertical position of the reference point of the GPS-antenna NVTX with respect to the reference point of the VLBI telescope we performed spirit levelling between NVTX and the elevation axis of the VLBI telescope. For this purpose we mounted the levelling instrument Jenoptik Ni002 which was available at the Geodetic Observatory on a mounting device close to the elevation axis on one side of the VLBI telescope (Fig. 7). Then we used an invar levelling metre to determine the vertical distance between NVTX and the levelling instrument (Fig. 8). We also determined the vertical distance between the elevation axis on the opposite side of the VLBI telescope and the levelling instrument using a small metal metre (Fig. 9). Finally the vertical distance between the reference point of NVTX and the elevation axis resulted with an accuracy of better than ± 1 millimetre.

By these classical survey measurements the position of the reference point of the newly installed GPS-antenna NVTX in the local coordinate system and thereby with respect to the reference point of the VLBI telescope is determined with accuracies of ± 1 millimetre in all three components. The coordinates of the reference point of NVTX in the local coordinate system are given in Table 1.

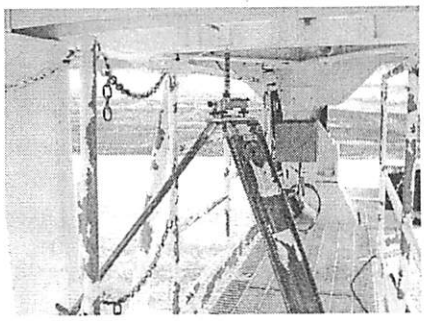

Figure 4. The survey target on the third balcony of the VLBI telescope for the determination of the horizontal position of GPS-antenna NVTX.

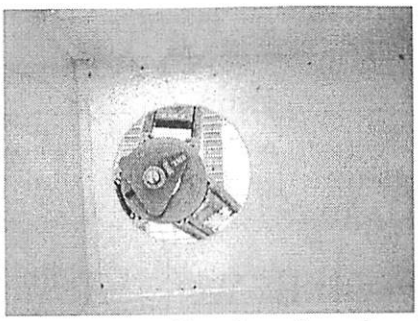

Figure 5. Looking down from the GPS-antenna NVTX to the survey target put up vertically below.

Figure 6. Measuring directions to the survey target from survey pillar #98 using a Wild T2 theodolite.

Figure 7. Spirit levelling with the instrument Ni002 on the third balcony of the VLBI telescope.

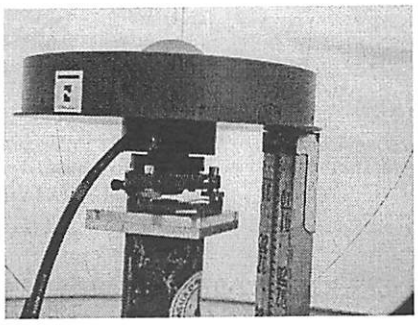

Figure 8. The invar levelling meter at the GPS-antenna NVTX.

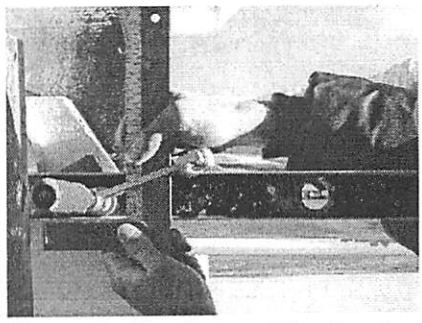

Figure 9. The short metal metre at the elevation axis of the VLBI telscope.

Table 1. Coordinates of the survey pillars #96, #98 and the VLBI reference point (Tomasi *et al.*, 2000) and the coordinates of the reference point of the GPS-antenna NVTX in the same local coordinate system.

	X [m]	Y [m]	Z [m]
#96	21.830 ± 0.001	18.787 ± 0.001	10.269 ± 0.001
#98	21.830 ± 0.001	18.787 ± 0.001	10.269 ± 0.001
VLBI	21.830 ± 0.001	18.787 ± 0.001	10.269 ± 0.001
NVTX	22.221 ± 0.001	18.345 ± 0.001	12.830 ± 0.001

5. GPS-data download, analysis and results

In the second half of our stay in Ny Ålesund we began to work on the download of the GPS-data from the GPS-receiver. The receiver flash card has a capacity that lasts in the setup we use for approximately 14 days of measurements. First we had to configure an old personal computer (PC) available at the Geodetic Observatory that could be used for the download process. Unfortunately it was not possible to install the Ashtech RCS-32 software on this PC which means that a fully automated download and data transfer is not possible. We had to remove the flash card from the receiver and download the recorded data on another computer. David Holland at the Geodetic Observatory gave us great support to make the downloading of the GPS-data working. Now it is possible to log GPS-data directly on the PC that is connected to the GPS-receiver. We agreed with the personnel at the Geodetic Observatory to log GPS-data for time spans of approximately one month before they will send out the data via ftp. Since the analysis of the measurements will always be done in post-processing, this seems a reasonable way to do data logging and to handle the data transfer although it is not automized and requires human interaction.

The aquired GPS-data were analysed with the Bernese GPS-analysis software (Beutler *et al.*, 1996). For this purpose we performed a network solution with the station NVTX and the two permanent GPS-stations NYA1 and NYAL. The new GPS-antenna NVTX receives only slightly less satellite signals than the permanent GPS-antenna NYA1 (Fig. 10 and Fig. 11). Obviously the supporting legs for the primary focus cabin of the VLBI telescope do not hinder satellite tracking seriously.

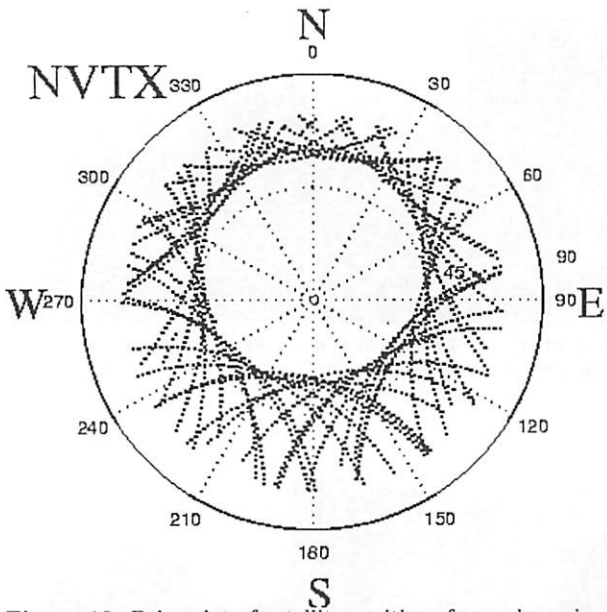

Figure 10. Polar plot of satellite positions from where signals were received by the GPS-antenna NVTX on July 21.

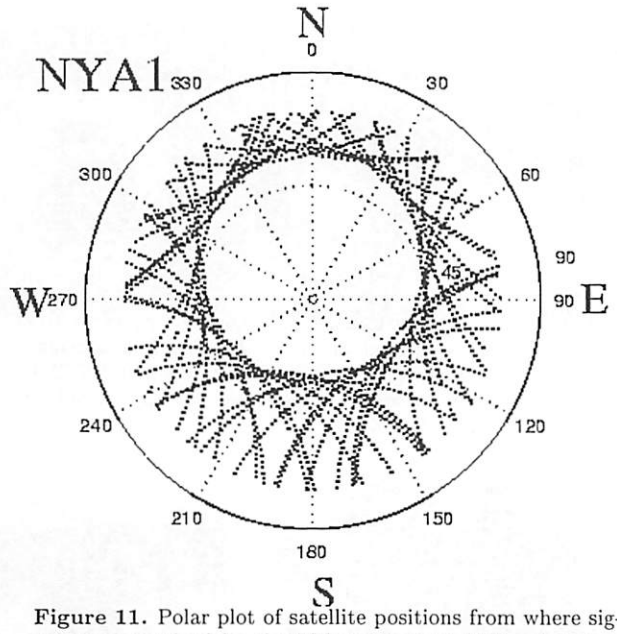

Figure 11. Polar plot of satellite positions from where signals were received by the IGS permanent GPS-antenna at Ny Ålesund NYA1 on for July 21.

Figure 12 shows the phase residuals for L1 and L2 from the analysis with the Bernese software for the baseline NVTX–NYAL on July 21. The low scatter of the residuals without larger systematics reflects the good quality of the GPS-data. Figure 13 and Fig. 14 show the phase residuals versus elevation of the observations on July 21 for NYA1 and NVTX. These results were obtained from analysis with the Gipsy software (Webb and Zumberge, 1993) in precise point positioning (PPP) mode. Both, residuals from NVTX and NYA1 show the typical behaviour to slightly reduce in magnitude with increasing elevation. But the residuals of NVTX have a significantly larger scatter than those of NYA1. This indicates that there is more multipath for NVTX than for NYA1. Nevertheless, the data of NVTX are of high quality and give high quality results on the baseline to NYA1, as shown in Fig. 12.

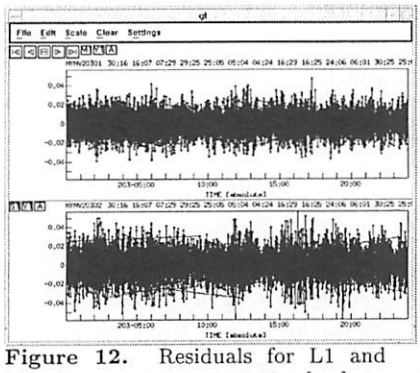

Figure 12. Residuals for L1 and L2 phase measurements in [cm] on the baseline NYA1–NVTX for July 21, analysed with the Bernese software.

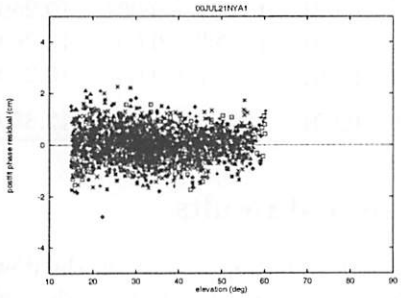

Figure 13. Post-fit phase residuals in [cm] versus elevation in degrees for NYA1 for July 21, analysed with the Gipsy software in PPP mode.

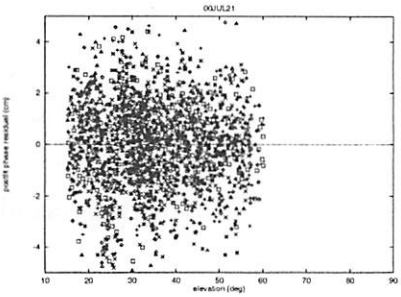

Figure 14. Post-fit phase residuals in [cm] versus elevation in degrees for NVTX for July 21, analysed with the Gipsy software in PPP mode.

NVTX is installed for 70 days with the end of September and we intended to analyse as many days as possible. The days when VLBI experiments were performed at Ny Ålesund had to be excluded of course, since the telescope was moving and therefore the acquired GPS-data cannot be used in a static analysis. Also some days when maintenance work at the telescope was done and when classical geodetic measurements were performed had to be excluded from the analysis. Unfortunately, the data logging program failed for some days therefore received data was lost since the receiver itself has only restricted memory. Finally a total number of 21 observation days remained which could be analysed. Figure 14 shows time series of the north, east and vertical component of NVTX as determined from the small network solution performed with the Bernese software. The repeatability of the measurements expressed as root-mean square errors (rms) are 2.8 mm, 2.1 mm and 5.7 mm for the east, north and vertical component of NVTX, respectively.

The repeatabilities for the permanent station NYAL which is only a few metres apart from NYA1 and has significantly more observation days are much better than those of NVTX. They are 0.2 mm, 0.2 mm and 0.7 mm for the east, north and vertical component, respectively (Fig. 15).

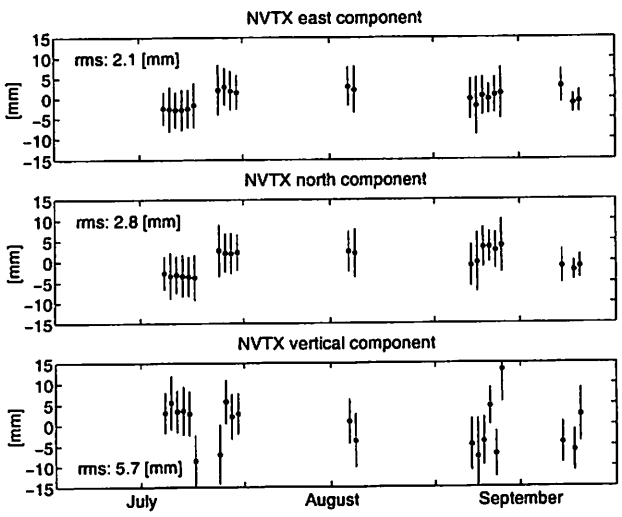

Figure 14. Time series of east, north and vertical component of NVTX between July 21 and end of September 2000.

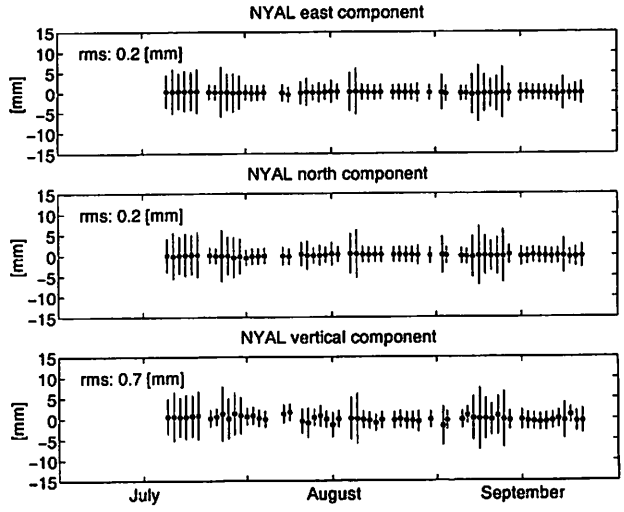

Figure 15. Time series of east, north and vertical component of NYAL between July 21 and end of September 2000.

The results for baseline measurements NVTX-NYA1 and NVTX-NYAL are shown in Fig. 16 and Fig. 17, respectively. The repeatabilities for the two baselines are 1.3 mm and thus stress the good quality of the new GPS-VLBI tie.

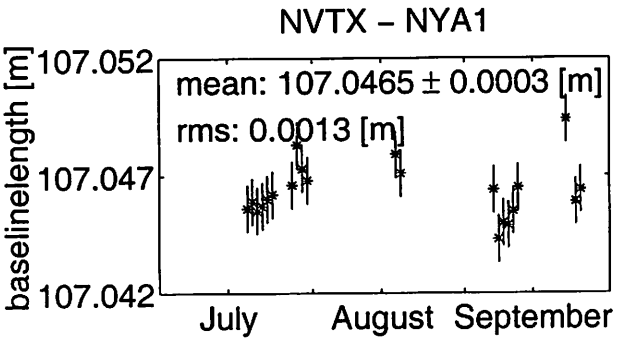

Figure 16. Time series of baseline length measurements between NVTX and NYA1.

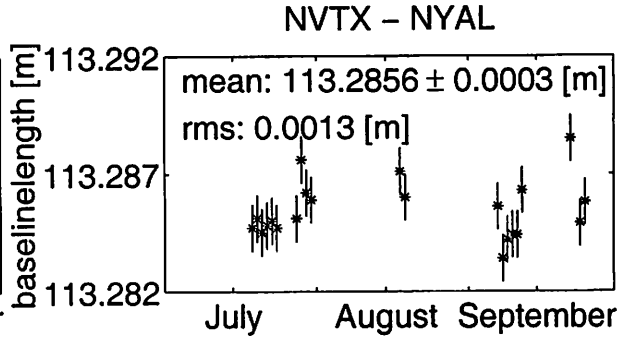

Figure 17. Time series of baseline length measurements between NVTX and NYAL.

Table 2 shows the results for geocentric cartesian coordinates of NVTX, NYAL and NYA1 from the small network solution. To express the reference point of the VLBI telescope in the same coordinate system, we have to transform the eccentricity from the local coordinate system to the geocentric cartesian coordinate system. To do this we need the coordinates of the survey pillars in the geocentric coordinate system. The coordinates of the survey pillars will result from the analysis of a measurement campaign performed by NMA during the summer 2000. Latter analysis is going on right now and therefore we have to postpone the transformation of the eccentricity by some time.

Table 2. Geocentric cartesian coordinates of NVTX, NYAl and NYA1 from the analysis of 21 days between July 21 and end of September 2000.

	X [m]	Y [m]	Z [m]
NVTX	1202463.4203 ± 0.002	252735.0870 ± 0.002	6237768.7383 ± 0.002
NYAL	1202430.5964 ± 0.002	252625.6676 ± 0.002	6237767.5407 ± 0.002
NYA1	1202433.9151 ± 0.002	252632.2571 ± 0.002	6237772.5513 ± 0.002

6. Discussion and outlook

The results for the position of the newly installed GPS-antenna NVTX on the VLBI telescope at NY Ålesund are very promising. The position of NVTX could be determined with repeatabilities of roughly 3 mm, 2 mm and 6 mm for the east, north and vertical component from 21 days of observations between July 21 and end of September. Though we found a higher level of phase residuals than for the permanent GPS stations at Ny Ålesund, the quality of the acquired GPS-data is high. Baseline measurement in the small network have repeatabilities of 1.3 mm which proves the high quality of the new GPS-VLBI tie.

The transformation of the eccentricity values of NVTX with respect to the reference point of the VLBI telescope into a geocentric coordinate system has to be postponed for some time until a recent measurement campaign by NMA is analysed. When these results get available we can also determine the position of the VLBI reference point in the same coordinate system as the reference points of the permanent GPS stations.

Unfortunately some of the acquired data between July and September could not be used in our static analysis since the VLBI telescope was moving for example due to VLBI experiments or maintenance work. There were also eventually data gaps of several hours due to data logging problems and those data have not been used so far in our analysis. There may be a chance to identify more precisely those periods when the telescope has been in stow-position and to rescue some of the data that have been left out so far from the analysis. This will require close cooperation with the personell at the Geodetic Observatory to point out periods that could be used and those that cannot be used.

Furthermore we also plan to analyse data that has been aquired during VLBI experiments in a kinematic way. Toghether with the elevation and azimuth readings from the VLBI logfile of the specific experiment, this approach may open the possibility to determine the VLBI reference point via fitting a sphere to the determined positions of NVTX. This would mean a determination of the local geodetic ties between the GPS and VLBI reference points without being dependent on the local eccentricity measurements. We also like to compare our results to results obtained by classical geodetic survey methods.

We are looking forward to continue acquiring GPS-data from NVTX in order to monitor the time stability of the geodetic tie. Since a radome was installed by Helge Digre recently at NVTX we expect that we will see some change in its position from our analysis, especially for the vertical component. The possible purchase of a new PC for data logging and transferring by NMA would make the data transfer more easy and reliable and help to acquire more data from NVTX.

Acknowledgements

This work was supported by LSF grant number NMA-23/2000. We would like to thank Helge Digre and David Holland for their help and support for our project. Rüdiger Haas is supported by the European Union under contract FMRX-CT960071.

References

[1] Beutler, G., E. Brockmann, S. Fankhauser, W. Gurtner, J. Johnson, L. Mervart, M. Rothacher, S. Schaer, T. Springer and R. Weber: Bernese GPS Software Version 4.0, 1996.

[2] Haas, R., S. Bergstrand and J. M. Johansson: A new GPS-VLBI tie at Ny Ålesund, Application to LSF Ny Ålesund, 2000.

[3] Nothnagel, A., C. Steinforth, and R. Haas: Conventional survey tie between VLBI and GPS reference points at Ny Ålesund, Application to LSF Ny Ålesund, 2000.

[4] Tomasi, P., P. Sarti, and M. Rioja: The determination of the "invariant point" of the VLBI antenna in Ny Ålesund, submitted to *Memoirs of National Institute of Polar Research*, Special Issue 54, Japan, 2000.

[5] Webb, F. H. and J. F. Zumberge: An introdution to GIPSY/OASIS-II Precision Software for the Analysis of Data from the Global Positioning System, *JPL Publ. No. D-11088*, JPL, 1993.

First Results from a New Dual-Channel Water Vapor Radiometer

Borys Stoew, Carsten Rieck, and Gunnar Elgered

Onsala Space Observatory, Chalmers University of Technology, 439 92 Onsala, Sweden, geo@oso.chalmers.se.

Abstract. A water vapour radiometer (WVR) measuring the sky brightness temperatures at 20.60 and 31.63 GHz has been designed and built. We describe the main features of the instrument and its specifications. We report on the first field measurements from July 2000 at Esrange, Kiruna, Sweden. Comparisons of estimated wet propagation delays are made with GPS data. We find that we have a significant bias of 27 mm in wet delay between GPS–WVR; the RMS difference is 31 mm (14 mm when the bias is removed). A large contribution to the difference is caused by a short term scatter in the WVR data and we discuss the options to improve the over all quality of the WVR.

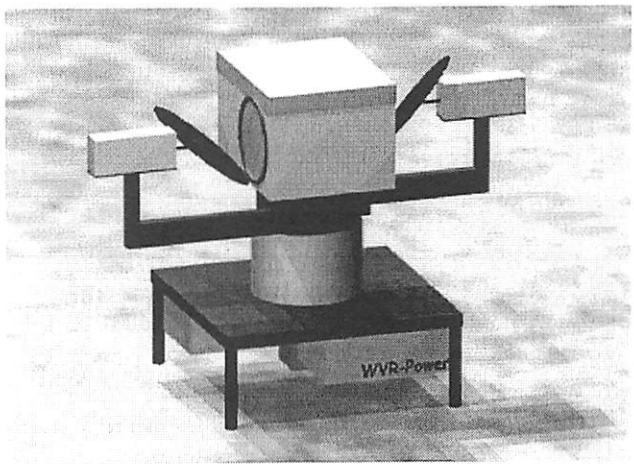

Fig. 1. The new dual-channel WVR.

1 Introduction

Observations of the sky brightness temperatures with a Water Vapor Radiometer (WVR) can be used to estimate the integrated amount of water vapor (IWV) in the atmosphere. Water vapor causes an additional delay (wet delay) which is equivalent to an excess path of radiowaves propagating through the atmosphere. The wet delay is a major error contributor in space geodetic techniques such as Very Long Baseline Interferometry (VLBI) and the Global Positioning System (GPS).

Compared to the ASTRID radiometer which is continuously operating at the Onsala Space Observatory, the new WVR was designed to have higher pointing accuracy, narrower antenna beams, higher resolution of the data acquisition units, superior stability of the calibration system, and mobility. The reduced beam width gives the possibility of studying IWV at low elevation angles and finer spatial structures. The mobility allows for making combined experiments with other instruments at various locations. Here we present the first field measurements of the WVR from July 2000 at Esrange, Sweden (Latitude: 67°88 N, Longitude: 21°06' E).

The instrument is described in Section 2. The results from the first campaign are presented in Section 3, followed by an assessment of the instrument performance in Section 4, and finally in Section 5 the conclusions and ideas for improvements are discussed.

Correspondence to: B. Stoew

2 Instrument Description

2.1 Overview

An outlook of the new Water Vapor Radiometer (WVR) is shown in Figure 1. The two antennas picking up sky emission around 20.6 and 31.6 GHz are placed facing opposite directions and are able to scan the sky by the aid of reflectors. The box containing the antennas rotates in azimuth, while the rotation of the mirrors performs the elevation scanning. The basic specifications of the instrument are presented in Table 1.

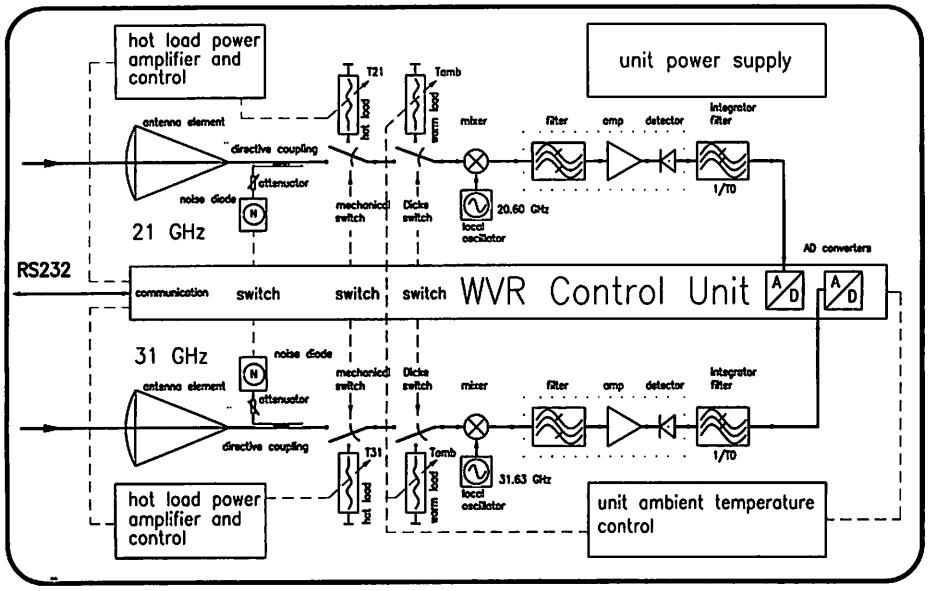

Fig. 2. Schematic representation of the control and data acquisition systems of the WVR. Each of the 20.60/31.63 GHz channels is supplied with a horn antenna, mechanical switch, ferrite switch, mixer, IF amplifier, detector, baseband amplifier and an A/D converter. At present the calibration noise diodes are not mounted; they are functionally substituted by calibrated noise sources (hot loads).

Table 1. Specifications of the WVR.

Microwave system	Channel 1	Channel 2
Center frequency	20.60 GHz	31.63 GHz
Channel bandwidth	190 MHz	190 MHz
Horn antenna beam width (E/H plane)	2.9°/3.4°	1.95°/2.3°
Side lobes, 5° from boresight	-18 dB	-23 dB
Calibration load stability	100°C ± 0.01°C	
Multiplexed inputs A/D converter resolution	16 bit	16 bit

Pointing system	Azimuth	Elevation
Gearing ratio (maximum pointing resolution)	1:100 (0.0072°)	1:50 (0.0144°)
Achieved pointing resolution (limited by the mechanics)	0.1°	0.05°
Pointing range	0-360°	0-360°
Slew rates of the motor drives	> 20°/s	> 30°/s

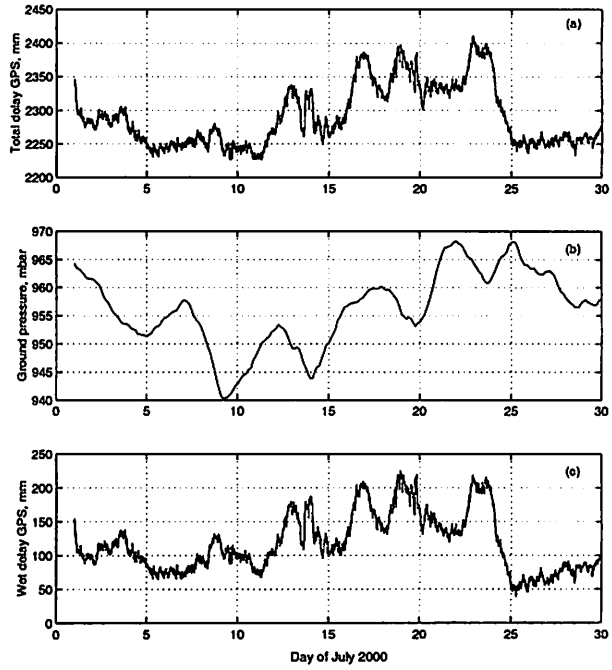

Fig. 3. Time series of a) the zenith total delay estimated from GPS data; b) interpolated ground pressure; c) the calculated wet path delay.

2.2 Microwave module

The components of the dual channel WVR are schematically shown in Figure 2. Stable internal temperature must be provided for the proper operation of the instrument, particularly the stability of the gain in each of the channels. The A/D and D/A converters, the switches, and the heaters of the calibration loads are controlled with a personal computer.

The hardware of the WVR and its operation modes are described in detail by *Rieck* [2000], *Elgered* [1993] and *Stoew* [1998].

3 First results

The first scientific use of the WVR have been observations at the Esrange Space Centre in Kiruna, within the EC project CLIWANET (http://www.knmi.nl/samenw/

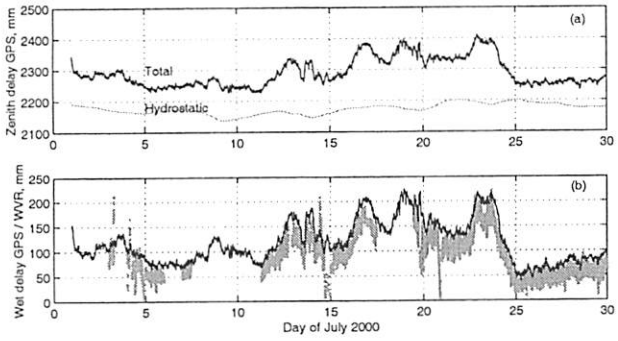

Fig. 4. Agreement between the estimated wet delay from GPS and the WVR. **a)** The total delay estimated from GPS data and the hydrostatic delay at Kiruna do not appear to be correlated – the short term variations are related to the water vapor. **b)** The GPS wet delay estimates are persistently higher than those from the WVR.

cliwanet/). A major goal for the usage of the observations are comparisons with the integrated cloud liquid inferred form different cloud models [see, e.g., *Meijgaard et al.,* 2000].

Several instruments for atmospheric studies are colocated with the WVR at the Kiruna site — a GPS receiver continuously operating in the SWEPOS network, a microrain radar, an infrared radiometer, and a ceilometer. Of these, the data acquired from GPS are used to validate the measurements by the WVR.

The equivalent total zenith delay estimated with GPS is calculated using the GIPSY processing software [*Webb and Zumberge,* 1993] assuming a horizontally stratified atmosphere. The wet delay is derived from the total delay estimates using ground pressure data [*Emardson et al.,* 1998]. The time series for July 2000 are shown in Figure 3. The hydrostatic (dry) delay is shown in Figure 4a together with the total delay from GPS. The total and dry zenith delays do not appear to be correlated; the difference (the wet delay from GPS) is strongly correlated, although biased, to the wet delay inferred from the WVR observations (Figure 4b).

4 Performance Assessment

4.1 Stability of performance

The gain in the two WVR channels is normally strongly correlated with temperature. In order to obtain observations with small uncertainties the monitoring of gain variations is necessary. This is done by using waveguide terminations as black body calibration loads whose physical temperatures are known. An example of the measured temperatures of the two hot loads and the ambient (warm load) temperatures are shown in Figure 5. It is clearly seen that the temperatures of the hot loads are actively controlled whereas the warm load temperature has a strong diurnal signature. The corresponding gains

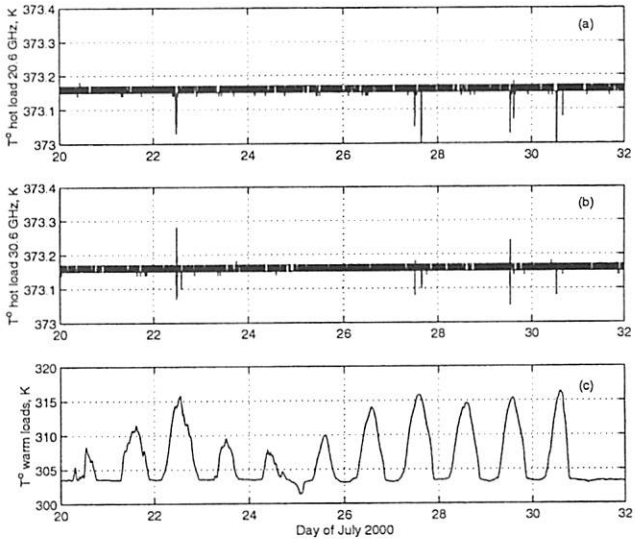

Fig. 5. Stability of the temperature, measured for the 20.6 GHz hot load, 31.6 GHz hot load, and the warm loads respectively. The hot load physical temperatures are regulated to within ± 0.01° at 100°C (373.15K). We note that the regulation experiences some difficulties during the periods of high warm load temperatures.

in the two channels are shown in Figure 6. We see the correlation with temperature in both channels but it is stronger for the 31.6 GHz channel. Possibly this is due to the larger waveguide attenuation in this frequency band. We also note a short term scatter in the gain estimates. We believe that this is caused by the limited integration time — according to *Janssen* [1993]

$$\Delta T = \frac{T_{sys}}{\sqrt{\tau \cdot B}} \tag{1}$$

where ΔT is an estimate of the RMS noise of the sky brightness temperature measured by the WVR in K; τ is the integration time in s; T_{sys} is the system temperature in K, and B is the bandwidth in Hz. Additionally, a small contribution arises from the limited resolution of the temperature and voltage measurements used in the

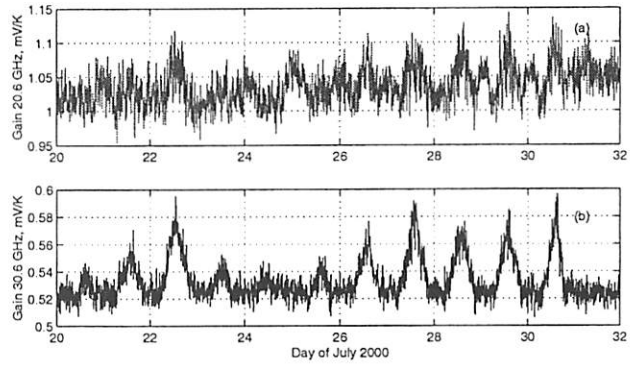

Fig. 6. Changes in the gain for the 20.6 GHz and the 31.6 GHz channels. The calculated gains apparently depend on the internal ambient temperature of the WVR (see Figure 5).

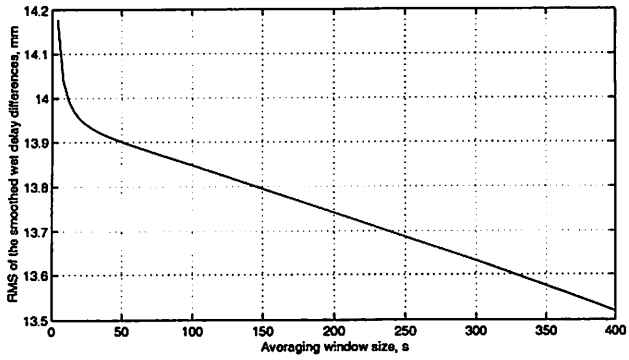

Fig. 7. RMS of the difference between GPS/WVR wet delay estimates with the bias removed. The differenced time series were smoothed with rectangular windows of various averaging times. The gain from smoothing is largest for integration times $\tau < 20$s.

gain calculation.

4.2 Bias and scatter

The systematic differences between the two techniques shown in Figure 4b may be attributed to biases in the WVR observations, miss-modeling in the algorithm used to derive wet delay from the sky emission, bias introduced by the a priori values for the dry and wet delays in the GIPSY processing, and the radome of the GPS receiver antenna [see e.g., *Emardson et al.*, 2000]. For the last 10 days of July the GPS technique produces wet delay estimates exceeding on the average those from the WVR by 27 mm. The RMS of the differenced time series is 14.2 mm after the removal of the bias.

The short-term scatter can be examined by studying the effect of data averaging over a set of time intervals. The differences between GPS and WVR wet delay estimates for the same 10-day period were smoothed several times by a moving average window whose length varied. In Figure 7 the RMS of the smoothed difference with the bias removed time series is plotted against the averaging time. The largest gain from smoothing is achieved for integration times up to 20 s; for longer integration times the RMS of the differences decreases at a much lower rate, e.g. for $\tau = 4000$ s the RMS of the difference is still about 10 mm. This suggests that in the process slowly varying components are being filtered from the differenced time series. These components may enter either through the GPS or the WVR estimates but we attribute the major contribution to the difficulty to model variations in the overall receiver gains.

In order to significantly increase the accuracy of the WVR, three major actions are planned: 1) improve the temperature stability of the whole WVR and especially that of the warm loads at ambient temperature; 2) investigate the effect of increasing the hardware/software integration time; 3) experimentally study the impact of using low noise RF amplifiers on decreasing the receiver system noise.

5 Conclusions

We have described the design and the first field experiment of a WVR. The data acquired in July 2000 show the level of agreement between GPS and WVR, particularly the bias of 27 mm between the two methods, and the large RMS scatter of 14 mm of the wet delay estimates from WVR. These results suggest the directions for further enhancement of the new radiometer. As a measure against the large scatter, temperature stability shall be improved, studies using different hardware integration times will be performed, and a replacement of the present RF amplifiers will be considered.

Acknowledgements

We appreciate the help from Bert Hansson and Lars Wennerback in the development of the WVR hardware as well as the support from Ola Widell and colleagues at Esrange, Sweden.

References

Elgered, G. Tropospheric radio-path delay from ground based microwave radiometry. In M. Janssen, editor, *Atmospheric Remote Sensing by Microwave Radiometry*, chapter 5. Wiley & Sons, Inc., New York, 1993.

Emardson, T.R., G. Elgered and J.M. Johansson. Three months of continuous monitoring of atmospheric water vapor with a network of Global Positioning System receivers. *J. Geophys. Res.*, 103:1807–1820, 1998.

Emardson, T.R., J.M. Johansson and G. Elgered. The systematic behavior of water vapor estimates using four years of GPS observations. *IEEE Transactions on Geoscience and Remote Sensing*, 38(1):324–329, 2000.

Janssen, M. An introduction to passive microwave remote sensing of atmospheres. In M. Janssen, editor, *Atmospheric Remote Sensing by Microwave Radiometry*, pages 1–35. Wiley & Sons, Inc., New York, 1993.

Meijgaard, E., U. Andrae and B. Rockel. Comparison of model predicted cloud parameters and surface radiative fluxes with observations on the 100 km scale. *Meteorology and Atmospheric Physics*, 2000. Submitted.

Rieck, C. A pointing control system for a microwave radiometer. Master's thesis, Department of Radio and Space Science, Chalmers University of Technology, Göteborg, Sweden, 2000.

Stoew, B. Data acquisition and software based temperature stabilization. Master's thesis, Department of Radio and Space Science, Chalmers University of Technology, Göteborg, Sweden, 1998.

Webb, F.H. and J.F. Zumberge. An introduction to the GIPSY/OASIS-II. JPL Publ. D-11088, Jet Propulsion Lab, Pasadena, California, 1993.

An Independent Stability Check of the Onsala 20 m Radio Telescope Using the Global Positioning System

Sten Bergstrand, Rüdiger Haas, Jan Johansson

Chalmers Centre for Astrophysics and Space Science, Onsala Space Observatory, SE-439 92 ONSALA

Contact author: Sten Bergstrand, e-mail: sten@oso.chalmers.se

Abstract

We present results from one year of Global Positioning System (GPS) measurements on the Onsala 20m radio telescope. Measurements have been made with the telescope pointing in the zenith direction during gaps in the ordinary observation schedule. Although the antennas are situateed inside a metal frame, the accuracy of the measurements is comparable that of data unaffected by multipath. The repeatability of the measurements are 4 mm, 2 mm and 6 mm in east, north and vertical components, respectively.

1. Introduction

The Onsala Space Observatory (OSO) participated in the first Mark I Geodetic trans-atlantic Very Long Baseline Interferometry (VLBI) experiment 1968 as well as in the first Mark III experiment 1979 and has been part of the Global Positioning System (GPS) satellite tracking network since 1987. As a collocated site with a long observing history for the International GPS Service (IGS) as well as the International VLBI Service for Geodesy and Astrometry (IVS) Onsala put important constraints on terrestrial reference frames. With the improved accuracy in space geodesy in recent years, the demand on accuracy of the local ties between such frames increases. The VLBI system ties a quasi-inertial celestial reference frame (CRF) of extragalactic radio sources to a terrestrial reference frame (TRF) that is not, or only weakly connected, to the centre of mass of the earth. Satellite methods, such as GPS, tie a dynamically based inertial reference frame to a terrestrial reference frame that is connected to the earth's centre of mass. The satellite orbits are influenced by a changing gravity field and also by solar wind and drag effects. To make sure that the references for the two systems are accurately given, the need of a good local tie is obvious. At OSO this is difficult to accomplish, since the 20m telescope presently used for geodetic measurements originally was constructed for astronomy purposes. To reduce impact of weather, the 20m telescope has a radome and in addition to this the geodetic reference point of the telescope, the intersection of the azimuth and elevation axes, is suspended in free air. Therefore, the reference point is hard to materialize and impossible to observe directly. Previous measurements [1, 2] of the local tie are based on combinations of drawings and measurements. This project aims at reducing the systematic errors of the local tie and, over a longer period of time, creating an independent millimetre-level VLBI–GPS tie at OSO.

2. Equipment

In order to establish this VLBI–GPS tie at Onsala and to check the stability of the construction, the 20m telescope has been equipped with two GPS antennas. The GPS antennas are rigidly attached to the telescope and thus keep the same azimuth and elevation as the 20m telescope. One of the antennas is permanently mounted on top of the subreflector support structure and is therefore referred to as the APEX antenna, the other antenna is intermittently mounted close to the vertex of the 20m paraboloid, hence called VTEX (cf. Fig. 1).

Since the telescope construction and the radome interferes with the satellite signals, some extra precautions have been made to suppress influences on characteristics of the GPS antenna. The APEX is not disturbed by any interfering constructions between the satellites and the antenna except the radome. The main precaution made for the APEX antenna was therefore to put it on a 50 cm pillar to make sure it is undisturbed by adjacent metallic objects. For VTEX the subreflector support structure, different horns and major parts of the 20m reflector are disturbing the environment above and around the GPS antenna. In

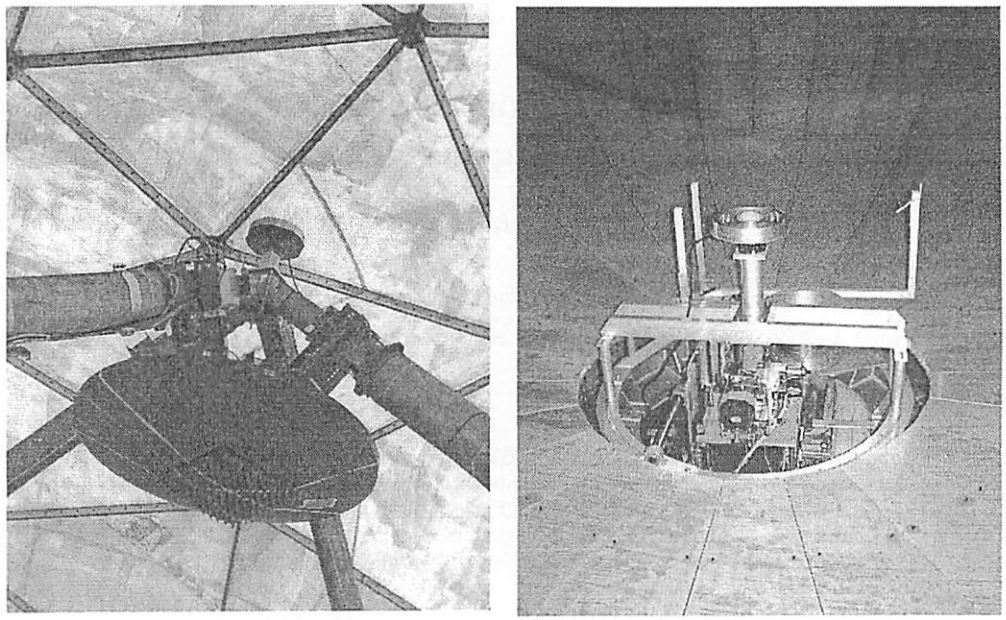

Figure 1. a) APEX antenna on top of the subreflector support structure b) VTEX antenna in the centre of the 20m paraboloid

order to get a reasonable elevation cut-off and to increase data availability, an aluminium antenna support was constructed to raise the antenna from the vertex of the paraboloid. To isolate the antenna from the telescope and retain the original phase-center of the antenna, a non-conducting plastic liner was put between the antenna and the supporting structure. Both GPS antennas are of Dorne Margolin choke ring type and supplemented with Turbo-Rogue receivers.

In order to monitor the vertical changes of the telescope tower an invar rod that monitors the concrete foundation height has been installed slightly off-center in the foundation tower [3, 4]. The invar measurements correlate very well with temperature recordings from sixteen temperature sensors placed in the four points of the compass at four different heights in the middle of the concrete wall of the telescope's foundation (cf. Fig. 2).

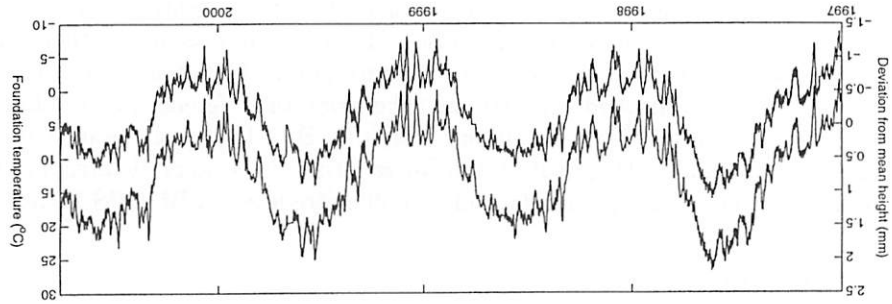

Figure 2. Temperature (upper curve) and height (lower curve) measurements of the conrete foundation at Onsala. Maximum height difference during the period is 2.5 mm.

3. Measurements

The Onsala 20m millimetre-wavelength radiotelescope is used both for geodetic and astronomic purposes and is, in all, occupied 70 % of total time for observations and maintenance. Therefore, GPS data have been recorded with APEX and VTEX in a campaign-like fashion. As no GPS satellites circle the poles, the GPS "hole in the sky" is a dominant feature at OSO (situated at latitude N 57.4°). This means that for a large portion of the sky, there are no satellites available. For normal measurements this is generally

not a problem, but if we were to measure while moving the telescope, the 20m reflector would act as a sky block and the amount of data would decrease significantly. Deformation of the telescope caused by different pointing directions is a yet unexplored factor, which impairs the hemispheric estimation of the moving telescope. The deformation is a small but visible signal that affects the scatter in the invar measurements height of the telescope foundation, cf. Fig. 3.

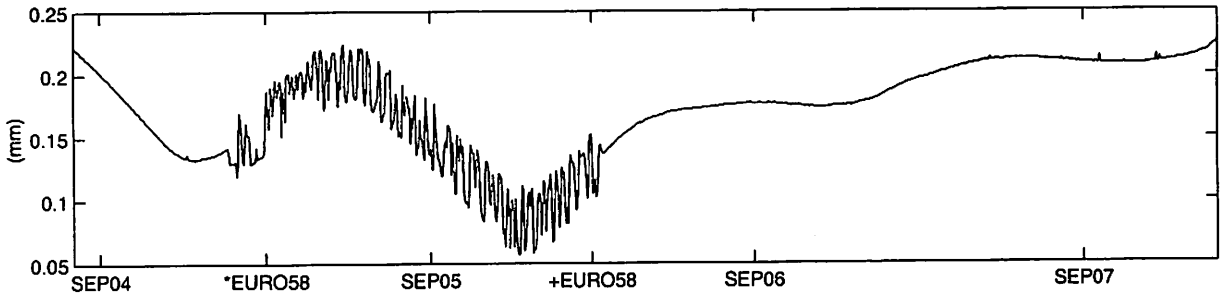

Figure 3. Invar height before, during and after Euro58. The frequent changes of observed radio sources affect the invar measurements, recorded 50 cm off the azimuth axis.

It is a plausible assumption that the difference in scatter 50 cm away from the azimuth axis between experiments with short observation times of each source and more static experiments indicates a larger off-set at the subreflector. In order to minimise the influences from these and other unknown factors, we have decided to measure with the antenna pointing to the zenith position.

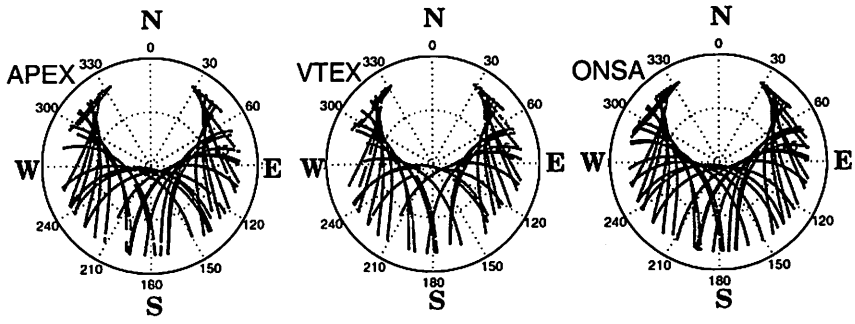

Figure 4. Satellite raw data availability for APEX, VTEX and IGS ONSA antennas, respectively. It is obvious that the radome affects the availability, APEX has 15 % less and VTEX 27 % less data than ONSA for this 24-hour period. (Recorded date: August 4th, 2000)

With this pointing, we have sampled GPS-data with an interval of 30 seconds during breaks in the ordinary observation schedule, i. e. during rainy weekends or summer/christmas holidays. Primary analysis of the data [5] has shown that a 24 hour period is a reasonable criterion for accepting recorded data in the final analysis.

4. Results

We used a baseline approach with three antennas and constrained the IGS site ONSA, so that the positions of APEX and VTEX are given with the IGS station as a fiducial point. Data were mainly processed with the Bernese software in a semiautomatical mode, using the graphical tool option to remove the most obvious outliers and phase ambiguities which the software was not able to adjust [6]. The postfit phase residual errors were studied also by using the GIPSY software [7]. Clearly, the new antennas are affected by the telescope construction and the radome, cf. Fig. 5. The root-mean-square (RMS) formal uncertainties of the antenna positions are, however, generally given with sub-millimeter precision and are thus comparable to data unaffected by complicated constructions such as the telescope and the radome. Formal errors of

the individual measurements have been upscaled with the scaling factor given by the Bernese software for each measurement day individually. The measurements have resulted in estimated positions of the GPS antennas with repeatabilities according to Table 1.

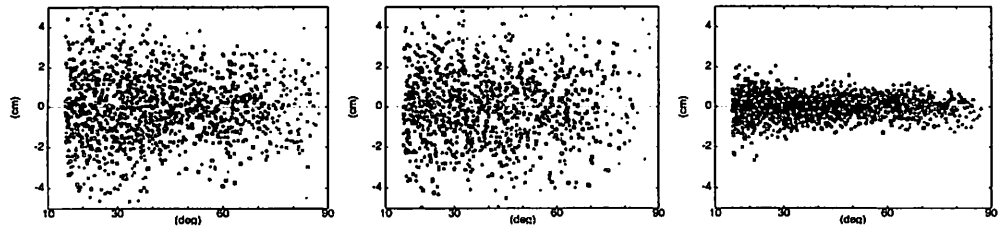

Figure 5. Postfit phase residuals from GIPSY software as function of satellite elevation for APEX, VTEX and ONSA antennas, respectively.

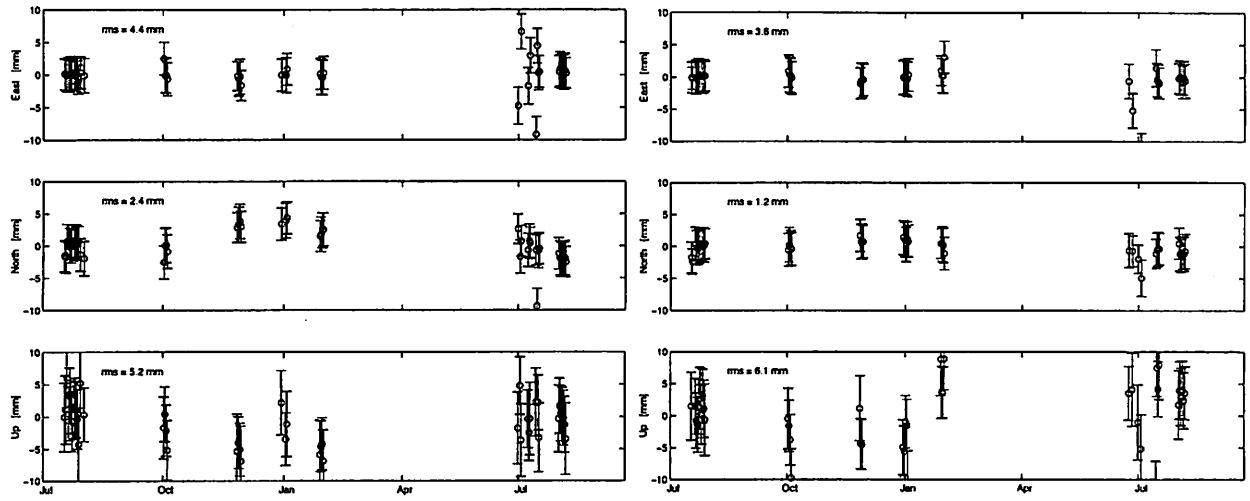

Figure 6. East, North and Up components for the two antennas July 1999–September 2000. APEX results to the left, VTEX to the right. Formal error bars have been upscaled with the factor given by Bernese software output. Some measurements are out of the picture range in order to improve comparability, cf. Fig. 7.

Table 1. Repeatabilities of estimated coordinates

Component	RMS scatter (1σ)	
	APEX	VTEX
	mm	mm
East	4.4	3.6
North	2.4	1.2
Up	5.2	6.1

5. Discussion

The increasing geodetic precision in VLBI measurements with time has created a need to check and monitor the position of the VLBI reference point with respect to GPS reference points and local "footprints". Following the reports of Combrinck and Merry and Matsuzaka et al. [8, 9], other VLBI stations have started to use GPS as an independent positioning check [10, 11]. The relatively slow position updating in the Turbo-Rogue receivers have made continuous measurement impracticable, as the receivers have proven to

lose satellite tracking during geodetic experiments. While performing similar GPS measurements of the telescope in Ny Ålesund [10], an Ashtech receiver with a quicker position update managed to keep track of the satellites while the telescope was moving. We plan a dedicated experiment with other receivers in the future in order to monitor the reference point as the centre of a hemisphere for comparison. A tie between the IGS and IVS reference points is yet to come, as the distances between the antennas and the IVS reference point remains undetermined. If everything proceeds according to plan. These measurements are planned for the coming spring.

The accuracy of the vertical component is, as expected, not sufficiently accurate to monitor the annual variation of APEX and VTEX heights due to thermal expansion of the telescope, cf. Fig. 7.

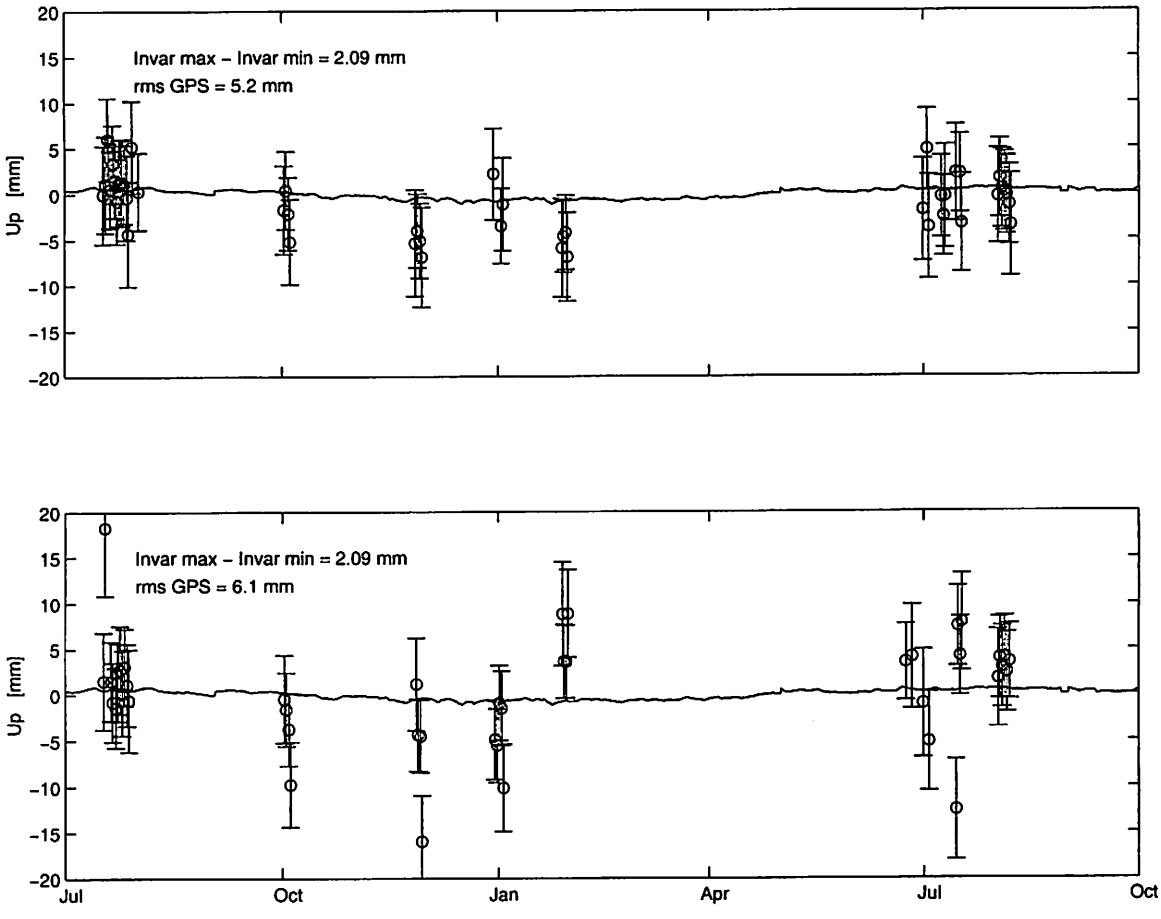

Figure 7. GPS antenna up components compared to results from the invar rod measurements, during the period July 1999–September 2000 (cf. Fig. 2). APEX antenna measurements above, VTEX measurements below.

6. Conclusion

Using GPS signals, we have measured the stability of the OSO 20m radio telescope inside a glassfiber-covered, metal frame-work radome. Formal accuracies of the measurements inside the radome are comparable to measurements made in open air. After fourty measurement days in a year on each of two GPS-antennas, repeatabilities are down to 4 mm, 2 mm and 6 mm levels in east, north, and vertical components, respectively. The measurements are not accurate enough to monitor annual variations, e. g. thermal deformation of the telescope, but a permanent movement or tilt of the telescope caused by reconstruction or local ground settlements, could use GPS as an independent check of the position.

Acknowledgements

Rüdiger Haas is supported by the European Union under contract FMRX-CT960071.

References

[1] Johansson J. M., Elgered G., Rönnäng B. O., The Space Geodetic Laboratory at the Onsala Observatory: Site Information, *Research Report No. 169*, Dept. of Radio and Space Science with Onsala Space Observatory, Chalmers Univ. of Tech., May 1992.

[2] Potash R., Accurate VLBI Geodetic Tie from Onsala VLBI Reference Point to Ground, Interferometrics/GSFC, Nov 31, 1992.

[3] Carlsson R., Site Dependent Error Sources in Geodetic Very-Long-Baseline Interferometry: Antenna Foundation and Cable length Instabilities, *Research Report No. 174*, Dept. of Radio and Space Science with Onsala Space Observatory, Chalmers Univ. of Tech., Jan 1996.

[4] Elgered G., Haas R., Geodetic Very-Long-Baseline Interferometry at the Onsala Space Observatory 1997-1998,*Proc. of the 13th Working Meeting on European VLBI for Geodesy and Astrometry*, Viechtach, February 12–13, 1999, edited by W. Schlüter and H. Hase, Bundesamt für Kartographie und Geodäsie, Wettzell, pp. 60–64, 1999.

[5] Bergstrand S., Haas R., Johansson J. M., A New GPS-VLBI Tie at the Onsala Space Observatory, First General Assembly of the IVS, *NASA CP/2000-209893*, editors N.R. Vandenberg and K.D. Baver, pp. 128–132, 2000.

[6] Beutler G., Brockmannn E., Fankhauser S., Gurtner W., Johnson J., Mervart L., Rotacher M., Schaer S., Springer T., Weber R., Bernese GPS Software Version 4.0, University of Berne, 1996.

[7] Webb F. H., Zumberge J .F., An Introduction to GIPSY/OASIS-II Precision Software for the Analysis of Data from the Global Positioning System, *JPL Publ. No. D-11088,* Jet Propulsion Laboratory, Pasadena, Cal., 1993.

[8] Combrinck W. L., Merry C. L., Very long baseline interferometry antenna axis offset and intersection determination using GPS, *Journal of Geophysical Research*, Vol.102, No.B11, pp. 24,741–24,743, Nov 1997.

[9] Matsuzaka S., Ishihara M., Nemoto K., Kobayashi K., Local tie between VLBI and GPS at Geographical Survey Institute,*Proc. of the international workshop on GEodetic Measurements by the collocation of Space Techniques ON Earth (GEMSTONE)*, Communications Research Lab., Koganei, Tokyo, pp. 68–72, 1999.

[10] Haas R., Bergstrand S., Johansson J. M., Establishing a new GPS-VLBI tie at Ny Ålesund, 14th Working Meeting on European VLBI for Geodesy and Astrometry, this volume, 2000.

[11] Sarti P., Vittuari L., Tomasi P., GPS and classical survey of the VLBI antenna in Medicina: invariant point, 14th Working Meeting on European VLBI for Geodesy and Astrometry, this volume, 2000.

Medicina and Noto Station Reports

A. Orfei[1], F. Mantovani[2], G. Tuccari[3] and C. Stanghellini[3]

1 - Istituto di Radioastronomia , Stazione di Medicina
2 - Istituto di Radioastronomia , Bologna
3 - Istituto di Radioastronomia , Stazione di Noto

In the following we will briefly summarize the relevant events, changes and upgrading at the two radio astronomy stations of Medicina and Noto during the recent past.

Medicina Station Report

Maintenance:

a) An inchworm motor broke. It was replaced with an EVN (spare part) inchworm;
b) a new degausser (model V91M) has been bought;
c) the Haystack dry air kit was mounted on the tape recorder;
d) both the write and read heads were replaced in 1999. The new heads are triple cap made by Spin Physics;
e) the last version of the Field System (9.4.14) was installed;
f) the 8-16 MHz bandbass problem was fixed with the substitution of VCs components;
g) the 0.125 MHz and 0.5 MHz filters were added to the first 8 VCs, which now have the full set of filters.

Telescope Upgrading:

a) Medicina will be a 'thin tape only' station from September 2000 on for astronomical observations;
b) the frequency agility project was slowed down; the main reasons for the delay are that the active surface project for the Noto antenna, which will allow the telescope to operate at 43 GHz with good sensitivity, was started, and because of unexpected problems with the grout supporting the azimuth rail of the antenna, which needed to be replaced.
c) The active surface project consists of a movable system for the primary mirror panels of the antenna to recover the gravity deformations of the surface. The components that are required are in mass production right now. The design for the network of electro-mechanical actuators is ready. The control software is almost completed.
About the installation see the Noto Station report below.
d) The grout supporting the rail was changed. A new approach was followed: the rail is placed on a continuous bed of steel plates (50mm thick); the interface between the foundation and plates is made by a reinforced fibers grout.

Geodetic VLBI Observations in year 2000:

Project	Date
EUROPE-53	27 January
VLBA19	31 January
EUROPE-54	07 February
VLBA20	13 March
EUROPE-55	16 March
EUROPE-56	15 May
VLBA21	22 May
VLBA23	23 October
VLBA24	04 December
EUROPE-60	06 December

Noto Station Report

Upgrading:

a) The MKIV formatter is now used as standard in the VLBA4 Terminal, improving the reliability of the station;
b) a new TTY distributor for the VLBA4 Terminal was completed. It was also produced for the following Stations: Cambridge, Effelsberg, Noto, Shanghai, Torun, Metsahovi, Yebes, Pico Veleta and Haystack (3)
c) the assembly of headstack boards (2) is almost completed. The tape recorders will be upgraded as fully two heads recording system for 1 Gbit/s recording;
d) the new SXL-UHF receiver is under construction;
e) A Heybond bonding machine was acquired in order to undertake studies of cryogenic low noise amplifiers for L, S and C front-ends;
f) the new panels plus the active surface will be installed in the last quarter 2001. The telescope will be stopped from September to December 2001.

Geodetic VLBI Observations in year 2000:

Project	Date
CORE-B801	12 January
EUROPE-53	27 January
EUROPE-54	07 February
EUROPE-56	15 May
EUROPE-57	07 August
EUROPE-58	04 September
CORE-B802	02 November
EUROPE-60	06 December

Matera CGS VLBI Station

G.Colucci(1), D.Del Rosso(1), L.Garramone(1) , E.Lunalbi(1) F. Vespe(2),

(1) telespazio spa (2) asi agenzia spaziale italiana

The System

The Matera VLBI system is operated, on behalf of Italian Space Agency (**ASI**), by Telespazio S.p.A. at **Centro di Geodesia Spaziale (CGS)** of Matera.
The **CGS** came into operation on 1983 in the framework of an agreement with the Basilicata Regional Government and **ASI**.
A fixed SLR system and a network of permanent GPS receivers (including one at Matera site) are also operated at **CGS**. Honeywell (formerly ATSC) is now installing a new SLR system: MLRO
The Matera VLBI system includes

- X/S bands receiver
- 20 meter diameter cassegrain antenna;
- ARK-IV D.A.T. and VLBA4 Recorder;

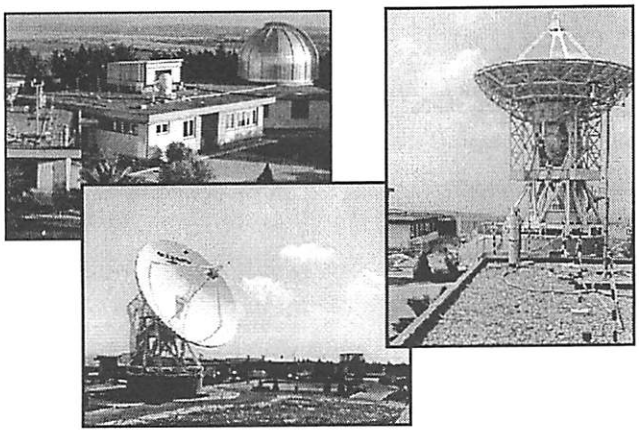

Acquisitions for 1999/2000

1999 2000	Europe			Core-A			Core-1		Core-3		RDV		Neos-A		Intensive		Other		TOT.		
	#	Tot. [hh]	Lost [hh]	#	Tot. [hh]	Lost [hh]	#	Tot. [hh]	#	Tot. [hh]	#	Tot. [hh]	#	Tot. [hh]	#	Tot. [hh]	#	Tot. [hh]	#	Tot. [hh]	Lost [hh]
January				2	48	(*) 48.0													2	48	48.0
February	1	24	(*) 24.0	2	48										5	10			8	82	24.0
March				2	48														2	48	0.0
April	1	24		1	24														2	48	0.0
May				2	48														2	48	0.0
June	1	24		3	72	2.5													4	96	2.5
July				1	24												1	24	2	48	0.0
August	1	24	0.3	2	48	1.0													3	72	1.3
September				2	48	0.3													2	48	0.3
October	1	24	24.0	2	48	(*) 24.0													3	72	48.0
November				3	72														3	72	0.0
December	1	24		1	24												1	5	3	53	0.0
January	1	24		2	48	1.0					1	24	1	24					5	120	1.0
February	1	24		1	24								1	24					3	72	0.0
March	1	24		1	24						1	24							3	72	0.0
April				1	24								1	24					2	48	0.0
May	1	24									1	24							2	48	0.0
June				1	24												1	11	2	35	0.0
July							1	24	1	24	1	24							3	72	0.0
August	1	24					1	24	1	24			1	24					4	96	0.0
Tot.	11	264	48.3	29	696	76.8	2	48	0.0	2	48	0.0	4	96	0.0	4	96	0.0	5	10	0.0	3	40	0.0	60	1298	125.1

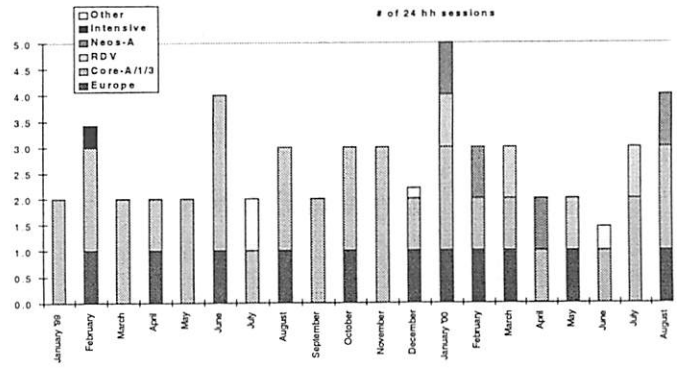

Summary of Acquisitions

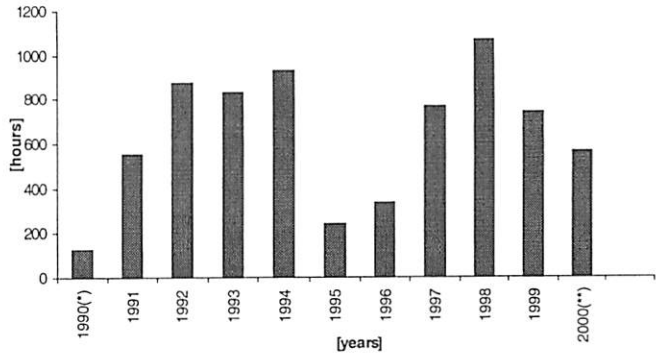

(*) From May
(**) Up to August

Correlators

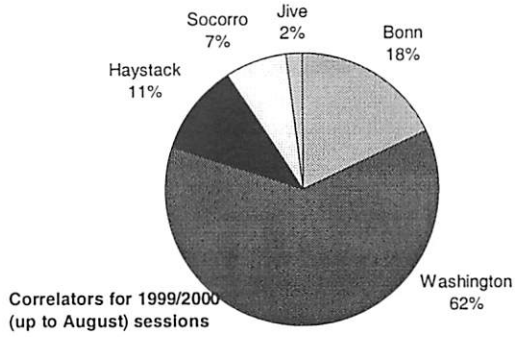

Performed Upgrades

- Mark-IV and Thin Tape upgrade. Performed by MIT Haystack.
- FS 9.4.13 on Linux PC.
- In order to minimize X-S band cross-talk, the old Down Converter was installed for S band.

Most Significant System Failures

January	Headstack/inchworm failure. Repaired by Haystack.
February	Azimuth #1 brake failure. Replaced with a spare one.
March	Cryogenic system failure. Repaired by maint. company.
August	L.O. Video Converter failure. Replaced with a spare one.
October	H-Maser minor failure. Repaired by Oscilloquartz.

H-Maser

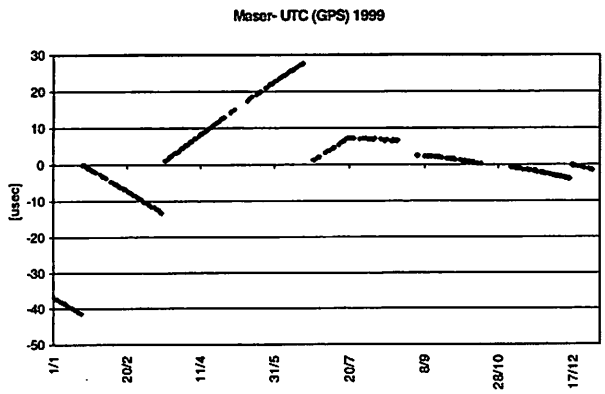

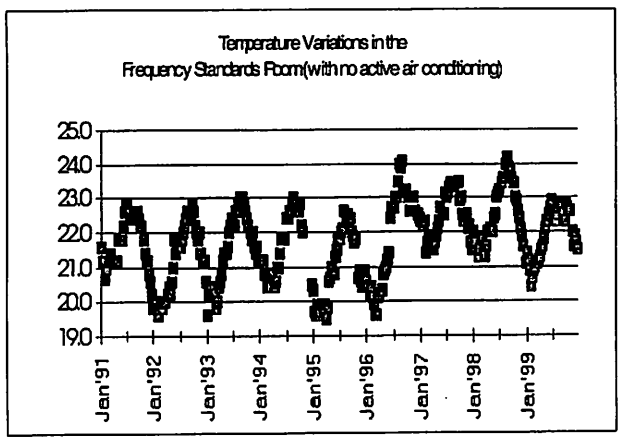

On-line resource and contact points

http://geodaf.mt.asi.it

VLBI Team at CGS
vlbi@asi.it

F. Vespe (ASI)
ASI CGS Geodesy Activities Manager
francesco.vespe@asi.it

D. Del Rosso (Tpz)
Telespazio Geodesy Activities Manager
domenico_delrosso@telespazio.it

L. Garramone (Tpz)
Station Engeneer
luciano.garramone@asi.it

G. Colucci (Tpz)
VLBI contact
giuseppe.colucci@asi.it

History and Status of the TIGO-Project

Hayo Hase, Armin Böer, Stefan Riepl, Wolfgang Schlüter, Adriano Cecioni

14th Working Meeting on European VLBI for Geodesy and Astrometry
Castel San Pietro Terme, September 8-9, 2000

Global geodetic networks require a *global* homogeneous distribution of reference points, otherwise undesirable systematic errors degrade the results of positioning. The number of fundamental stations for geodesy is low and they are concentrated on the northern hemisphere.

Based on this background the German *Research Group for Space Geodesy* (FGS)[1] proposed in its research program from 1989 the development of a *mobile integrated geodetic measuring platform.* The idea was to build a new transportable fundamental station which can be operated at remote locations in order to improve the distribution of fundamental stations in the global network.

In 1992 the IfAG (now BKG) got the fundings to build the *Transportable Integrated Geodetic Observatory* (TIGO). In May 1992 the specification of TIGO had been finished and had been used for an invitation to bid. In December 1992 the main orders for TIGO components were placed.

During June/July 1995 a platform for testing the TIGO components was built at the Fundamental Station Wettzell.

In November 1997 the first VLBI test experiment was carried out with the VLBI-module of TIGO[2]. In January 1998 the first SLR measurements were done with the SLR-module of TIGO[3]. Since then TIGO is continously improved and equipped by additional sensors, measuring devices and spare parts.

In July 1999 the *Announcement of Opportunity*[4] was published in order to find hosting countries for TIGO. By the due date of September 30, 1999, promising proposals from Brazil, Argentine, Chile, India, Philippine and Indonesia had been sent to BKG. In November/December 11 proposed locations in the countries above had been reconnitered (fig. 1). All applicants were challenged to send a *Letter of Intend* by January 15, 2000, in which the fulfillments of requests by BKG for the joint operation of TIGO had to be confirmed.

On January 21, 2000, the steering committee of FGS decided to give the highest priority to the application of a consortium from Concepción, consisting of

- *Universidad de Concepción* (UdeC) as main partner for BKG,
- *Universidad del Bio Bio* (UBB),
- *Universidad Catolica de la Santisima Concepción* (UCSC),
- *Instituto Geografico Militar* (IGM) in Santiago.

In March 6-16, 2000, the location for the TIGO-platform was defined at the campus area of UdeC with respect to protection of existing microwave sources in Concepción (see fig. 2). During that period an *Arrangement* between BKG and UdeC as main partner had been drafted.

The final version of the *Arrangement* was signed on behalf of the consortium by the rector of UdeC Prof. Lavanchy and the president of BKG Prof. Grünreich in Frankfurt a.M. on June 21, 2000. The minimum period of TIGO being in Concepción will be 3 years with the option of extension on a year-by-year base.

[1] The *Forschungsgruppe Satellitengeodäsie* (FGS) coordinates common research activities of the Technische Universität München (TUM), the Geodätisches Institut Universität Bonn (GIUB), the Deutsches Geodätisches Forschungsinstitut München (DGFI) and the Bundesamt für Kartographie und Geodäsie (BKG) with respect to the tasks of the Fundamentalstation Wettzell.

[2] http://http://www.wettzell.ifag.de/veranstaltungen/vlbi/euro13/postscript/hase1.ps.gz

[3] http://www.wettzell.ifag.de/veranstaltungen/slr/11thlaserworkshop/postscript/wtigoreportboer.ps.gz

[4] http://www.wettzell.ifag.de/tigo/announce/announce.html

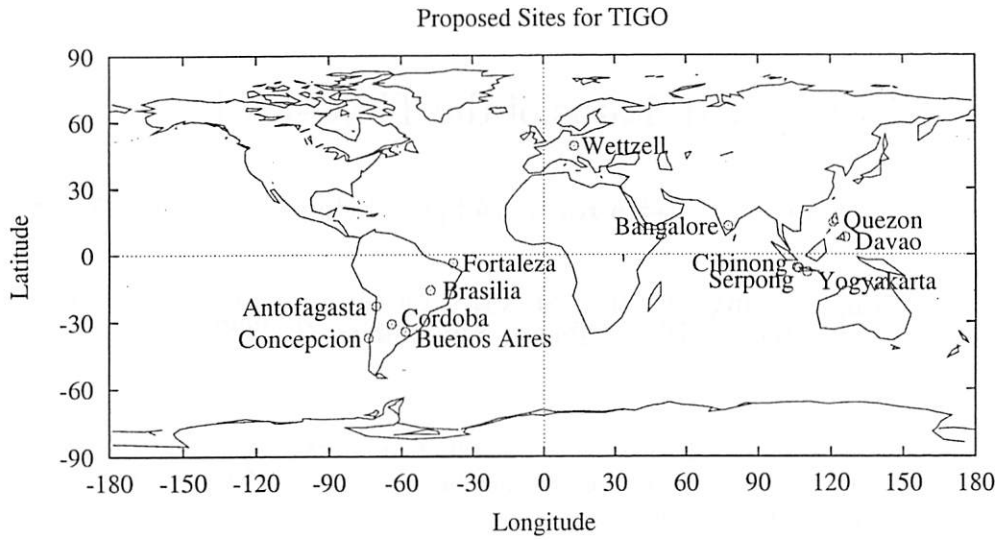

Fig. 1: Proposed sites for TIGO by instititutions of the hosting countries, September 30, 1999. TIGO was developed at the fundamental station Wettzell.

Fig. 2: The selected site for TIGO in March 2000. TIGO will be installed on the left side on top of the hill. The site is still located at the campus area of Universidad de Concepción in about 2 km distance to the university institutes. It is protected against manmade electromagnetic noise by the surrounding hill chains.

During the second half of 2000 a platform for TIGO and a way to it will be constructed in Concepción in order to receive TIGO in early 2001.

Beginning in November 2000 TIGO will be prepared at Wettzell for the transportation to Chile. For the move to Chile a formal note on TIGO must be exchanged between the German and Chilean government.

It is envisaged that TIGO starts its operation as a joint venture among the Chilean partner consortium providing 11 engineers and BKG providing 3 TIGO-experts in the beginning of 2001.

Approx. coordinates of TIGO site Concepción	
Longitude	W 73.0236°
Latitude	S 36.8417°
Altitude	150 m
X	1492201 m
Y	-4887972 m
Z	-3803436 m

MDSCC Station Report

D. Behrend[a], A. Alberdi[b,c], A. Rius[a,b], J.F. Gómez[b],
C. García-Miró[b], C. Calderón[d], J.A. Perea[d]

[a]Institut d'Estudis Espacials de Catalunya (IEEC/CSIC), Barcelona, Spain
[b]Laboratorio de Astrofísica Espacial y Física Fundamental (LAEFF/INTA), Madrid, Spain
[c]Instituto de Astrofísica de Andalucía (IAA/CSIC), Granada, Spain
[d]Madrid Deep Space Communications Complex (MDSCC/NASA), Madrid, Spain

1 Introduction

The NASA Madrid Deep Space Communications Complex (MDSCC) forms part of the Deep Space Network (DSN) whose primary goal is to track spacecrafts. Apart from its tracking activities the MDSCC also participates in radio astronomy and geodetic programs making use of the high quality equipment at the station such as the large radio antennas, precise and accurate clocks, and low noise receivers. In this report we give an outline of the radio astronomical and geodetic activities done in the year 1999 and in the first half of the year 2000.

2 Programmes and Instrumentation

2.1 Radio Astronomy Programmes of the DSN

The radio astronomy programmes within DSN may be characterized by the following items:

- **Applied Radio Astronomy:** Direct support of the DSN.
- **Support of the NASA:** Office of Space Sciences and Applications (OSSA).
- **Host Country Observations:** These include both single-dish and interferometric observations.
- **Radio Astronomical Observations which require the unique capabilities of the DSN:** An agreement has been signed with the EVN (European VLBI Network) permitting the participation of the NASA dishes in a few projects, requiring very high sensitivity, in each EVN observing session. The proposals must be submitted to the Program Committees of the VLBA (Very Long Baseline Array) and of the EVN.
- **Co-observations with VSOP at 18 cm:** The co-observations were taken twice a week. Due to (i) satellite eclipse problems and (ii) malfunctioning of the satellite some planned observations could not be performed.

2.2 Instrumentation

Detailed accounts of the available instrumentation can be found in the "Radio Astronomy and the Deep Space Network" reports generated annually by the JPL Telecommunications and Data Acquisition Science Office (M/S 303-401, Pasadena, California 91109). Here we give a very brief summary.

- **VLBI Antennas:** There are two radio antennas available for VLBI work: the DSS63 (cf. Table 1) and the DSS65 (cf. Table 2). The latter is employed in the geodetic VLBI experiments of the Europe series.

Table 1: DSS63 VLBI antenna (70 m dish).

Band	**L**	**S**	**X**	**K**
Frequency range (GHz)	1.60–1.70	2.2–2.3	8.4–8.5	18–26[a]
Antenna beamwidth (arcmin)	10.8	6.5	1.8	0.75
Apert. efficiency (%)	60	72	65	50
Sensitivity (K/Jy)	0.84	1.0	0.9	0.7
Feed polarization	LCP	RCP-LCP	RCP-LCP	RCP-LCP
Low noise amplifier	FET	Maser	Maser	HEMT
Tsys (K)	35	16	21	70

[a]Expected to be operational in 2001

Table 2: DSS65 VLBI antenna (34 m dish).

Band	**S**	**X**	**X**
Frequency range (GHz)	2.2–2.3	8.4–8.5	8.2–8.6
Antenna beamwidth (arcmin)	16.2	4.2	4.2
Apert. efficiency (%)	57	72	72
Sensitivity (K/Jy)	0.19	0.24	0.24
Feed polarization	RCP-LCP	RCP-LCP	RCP-LCP
Low noise amplifier	FET	Maser	HEMT
Tsys (K)	40	21	38

- **Recording Terminals:**
  - 1 Mark IV A DAT (with two WCB recorders). It is controlled by the standard Linux-based field system (version 9.4.0).
  - The Video Converters have 2, 4, 8 and 16 MHz filters, with the capability to use them in the USB or LSB or both at the same time. 4 of the Video Converters have 125 KHz and 500 KHz filters available.
- **Local Oscillators:** X-band (8100 MHz), S-band (2000 MHz), K-band (tunable from 18 to 26 GHz), L-band (1380 MHz).
- **Time and Frequency:** 2 redundant Hydrogen MASERS.
- **Spectrometer:** Autocorrelation spectrometer with 256 channels. Bandwidth, variable between 1 and 10 MHz, which provides a maximum velocity resolution of $\sim$ 0.05 km/s at 22 GHz. This spectrometer was originally installed at the Canberra station.
- **Other Equipment:** SNR-8 ROGUE GPS Receiver; pressure, humidity and temperature sensors integrated in the system; JPL-D2 Water Vapour Radiometer (WVR).

3 News about the MDSCC

- José Antonio Perea retired from his job as Radio Astronomy Engineer of MDSCC on June 15th, 2000. His successor is Cristina Calderón.

- A new spectrometer has been installed. The control program was adapted from original settings for Canberra to those suitable for Madrid. First observational tests were performed with H_2O, NH_3, and CCS molecular lines at K band. The spectrometer proved operational in the frequency switching mode, with full control of MMS frequency. So far the spectrometer is not equipped with an interface to control the antenna motion, thus this has to be done

Table 3: VLBI experiments in 1999 and first half of 2000.

Code	Year	DOY	Antenna	Band	Comments
CB601	1999	69	DSS65	S/X	CORE-B
BR063	1999	72	DSS63	X	global VLBI, dual polarization, problems reported
EURO48	1999	116	DSS65	S/X	problems reported
BR063B	1999	135	DSS63	X	global VLBI, dual polarization, problems reported
CB602	1999	139	DSS65	S/X	CORE-B, problems reported
BM112HRO	1999	146	DSS63	K	RAES
GB033B	1999	155	DSS63	L	global VLBI
GB033C	1999	156	DSS63	L	global VLBI
GR016B	1999	159	DSS63	X	global VLBI
EURO49	1999	179	DSS65	S/X	Europe, problems reported
CB603	1999	181	DSS65	S/X	CORE-B
EURO50	1999	228	DSS65	S/X	Europe
BR063C	1999	261	DSS63	X	global VLBI, dual polarization
GB035	1999	271	DSS63	L	global VLBI
CB605	1999	277	DSS65	S/X	CORE-B
EURO51	1999	284	DSS65	S/X	Europe
CB606	1999	291	DSS65	S/X	CORE-B
EM035A	1999	317	DSS63	L	EVN
EM035B	1999	318	DSS63	L	EVN
ES028	1999	318	DSS63	L	EVN
BR063D	1999	343	DSS63	X	global VLBI, dual polarization
EURO52	1999	347	DSS65	S/X	Europe
GB034	2000	55	DSS63	X	global VLBI, dual polarization
CB701	2000	131	DSS65	S/X	CORE-B, problems reported: power plant failure
BR067	2000	136	DSS63	X	global VLBI, dual polarization
EURO56	2000	136	DSS65	S/X	Europe
GO003	2000	147	DSS63	L	global VLBI, predicts problem
185-00	2000	186	DSS63	X	Host-Country R/A, dual polarization, problems reported: MarkIV failure

manually by the operator. Science operations with the spectrometer pending on improvement of K-band receiver. K-band is not operational yet.

- The communication between the antenna equipment and the Radio Astronomy Controller (RAC) has been improved. A transition of the cone R&D instrument architecture from an HPIB extended bus approach to an HPIB-LAN gateway has been carried out.

4 VLBI and Radio Astronomy Observations at MDSCC

Table 3 lists the VLBI experiments that have been conducted at MDSCC during the report period. Further, non-VLBI, radio astronomical experiments (Host-Country R/A experiments) are compiled in Table 4. In addition to these experiments multiple VSOP co-observing sessions (2 per week) have been performed.

Table 4: Radio astronomical experiments (non-VLBI) in 1999 and first half of 2000 in the frame of Host-Country R/A.

Year	DOY	Antenna	Band	Comments
1999	355	DSS63	X	target of opportunity
1999	357	DSS63	X	target of opportunity
2000	27	DSS63	X	sensitivity test
2000	89	DSS63	K	continuum and spectrograph observations
2000	123	DSS63	X	continuum, problems reported
2000	124	DSS63	X/K	X (continuum), K (line)
2000	125	DSS63	X	continuum
2000	127	DSS63	X	continuum
2000	128	DSS63	X	continuum
2000	132	DSS63	X	continuum, problems reported
2000	142	DSS63	X	continuum
2000	148	DSS63	X	continuum
2000	153	DSS63	X	continuum
2000	156	DSS63	X	continuum
2000	158	DSS63	X/K	X (continuum), K (line)
2000	160	DSS63	X	continuum
2000	161	DSS63	X	X (continuum), K (line)
2000	162	DSS63	X	continuum
2000	163	DSS63	X	continuum

5 Observational Problems

Different circumstances have affected the VLBI system and prevented fringes from being found. Here we summarize the major observational problems:

- Quasar meter (system temperature meter) unavailable on and after DOY 001 (2000): not Y2K compliant.

- Station power failure on DOY 131 (2000). Experiments CORE-B701 on DOY 131 and Host-Country R/A on DOY 132 failed.
- Formatter power supply system problem on DOY 169 (2000).
- Formatter failing synch test on DOY 261 (2000).

Moreover, some other experiments suffered from operational problems.

6 Scientific Objectives and Results

The scientific objectives and results included the following items:

- **Study of the parsec-scale relativistic jets** associated with quasars and Active Galactic nuclei. DSS63 has taken part in dual polarization VLBI experiments at X-band .
- **VLBI differential astrometry**. High precision VLBI differential astrometry observations have permitted to i) study the stability of the cores of the compact radio sources and ii) determine absolute motions of the VLBI components with precisions better than a tenth of a milliarcsecond.
- **Single-dish monitoring** of variable radiostars and galactic plane variable radio sources. The 70 meter antenna (DSS63) has been used to monitor the flux density of variable radiostars (as X-ray binaries, flare stars). Several campaigns were performed coordinated with X-ray, millimetre and sub-millimetre observations at other observatories.
- **Single-dish monitoring** of a selected sample of Blazars. Several observations have been made in X-Band (8.4 GHz) with the 70 meter antenna (DSS63) to study the emission variability of Blazars in time-scales of the order of days. This variability is interpreted as produced by the propagation of shock waves downstream the strong relativistically beamed jet.
- **Search for very low mass objects** around nearby radio stars. VLBI phase-referencing observations using the DSS63 antenna in combination with the MPIfR antenna at Effelsberg are part of a long-term program to search for possible planetary companions down to 1 Jupiter massi orbiting single M dwarfs.
- **VSOP observations at 1.6 GHz.** In the report period, DSS63 has been regularly co-observing with VSOP compact radio sources at 18 cm.
- **Applications of GPS to Meteorology:** Data obtained at the MDSCC and in a local network of GPS receivers, have been used to study the spatial and temporal distribution of the atmospheric delays for meteorological applications. Furthermore, MDSCC is included in a list of stations for which "near real time estimates" of the total zenith delay are computed using data stored hourly at the BKG and CDDIS servers.
- **Applications of VLBI to Geodynamics.** The antenna DSS65 has participated in geodetic VLBI campaigns, in particular in the *Europe* and in the *CORE* experiments. The DSS65 antenna has again been surveyed to determine possible displacements of the VLBI reference point. It appears that the antenna has been stable at the few mm level after the track-and-wheel repair in April/May 1997 (see Table 5).

Table 5: Reference point stability of the DSS65 antenna. UTM30 coordinates of the reference point; average orthometric height of the "yellow marker" of the elevation axis.

Campaign	Northing [m]	Easting [m]	Orth. Height [m]
December 1988	4 476 130.999	393 955.935	781.261
March 1997	131.005	955.933	781.278
June 1997	130.998	955.934	781.284
April 1998	130.998	955.934	781.284
March 1999	131.000	955.936	781.284

- **Spectroscopy of Molecular Clouds:** Spectral line studies of molecular lines at K-band will be performed with the spectrometer, using antenna DSS63. In particular, it will be dedicated to surveys of H_2O maser, NH_3, and CCS surveys of catalogued molecular clouds.
- **Spectrometer observations:** It will also give support to interferometric (VLA) observations, by checking the detectability of variable lines before a VLA observation, and by determining the missing extended emission due to lack of short baselines in the interferometer.
- **Targets of Opportunity:** The Gamma Ray Burst GRB 991208 was observed with the antenna DSS63. The observations were based on two observing runs carried out on Dec 22.2491-22.6488 UT and Dec 23.3243-23.6095 UT 1999. An 1 sigma upper limit for the flux density of 3.5 mJy for the afterglow was derived.

7 Recent Publications

7.1 Refereed Journals

1. Arbizzani, E., Giovannini, G., Taylor, G.B., Bondi, M., Cotton, W.D., Feretti, L., Lara, L., Venturi, T. 1999, "VLBI observations of B2 1144+35: a peculiar radio galaxy.", Memorie della Societa Astronomica Italiana, 70, 125.
2. Behrend, D., Cucurull, L., Vilà, J., Haas, R. 2000, "An Inter-comparison Study to Estimate Zenith Wet Delays Using VLBI, GPS, and NWP Models.", Earth Planets and Space, accepted for publication.
3. Behrend, D., Rius, A. 1999, "Institut d'Estudis Espacials de Catalunya.", In: International VLBI Service for Geodesy and Astrometry 1999 Annual Report, edited by N.R. Vandenberg, NASA/TP-1999-209243.
4. Cotton, W.D., Feretti, L., Giovannini, G., Lara, L., Venturi, T. 1999, "A Parsec-Scale Accelerating Radio Jet in the Giant Radio Galaxy NGC 315", Astrophysical Journal, 519, 108.
5. Elósegui, P., Davis, J.L., Gradinarsky, L.P., Elgered, G., Johansson, J.M., Tahmoush, D.A., Rius, A. 1999, "Sensing atmospheric structure using small-scale space geodetic networks", Geophysical Research Letters, 26, 2445.

6. Garrett, M.A., Muxlow, T.W.B., Garrington, S.T., Alef, W., Alberdi, A., Venturi, T. et al. 2000, "EVN Observations of the Hubble Deep Field", Astronomy & Astrophysics, in preparation.

7. Giovannini, G., Cotton, W.D., Feretti, L., Lara, L., Venturi, T. 1999, "Space VLBI and VLBA observations of MKN 501 and MKN 421.", Memorie della Societa Astronomica Italiana, 70, 161.

8. Giovannini, G., Cotton, W.D., Feretti, L., Lara, L., Venturi, T. 2000, "Space VLBI Observations of Mkn 501", Advances in Space Research, 26, 693.

9. Giovannini, G., Taylor, G.B., Arbizzani, E., Bondi, M., Cotton, W.D., Feretti, L., Lara, L., Venturi, T. 1999, "B2 1144+35: A Giant Low-Power Radio Galaxy with Superluminal Motion", Astrophysical Journal, 522, 101.

10. Gómez, J.L., Marscher, A.P. 2000, "Space VLBI Observations of 3C 371", Astrophysical Journal, 530, 245.

11. Gómez, J.L., Marscher, A.P., Alberdi, A. 1999, "86, 43, and 22 GHZ VLBI Observations of 3C 120", Astrophysical Journal, 521, L29.

12. Gómez, J.L., Marscher, A.P., Alberdi, A. 1999, "Outburst in the Polarized Structure of the Compact Jet of 3C 454.3", Astrophysical Journal, 522, 74.

13. Gómez, J.L., Marscher, A.P., Alberdi, A., Gabuzda, D.C. 1999, "The Twisted Parsec-Scale Structure of 0735+178", Astrophysical Journal, 519, 642.

14. Guirado, J.C., Jones, D.L., Lara, L., Marcaide, J.M., Preston, R.A., Rao, A.P., Sherwood, W.A. 1999, "Dual-frequency VLBI observations of the gravitational lens system PKS 1830-211", Astronomy & Astrophysics, 346, 392.

15. Guirado, J.C., Marcaide, J.M., Pérez-Torres, M.A., Ros, E. 2000, "VLBI difference astrometry at 43 GHz", Astronomy & Astrophysics, 353, L37.

16. Hough, D.H., Zensus, J.A., Vermeulen, R.C., Readhead, A.C.S., Porcas, R.W., Rius, A., Rector, T.A., Lenz, G.C., Davis, M.A., Snowdall, J.C. 1999, "Deep 8.4 GHZ VLBI Images of Seven Faint Nuclei in Lobe-dominated Quasars", Astrophysical Journal, 511, 84.

17. Lara, L., Alberdi, A., Marcaide, J.M, Muxlow, T.W.B. 1999, "Space-VLBI observations of the twisted jet in 3C395", Astronomy & Astrophysics, 352, 443.

18. Lara, L., Feretti, L., Giovannini, G., Baum, S., Cotton, W.D., O'Dea, C. P., Venturi, T. 1999, "The Radio-Optical Jet in NGC 3862 from Parsec to Subkiloparsec Scales", Astrophysical Journal, 513, 197.

19. Lara, L., Mack, K., Lacy, M., Klein, U., Cotton, W.D., Feretti, L., Giovannini, G., Murgia, M. 2000, "The giant radio galaxy 8C 0821+695 and its environment", Astronomy & Astrophysics, 356, 63.

20. Lara, L., Márquez, I., Cotton, W.D., Feretti, L., Giovannini, G., Marcaide, J.M., Venturi, T. 1999, "Restarting activity in the giant radio galaxy J1835+620", Astronomy & Astrophysics, 348, 699.

21. Lazio, T.J.W., Fey, A.L., Dennison, B., Mantovani, F., Simonetti, J.H., Alberdi, A., Foley, A.R., Fiedler, R., Garrett, M.A., Hirabayashi, H., Jauncey. D.L., Johnston, K.J., Marcaide, J.M., Migenes, V., Nicolson, G.D. 2000, "The extreme scattering event towards PKS 1741-038: VLBI Images", Astrophysical Journal, 534, 706-717.

22. Marcaide, J.M., Alberdi, A., Lara, L., Pérez-Torres, M.A., Diamond, P.J., Preston, R.A. 1999, "A decade of unchanged 1.3 cm VLBI structure of SgrA*", Astronomy & Astrophysics, 343, 801-805.

23. Murphy, D.W., Tingay, S.J., Preston, R.A., Meier, D.L., Guirado, J.C., Polatidis, A., Conway, J.E., Hirabayashi, H., Kobayashi, H., Murata, Y. 2000, "VSOP Monitoring of the Quasar 1928+738", Advances in Space Research, 26, 665.

24. Pérez-Torres, M.A., Marcaide, J.M., Guirado, J.C., Ros, E., Shapiro, I.I., Ratner, M.I., Sardón, E. 2000, "Towards global phase-delay VLBI astrometry: observations of QSO 1150+812 and BL 1803+784", Astronomy & Astrophysics, 360, 161.

25. Ros, E., Guirado, J.C., Marcaide, J.M., Pérez-Torres, M.A., Falco, E.E., Muñoz, J.A., Alberdi, A., Lara, L.J. 2000, "VLBI Imaging of the quad gravitational lens PKS 0411+05", Astronomy & Astrophysics, in press.

26. Ros, E., Marcaide, J.M., Guirado, J.C., Ratner, M.I., Shapiro, I.I., Krichbaum, T.P., Witzel, A., Preston, R.A. 1999, "High precision difference astrometry applied to the triplet of S5 radio sources B1803+784/Q1928+738/B2007+777", Astronomy & Astrophysics, 348, 381.

27. Ros, E., Marcaide, J.M., Guirado, J.C., Sardón, E., Shapiro, I.I. 2000, "A GPS-based method to model the plasma effects in VLBI observations", Astronomy & Astrophysics, 356, 357.

28. Ruffini, G., Kruse, L.P., Rius, A., Bürki, B., Cucurull, L., Flores, A. 1999, "Estimation of tropospheric zenith delay and gradients over the Madrid area using GPS and WVR data", Geophysical Research Letters, 26, 447.

29. Venturi, T., Giovannini, G., Fertti, L., Cotton, W.D., Lara, L. 1999, "Nuclear properties in radio galaxies.", Memorie della Societa Astronomica Italiana, 70, 147.

7.2 Conference Proceedings

1. Alberdi, A., Gómez, J.L., Marcaide, J.M., Pérez-Torres, M.A., Marscher, A.P. 1999, "The parsec-scale radio jet of 4C39.25: witnessing the interaction between a superluminal and stationary component", in "BLLac Phenomenon", ed. L.O. Takalo, ASP Conference Series 159, 1999.

2. Alberdi, A., Gómez, J.L., Marcaide, J.M., Pérez-Torres, M.A., Marscher, A.P. 1999, "4C 39.25: Multi-epoch polarisation observations at 15, 22 and 43 GHz", New Astronomy Review, 43, 731.

3. Behrend, D., Rius, A. 1999, "Geodetic Control of the Madrid DSS65 VLBI Antenna.", In: W. Schlüter and H. Hase (Ed.): Proceedings of the 13th Working Meeting on European VLBI for Geodesy and Astrometry. Viechtach, February 12-13, 1999, Bundesamt für Kartographie und Geodäsie, Wettzell, 1999.

4. Behrend, D., Rius, A., Gradinarsky, L.P., Haas, R., Johansson, J.M., Keihm, S.J. 1999, "Comparison of Independently Derived Atmospheric Parameters", IUGG XXII General Assembly, Birmingham, England, A.409.

5. Giovannini, G., Taylor, G.B., Arbizzani, E., Bondi, M., Cotton, W.D., Feretti, L., Lara, L., Venturi, T. 1999, "1144+35: A giant radio galaxy with superluminal motion", New Astronomy Review, 43, 651.

6. Gómez, J.L., Marscher, A.P., Alberdi, A.,Marti, J.M., Ibanez, J.M., Marchenko, S.G. 1999, "A Close-Up Look at Superluminal Motion: Subparsec Radio Observations of 3C120 and its Comparison with Numerical Simulations", ASP Conf. Ser. 159: BL Lac Phenomenon.

7. Haas, R., Nothnagel, A., Behrend, D. 2000, "VLBI Determinations of Local Telescope Displacements.", In: N.R. Vandenberg and K.D. Baver (Eds.): International VLBI Service for Geodesy and Astrometry 2000 General Meeting Proceedings, pp. 133-137.

8. Lara, L., Mack, K., Lacy, M., Klein, U., Cotton, W.D., Feretti, L., Giovannini, G., Murgia, M. 1999, "GRG 8C 0825+695 and its environment", AG Abstract Services, vol. 15. Abstracts of Contributed Talks and Posters presented at the Annual Scientific Meeting of the Astronomische Gesellschaft, in Göttingen, 20-25 September 1999.

9. Lara, L., Márquez, I., Cotton, W.D., Feretti, L., Giovannini, G., Marcaide, J.M., Venturi, T. 1999, "The broad-line radio galaxy J2114+820", New Astronomy Review, 43, 643.

10. Murphy, D.W., Tingay, S.J., Preston, R.A., Meier, D.L., Guirado, J.C., Polatidis, A., Conway, J.E., Hirabayashi, H., Kobayashi, H., Murata, Y. 2000, "VSOP Monitoring of the Quasar 1928+738", New Astronomy Review, 43, 727.

11. Nothnagel, A., Behrend, D., Campbell, J., Gueguen, E., Haas, R., Tomasi, P. 2000, "Height Variations Determined with the European Geodetic VLBI Network - Preliminary Results", European Geophysical Society General Meeting, Nice, 2000.

12. Pérez-Torres, M.A., Marcaide, J.M., Guirado, J.C., Ros, E. 1999, "Differential astrometry over 15 deg", New Astronomy Review, 43, 587.

13. Rioja, M.J., Porcas, R.W., Garrington, S., Alberdi, A., Saikia, D.J. 1999, "Phase-reference mapping of a weak-cored double-lobed source in the 1636+473 system using MERLIN and Global VLBI", New Astronomy Review, 43, 593.

14. Rius, A., Alberdi, A., Behrend, D., García-Miró, C., Perea, J.A. 1999, "Radioastronomy at the NASA Madrid Deep Space Communications Complex (MDSCC) - Status Report.", In: W. Schlüter and H. Hase (Ed.): Proceedings of the 13th Working Meeting on European VLBI for Geodesy and Astrometry. Viechtach, February 12-13, 1999, Bundesamt für Kartographie und Geodäsie, Wettzell, 1999.

7.3 Circulars

1. García-Miró, C., Gorosabel, J., Calvo, J., Castro-Tirado, A.J. 2000, "The GRB Coordinates Network -GCN- notice #531: GRB 991208 Radio Observation Report.",

Geodetic Very Long Baseline Interferometry at the Onsala Space Observatory 1999–2000

Sten Bergstrand, Rüdiger Haas, Gunnar Elgered

Onsala Space Observatory, OSO

Contact author: Sten Bergstrand, e-mail: geo@oso.chalmers.se

Abstract

We review the performed geodetic VLBI experiments that Onsala has participated in during the period 1999–2000. We concentrate on the performance of the VLBI system, recordings and hardware development. In 1999, eighteen experiments were planned and carried out without major problems. In 2000, twentyfive experiments were originally planned whereas due to limitations in correlator capacity only fourteen will be observed.

1. VLBI Observations

The Onsala 20 m antenna regularly participates in the Europe experiment series. Six experiments were planned and carried out in 1999. In 2000 eight were originally planned, six have been observed so far and one more is scheduled. In addition to this, Onsala participated in six CORE-B experiments in 1999. In 2000, seventeen CORE-3 experiments were originally planned, two have been carried out and three more are scheduled this year. The number of experiments was cut down due to limitations in correlator capacity. Six VLBA experiments were carried out in 1999, and two in 2000 although none were originally planned. All experiments for the period 1999–2000 are listed in Table 1.

Table 1. Geodetic VLBI experiments at the Onsala Space Observatory 1999–2000

Experiments	1999				
Europe-47	Europe-50	CORE-B601	CORE-B604	VLBA13	VLBA16
Europe-48	Europe-51	CORE-B602	CORE-B605	VLBA14	VLBA17
Europe-49	Europe-52	CORE-B603	CORE-B606	VLBA15	VLBA18
Experiments	2000	(up to Oct.	15)		
Europe-53	Europe-55	Europe-57	CORE-3001	VLBA19	
Europe-54	Europe-56	Europe-58	CORE-3002†	VLBA20	
Scheduled	experiments	2000			
Europe-59	CORE-3004	CORE-3005	CORE-3006		

We anticipate correlation problems for the Onsala recordings for Europe-57 in August 2000 due to high receiver temperatures and tape problems in the beginning of the experiment (cf. Figs. 1, 2). The 20m telescope had pointing problem during CORE-3002. However, today only the correlator report for CORE-3002 had been issued. As expected Onsala data were rejected due to low fringe amplitudes.

2. Technical Developments during 1999-2000

Different actions have been made to improve the Mark-IV recorder performance. A dry-air kit with humidity and temperature sensors/regulators has been installed in the tape recorder to ensure satisfying tape environment during recordings. Due to problems with hardware stability when changing between the pressures for thick and thin tape with the field system, a mechanical switch has been installed. The overall system performance is checked regularly, monitoring key parameters like the cable delay, difference between formatter and GPS time, the physical temperatures in the dewar for the front end HEMT amplifiers of the receivers and the measured system temperatures (cf. Fig. 1).

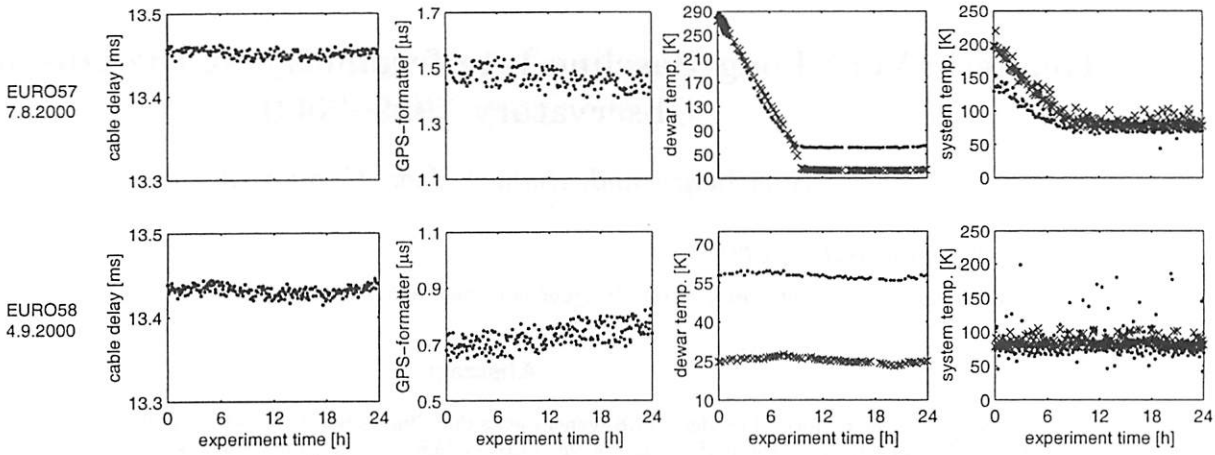

Figure 1. Cable delay, GPS-formatter time difference, dewar temperatures (20K station marked with crosses, 70K station marked with dots) and system temperatures (IF1 marked with crosses, IF2 marked with dots) for the last two Europe experiments. The high initial dewar and system temperatures for Europe-57 will cause a degradation in the signal-to-noise ratio.

After each experiment the parity errors of the recordings are being monitored and checked by track over time, so that any large systematic behaviour can be detected at an early stage (cf. Fig. 2). Tape recorder heads were changed in 1998 and has been sent back to Haystack twice due to inchworm and head tilting problems, respectively. No major changes have been made since May 1999. Presently the run time for the heads is six thousand hours and the performance seems to deteriorate. Recent astronomical observations showed large parity errors and an investigation by the technical staff is ongoing.

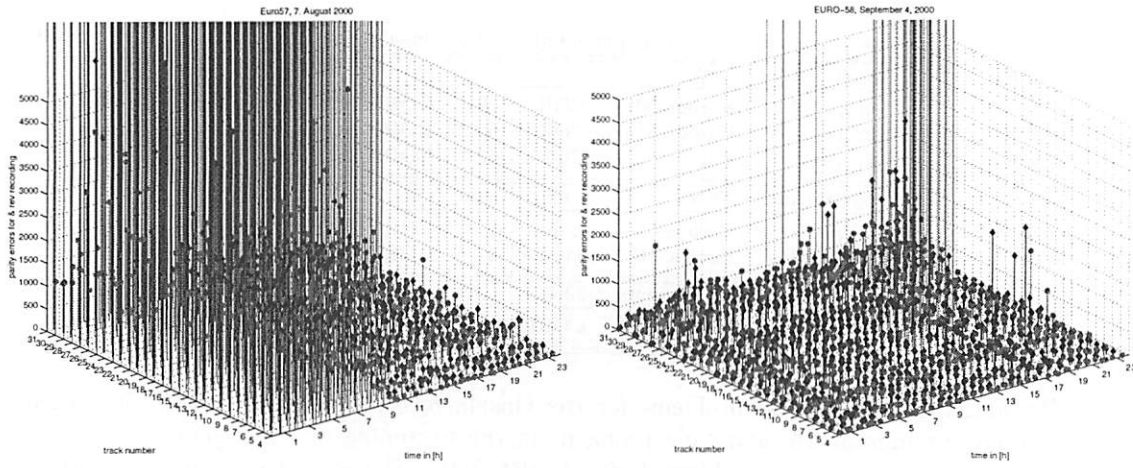

Figure 2. Parity errors for Europe-57 and Europe-58: The large parity errors in the beginning of Europe-57 are due to usage of the wrong tape pressure for the first tape.

The development of a new S/X-band feed as reported previously [1] continues. The current version of the feed did not live up to the pre-set requirements and therefore has to be redesigned.

References

[1] Elgered, G., Haas, R.: Geodetic Very-Long-Baseline Interferometry at the Onsala Space Observatory 1997-1998, 13th Working Meeting on European VLBI for Geodesy and Astrometry, Proceedings, 60–64, 1999.

14th Working Meeting on European VLBI for Geodesy & Astrometry

EFFELSBERG OBSERVATORY REPORT

R. W. Porcas & W. Alef

MPIfR, Bonn

1) The present "Friend of VLBI" in Effelsberg is Dr. Alex Kraus (akraus@mpifr-bonn.mpg.de)

2) The VLBI interface to the Effelsberg drive program has been modified for automatic recognition of SKED-created commands specifying the azimuth drive direction in the azimuth overlap region.

3) The tape drive electronics of the MK4 recorder have been upgraded to VLBA style (it is now a "VLBA4 recorder") to increase recording reliability, and also to permit its use as a second recorder with the VLBA terminal. However, since both thick and thin tapes are still in use in the geodetic and astronomical observing communities, the MK4 recorder is at present only used for recording THICK tapes. We hope this will produce more reliable recordings and reduce head wear. Astronomical programs requiring use of thin tapes are recorded using the VLBA terminal.

4) An additional 4 BBCs have been added to the VLBA terminal, bringing the total to 8, making better compatibility for joint observations with the VLBA. An upgrade of the VLBA formatter is also planned, to permit dual-recorder 512 Mb/s operation together with the VLBA.

5) It is planned to install an Ashtech Z-12 GPS receiver (from the BKG) in Effelsberg to provide positioning data.

6) The new 8.4 GHz receiver has not yet been installed in the telescope. This receiver will support the "R&D" wide frequency range at X-band.

7) Worn gears on the azimuth drive have resulted in a restriction on the drive rate to a maximum of 20 deg/minute. New gears are expected in October 2001.

September 2000

Section 3

Correlators Reports

The new MPIfR-BKG MK IV correlator

W. Alef, D.A. Graham, J.A. Zensus
Max-Planck-Institute for Radioastronomy, Bonn

A. Müskens
Geodetic Institute, University of Bonn

W. Schlüter
Bundesamt für Kartographie und Geodäsie

9th November 2000

Abstract

A MK IV correlator was installed at the MPIfR, Bonn in December 1999 by MIT Haystack Observatory. Is is jointly operated by the MPIfR and the BKG. We present an overview of the correlator system with emphasis on the major differences to the old MK IIIA data processor. We give a summary of the present correlator operation at Bonn for both the MK IV and the MK IIIA correlators.

1 Introduction

Nearly 10 years ago the Max-Planck-Institute for Radioastronomy (MPIfR) and the Institut für angewandte Geodäsie (IFAG, now Bundesamt für Kartographie: BKG) agreed to jointly acquire and operate a MK IV VLBI correlator. In December 1999 a standard MK IV correlator was installed at the MPIfR in Bonn by MIT Haystack Observatory. The old MK III and MK IIIA correlators in Bonn which have served both the astronomical and geodetic community for nearly 20 years will be taken out of operation this year.

Like the MK III correlator the MK IV will be used for geodetic observations and MPI based astronomical observations, where the emphasis is on mm-wavelengths and the developement of new techniques.

Overview of the timeline of the MK IV correlator project:

- In 1991 IFAG (now BKG) and MPIfR agreed to jointly buy and run a MK IV correlator.
- In 1992 IFAG and NASA signed a contract about delivery of a MK IV correlator to Bonn
- Fall 1993: Start of the project by the IACC (International Advanced Correlator Consortium)
- Jan 1995: First prototype VLSI correlator chip
- Jul 1996: Chips produced by HP foundry
- Oct 1997: First fringes from tape
- Apr 1998: First 2 tape-drive fringes (Haystack)
- Nov 1999: The MK IV correlator replaces the MK III correlator at Haystack
- Dec 1999: Installation of MK IV correlators at USNO, Washington and MPIfR, Bonn

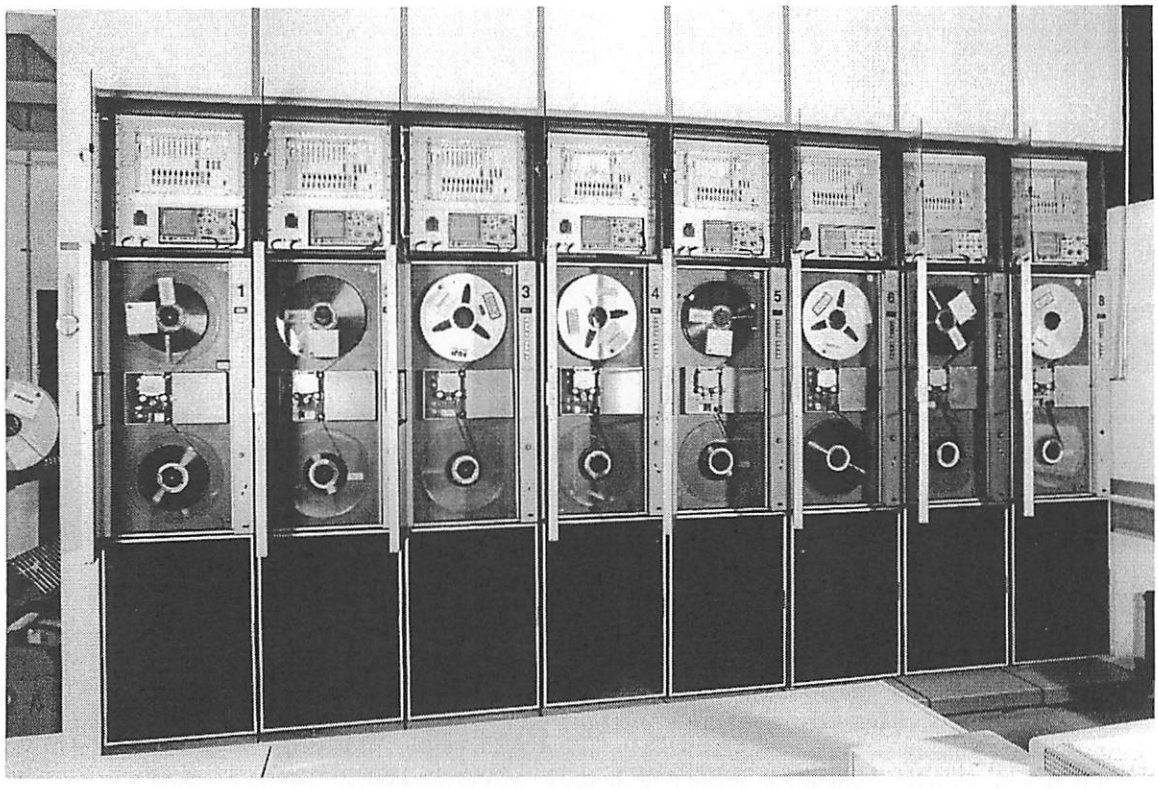

Figure 1: 8 of the 9 tape drives of the new MK IV processor in Bonn. Above each tape drive there is a station unit, which controls the tape drive, handles the station based aspects of the data processing, and sends the data to the correlator proper via high speed serial links.

2 MK IV Correlator Major Design Features

The MK IV data processor is roughly 1.5 orders of magnitude more powerful than the MK IIIA correlator. Its major design features are:

- It can handle bit rates of up to 1 Gbps/station
- Up to 16 stations can be correlated simultaneously
- It can process 1 or 2 bits/sampled data
- The correlator is lag-based, implemented on a new VLSI correlator chip
- It has a fully station-based architecture; station model parameters are embedded in the data streams
- The MK IV data processor is fully compatible with MK IIIA, MK IV, and VLBA formats
- Full space-VLBI compatibility is provided (high delay rate and acceleration are possible)
- Multi-tone phase-cal extraction can be used
- Station based pulsar gating
- High speed serial links are used for efficient data distribution
- correlation can be done at 3.5 times the standard recording speed
- The correlator is real-time compatible
- Efficient and flexible post-correlation software (HOPS, MPIS, FITS) is available

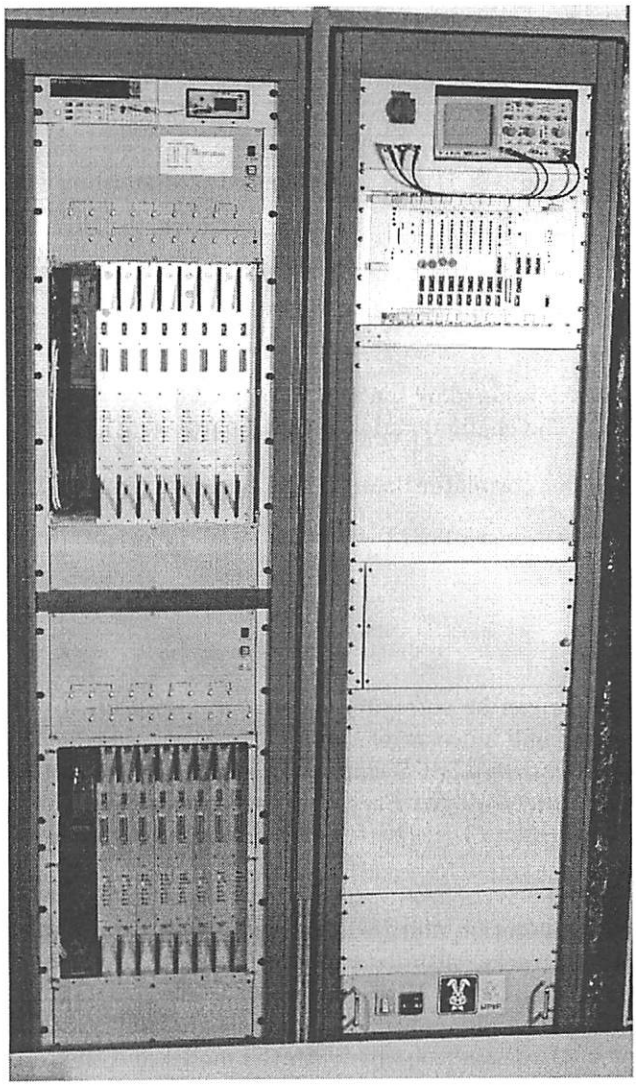

Figure 2: The rack on the left shows the 2 crates of the MK IV correlator. In each crate 8 oversized correlator boards are visible. The crate control computer is in the dark slot on the left of each crate. In the rack on the right the station unitand scope for recorder 0 can be seen.

- A smooth transition from MK IIIA

3 The Hardware

A fast HP workstation serves as the so called Correlator Control Computer (CCC). It initiates and controls the correlation process, runs the operator interface, supervises all other computers in the correlator system, and receives the data from the correlator. In addition it performs all of the required post-processing. CCC and all other computers are connected via ethernet; an RS-422 connection to the tape drives is used to speed up tape operations.

3.1 The Correlator

The correlator consists of 2 crates. Each crate hosts 8 correlator boards,2 data input units, and a crate control computer. Furthermore there are a clock and a timing module.

MK IV	MK IIIA
~128,000 lags (real; 64,000 complex)	1344 complex lags
1 or 2 bits/sample	1 bit/sample only
operating at 32 Msamples/sec	operating at 4 Msamples/sec
16 (9) playback systems up to 1 Gbps each	$\leq$ 8 playback systems up to 128 Mbps each
flexibly configurable using ASCII files	limited configurability using ASCII files
16 input channels	28 input channel of 4 Mbps
software incomplete, many bugs	stable, well debugged software

Table 1: Overview of the most important differences between the **MK IIIA and MK IV correlators**

The correlator board was developed by the International Advanced Correlator Consortium (IACC: USNO/Haystack/JIVE/BKG). The characteristics of each board are:

- 32 VLSI correlator chips per correlator board
- 64 2-bit data streams input to each board
- 16,384 lags/board
- $\leq$128 baselines/board

With the 16 modules 16 stations can be correlated at a data rate of up to 1 Gbit/sec/station with 32 lags per baseline including cross- and auto-correlation.

The correlator chip is a full-custom CMOS chip with ~1,000,000 transistors. The chip has 512 lags and can run at a clock rate of up to 64 MHz. Each chip costs about $150.

3.2 The Station Unit

Each tape drive is controlled by a station unit (SU) via an RS-232 serial link. Each SU can reconstruct up to 16 channels from up to 64 tracks [1]at a data rate of up to 16 Mbits/sec/track. The data are pre-delayed according to the model sent to the SU from the CCC. The tones of the phase-calibration signal are extracted, and pulsar gating may be applied. The data is transmitted to the correlator modules via 4 high speed serial links ($\leq$1.6 GBits/sec) together with the model and the recovered phase-cal signals.

4 The Software

4.1 Control files

All control files for the correlator, the station unit, and the observations are stored as ASCII files. All files use the VEX language, which was invented for VLBI observing. The following files are used:

- Global initialization file: `global.ivex`
- Correlator initialization: `global.cvex`
- Station unit initialization: `global.svex`
- Definition of experiments: `global.evex`
- Experiment specific observe file: `xxxx.ovex`
  (where `xxxx` is the experiment number)
- Log-file summary in vex format: `xxxx.lvex`

[1]In Bonn the playbach units are only equipped with 1 head so that only up to 32 tracks can be used.

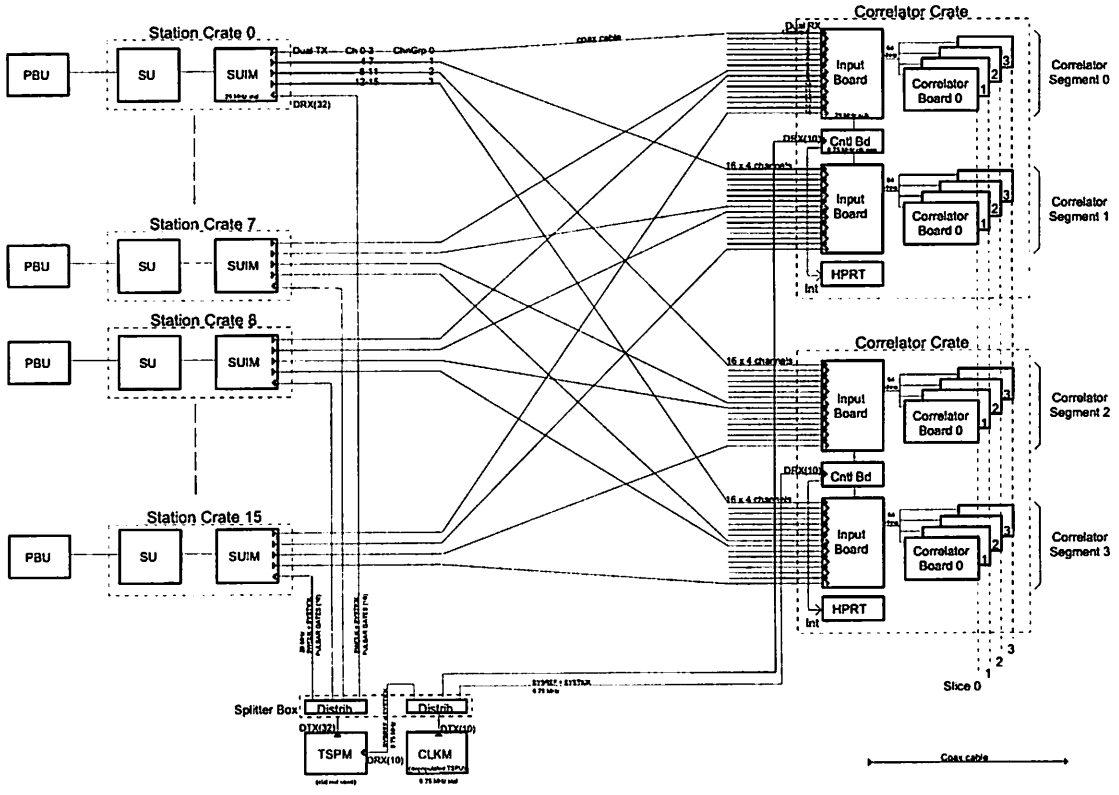

Figure 3: Correlator signal interconnection diagram. The figure shows a 16 station setup.

4.2 Programs

The software is written in C and tcl/tk. The correlation is organized by scan. The only correlation mode presently implemented is a start/stop mode of correlation, which is a sequence of set-up, finding the first time on tape, synchronizing the tapes and correlation. A scan is a single entity in the `$SCHED` section of a vex observing file.

The central task dispatching and synchronization is implemented in a so called 'state machine' in the program `CONDUCTOR`. The operator supervises the correlation process via a gui driven operator interface `OPERA`. Other major parts of the software are the root-file generator, the correlator manager `CORRMAN` and the station unit manager `SUMAN` (see fig. 4). The communication between the programs is realized via a messaging system.

4.3 Data files

The correlation of a scan results in a *fileset* with a single *root* file. There may be multiple filesets for a scan resulting from more than one correlation. All member files in a fileset share the same root extension code as a suffix. This extension code is the encoded creation time of the root file.

- Root file (type 0 file)
  ASCII, 1 per scan. E.g.: `3C345.nopqrs`
  ({source name '.' mapped to '-'}.{root extension code: date of creation})
- Correlated data file (type 1 file)
  binary, 1 per baseline. E.g.: `BL..nopqrs`
  ({baseline}..{root extension code})

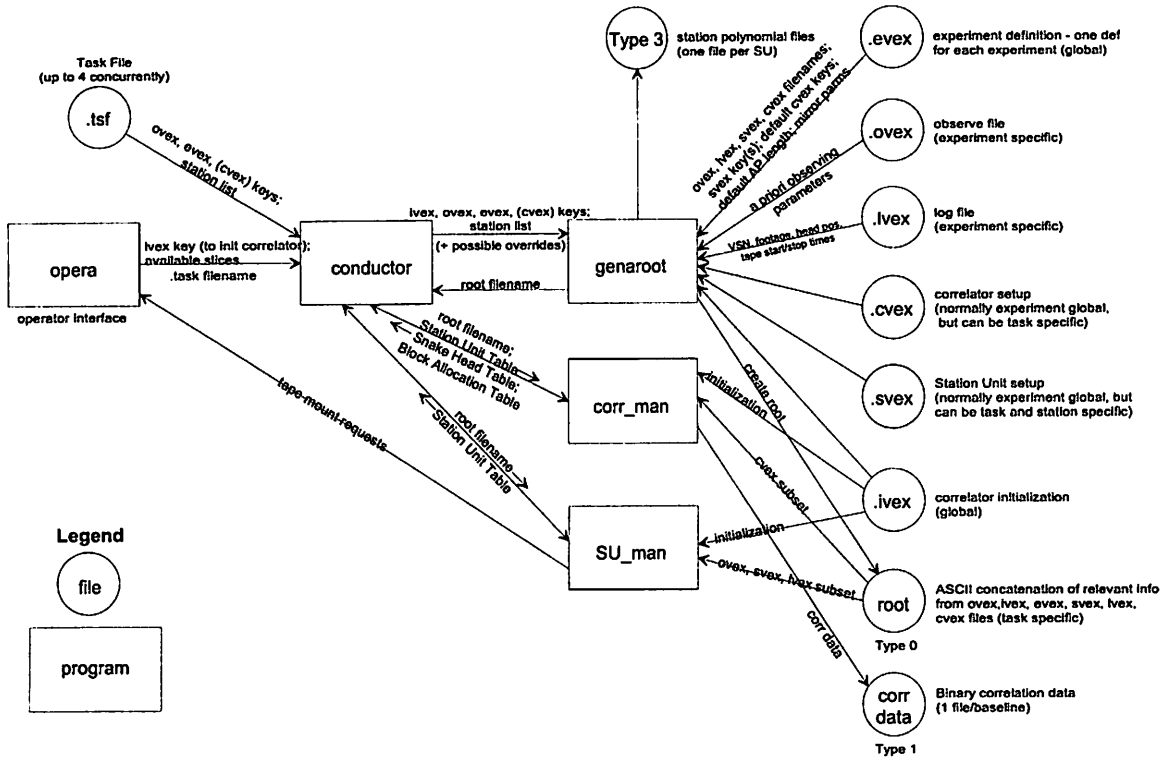

Figure 4: Block diagram of the correlator software.

- Fringe fitted data file (type 2 file)
  binary, many per baseline. E.g.: `BL.X.1.nopqrs`
  ({baseline}.{freq.}.{seqno}.{root extension code})
- Station data file (type 3 file)
  binary, 1 per station. E.g.: `L..nopqrs`
  ({station}..{root extension code})
- FITS correlation data file (type 5 file)

4.4 Post-processing software (HOPS)

The post-processing software is a further development of the MK IIIA post-processing software. It's major components are:

- `fourfit`: a fringe-fitting program. It is used to check the quality of the correlated data and to determine the precise parameters of the interference fringes.
- `aedit`: is used for overall data inspection (after fringe-fitting) and for data selection in the case of multiple correlation passes
- `fringex`: data export and segmentation of scans into smaller entities
- `mk4fits`: (fits writer for MK4 data, under development)

After the correlation is finished the data is archived on DAT cassettes with the UNIX tar command.

5 Present Status:

5.1 Highlights at Bonn

Following installation in December 1999 and an extensive period of test and development, the MPIfR MK IV correlator is now in use for both astronomy and geodesy experiments. Tests included correlation of an astronomical experiment (C99L3) and a geodesy experiment (IRIS-146) on both the MK IV and MK IIIa correlators. A comparison between the two correlators gave encouraging results. Proper production correlation started after the implementation of the phase-cal extraction in April 2000.

A backlog of about 1.5 month exists for both geodetic and astronomical observations. The correlation efficiency for 1-pass correlation is still worse than that of the old MK III correlator.

Exporting geodetic data to CALC/SOLVE is standard. A simple (but not sufficient) interface to the Caltech software exists.

Although many correlation modes remain to be developed or tested, the present tested capabilities include:

- 15 DEC 1999 - First fringes in MK3-Mode C using a 4-channel subset
- 21 JAN 2000 - Increase of the useable number of playback drives from 4 to 6.
- 16 FEB 2000 - First fringes with a VLBA mode (64-16-1) from a VLBA formatter (test experiment Eb-Mc, Feb 2000)
- 15 MAR 2000 - Playback of a fan-out 1:2 mode
- 5 APR 2000 - Correlation of dissimilar tape speeds
- 6 APR 2000 - Extraction of the phase-cal signal
- 7 APR 2000 - Replay of 2-bit sampling mode
- 7 APR 2000 - Playback of a fan-out 1:4 mode
- 12 APR 2000 - Playback of a mode using "barrel roll"
- 10 AUG 2000 - Allow integration times larger than 0.5 s
- 10 AUG 2000 - Decrease the scan set-up time
- 10 AUG 2000 - Decrease the synchronization time for most scans to less than 1 s

5.2 Wishlist

High priority items which have to be implemented still are:

- Increase number of useable playback drives to 9. For the end of 2000 it is expected to be able to correlate with 8 tape drives.
- Double-speed playback (extra equalizers planned, switchable; ready by the end of 2000)
- Dual LHC/RHC fringe-fitting in `fourfit` (end of 2000)
- Implement `fringex` (end of 2000)
- Implementation of a data route into AIPS: `mk4fits` (beginning of 2001)
- More than 256 lags for spectral line observations
- software to automatically generate re-correlation lists
- continuous correlation (increase throughput)

- multiple correlation streams
- 2-tone phase-cal in fourfit
- ... and of course: fix more bugs (mostly in the station unit)

5.3 Correlation

5.3.1 MK IIIA

The MK IIIA correlator is still in use for 2 astronomical and 1 geodetic observation. It will be switched off on 1.10.2000.

5.3.2 MK IV

The first production correlation was performed in February 2000.

Correlation is being ramped up since April 2000 after the extraction of the phase-cal signal was implemented. The correlation efficiency is still 20 - 30% lower than with MK III for 1-pass correlation. This is mostly due to slow and somewhat fragile station unit.

6 Official opening of the MPIfR/BKG MK IV correlator will be on 17th November

The EVN MkIV Data Processor at JIVE

R. M. Campbell[1]

Joint Institute for VLBI in Europe, Oude Hoogeveensedijk 4, 7991 PD Dwingeloo, the Netherlands

The inauguration of the EVN MkIV data processor at JIVE took place at the 4 EVN/JIVE Symposium. Since then, we have been increasing the capabilities, flexibility, and reliability of the correlator, and have now processed several test, pilot, and user experiments. Milestones include the first scientific publication resulting from data correlated at JIVE: detection of HI absorption within 20 light-years of the nucleus of NGC4261. We will discuss these developments and accomplishments at the JIVE correlator, with a few concluding thoughts on processing geodetic experiments.

1. Introduction

A key item in the MkIV upgrade of the EVN was the construction of the EVN MkIV data processor at the Joint Institute for VLBI in Europe (JIVE). JIVE is hosted by ASTRON in Dwingeloo, the Netherlands, and is funded by science councils in a number of European countries. Special projects have been funded directly by the EU. The EVN MkIV data processor was constructed in the context of the International Advanced Correlator Consortium, through which the other MkIV (geodetic) correlators were also built (see Casse 1999 for details of the IACC), with significant contributions, from European members, in hardware from CNR/IRA, control software from Jodrell Bank, and correlator software from ASTRON.

The first fringe on the EVN MkIV data processor was seen on 21 July 1997, and its official inauguration took place on 22 October 1998. Casse (1999) and Phillips & Van Langevelde (1999) provide a description of the correlator and the detection of fringes at that time. The "first science" resulting from data correlated on the EVN MkIV data processor detected HI absorption against the counterjet very close to the nucleus of NGC4261, providing the ability to see the transition from molecular to atomic gas in the disk, and hence to say something about its thermal structure (Van Langevelde *et al.* 2000; Pihlström 2000).

Since the previous EVN Symposium, we have made a great deal of improvements in the capability and operation of the JIVE correlator. This paper will concentrate on areas of interest to the user having data correlated at JIVE: tools for planning observations with regard to the correlator's capabilities, current operational and communication flow between JIVE and the PI, and what we at JIVE do to get your data to you in a usable form. More information about using the EVN and JIVE can be found at the (newly redesigned) JIVE website: `www.jive.nl/jive`. A brief concluding section looks at some of the issues relating to future processing of geodetic experiments on the JIVE correlator. It is possible to support geodetic processing at some point in the future, however neither a detailed plan nor funding for such a project currently exists.

[1]On behalf of the JIVE Data Processor Group

2. Capabilities

Basic characteristics of the design of the EVN MkIV data processor include: correlation of up to 16 stations, with 16 channels per station, 1 Gb/s recording (via 2 head-stacks × 32 heads × 16 Mb/s/track), and use of either MkIV and VLBA format recordings. The principal science drivers behind the development of the correlator and associated software include the ability to handle continuum dual-polarization observations, spectral line experiments (*i.e.*, providing lots of frequency points and narrow bandwidths), and phase-reference mapping.

Current capabilities include:

- 2-bit sampling.
- cross-polarization.
- up to 512 frequency points for correlation of up to 8 stations; up to 128 frequency points for 9–16 stations (see the discussion following equation 2-1).
- fan-out modes, where 1 channel was written onto 2 or 4 tracks, increasing bandwidth without using higher tape-speeds.
- processing of both MkIV and VLBA type recordings.
- sustained 256 Mb/s recordings, a capability that is currently unique to the EVN (see, *e.g.*, Garrett, Muxlow, Garrington, *et al.* 2000).

Capabilities whose development is still underway or not yet fully tested include:

⊙ Oversampling at 2, 4, 8, or 16 times the Nyquist frequency in order to provide bandwidths down to 125 kHz (*i.e.*, 2 MHz ÷ 16). Oversampling up to a factor of 4 will also provide a finer fractional bit-shift correction, and hence some SNR improvement.

⊙ MkIII modes.

⊙ Pulsar gating. (The replication of individual channels useful in pulsar-gate fitting can also be applied to one-pass correlation of multiple field centers.)

Capabilities that are yet to come include:

- Reading observations with barrel-rolling.
- Playback at tape speeds different than used in recording.
- 1 Gb/s data rates — 320 ips and 2-head recording/playback each contributing a factor of 2 increase from the current 256 Mb/s.
- Recirculation — achieving >2048 frequency points via time-sharing the correlator.
- Sub-netting.
- Multi-pass correlation (>16 stations).
- Phase-cal extraction.
- Space VLBI.

There are two equations that are useful when planning observations that will be correlated on the EVN MkIV data processor. The first relates to total correlator capacity:

$$N_{\rm sta}^2 \cdot N_{\rm sb} \cdot N_{\rm pol} \cdot N_{\rm frq} \leq 131072 \quad (= 2^{17}). \tag{2-1}$$

We are currently limited to one-quarter of this capacity (*i.e.*, 32768 vice 131072) pending installation of local processing capacity (DSP's) onto all correlator boards, which we anticipate to be in place before the end of 2000. In equation (2-1), $N_{\rm pol}$ is the number of polarization combinations wanted in the correlation (1, 2, or 4). $N_{\rm sb}$ represents the number of different frequency subbands, counting lower- and upper-sidebands from the same BBC as distinct subbands, but not multiple polarizations in the same sideband (these enter via $N_{\rm pol}$). The value to use for $N_{\rm sta}$ is currently either 8 or 16: if you have 7 stations, use "8"; if you have 9, use "16". We plan in the future to reduce this granularity in $N_{\rm sta}$ from multiples of 8 to multiples of 4. When recirculation is operational, the constant term 131072 will be multiplied by the recirculation factor used. Equation (2-1) takes into account all correlator products, both cross- and auto-correlations. You should pick the various N parameters in designing your observation such that the equation holds, otherwise you will have to compromise on at least one of them when it's time to correlate.

The second equation relates to output capacity:

$$\frac{N_{\rm sta}^2/2 \cdot N_{\rm sb} \cdot N_{\rm pol} \cdot 2N_{\rm frq} \cdot 8\,\text{bytes}}{t_{\rm int}} \quad = \quad \text{Output Rate.} \tag{2-2}$$

Our current peak output rate is ~250 kB/s (which puts a lower limit to integrations times for experiments using the full correlator of ~4 s). In the future, with the Post-Correlator Integrator operational, the output rate may go as high as 40 MB/s.

3. Operational Concerns

Figure 1 summarizes operational and communication flow between the PI, JIVE, and the various EVN assets during an EVN astronomical experiment (this figure is available in color, clarifying the lines of data/communication flow, at `www.jive.nl/~campbell`). The user deposits SCHED output on VLBEER, from which individual stations draw their observing instructions. Help from JIVE of course may be requested during the scheduling process. Following the observations, the stations deposit logs and GPS data on VLBEER, sends tapes to JIVE, and posts comments to the JIVE website. We pull necessary information off VLBEER, prepare files that will drive the correlation, and send e-mail to the PI describing what we envision the correlation of the experiment to entail. The PI has the opportunity to review the parameters in our e-mail and all other available information (information about items with a check in figure 1 are available on the JIVE website or anonymous FTP server), and writes back to pass along any requests for changes (*e.g.*, improved source coordinates, *etc.*) and/or confirm that correlation can go ahead.

We operate the correlator 80 hours per week, from which time system testing and development must also come. When correlation of the experiment is finished we review the output, make diagnostic plots (which we put on our anonymous FTP server), and send post-correlation e-mail to the

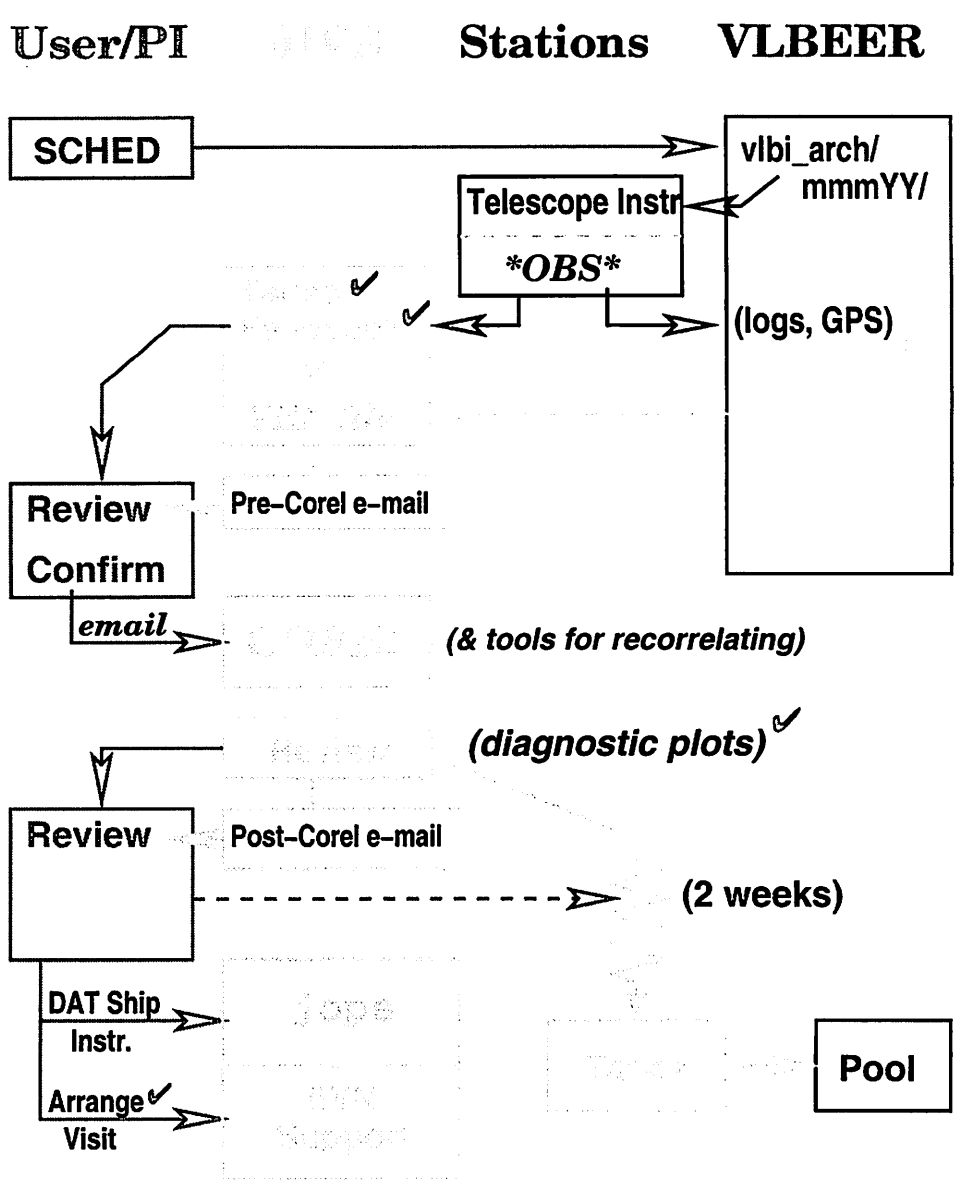

FIGURE 1: Operational flow for the observation and correlation of an experiment.

PI summarizing the results of the correlation. After reviewing the e-mail and plots, and after any further discussions with the responsible JIVE support scientist if necessary, the PI can then arrange for the shipment of the FITS-file DAT and also for visiting the EVN support group at JIVE for help in data reduction if desired. We usually request that you let us know by a certain date whether it's okay to release the tape back into the pool. It greatly benefits the whole network if PIs could give us this authorization in a timely fashion, especially for thin tapes.

Our internal data review process begins by transforming the lag-based correlator output into lag- and frequency-based AIPS++ Measurement Sets (MS). These MS contain a data-cube of the real & imaginary components of the correlation-function per subband per baseline/autocorrelation. We can then investigate slices of the correlation functions in time and lag/frequency channel, allowing us to detect and diagnose various problems with the recorded data or the correlation itself, and to determine any scans for which recorrelation would be profitable. There are also various plots more

suited to providing feedback to the stations rather than to the PI. We usually flag subsets of the data for low weights or other known problems resulting in spurious correlation amplitudes and phases. The last step is converting the final MS into a FITS file, which can be read into AIPS directly using FITLD.

As of 8 October 2000, we have completed correlation of 24 user and 15 test experiments. A further 7 user and 1 test experiments were then in the process of running or in the queue (not including experiments from the September 2000 session). Nine user experiments were on hold awaiting either further PI liaison (6) or specific correlator features (3). We have so far processed and distributed data from experiments having goals including:

- continuum mapping (including a global experiment).
- HI absorption (1420 MHz & UHF).
- OH megamasers.
- Phase-reference mapping.

4. Geodetic Considerations

As mentioned in the itemized list of current and future capabilities in § 2, we can not yet extract phase-cal tones. We must have this capacity before processing geodetic experiments in order to allow computation of the multi-band delays.

However, output data formats seem to be the major issue. For geodetic or astrometric experiments, the final desired "product" is a time-series of "total" multi-band delays, (phase) delay rates, and phase delays for each baseline. Here "total" denotes that the correlator model, which shifted and slowed down the fringes sufficiently to allow correlation over a reasonable number of lags and integration time, has been added back into the correlator (model-residual) output. These totals are then used as constraints in CALC/SOLV, MODELFIT, VLBI3, *etc.* to refine various subsets of model parameters (*e.g.*, Earth orientation, shape, and rotation; tropospheric propagation; source position). As discussed in the latter part of § 3, the correlator outputs lag-based correlation-function data in a JIVE-specific binary ("CDF") format. This format has no relation to the root/corel/fringe/sudata file- and record- structure inherited from the MkIII type 50/51/52 files, which feed directly into HOPS for fringe-fitting (`fourfit`) and exporting totals (`fringex`). Of course, this variance of correlator-output binary formats is not an unprecedented occurrence: data processed on the VLBA correlator also do not have a direct way into HOPS — the resulting FITS files need to be processed through AIPS in order to obtain the desired totals data-files for final geodetic/astrometric analysis.

At first thought, there appear to be three possibilities for the path for geodetic data:

- As described in § 3, we already are able to create FITS files that can be processed through AIPS just as one would do with a FITS file from the VLBA correlator. Therefore, the procedures used for analyzing VLBA-correlated geodetic observations could simply be carried over. However, we first need to be able to write the associated IM and MC tables containing model information to allow calculation of totals. The model polynomials used by the station units (*viz.*, delay application) and correlator (*viz.*, fringe rotation) are written to the output-data directory during the correlator-job preparation stage, but do not currently find their way into the Measurement Set (nor, hence, into the FITS data).

- Currently, our output data passes through an AIPS++ Measurement-Set stage on their way to becoming a FITS file. Like the old type-51's, the MS contains the correlation-function real and imaginary components for all the correlated baselines. In principle, functionality equivalent to HOPS `fourfit` and `fringex` could be created in `glish` (the high-level AIPS++ control language) for operation directly on the MS itself and direct export of the desired totals, bypassing the FITS-file stage.
- Rather than conversion of the CDF file into a Measurement Set, it may also in principle be possible to transform it into the root/corel/fringe/sudata file-/record-structure for direct analysis via HOPS. EVN document #68 (van Langevelde & Noble 1996) discussed various aspects of data output formats and consequences on processing — notably for HOPS-compatible file structure, the difficulty of maintaining separate baseline-specific files when up to 16 stations can be mounted at once.

Each of these options, especially the latter two, will require quite a significant amount of new software to be written. Testing/validation for the latter two would also have to begin essentially from scratch, using data correlated at JIVE and on another MkIV correlator. Even validation of the data path through FITS will require a substantial amount of verification, as was/is needed for the VLBA.

References.

Casse, J.L. 1999, in *Proceedings of the* 4$^{\rm th}$ *EVN/JIVE Symposium*, eds. M.A. Garrett, R.M. Campbell, & L.I. Gurvits, *New Astron. Rev.*, **43**, 503. "The European VLBI Network MkIV Data Processor."

Garret, M.A., Muxlow, T.W.B., Garrington, S.T., *et al.* 2000, *Astron. & Ap.*, submitted. "EVN Observations of the Hubble Deep Field."

Phillips, C.J. & Van Langevelde, H.J. 1999, in *Proceedings of the* 4$^{\rm th}$ *EVN/JIVE Symposium*, eds. M.A. Garrett, R.M. Campbell, & L.I. Gurvits, *New Astron. Rev.*, **43**, 609. "Fringes on the EVN MkIV Data Processor at JIVE."

Pihlström, Y.M. 2000, in *Proceedings of the* 5$^{\rm th}$ *EVN Symposium*, eds. J. Conway, A. Polatidis, & R. Booth (Gothenburg: Onsala Space Observatory, Chalmers Technical University), in press. "A Thin HI Circumnuclear Disk in NGC4261."

Van Langevelde, H.J. & Noble, R. 1996, *EVN Document #68.* "JIVE/EVN Correlator Output; Formats & Diagnostic Tools."

Van Langevelde, H.J., Pihlström, Y.M., Conway, J.E., Jaffe, W., & Schilizzi, R.T. 2000, *Astron. & Ap.*, **454**, L45. "A Thin HI Circumnuclear Disk in NGC4261."

Comparison of MK III and MK IV Correlation using a 4–station IRIS–S experiment

Arno Müskens, Klaus Börger, Mauro Sorgente, James Campbell

Geodetic Institute, University of Bonn, Nussallee 17, 53115 Bonn

contact: mueskens@mpifr-bonn.mpg.de ; campbell@sn-geod-1.geod.uni-bonn.de

September 2000

Abstract:
A 4–station IRIS–S VLBI experiment has been used to compare the performance of the new MK IV correlator and the existing MK III correlator that will be phased out this year. At the correlation center of the *Max–Planck–Institute for Radioastronomy (MPIfR)* in Bonn, the new MK IV correlator, which is based on an entirely new design, has been installed in December 1999 and is presently being phased into operation. The routine 4–station processing level including phase calibration has been achieved in May 2000. At this point it made sense to carry out a first full–scale comparison that includes the single–session geodetic results. The outcome of the comparison both in terms of correlator/fringe output as well as delay residuals and geodetic baseline parameters is presented.

1 Introduction

Back in 1990 a "Prototype Next Generation Correlator" Project was initiated by a consortium of institutions on the East Coast of the United States. In 1993 the construction of a completely new designed successor for the existing MK III(A) VLBI data acquisition and recording system was started at Haystack Observatory under the designation "MK IV Correlator Project". The first hardware was delivered in June 1999 and in December 1999 the first operational correlator tests were performed at the Washington VLBI correlator at the *United States Naval Observatory (USNO)* [*Kingham and Martin*]. Nearly at the same time the era of MK IV started at the Bonn VLBI correlator center at the *MPIfR* [*Alef et al.*]. An identical correlator as had been set up at *USNO* was installed by members of the Haystack Observatory at the *MPIfR* in December 1999. This correlator is used partly by the *MPIfR* for astronomical observations and partly by the *Bundesamt für Kartographie und Geodäsie (BKG)* in cooperation with the *Geodetic Institute of the University of Bonn (GIUB)* for geodetic applications. In the first months of the MK IV correlator operations *Kingham and Martin* as well as *Alef et al.* reported about the teething problems of the new correlator, which of course had to be expected with an entirely new system of such high complexity. Therefore it will take some time until the full potential of MK IV will be reached.

Starting in December 1999 with only 4 playback units and processing of a maximum of 6 baselines with 8 tracks, by August 2000 we had a 6 station correlator capable of processing all 15 baselines with 16 tracks including phasecal. The full operation at Bonn will include all 9 stations with all modes and other promised features. Due to the special circumstance, in the first part of 2000, of having both the old MK III and the new MK IV correlator in operation, we were able to perform a full–scale correlator comparison. This comparison will go beyond the pure correlation and includes FOURFIT analysis and as well as geodetic post–processing.

For this purpose an IRIS–S experiment has been used which belongs to the series of experiments that are usually correlated in Bonn. The chosen experiment is of March 27, 2000, with the official name IRIS–S 148. It is a standard IRIS–S experiment with four stations participating, i.e. *Fortaleza*, *HartRAO*, *Westford* and *Wettzell*. *Gilcreek* was scheduled but did not observe, because the antenna tracking computer was down.

2 Steps of Data Analysis

This section shortly describes the data flow in the MK III/MK IV VLBI data analysis in order to point out those places where a comparison of MK III and MK IV data can be made without excessive difficulties.
The received signals from the radio sources are combined at the correlator and in a subsequent fringe–fitting process using the MK3FIT software in MK III and FOURFIT in MK IV the group delay observables are determined. Then the software module DBEDIT sorts the data by time and filters them in such a manner that only the "best" observations enter the post–correlation analysis. The data is placed into a first version of X–Band and S–Band database.

The next step in the MK III / MK IV VLBI data analysis is to compute the contributions which in their sum form the theoretical delay as well as all theoreticals and partial derivatives which go into the parameter estimation. This is done by the CALC software module and in this way version 2 of the X–Band and S–Band database is generated. Furthermore, the original observations have to be corrected due to several systematic effects, in particular atmospheric refraction. This correction is called calibration. In order to determine the cable and weather calibration XLOG is used which is an automatic controlled version of the old PWXCB. The DBCAL–program then writes the respective corrections into the X–Band database.

The steps just described prepare the data for use in the adjustment and they finally deliver version 3 of X–Band database and version 2 of S–Band database which now are ready to enter the parameter estimation. For this purpose the SOLVE run is launched, but before the final analysis some preparatory work is necessary again. The group delay ambiguities have to be eliminated and then the analyst has to apply the ionosphere correction in order to calibrate the X–Band database. An update saves all steps and results and provides version 4 of the X–Band database.
Now the analyst creates the final solution. At this stage the data should be calibrated and set up correctly by the preceding steps. The further handling serves to determine the parameters with the aim to obtain an optimized least–squares–fit to the data. In the end the adjustment of the observation weights is made using the $\chi^2 = 1$ citerion.

3 Correlator Status during comparison

It should be mentioned, that the hardware structure of both correlators is completly different. The newly designed MK IV VLBI processor requires therefore also a completly new developed software.
At the comparison epoch (July 2000) the newly written MK IV software had not yet been completed in every detail. Therefore setting up and running the correlation process took more time as in the earlier MK III software. Also, the correlator processing analysis software is still incomplete (in particular the *Haystack post processing software package (HOPS)*) which causes a large additional effort in time for the analysis. Here some of the main problems are pointed out which caused extra work during the comparison:

- hand editing of vex files
- hand editing of the processor task files

- correlator control software problems
  - o head peaking software unreliable
  - o synchronisation of tapes unreliable
  - o messenger problems in correlator control software
  - o accumulation periods still too short (0.5s)
  - o Station Units have "forks" problem; this causes FOURFIT to generate a quality factor of "G" (unusable obs.)
- HOPS (in particular AEDIT module) incomplete
- Reprocessing not yet available
- FOURFIT problems in some cases (FQ=0/9)

The present MK IV correlator software status (Sept. 2000) corresponds no longer exactly to the one which was available under the comparison conditions (July 2000). Every second week improvements are bringing significant progress towards the successful completion of the system.

	MK IIIA	MK IV
hardware	HP1000(A900) 2 CAMAC system 9 MK3A playback rec. parallel twisted pair	HP-WS C360 HP-UX 9 SU (station units) 9 MK4 playback rec. HighSpeed serial Links
software	TLUP, TRACK (NRAO) control files correlator software (COREL etc.) transfer files MK3FIT (FRNGE), HOPS Reprocessing sofware	TUBA, TRACK (NRAO) vex files, global vex files correlator control software (CONDUCTOR etc.) task files FOURFIT, HOPS (incomplete) Reprocessing software missed

Tab. 1: Overview of MK III/MK IV hardware and software

4 Comparison of the correlator output

In principle, we have to mention that every scan which is reprocessed several times at the same correlator, produces slightly differing results. This is true for both correlators and has its reasons in many different technical problems during recording and processing the data. In order to

bsl/frq	MK III			MK IV		
	FQ = 1-2	FQ = 0	FQ = 7-9	FQ = BEG	FQ = 0	FQ = 7-9
FJ:X	0	15	118	1	17	117
FJ:S	0	2	130	2	4	129
FE:X	0	15	139	2	14	133
FE:S	0	7	146	1	8	140
FV:X	0	8	109	1	7	109
FV:S	0	1	116	0	4	113
JE:X	0	3	51	0	2	52
JE:S	0	0	54	1	0	53
JV:X	0	17	104	3	3	114
JV:S	0	0	121	0	15	105
EV:X	1	20	195	2	12	205
EV:S	0	2	216	1	4	214
SUM	1	90	1499	13	90	1484

Tab. 2: Fringe/Fourfit Quality Codes (FQ) statistics

establish a more precise statement about the level of "correlator noise", a full recorrelation of the same IRIS–S experiment on the MK III correlator is planned before this correlator will be phased out definitively.

At first we have a look at all processed baselines with the different MK3FIT/FOURFIT Quality codes of both correlators. The FQ code 1-2 in MK III describes a fringe error code in which one or two frequency channels are affected by spurious signals. The MK IV FQ code G for example, has its origin within the Station Unit (SU), and is related to a TRM firmware mistake which causes sporadic data transmission delays. All mentioned FQ 7-9 for MK III and MK IV are of good proccessed quality and are used for further analysis. With the existing software (i.e.

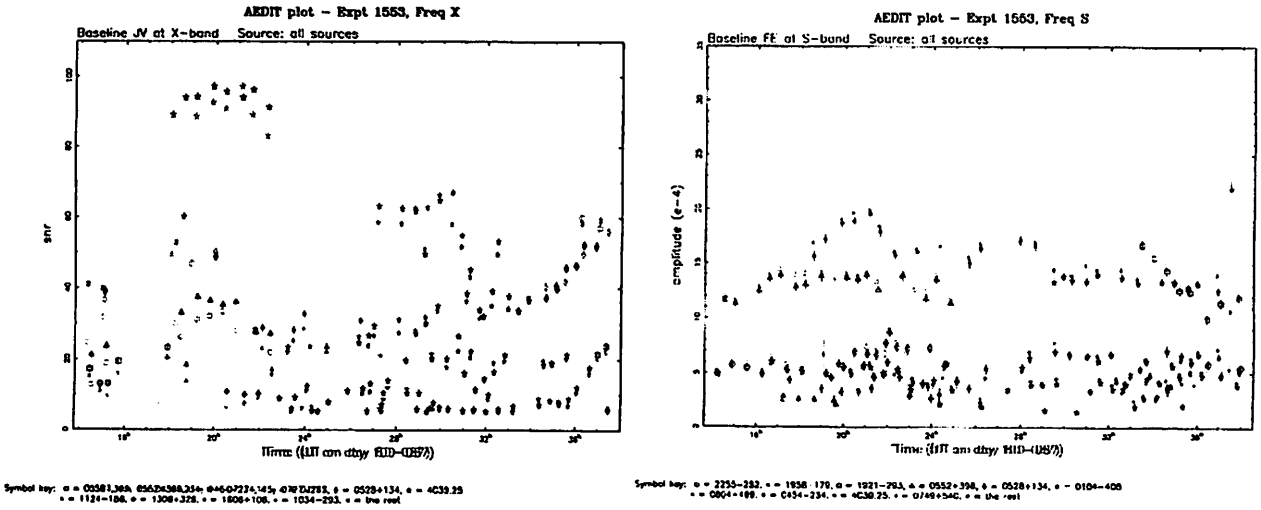

Fig. 1: Comparison of MK III (green) data against MK IV data (black) for i.e. SNR and AMP

AEDIT part of HOPS) we were able to produce the same dataplots for both the MK III and MK IV processed data, which makes the comparison of these data easier. The plots are printed in color. The MK IV data are all shown in black while the correlated MK III data are shown in green/yellow (see *Fig. 1*). It is interesting that the SNR comparison plot shows in general slightly larger SNR levels for nearly all MK IV data points. This result is also reproduced in Fig. 2 over all baselines in both frequencies. In the other example the data is slightly lower in amplitude for all MK IV baselines over the whole 24 hour experiment. Larger SNR with lower amplitudes means more integration time per scan which is an indication of a faster tape synchronization process (i.e. less loss of time). Again we can see this fact in all baselines.

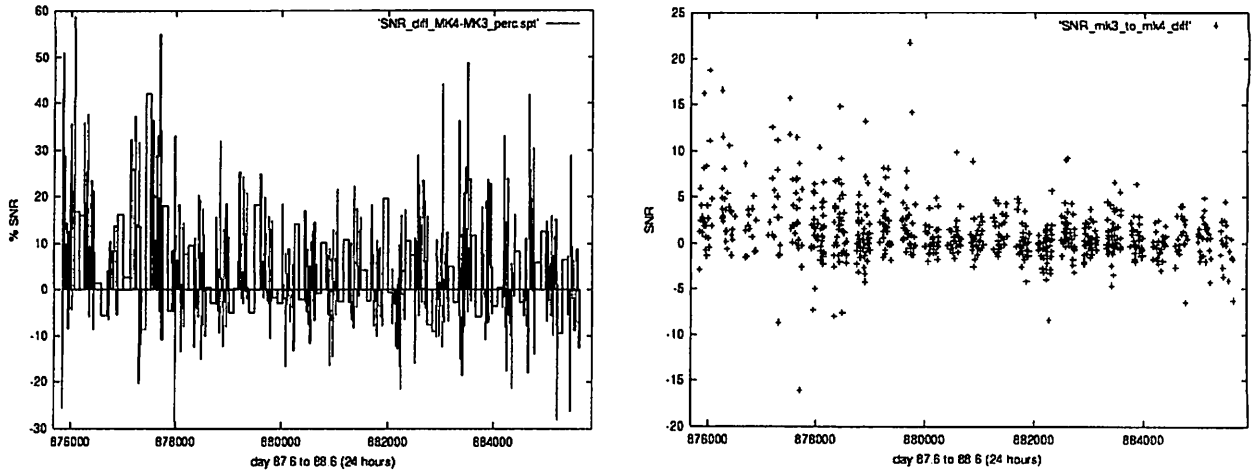

Fig. 2: SNR differences in percentage and net values

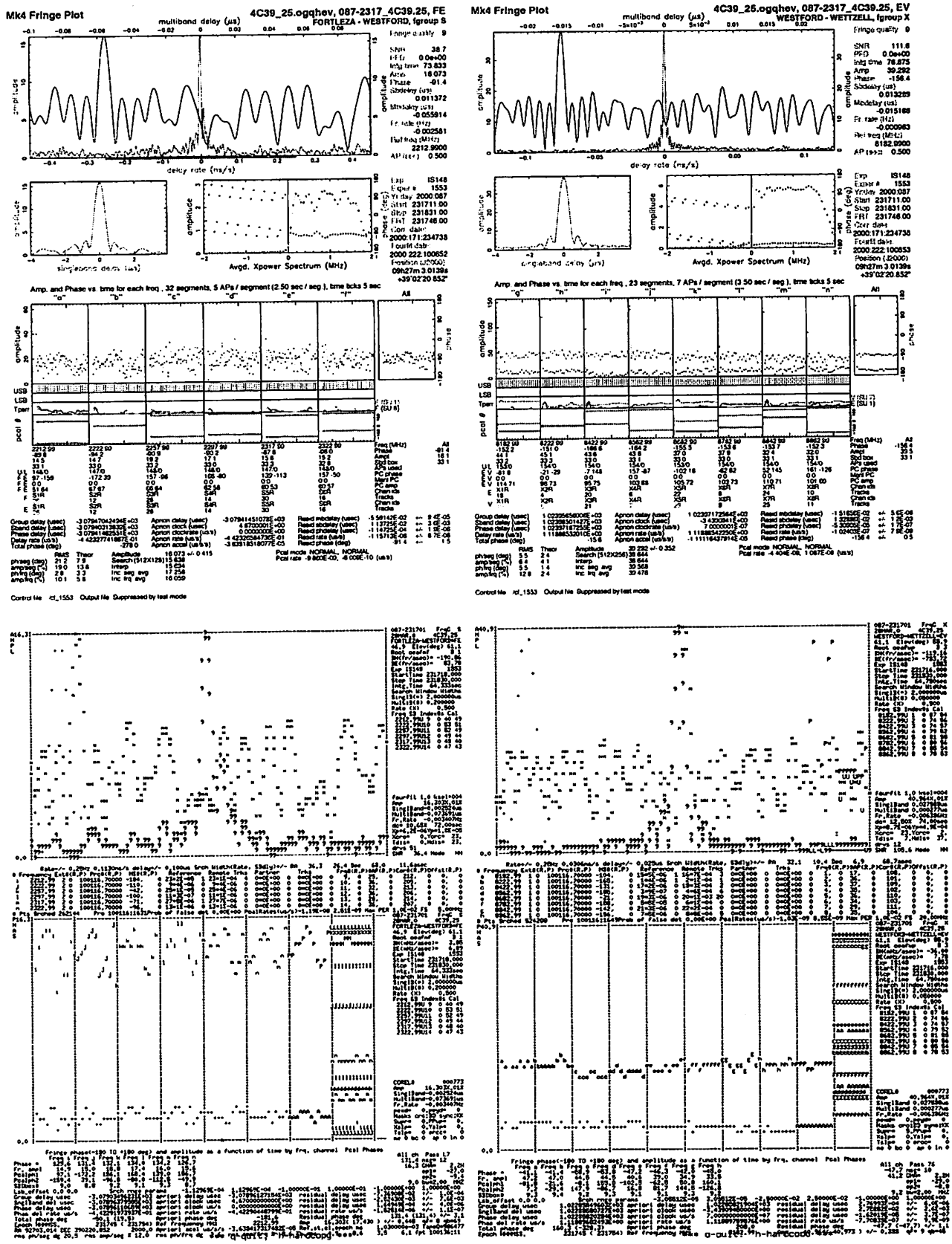

Fig. 3: Comparison of MK III fringe (MK3FIT) plots and the MK IV fourfit plots

Fig. 2 gives an overview of all good observations (FOURFIT Quality Code (FQ) = 7 to 9). It shows the differences in SNR where we subtracted the MK IV data from the MK III data. A similar plot shows the same data in percentage of the SNR level.
Fig. 3 shows some more detailed information for both examples. We can see two scans processed and fitted by MK III and MK IV. The plots shown on the right hand side give a good example how identical both correlators outputs can be. Even the bad data of track 20 (freq. 8682) can be seen in the FRNGE (MK3FIT) and FOURFIT plots. The plots on the left hand side show small differences which are not unusual, because we know, due to our practical experience on the processor side, that the reasons are small technical problems during recording and processing.

5 Inconsistencies in SNR determination in MK3FIT/ FOURFIT

Let us look at some of those plots, which belong to the problematic scans, i.e. those which are still acceptable in terms of data quality but which are at the limits of good or bad data. These scans show us in detail that there are strong divergences in some of the processed frequently channels. Some channels have a particularly poor data yield in each AP, and therefore the channel fringe amplitudes are biased to artificially high values. The reason can be traced to a deficiency in the way the frequency channels are weighted when computing the coherent fringe amplitude. The fact that all channels have nearly the same APs means that they will be weighted nearly equally in the average. As a result, also those frequency channels with lower amplitude will be weigthed in the same way as the channels with high amplitudes, i.e. higher than it should be. The SNR, which is calculated from the fringe amplitude and the total number of APs, is therefore always too high and the quality code of "9" follows from the high SNR. In some cases FOURFIT can turn a non-detection into an apparent detection, or it can influence the delay estimation. Some examples are shown in Fig. 4.

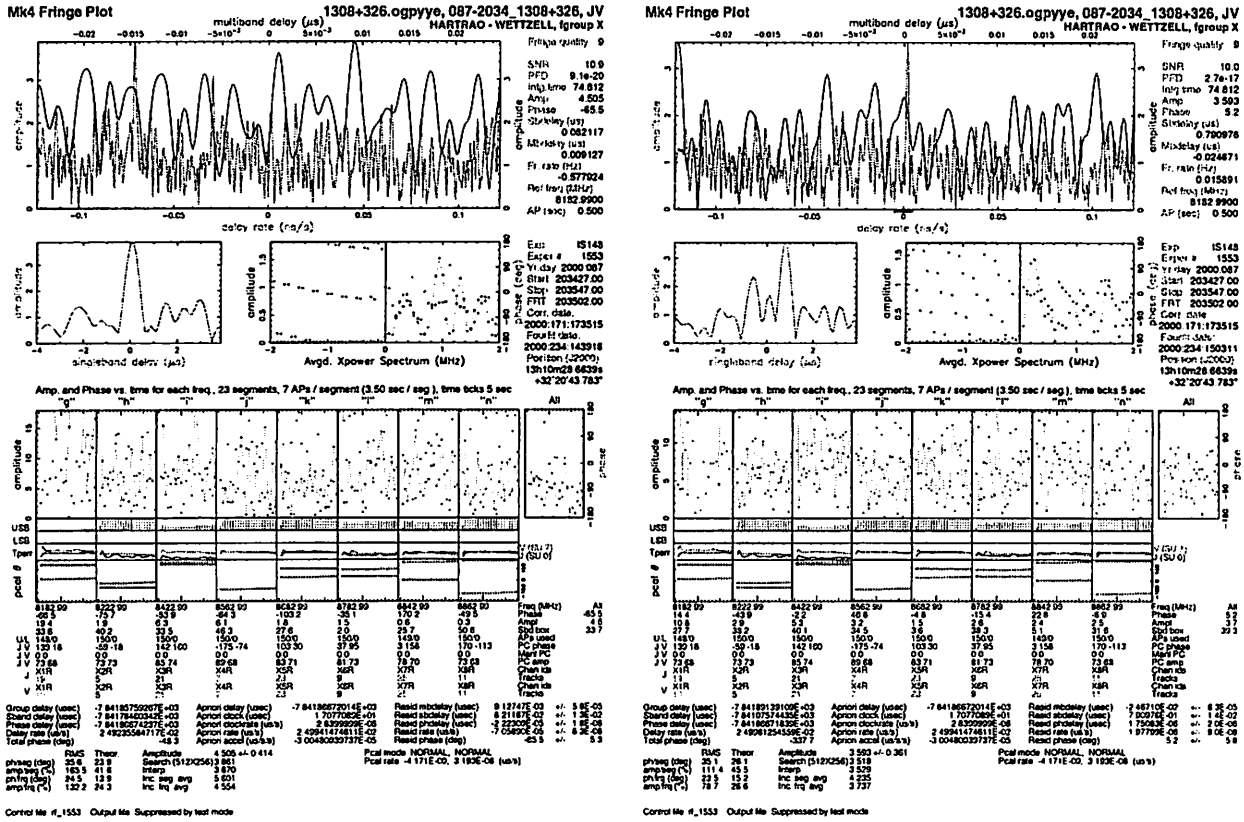

Fig. 4: Example of Inconsistencies in SNR determination by FOURFIT

6 Comparison of CALC/SOLVE geodetic results

The geodetic data analysis has been performed as described in section 2. A first useful comparison of MARK III data and MARK IV data is possible before the final solution. It is a comparison of the respective ambiguity–free and ionosphere–free X–Band databases (for the time being version 4). This comparison occurs before reweighting. For the solution a very simple parametrization is used in order to check the preceding steps and in order to obtain a first impression of the residuals. Taking this *intermediate solution*, the following phenomena were detected:

- The MK III X–Band database (version 4) contains 795 observations whereas the MK IV X–Band database (version 4) contains only 773 observations
- The MK IV X–Band database (version 4) contains some observations which are not contained in the MK III X–Band database (version 4)
  (see Figure 5)
- Several MK IV observations have significantly larger residuals than the respective MK III observations
  (see table 4 for example)

	WRMS (MK III) [ps]	WRMS (MK IV) [ps]
Fortaleza–HartRAO	112	119
Fortaleza–Westford	138	136
Fortaleza–Wettzell	95	93
HartRAO–Westford	108	140
HartRAO–Wettzell	75	80
Westford–Wettzell	71	78

Tab. 3: baseline statistics of the intermediate solution

The fact that the MK IV database holds only 773 observations instead of 795 observations as the MK III database, is explained by hardware–errors in the station units (SU) of the MK IV correlator which lead in some cases to a fringe–quality factor (FQ) of "G" (see also *section 3*). Such marked observations do not pass the DBEDIT–filter and therefore do not enter the database.

Figure 5 shows in the upper frame the original MK IV residual plot for the baseline Fortaleza–Westford as it comes out of the intermediate solution (before reweighting). The lower frame of figure 5 is the corresponding original MK III plot. This means that the MK IV database contains observations which are not included in the MK III database. Eliminating the doubtful MK IV observations yields a picture which is similar to the MK III plot (middle frame). This phenomenon appears at each baseline. A more detailed investigation of these observations showed that they all have a low SNR (< 10). These critical cases obviously cause problems for the MK IV correlator, for MK IV assigns a fringe–quality factor of "9" which tells DBEDIT to accept this observation whereas MK III assigns a fringe–quality factor of "0" which does not pass the DBEDIT filter. Considering the baseline statistics, i.e. the Weighted Root Mean Square (WRMS) of the respective baselines of the intermediate solution (see *table 3*), the MK III results are slightly better than MK IV. In particular, the baseline HartRAO–Westford is very striking, because the WRMS of MK IV is about 30 % worse than the WRMS of MK III. A detailed comparison of the MK IV residuals with the MK III residuals showed that several MK IV observations are less "good" than the respective MK III observations.

Original MK IV plot:

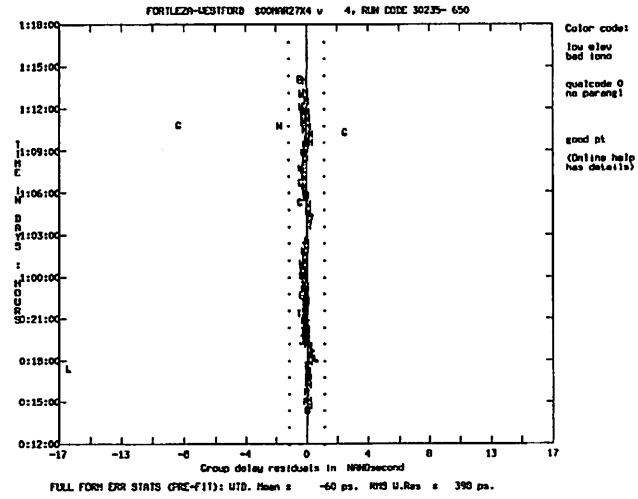

Corrected MK IV plot:

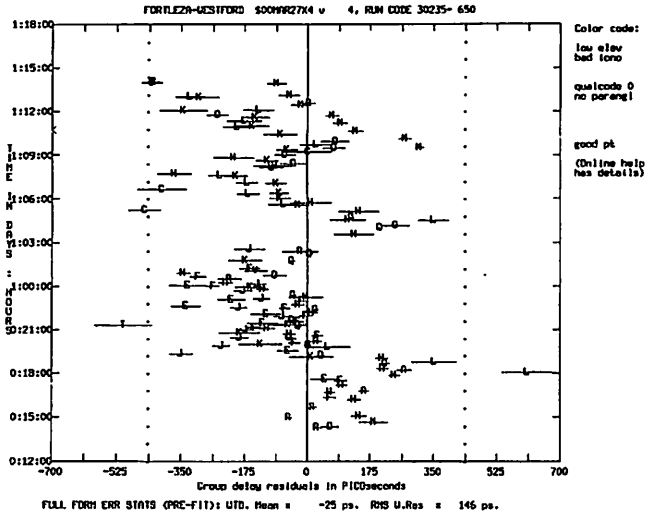

Original MK III plot:

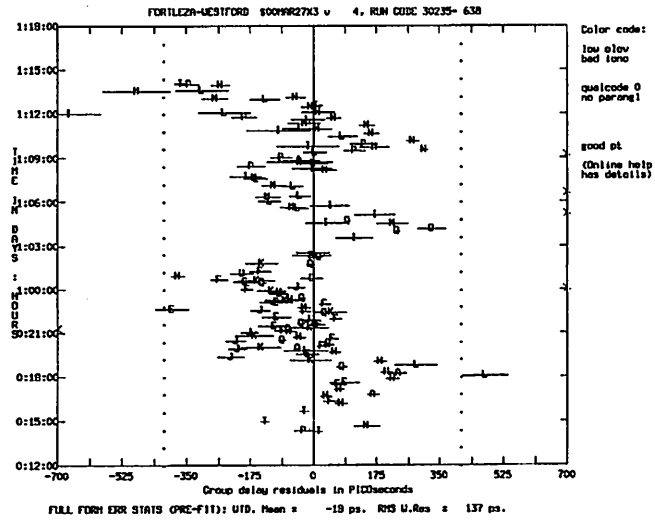

Fig. 5: Residual Plots (upper, middle MK IV, lower MK III) for the baseline Fortaleza–Westford of the intermediate solution (before reweighting)

Table 4 gives an example for such a doubtful observation. The observation has different observed group delays and significantly different residuals.

Correlator Type	Baseline	source	date	time	SNR	delay residual [ps]
MARK III	HART-WEST	0727-115	0 3 27	21 50	25	-16
MARK IV	HART-WEST	0727-115	0 3 27	21 50	26	-825

Tab. 4: Bad observation detected in the intermediate solution (before reweighting)

OPTIONS FOR LSQ-SOLUTION			
calibrations	contributions	sites	last page
default	MTTDRFLY APPLIED cable NOT APPLIED	"automatic" clock: interval: 360 min "automatic" atm: interval: 180 min (coordinates YES)	UT1 rate YES Dpsi, Deps YES

Tab. 5: Setup of the least-Squares-fit

For investigating the differences in the residuals an X-Band-only and S-Band-only solution has been created for both data types. These solutions will be ionosphere-influenced but ambiguity-free. Clock parameters are estimated and they should not differ by any large amount. The general setup of the least-squares-fit is shown in table 5. The station of Wettzell serves as a reference for the clock as well as for the stations. Table 6 shows the results for the estimated clock parameters. They agree at the *ns* level, apart from the S-Band-only solution which shows small differences which may be caused by the ionosphere.

Again the residuals of the "bad observation" (see *table 4*) are considered. Table 7 shows this bad observation in different types of solution. The X-Band-only solution yields nearly identical residuals for MK III and MK IV, whereas the S-Band-only solution shows a very large difference. The SNR of the S-Band-only solution is close to 10 and it seems again that in particular those weak SNRs (close to and below 10) cause problems in the MK IV fringe analysis (see *section 5*).

X-Band-only solution					
Station	Clock parameter	MARK III Adjustment	σ_{MK3}	MARK IV Adjustment	σ_{MK4}
Fortaleza	offset [ns]	-1229.01	.026	-1229.11	.022
Fortaleza	rate [fs]	-976.57	11.86	-970.13	11.78
Fortaleza	q-term [fs/day]	299.86	6.34	294.41	6.21
HartRAO	offset [ns]	-17056.63	.046	-17056.73	.042
HartRAO	rate [fs]	-2342.17	12.76	-2367.92	12.65
HartRAO	q-term [fs/day]	95.80	7.90	123.88	7.78
Westford	offset [ns]	3429.22	.026	3428.93	.022
Westford	rate [fs]	-570.29	11.35	-566.02	11.29
Westford	q-term [fs/day]	-173.87	5.35	-173.62	5.21
S-Band-only solution					
Fortaleza	offset [ns]	-1265.04	.160	-1284.19	.154
Fortaleza	rate [fs]	-2088.84	19.94	-1438.08	19.79
Fortaleza	q-term [fs/day]	1253.10	17.01	542.89	16.93
HartRAO	offset [ns]	-17088.63	.236	-17112.63	.236
HartRAO	rate [fs]	-2250.05	20.24	-1513.74	20.13
HartRAO	q-term [fs/day]	33.89	17.29	-484.76	17.24
Westford	offset [ns]	3321.78	.143	3346.54	.133
Westford	rate [fs]	-20.743	19.34	464.65	19.03
Westford	q-term [fs/day]	-640.46	16.45	-1390.71	16.16

Tab. 6: Estimated clock parameters in the X-Band-only and S-Band-only solution (q-term stands for quadratic term*)*

Bad observation detected in the intermediate solution (before reweighting)							
Correlator Type	Baseline	source	date	time	SNR	observed delay [ps]	delay residual [ps]
MARK III	HART-WEST	0727-115	00 3 27	21 50	25	-1,419,737,806	-16
MARK IV	HART-WEST	0727-115	00 3 27	21 50	26	-1,421,634,046	-825
Bad observation in X-Band-only solution							
Correlator Type	Baseline	source	date	time	SNR	observed delay [ps]	delay residual [ps]
MARK III	HART-WEST	0727-115	00 3 27	21 50	25	-1,419,737,806	-133
MARK IV	HART-WEST	0727-115	00 3 27	21 50	26	-1,421,634,046	-129
Bad observation in S-Band-only solution							
Correlator Type	Baseline	source	date	time	SNR	observed delay [ps]	delay residual [ps]
MARK III	HART-WEST	0727-115	00 3 27	21 50	14	-1,419,854,363	-177
MARK IV	HART-WEST	0727-115	00 3 27	21 50	11	-1,421,690,194	5732

Tab. 7: The behaviour of a bad observation in different types of solution

Finally the effect of using different correlator types on the parameter adjustments is considered. Table 8 shows the results and the adjustments confirm the existing discrepancies between Mark III and Mark IV. Δ means the difference in coordinates between MK III and MK IV. This difference is formed between the X-, Y-, Z-components as well as between Up (U), East (E) and North (N). Due to the problems described above the adjustment yields differences as large as one sigma.

	$\lvert\Delta\rvert$ [mm]	σ_{MKIII} [mm]	σ_{MKIV} [mm]
Fortaleza X	9.46	13.39	15.83
Fortaleza Y	10.10	8.59	9.77
Fortaleza Z	13.08	7.29	8.29
Fortaleza U	12.78	14.55	17.07
Fortaleza E	2.03	5.98	6.81
Fortaleza N	13.99	7.68	8.78
HartRAO X	13.03	17.82	22.35
HartRAO Y	0.27	8.25	10.66
HartRAO Z	10.06	9.40	11.36
HartRAO U	14.89	18.72	23.74
HartRAO E	5.82	5.46	6.58
HartRAO N	3.96	9.67	11.63
Westford X	1.17	9.30	10.54
Westford Y	10.39	8.91	10.90
Westford Z	11.47	12.07	13.74
Westford U	15.29	14.98	17.49
Westford E	2.19	7.72	8.73
Westford N	1.51	5.25	6.05

Tab. 8: parameter adjustments

7 Conclusions

First of all we have to state that the comparison of the results from the MkIII and the MkIV correlators as presented here are referring to an interim situation where several of the MkIV hardware and software components have not yet reached their final form.

Using the same IRIS experiment at both correlators, we found that the most serious deficiencies (well known to the system developers) are related to the station units on the one hand and to the fringe fitting program FOURFIT on the other. These are problems that have a direct influence on the results of our comparison:

- the station units occasionally produce incorrect data quality codes that lead to the loss of good observations
- FOURFIT does not handle correctly the observations with low SNR. This bears down more heavily on the IRIS experiment used here because of the large number of weak scans involved.

The differences in the final adjustments of the CALC/SOLVE solution reach a level of up to 15 mm in the station coordinates which is on the order of one formal sigma. We expect these differences to become much smaller after the problems cited above have been eliminated.

We are planning to analyse the two independent correlations made with the old MkIII correlator

in the same way as the procedures presented here, in order to establish the intrinsic noise floor for one system. This will provide a standard of comparison to assess the progress made with the new system. Moreover, a suitable software tool will be written to make a comparison between the raw delays from two independent correlations easier (using the Data Base Version 1).

8 References

Alef W, Graham D A, Zensus J A, Müskens A, Schlüter W (2000) The Bonn MK IV Correlator Project, Proceedings of the First IVS General Meeting, N.R.Vandenberg and K.Baver, Eds., NASA Center for AeroSpace Information, 7121 Standard Drive, Hanover, MD 21076–1320, Publ.No. NASA/CP-2000-209893.; p.210-214

Kingham K A, Martin J O (2000) Early Experiences with the Mark 4 Correlator, Proceedings of the First IVS General Meeting, NASA Center for AeroSpace Information, 7121 Standard Drive, Hanover, MD 21076–1320

Nothnagel A (2000) VLBI Data Analysis User's Guide, unpublished paper

Nothnagel A (1997) On the Effect of Missing Tracks, Proceedings of the 12th Working Meeting on the European VLBI for Geodesy and Astrometry, Edited by Bjorn R. Pettersen, Statens Kartverk Geodesidivisjonen, p.66-73

Section 4

Astrometric VLBI and Phase-Reference Mapping

Space VLBI Astrometry and Phase-Reference Mapping with VSOP

RICHARD W. PORCAS[1] AND MARÍA JOSÉ RIOJA[2,3]

[1] *MPIfR, Bonn, Germany*
[2] *OAN, Alcalá de Henares, Spain*
[3] *IRA, Bologna, Italy*

Abstract

We discuss the use of the VLBI phase-referencing technique for astrometry and mapping, for observations made with a spaceborne antenna orbiting the Earth. Such observations made with the Japanese-lead Space VLBI mission VSOP are limited to close source pairs where both target and reference are within the primary beam of the "HALCA" spacecraft antenna. We present an analysis of 5 GHz data from the source pair 1308+326 and 1308+328. For these observations the HALCA orbit was sufficiently well determined that it was possible to make a phase-reference map of 1308+326 and to perform the first ever Ground-Space VLBI relative astrometry between physically unrelated sources.

1 Introduction

Phase-reference mode observing has proved to be a useful technique for astronomical VLBI. The basic idea is that unwanted contributions to the visibility phase (e.g. from tropospheric and ionospheric path fluctuations) are nearly the same for two closely-spaced sources observed simultaneously or in rapid succession. For strong sources the visibility phase difference can be used directly for precision relative astrometry, whilst phase-reference mapping can also be used for astrometry of, and imaging, sources too weak for self-calibration (Alef 1988, 1989; Beasley & Conway, 1995; Porcas & Rioja, 1996). Prerequisites for success are a sufficiently strong, compact reference source, instrumental phase coherence between the sites and an accurate correlator model for the path delay difference between antennas; any uncompensated path differences arising in the propagation medium or from imperfect interferometer geometry appear in the relative phase, diluted by the source separation measured in radians, and reduce the "coherence" in the phase-referenced map.

In 1997 the Japanese-lead VLBI Space Observatory Program (VSOP) launched the first spacecraft ("HALCA") dedicated to ground-space VLBI observations (Hirabayashi et al, 1998). HALCA carries an 8 metre radio dish, and orbits the Earth every 6.32 hours, with an apogee height of 24,400 km and perigee 560 km. Together with radio telescopes on the ground it can form part of a VLBI array with baselines some 3-4 times longer than those obtainable with ground arrays alone.

In principle the phase-referencing technique can be extended to Space VLBI (e.g. Bartel, 1993). In practice there may be special problems: candidate reference sources are more likely to be resolved out at higher resolution; the number of such reference sources is further reduced by the relatively poor sensitivity achievable with small orbiting antennas; instrumental coherence may be limited by the space-ground link; and uncertainties in the spacecraft orbit may produce large geometric delay errors. The VSOP mission was not designed with phase-referencing - or geodesy - in mind ! The mission specification for the HALCA orbit accuracy was only < 80 m, and the rapid source changes required for both techniques cannot be performed by HALCA. Phase-reference observations are thus limited to close source pairs where both target and reference sources are simultaneously within the HALCA primary beam. The first such observation, of the pair 1038+528A/B (separation 33 arcsec), was reported by Porcas & Rioja (2000). Here we report on observations of the pair 1308+326/8.

2 VSOP observations of 1308+326/1308+328

The two strong, flat-spectrum sources 1308+326 and 1308+328 are separated by 14.3 arcmin in PA 27°, about half of the HALCA primary beam at 5 GHz (FWHM 26 arcmin). They thus provide an ideal case for investigating the limits of phase-reference observing with VSOP. 1308+326 (z=0.996) is highly variable (S = 2-4 Jy) and has been studied by Gabuzda et al (1993). Geodetic VLBI observations show that its structure is also variable. 1308+328 (z=1.65; Machalski & Engels, 1994) is also variable but weaker (S = 0.3-0.6 Jy). Rioja et al (1996) showed that it is essentially unresolved on ground baselines at 8.4 GHz, and measured the separation between the two sources to sub-mas accuracy (Rioja and Porcas, 1996).

VSOP observations of this pair were made from UT 1630-2230 on 29th June 1998 at 5 GHz. The ground array telescopes (VLBA and Effelsberg), which have smaller primary beams, were switched between the sources every 3 or 4 minutes. The HALCA data (2.5 h) were relayed via the Tidbinbilla tracking station. Correlation was done at the VLBA correlator and calibration and further analysis was made using AIPS.

Fig. 1 shows the visibility amplitude vs. resolution for the two sources; both showed strong fringes on ground-space baselines. The weaker, but highly compact nature of 1308+328 is also evident. Maps using ground baselines only are shown in Fig. 2. At this epoch, 1308+326 consists of two, nearly equal components, separated by 1 mas. 1308+328 is almost point-like, apart from a faint (10 mJy/beam) extension of 2 mas in PA -45°. For simplicity we chose this as the reference source in our analysis.

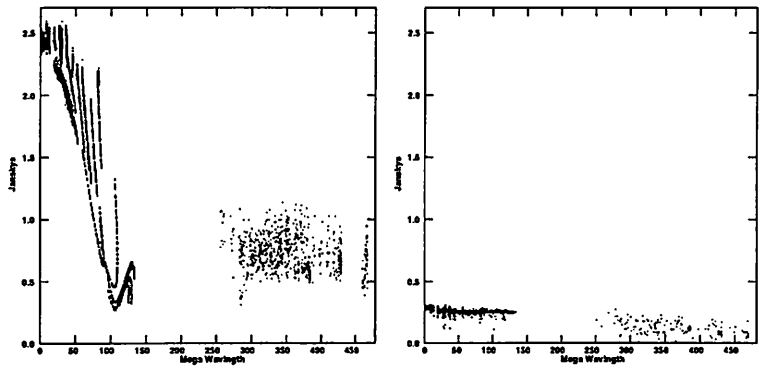

Figure 1: Visibility amplitude vs (u,v)-distance for **a** (left) 1308+326 and **b** (right) 1308+328

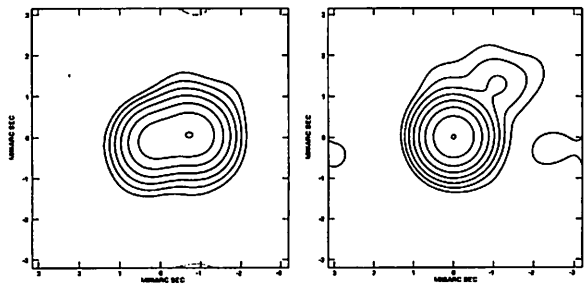

Figure 2: GRT-only maps, CLEAN beam 1x1 mas: **a** (left) 1308+326: phase-ref map, peak 1294, base contour 20 (mJy/beam); **b** (right) 1308+328: hybrid map, peak 258, base contour 2 (mJy/beam)

3 Phase-reference analysis

We started our phase-reference analysis by making VSOP hybrid maps of 1308+328 (using only the single phase self-calibration step in FRING). Maps with uniform weighting and equal data weights for all baselines are shown in Fig. 3. As expected, these show a single, compact component; in a map made with baselines to HALCA alone (Fig 3b), 100 mJy is still detected.

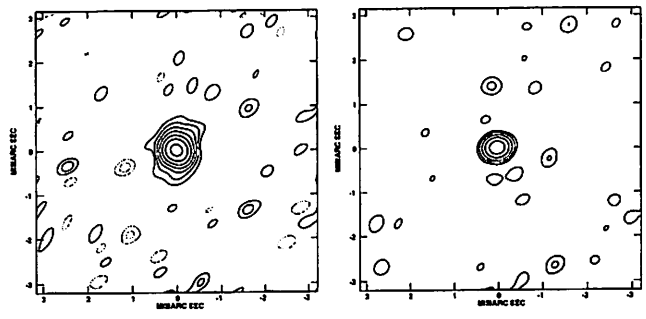

Figure 3: VSOP maps of reference source 1308+328, CLEAN beam 0.35x0.35 mas: **a** (left) Using data from all baselines: peak 171, base contour 2 (mJy/beam); **b** (right) Using only baselines to HALCA: peak 105, base contour 4 (mJy/beam)

The antenna phase calibrations determined from 1308+328 were then used to correct the data of the "target" source, 1308+326, after interpolation across the observing gaps. Visibility phase plots on two baselines are shown in Fig. 4. Both are smoothly varying functions over the observing period, and represent the sum of target source structure phase, errors due to interpolation and correlator model errors (including the absence of an ionospheric path correction). It is clear that the position determination of HALCA is much better than the nominal 80 m requirement for the VSOP mission (from which one might expect phase changes up to 5 turns for the source separation of 0.004 radians).

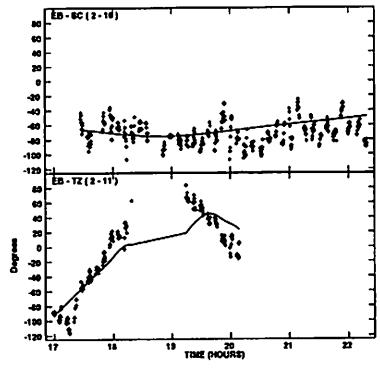

Figure 4: Phase of the 1308+326 visibility function on baselines from Effelsberg to (top) VLBA-SC and (bottom) HALCA, after applying instrumental phase corrections determined using the reference source 1308+328. Solid line is the prediction from the hybrid map in Fig 6a.

We next made phase-reference maps of 1308+326 (Fig. 5) using these calibrated visibilities, with no further phase self-calibration step. The uniform-weighted map, using all baselines with equal weight (Fig. 5a) shows clearly the two compact source components, with the suggestion of an arching bridge between the two. A map made using only baselines to HALCA (Fig. 5b) shows only

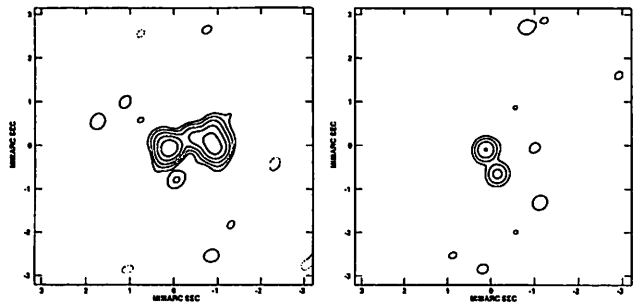

Figure 5: VSOP phase-reference maps of the target source 1308+326, CLEAN beam 0.35x0.35 mas; **a** (left) Using data from all baselines: peak 579, base contour 20 (mJy/beam); **b** (right) Using only baselines to HALCA: peak 372, base contour 45 mJy/beam

one (the eastern) of these components, with a peak flux of 372 mJy/beam. A secondary component in PA -140° is clearly spurious, and can be attributed to phase errors.

The difference in the positions of the peaks between Figs. 5 and 3 define **astrometric corrections** (δRA, δDec) to the separation between the assumed source positions (given below):

1308+326 RA=13:10:28.663639 DEC=+32:20:43.78908 (J2000) ref: GLB923Z
1308+328 RA=13:10:59.4025262 DEC=+32:33:34.455578 (J2000) ref: ER1

Preliminary estimates give +100, −60 μas between the peaks in the maps using all the data (Figs. 5a,3a) and +90, −100 μas between the maps using baselines to VSOP only (Figs. 5b,3b).

Finally, we made hybrid maps of 1308+326 by performing five iterations of phase self-calibration using CALIB, starting with the phase-reference map of Fig. 5a. These are shown in Fig. 6, with the mapping parameters as for Fig. 5. Compared to the phase-referenced maps the noise levels are much less; in particular the strong, spurious feature in Fig. 5b is considerably reduced in Fig. 6b. The peak brightness (on the eastern "core") is also increased in the hybrid maps - by 11 % in Fig. 6a and 55 % in Fig. 6b.

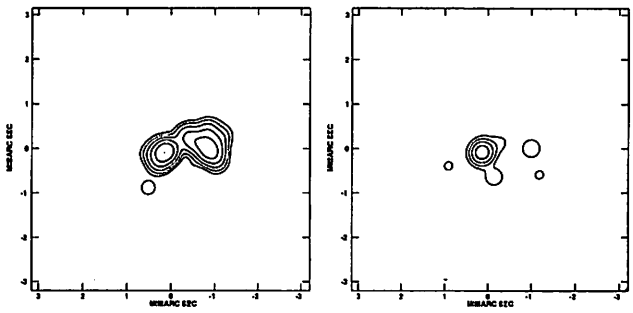

Figure 6: Hybrid maps of 1308+326: **a** (left) Using all baselines: peak 641, base contour 20 (mJy/beam); **b** (right) Using only baselines to HALCA: peak 578, base contour 45 (mJy/beam)

The phase corrections derived in the CALIB phase self-calibration steps for the VLBA-SC and HALCA antennas are shown in Fig. 7. These represent the residual, differential path length errors between the two sources (with respect to the reference antenna Effelsberg), after removal of the phase terms arising from the source structure of 1308+326 and the small offset in the assumed separation between the sources.

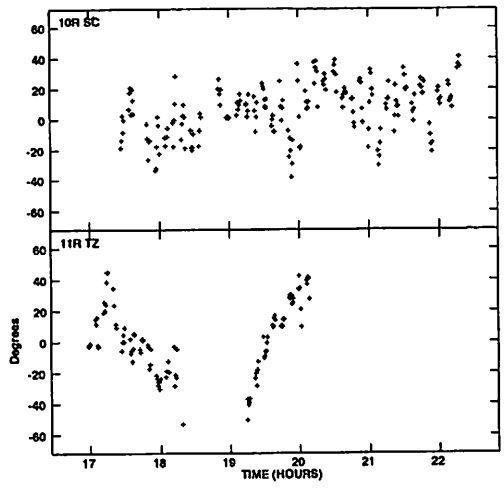

Figure 7: Antenna phase corrections for (top) VLBA-SC and (bottom) HALCA, determined using the referenced phase of 1308+326 and a hybrid map (Fig 6a)

4 Conclusions

Our preliminary analysis of 5 GHz VSOP observations of the close pair of sources 1308+326/8 has shown that phase-reference observations are indeed feasible with Ground-Space VLBI. We were able to make a phase-reference map of 1308+326 (albeit with limited dynamic range), using the compact reference source 1308+328 within the HALCA beam, 14.3 arcmin away, and making a temporal phase interpolation using a source switching cycle of 7 minutes.

It is apparent from the phase-reference and hybrid maps of 1308+326 that the western (jet) component - the strongest in the GRT-only map - is heavily resolved by the extra resolution provided by HALCA; it is essentially resolved out in the maps made with baselines to HALCA alone, where only the eastern, core component is seen. By measuring the offset between the core peaks and the map centres for both sources, and taking the difference, we were able to determine an astrometric correction to the assumed position difference for the sources. This is the first time that such a measurement between two independent sources has been made with Space VLBI. Although it is difficult to assign a realistic error to this correction, the size and direction (ca. 120 micro-as in PA 120°) could correspond to a small shift along the structural axis of 1308+326; our assumed separation was measured in February 1995, when this source was smaller, and our "peak" position may have corresponded to a blend of "core" and "jet". (Geodesists, take note that "positions" of such sources are not stable when measured with mas-size beams !)

The residual relative phase errors for the source separation of 14.3 arcmin produce significant spurious features when using the ground-space baselines alone, and result in the loss of about 33 % of the expected flux. However, the orbit determination for HALCA is clearly much better than the 80 m mission requirement. The residual relative phase errors (up to 60°) imply HALCA position accuracies in the range 2-5 m. This agrees well with the estimate of 1-6 m given by You et al (1998) from JPL Navigation measurements, and preliminary results from the Space VLBI Geodesy Demonstration Experiment (GEDEX) of "a few meters" (Frey et al, 2000a,b). Such errors are comparable to the delay path differences introduced by the ionosphere at lower frequencies (e.g. 1.6 GHz), which can produce similar map coherence losses if left uncorrected.

The residual relative phase errors should scale with target/reference source separation, and observing frequency. Thus phase-reference observations with closer source pairs should be possible

with VSOP. For observations at wavelength λ, source separation of S radians, and orbit error X, the expected phase error is: $\Delta\phi \sim 2\pi SX/\lambda$. For successful phase-referencing between 2 sources anywhere within the primary beam of an antenna of diameter D (FWHM $= \lambda/D$) the phase error should be less than one radian, leading to the condition :

$$X < D/2\pi$$

However, a more general application of phase referencing to wider target/reference separations with future Space VLBI missions will need more precise orbit determinations. For example, Reid (1984) estimated a required baseline precision for the QUASAT mission of 0.1 m for astrometric measurements of 22 GHz water-vapour masers.

Acknowledgements. We gratefully acknowledge the VSOP Project, which is led by the Japanese Institute of Space and Astronautical Science in cooperation with many organizations and radio telescopes around the world. We thank P. Edwards and M. Claussen for assistence in scheduling and correlating the observations.

References

Alef, W. 1988, in *IAU Symp. 129: The Impact of VLBI on Astrophysics and Geophysics*, eds. M.J. Reid & J.M. Wrobel (Dordrecht: Kluwer), 523

Alef, W., 1989 in *NATO ASI Ser. : Very Long Baseline Interferometry: Techniques and Applications*, eds. M.Felli & R.E.Spencer (Dordrecht: Kluwer), 261

Bartel, N., 1993 in *Propagation Effects in Space VLBI*, ed. L. Gurvits (Arecibo: NAIC Arecibo Observatory), 90

Beasley, A.J. & Conway, J.E., 1995 in *ASP Conf. Ser.* **82**: *Very Long Baseline Interferometry and the VLBA*, eds. J.A. Zensus, P.J. Diamond & P.J. Napier (San Francisco: Astron. Soc. Pac.), 327

Frey, S., Fejes, I. & Paragi, Z., 2000a in *Astrophysical Phenomena Revealed by Space VLBI*, eds. Hirabayashi et al, ISAS, Sagamihara, Japan, 285

Frey, S., Meyer, U., Fejes, I., Paragi, Z., Charlot, P. & Biancale, R., 2000b, presented in *New Trends in Space Geodesy*, 33rd COSPAR Scientific Assembly, Warsaw

Gabuzda, D.C., Kollgaard, R.I., Roberts, D.H. & Wardle, J.F.C., 1993, *ApJ*, **410**, 39

Hirabayashi, H. et al, 1998, *Science*, **281**, 1825

Machalski, J. & Engels, D., 1994, *MNRAS*, **266**, L69

Porcas, R.W. & Rioja, M.J.,1996, in *Proceedings of the 11th working meeting on European VLBI for Geodesy and Astrometry*, Onsala, 209

Porcas, R.W. & Rioja, M.J., 2000, *Adv. Sp. Res.*, **26**, 673

Reid, M.J., 1984 in *QUASAT - a VLBI observatory in space*, comp. W.R.Burke (Paris: ESA SP-213), 181

Rioja, M.J. & Porcas, R.W.,1996, in *Proceedings of the 11th working meeting on European VLBI for Geodesy and Astrometry*, Onsala, 219

Rioja, M.J., Porcas, R.W. & Machalski, J., 1996, in *IAU Symp. 175: Extragalactic Radio Sources*, eds. R.Ekers, C.Fanti & L.Padrielli (Dordrecht: Kluwer), 122

You, T.H., Ellis, J., Mottinger, N., 1998, in *Spaceflight Dynamics 1998, Advances in the Astronautical Sciences*, Univelt, San Diego, Ca., **100**, 873

On the way to global phase-delay astrometry

E. Ros[1], J.M. Marcaide[2], J.C. Guirado[2], M.A. Pérez-Torres[3]

[1] *Max-Planck-Institut für Radioastronomie, Bonn, Germany*
[2] *Dep. Astronomia i Astrofísica, Universitat de València, Burjassot (Valencia), Spain*
[3] *Istituto di Radioastronomia/CNR, Bologna, Italy*

The use of the phase-delay improves substantially the accuracy obtained in VLBI astrometry with respect to the group-delay observable. Recently, Ros et al. (1999) have extended the related phase-connection technique to a triangle of radio sources with relative separations up to 6.8° (the S5 sources BL 1803+784/QSO 1928+738/BL 2007+777). This technique has also been extended for separations up to 15° in the studies of the pair of S5 radio sources QSO 1150+812/BL 1803+784 (Pérez-Torres et al. 2000). We are carrying out a long-term astrometric programme at 8.4, 15, and 43 GHz to determine the absolute kinematics of radio source components in the 13 members of the complete S5 polar cap sample. For each epoch, all the radio sources are observed at the same frequency for 24 hours in total. Bootstrapping techniques are used to phase-connect the data jointly for the 13 objects throughout the observations. An accurate registration of the maps of the radio sources at different frequencies will allow a study of jet components with unprecedented precision and provide spectral information. This observing scheme could be extended in the future to other regions of the sky and eventually lead to global phase-delay astrometry.

1 Introduction

The improvement by four orders of magnitude in wide-angle astrometric measurements in the last 30 years, provided mainly by Very Long Baseline Interferometry (VLBI), have resulted in a better definition of the fundamental astronomical reference frame (Johnston & de Vegt 1999), the International Celestial Reference Frame (ICRF), based on the radio positions of 212 compact extragalactic radio sources. Up to the present, the group delay VLBI observable has been regularly used for such a task. The use of the more precise phase delay observable should provide an immediate improvement in accuracy. A phase-connection process is needed (Shapiro et al. 1979) to overcome the inherent 2π ambiguity of the phases. When used with radio source pairs, the phase delay becomes the most accurate observable in astrometry. The phase-delay astrometric technique has been applied to different pairs of radio sources with separations from minutes to some degrees in the sky (among others, 3C 345/NRAO512, Shapiro et al. (1979), Bartel et al. (1986); 1038+528 A/B, Marcaide et al. (1983, 1995) and Rioja et al. (1997); 4C 39.25/0920+390, Guirado et al. (1995b); QSO 1928+738/BL 2007+777, Guirado et al. (1995a, 1998); 3C 395/3C 382, Lara et al. (1996)).

A significant technical problem in the astrometric data reduction is the modelling and removal of the ionospheric effect. Since the latter is a frequency-dependent effect, the removal was done in the past by observing at two frequencies. The Global Positioning System (GPS) allows now to obtain ionospheric data of unprecedented accuracy. Ros et al. (2000a) and Pérez-Torres et al. (2000) used GPS data to successfully remove the ionospheric effect. Such

an approach can be applied to any VLBI astrometric observations, without the need for dual-frequency observations.

Many compact radio sources show variable structures on scales larger than the accuracy of their position estimates. If the source structure is ignored, the group-delay astrometric results may incorrectly be interpreted as a proper motion of the radio sources. Because the radio sources, with typical redshifts of 1.0, are very distant proper motions should not be detectable. It is true that most of the emission is generally produced in the core (brightest feature) of the source, but for low frequencies, due to opacity effects, this core may not be close to the central engine of the source. Until the efforts of Fey et al. (1996) and Fey & Charlot (1997, 2000) the effect of source structure had been ignored in the group-delay based reference system maintenance. These authors have initiated a programme to image the radio reference frame sources and define a source "structure index" to provide a quantitative estimate of the possible astrometric quality of them. In contrast, the phase-delay analysis from the early studies of Shapiro et al. (1979) takes into account the effect of the structure and to date, the phase-delay astrometry is the only rigorous way to register radio maps with precisions of 100 μas or better. As mentioned above, this is the technique that we use in our astrometric data analysis.

2 Phase-delay astrometry of S5 polar cap sample sources

Eckart et al. (1986,1987) selected 13 radio sources from the MPIfR-NRAO 5 GHz survey (abbreviated as S5, Kühr et al. 1981) with declinations over 70°, flat spectral indices and flux densities over 1 Jy at λ6 cm. These sources, given in Table 1 (IERS coordinates, optical magnitude and redshift) constitute the S5 polar cap sample. The sky distribution of the members of the sample, with their angular separations indicated, is given in Fig. 1.

Table 1: S5 polar cap sample.

Name	R.A.	Dec	V	z
QSO 0016+731	$0^h19^m45\overset{s}{.}78645$	73°27′30.″0175	18.0	1.781
QSO 0153+744	$1^h57^m34\overset{s}{.}96500$	74°42′43.″2305	16.0	2.338
QSO 0212+735	$2^h17^m30\overset{s}{.}81337$	73°49′32.″6218	19.0	2.387
BL 0454+844	$5^h\ 8^m42\overset{s}{.}36340$	84°32′ 4.″5438	16.5	0.112
QSO 0615+820	$6^h26^m\ 3\overset{s}{.}00612$	82° 2′25.″5680	17.5	0.710
BL 0716+714	$7^h21^m53\overset{s}{.}44848$	71°20′36.″3634	14.2	–
QSO 0836+710	$8^h41^m24\overset{s}{.}36529$	70°53′42.″1735	16.5	2.172
QSO 1039+811	$10^h44^m23\overset{s}{.}06255$	80°54′39.″4430	16.5	1.254
QSO 1150+812	$11^h53^m12\overset{s}{.}49923$	80°58′29.″1546	18.5	1.250
BL 1749+701	$17^h48^m32\overset{s}{.}84022$	70° 5′50.″7687	16.5	0.770
BL 1803+784	$18^h\ 0^m45\overset{s}{.}68393$	78°28′ 4.″0184	16.4	0.684
QSO 1928+738	$19^h27^m48\overset{s}{.}49521$	73°58′ 1.″5699	15.5	0.302
BL 2007+777	$20^h\ 5^m30\overset{s}{.}99855$	77°52′43.″2478	16.5	0.342

Guirado et al. (1995a, 1998) studied astrometrically two sources of this sample at 2.3, 5, and 8.4 GHz, QSO 1928+738 and BL 2007+777. Ros et al. (1999) added a new source

to this pair, BL 1803+784, studied the trio at 2.3 and 8.4 GHz, and determined the relative positions with $\sim 130\,\mu$as precisions at 8.4 GHz. The phase connection technique was thus extended to angular separations of 6.8°. Later, Pérez-Torres et al. (2000) phase-connected data on the pair QSO 1150+812/BL 1803+784, separated by 14.9°. The situation now allows us to design a strategy to extend the phase-delay astrometric technique to larger sets of radio sources. The S5 polar cap sample, given the high flux densities of the radio sources and their situation on the sky, is optimal for carrying out phase-delay astrometry simultaneously for the complete sample.

All sources have neighbours at angular distances such that the use of the phase-connection technique is possible throughout a 24 hr VLBA observing run. Using the phase-delay data from the 13 radio sources we should obtain their relative positions with accuracies better than 0.1 milliarcseconds (mas).

We have observed all the 13 members of the sample at 8.4 GHz at epochs 1997.93 and 1999.41, and at 15 GHz in 1997.57 and 2000.46 using a phase-reference scheme. In each of the 24-hour observations at each wavelength, each source was observed on average for 5 hours, enough to produce high-quality hybrid maps. In Fig. 2 we show the 8.4 GHz hybrid maps from those sources of the S5 polar cap sample that were studied astrometrically in the past — Guirado et al. (1995a, 1998, 2000), Ros et al. (1999), Pérez-Torres et al. (2000).

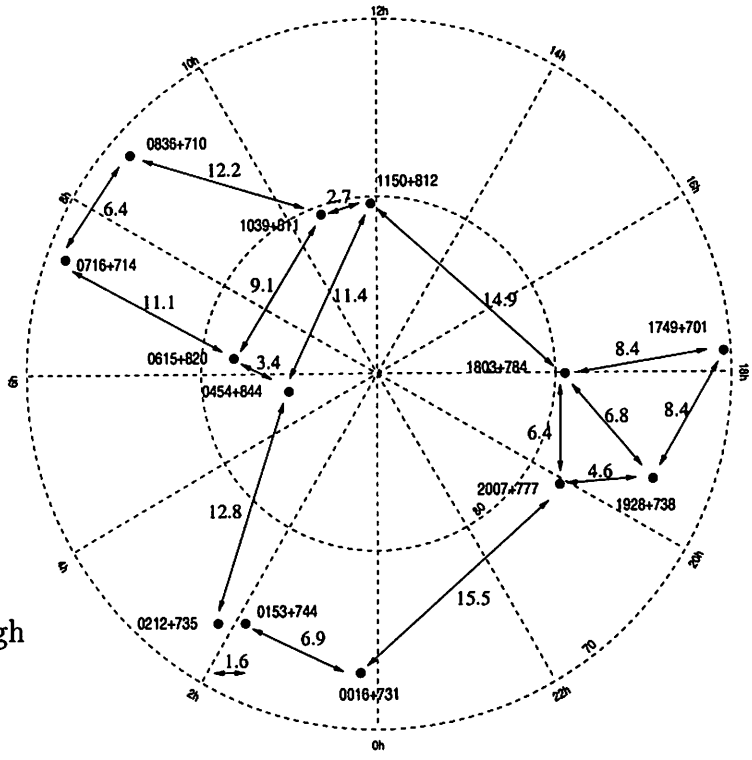

Figure 1: Distribution of the S5 polar cap sample in the northern sky, centered at the celestial north pole. The black dots represent the positions of radio sources, and the angular distances between them are indicated in arc degrees with arrows.

It is possible to observe some morphological changes just from the present mapping results at 8.4 GHz, as is the case for the sources QSO 0016+731 and QSO 1928+738 (Ros et al. 2000b). As an example, we present in Fig. 3 the changes in the inner jet features of QSO 0836+710 after convolving the CLEAN-components of the map with a 0.6 mas circular beam to better compare the images. The evolution within 3 mas of the core (P.A. $-140°$) is evident during the 1.5 years elapsed between the observations.

The astrometric data reduction of the S5 polar cap sample data is in progress. We can report very interesting preliminary astrometric results from the observations of epoch 1997.93. The joint phase-delay analysis for all the 13 radio sources did not present particular difficulties. The quality of our analysis is demonstrated by the low root-mean-square (30 ps)

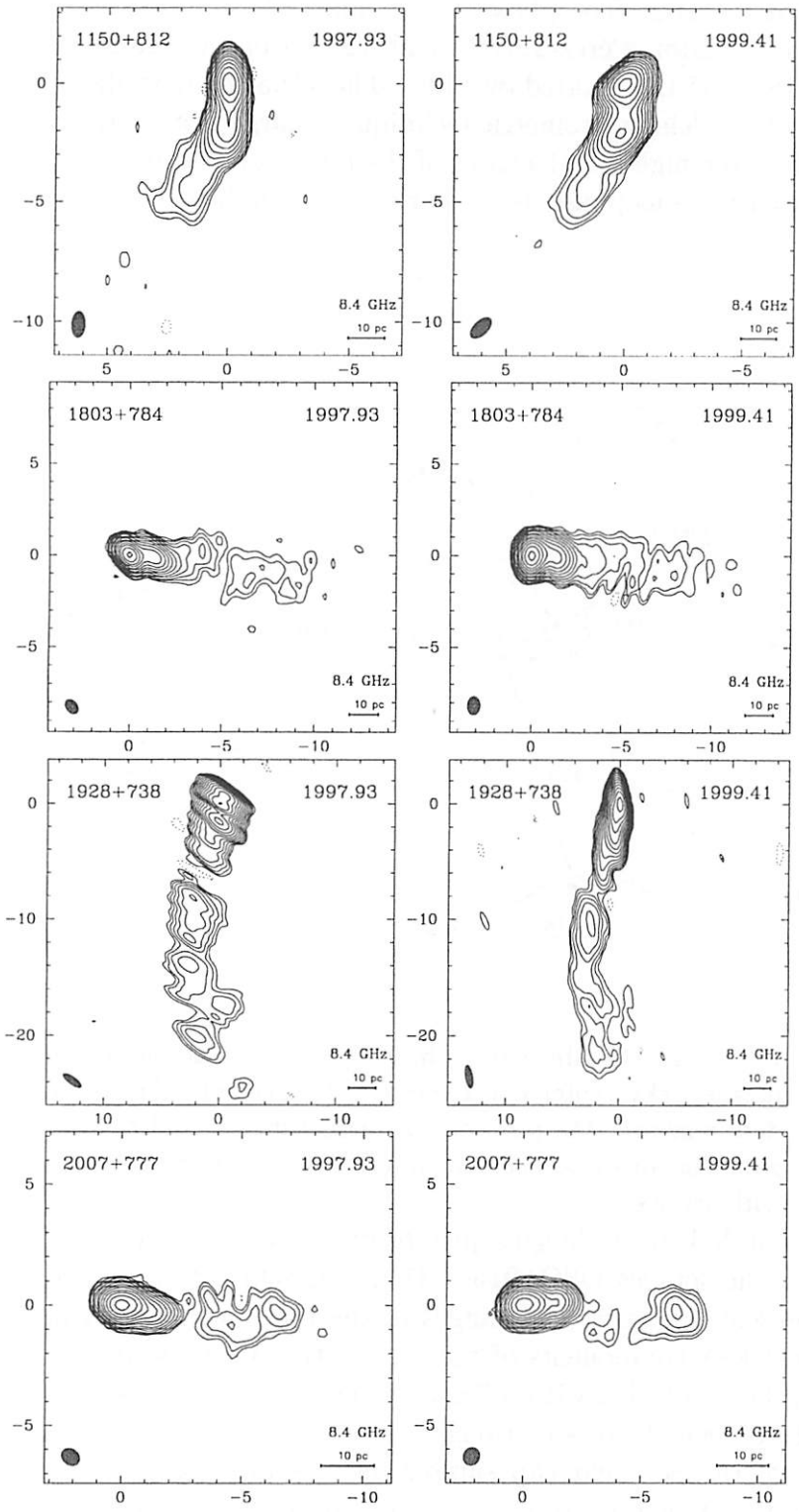

Figure 2: VLBA images of QSO 1150+812, BL 1803+784, QSO 1928+738, and BL 2007+777 from observations on 6 December 1997 (1997.93) and 28 May 1999 (1999.41). Axes are relative α and δ in mas. Minimum contour levels are of 1.0 mJy/beam for QSO 1150+812 and BL 1803+784, 1.4 mJy/beam for QSO 1928+738, and 0.9 mJy/beam for BL 2007+777. Note that the convolution beam of a given source in a given epoch substantially differs from those of other sources and epochs, due to the different coverages of the (u, v) plane.

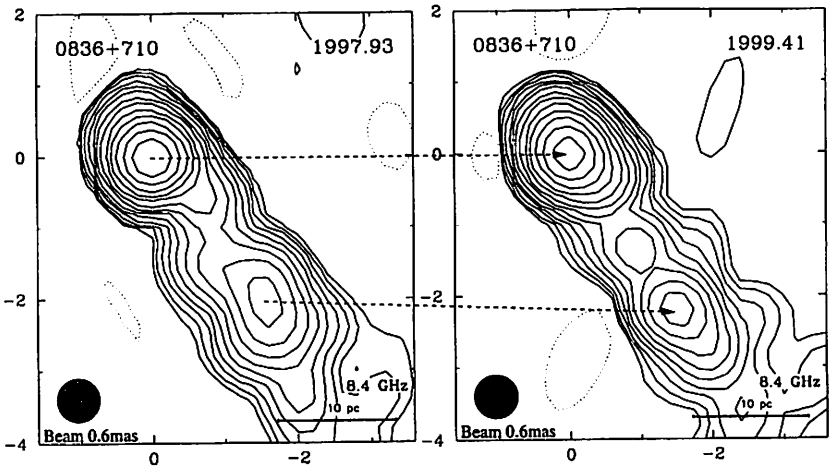

Figure 3: VLBA images of QSO 0836+710 convolved with a 0.6 mas circular beam. We observe the small structural changes in the inner part of the jet. The dashed lines draw a tentative association between features from one epoch to another.

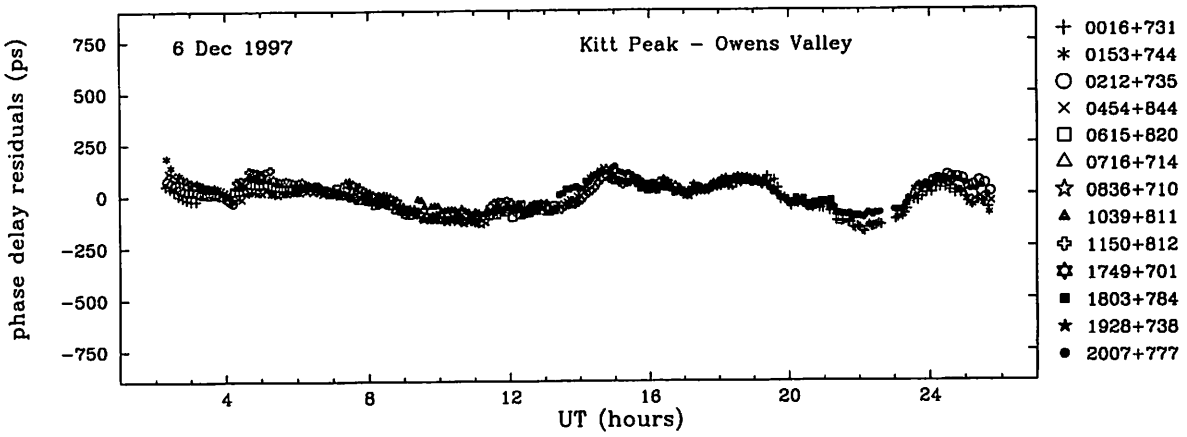

Figure 4: Postfit residuals of the (undifferenced) phase-delays at 8.4 GHz after a weighted least-squares analysis that estimates the relative separations between the radio sources. One phase-cycle at 8.4 GHz corresponds to 120 ps of phase-delay. Notice a similar trend for all sources. These trends cancel out in the differences to yield a global residual rms of $\sim$ 30 ps.

post-fit residuals shown in Fig. 4. The phase-connection process has also been eased by the availability of an interactive, PGPLOT-based software developed in our group, which permits us to efficiently correct for phase-delay ambiguities. The expected average precision (including all systematic errors) of the relative position determination of all radio sources in the sample is of $\sim$80 μas at 8.4 GHz. If extrapolated, these results indicate that our observations at 15 GHz should yield a precision of $\sim$50 μas.

Related to this work, Guirado et al. (2000) have shown the feasibility of precision differential phase-delay astrometry at 43 GHz (λ7 mm) by studying the pair of S5 radio sources QSO 1928+738 and BL 2007+777, separated by $\sim$ 5°. For their results, the root-mean-square of the postfit residual delays is $\sim$ 2 ps, or equivalently $\sim$ 30° of phase at this frequency. There can be little doubt that the entire S5 sample can thus be studied at 43 GHz, following studies at 8.4 and 15 GHz, and the relative positions of all the sources determined with $\sim$ 20μas precision. The VLBA has allocated time to observe the S5 polar cap sample also at 43 GHz

in late 2000. Thus, the observations at 8.4 and 15 GHz will be complemented with those at mm-wavelength.

3 Conclusions

Following recent progress in the phase-delay astrometric technique (extension to larger distances, larger sets of radio sources, and higher frequencies) we have initiated a program to study the 13 radio sources of the S5 polar cap sample. We observed the sources twice at 8.4 GHz and twice at 15 GHz, and new observations are planned at these frequencies and at 43 GHz. The astrometric data reduction includes the modelling of the atmospheric, ionospheric and source-structure effects. Our first results show the feasibility of phase-connecting the 13 radio sources at 8.4 GHz, and obtain precisions in the relative separation determinations better than 0.1 mas. The absolute kinematics of the radio sources will thus be determined unambiguously. Furthermore, using the astrometric information available at 8.4, 15 and 43 GHz, it will be possible for the first time to make rigorous spectral-index maps, together with a multiwavelength study of the absolute kinematics of the S5 polar cap sources. This observing scheme could be extended in the future to further regions of the sky, on-route towards global phase-delay astrometry.

References

- Bartel et al. *Nature*, **319**, 733 (1986)
- Blandford & Königl *ApJ*, **232**, 34 (1979)
- Eckart et al. *A&A*, **168**, 17 (1986)
- Fey et al. *ApJS*, **105**, 299 (1996)
- Fey & Charlot *ApJS*, **111**, 95 (1997)
- Fey & Charlot *ApJS*, **128**, 17 (2000)
- Gómez et al. *ApJ*, **435**, L19 (1995)
- Guirado et al. *A&A*, **293**, 613 (1995a)
- Guirado et al. *AJ*, **110**, 2586 (1995b)
- Guirado et al. *A&A*, **336**, 385 (1998)
- Guirado et al. *A&A*, **353**, L37 (2000)
- Johnston & de Vegt *ARAA*, **37**, 97 (1999)
- Kühr et al. *A&ASS*, **45**, 367 (1981)
- Lara et al. *A&A*, **314**, 672 (1996)
- Marcaide et al. *AJ*, **88**, 1183 (1983)
- Marcaide et al. *AJ*, **108**, 368 (1994)
- Pérez-Torres et al. *A&A*, **360**, 161 (2000)
- Rioja et al. *A&A*, **325**, 383 (1997)
- Ros et al. *A&A*, **348**, 381 (1999)
- Ros et al. *A&A*, **356**, 357 (2000a)
- Ros et al. *Proc. of 5th EVN VLBI Symp.*, Polatidis A., Conway J., Booth R., (eds.), Onsala Space Observatory, in press (2000b)
- Shapiro et al. *AJ*, 84, 1459 (1979)

List of Participants

Alef, Walter Max-Planck-Institut für Radioastronomie, Germany
alef@mpifr-bonn.mpg.de

Behrend, Dirk IEEC - CSIC, Spain
behrend@ieec.fcr.es

Bergstrand, Sten Onsala Space Observatory, Sweden
sten@oso.chalmers.se

Böhm, Johannes Institute of Geodesy and Geophysics, Austria
jboehm@luna.tuwien.ac.at

Campbell, Bob Joint Institute for VLBI in Europe, The Netherlands
campbell@jive.nl

Campbell, James Geodetic Institute, Univ. of Bonn, Germany
CAMPBELL@sn-geod-1.geod.uni-bonn.de

Colucci, Giuseppe ASI/Telespazio, S.P.A, Italy
giuseppe.colucci@asi.it

Elgered, Gunnar Onsala Space Observatory, Sweden
kge@oso.chalmers.se

Engelhardt, Gerald Bundesamt für Kartographie und Geodäsie, Germany
engelhardt@leipzig.ifag.de

Gandolfi, Stefano Università di Bologna, Italy
stefano.gandolfi@mail.ing.unibo.it

Garrett, Mike Joint Institute for VLBI in Europe, The Netherlands
garrett@jive.nl

Gueguen, Erwan Istituto di Tecnologia Spaziale - CNR, Italy
gueguen@itis.mt.cnr.it

Haas, Rüdiger Onsala Space Observatory, Sweden
haas@oso.chalmers.se

Kierulf, Halfdan Norwegian Mapping Authority, Norway
halfdan.kierulf@statkart.no

Lanotte, Roberto Agenzia Spaziale Italiana, Italy
roberto.lanotte@asi.it

Lunalbi, Eustachio Agenzia Spaziale Italiana, Italy
vlbi@asi.it

Mantovani, Franco Istituto di Radioastronomia, Italy
fmantovani@ira.bo.cnr.it

Müskens, Arno
mueskens@mpifr-bonn.mpg.de
Geodetic Institute, Univ. of Bonn, Germany

Nothnagel, Axel
nothnage@picasso.geod.uni-bonn.de
Geodetic Institute, Univ. of Bonn, Germany

Pérez-Torres, Miguel-Angel
torres@ira.bo.cnr.it
Istituto di Radioastronomia, Italy

Plag, Hans-Peter
plag@statkart.no
Norwegian Mapping Authority, Norway

Porcas, Richard
p222rwp@mpifr-bonn.mpg.de
Max-Planck-Institute für Radioastronomie, Germany

Rioja, Maria
rioja@oan.es
Observatorio Astronomico Nacional, Spain

Roy, Alan
aroy@mpifr-bonn.mpg.de
Max-Planck-Institute for Radioastronomy, Germany

Sarti, Pierguido
pierguido.sarti@mail.ing.unibo.it
University of Bologna, DISTART, Italy

Schlüter, Wolfgang
schlueter@wettzell.ifag.de
Bundesamt für Kartographie und Geodäsie, Germany

Schuh, Harald
hschuh@luna.tuwien.ac.at
Institute of Geodesy and Geophysics, Austria

Schwegmann, Wolfgang
schwegma@ira.bo.cnr.it
Istituto di Radioastronomia, Italy

Sorgente, Mauro
sorgente@mpifr-bonn.mpg.de
Geodetic Institute, Univ. of Bonn, Germany

Steinforth, Christoph
steinfor@chagall.geod.uni-bonn.de
Geodetic Institute, Univ. of Bonn, Germany

Tesmer, Volker
tesmer@dgfi.badw.de
Institute of Geodetic Research, Germany

Thorandt, Volkmar
vt@leipzig.ifag.de
Bundesamt für Kartographie und Geodaesie, Germany

Tomasi, Paolo
tomasi@ira.bo.cnr.it
Istituto di Tecnologia Spaziale - CNR, Italy

Tornatore, Vincenza
vin@ipmtf4.topo.polimi.it
Politecnico di Milano, DIIAR, Italy

Vittuari, Luca
luca.vituari@mail.ing.unibo.it
University of Bologna, DISTART, Italy